



Cessna Aircraft Company Raytheon Missile Systems AIAA Foundation

The 2012 Cessna Aircraft Company/Raytheon Missile Systems/AIAA Design/Build/Fly Competition Flyoff was held at Cessna East Field in Wichita, KS on the weekend of April 13-15, 2012. This was the 16th year the competition was held. A total of 68 teams submitted written reports to be judged. At least 57 teams attended the flyoff, 54 of which completed the technical inspection. Approximately 500 students, faculty, and guests were present. Attendance was down this year due to a new rule limiting universities to a single team, however, the quality of the teams, their readiness to compete, and the execution of the flights was extremely high.

The primary design objectives for this year were performance based:

- Mission 1 was scored on the number of laps which could be flown in 4 minutes, so speed was important
- Mission 2 simulated carrying a specified passenger load for three laps, testing load-carrying ability.
- Mission 3 measured airplane time to climb with a two-liter water payload.

Total flight score was the sum of the three mission flight scores. As usual, the total score is the product of the flight score and written report score, divided by airplane empty weight. More details can be found at the competition website: <http://www.aiaadbf.org>

This year the flyoff was affected by significant weather events. Flights were suspended Saturday at 12:45PM by high winds, and when they did not subside by 2PM activities were terminated for the day. That night, a severe storm cell hit southeast Wichita and a tornado passed approximately $\frac{1}{4}$ mile from Cessna East Field (see below). The hangar escaped damage – except for the food vendor trailer which was flipped – but downed power lines forced closure of the road to the site and prevented normal access. It was determined that the flyoff could not continue and a recovery plan was implemented to provide access through the main Cessna plant for teams to recover their property. We are all thankful that none of the teams experienced any property loss, and also that there weren't serious injuries to any of the Wichita population.

Despite this unprecedented weather event, two complete rotations through the flight queue were completed, and there were ten attempts at a third flight. By unanimous consensus of the DBF Organizing Committee, it was ruled that the winners of the competition would be based on the scores from the two complete rotations. This was considered the most fair, as the overwhelming majority of teams did not get an opportunity for a third attempt.

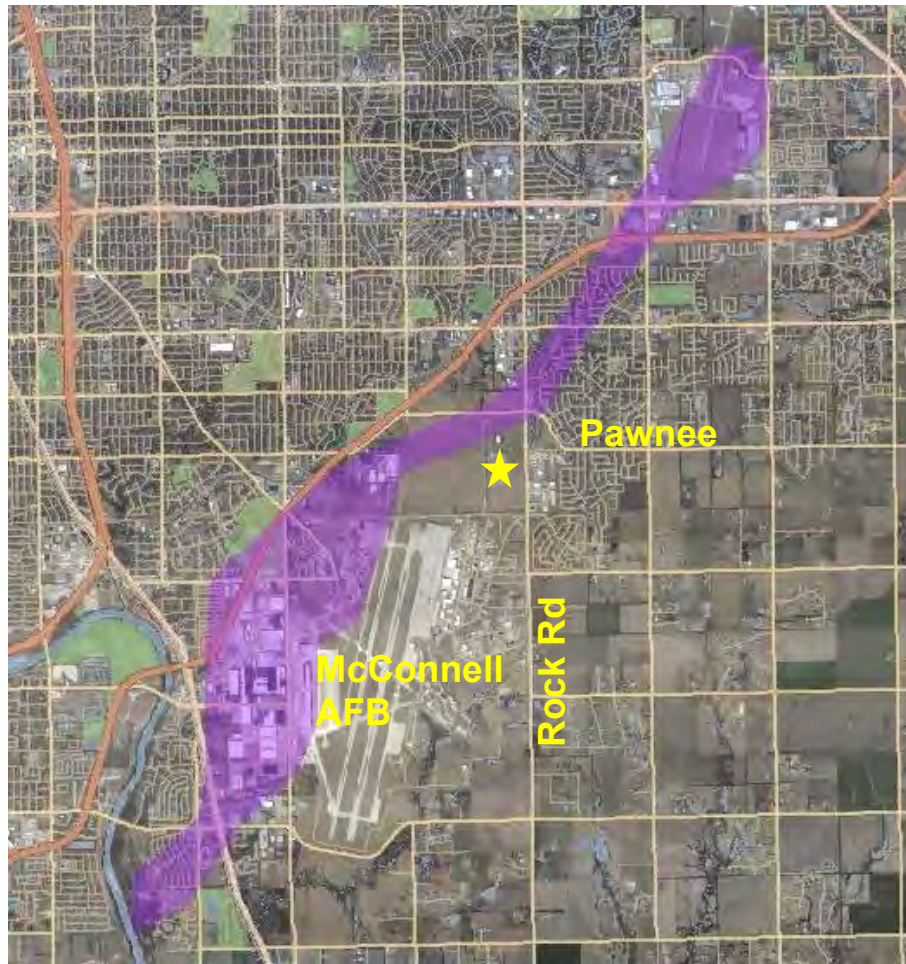
First place is awarded to San Jose State University: Team PhalanX, with the second highest report score, excellent flight scores, and second lowest RAC. Second place goes to University of California at Irvine: Angel of Attack, and third place to University of Colorado: H2Buffalo. It

should also be noted that Colorado and Irvine were the only two teams to complete all three missions, even though the third score ultimately was not used. This is a testament to their readiness to fly and to their final execution of the missions. Finally, special mention goes to Wichita State University for the highest report score at 96.50 (WSU also had the low RAC at 1.72 lb). The complete standings are listed in the table below.

We owe our thanks for the success of the DBF competition to the efforts of many volunteers from Cessna Aircraft, the Raytheon Missile Systems, and the AIAA sponsoring technical committees (Applied Aerodynamics, Aircraft Design, Flight Test, and Design Engineering). These volunteers collectively set the rules for the contest, publicize the event, gather entries, judge the written reports, and organize the flyoff. Thanks also go to the Corporate Sponsors: Cessna Aircraft, Raytheon Missile Systems, and the AIAA Foundation for their financial support. Special thanks go to Cessna Aircraft for hosting the flyoff this year.

Finally, this event would not be nearly as successful without the hard work and enthusiasm from all the students and advisors. If it weren't for you, we wouldn't keep doing it.

David Levy
For the DBF Governing Committee



Path of Tornado near 2012 DBF Competition Site, 4/14/2012

WICHITA STATE UNIVERSITY



AIAA/Cessna/RMS
Design/Build/Fly
Design Report 2011/2012

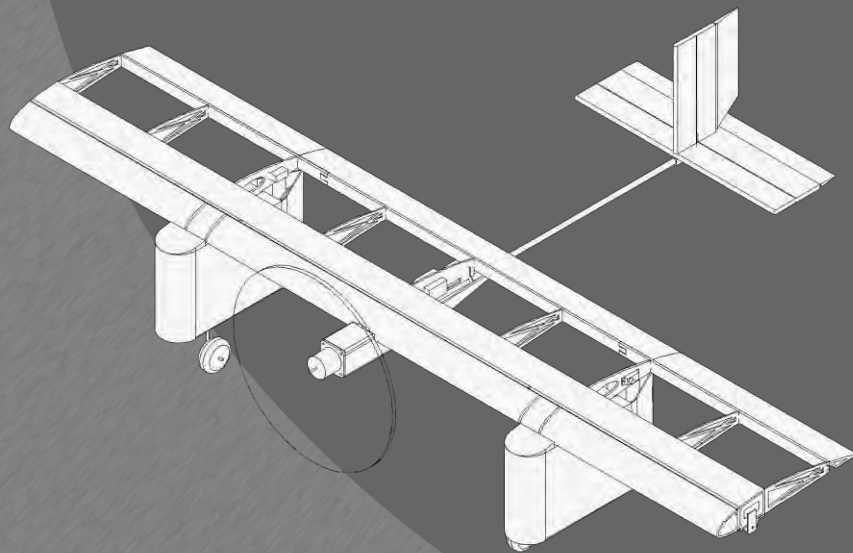




Table of Contents

1.0	Executive Summary	5
2.0	Management Summary	6
2.1	Team Organization.....	6
2.2	Design Schedule	7
3.0	Conceptual Design	8
3.1	Mission Requirements.....	8
3.1.1	<i>Mission One: Ferry Flight¹</i>	8
3.1.2	<i>Mission Two: Passenger Flight¹</i>	9
3.1.3	<i>Mission Three: Time-to-Climb¹</i>	9
3.1.4	<i>Total Score¹</i>	9
3.2	Competition Scoring Analysis	9
3.3	Translating Mission Requirements into Design Requirements	11
3.4	Conceptual Design Selection	12
3.4.1	<i>Configuration Selection</i>	13
3.5	Component Layout Selection.....	13
3.5.1	<i>Propeller Configuration and Location Selection</i>	13
3.5.2	<i>Control System Selection</i>	14
3.5.3	<i>Payload Configuration and Location Selection</i>	15
3.6	Selected Conceptual Design.....	15
4.0	Preliminary Design	16
4.1	Design and Analysis Methodology.....	16
4.2	Mission Model	17
4.3	Initial Sizing – Design Method.....	17
4.4	Aerodynamics	18
4.4.1	<i>Aerodynamics Model</i>	19
4.4.2	<i>Airfoil Selection</i>	20
4.4.3	<i>Aerodynamic Performance Predictions</i>	21
4.5	Stability and Controls	22
4.5.1	<i>Stability and Controls Model</i>	22
4.5.2	<i>Stability and Control Performance Predictions</i>	24
4.6	Propulsion	25
4.6.1	<i>Propulsion Model</i>	25
4.6.2	<i>Propulsion System Constraints</i>	25
4.6.3	<i>Propulsion Sizing</i>	26
4.6.4	<i>Propeller Analysis</i>	26
4.6.5	<i>Battery Analysis</i>	27
4.6.6	<i>Motor Analysis</i>	28
4.7	Structures	28



4.7.1	<i>Structures Model</i>	29
4.7.2	<i>Structural Layout and Load Paths</i>	29
4.7.3	<i>Material Selection</i>	30
4.7.4	<i>Wing Design</i>	30
4.7.5	<i>Fuselage Design</i>	31
4.7.6	<i>Boom, Tail, and Landing Gear Design</i>	31
4.7.7	<i>Critical Load Analysis</i>	31
4.7.8	<i>Landing Analysis</i>	33
4.7.9	<i>Weight Buildup</i>	33
5.0	Detail Design	34
5.1	Dimensional Parameters.....	35
5.2	Structural Characteristics	35
5.2.1	<i>Wing</i>	35
5.3	System Design, Component Selection and Integration	36
5.3.1	<i>Payload Systems</i>	36
5.3.2	<i>Propulsion System Integration</i>	38
5.3.3	<i>Electronic Component Selection</i>	39
5.4	Aircraft Component Weight and CG Buildup	40
5.5	Flight Performance Summary	40
5.6	Mission Performance Summary	41
5.7	Drawing Package	41
6.0	Manufacturing Plan and Processes	46
6.1	Manufacturing and Material Selection.....	46
6.1.1	<i>Material Selection</i>	47
6.2	Manufacturing Schedule	47
6.3	Aircraft Manufacturing Process	47
7.0	Testing Plan	48
7.1	Aerodynamic Testing	49
7.1.1	<i>50% Scaled Wind Tunnel Model Test</i>	49
7.1.2	<i>Full Scale Wind Tunnel Model</i>	49
7.2	Propulsion System Testing	50
7.2.1	<i>Battery Testing</i>	50
7.2.2	<i>Propulsion System Testing</i>	51
7.3	Structural Testing	52
7.3.1	<i>XPS Foam Material Properties Validation</i>	52
7.3.2	<i>Wing Testing</i>	53
7.4	Flight Testing.....	53
7.4.1	<i>Initial Flight Testing</i>	53
7.4.2	<i>Competition Prototype</i>	55



8.0	Performance Results	56
8.1	Aerodynamic Performance.....	56
8.2	Stability and Controls Performance	57
8.3	Structures Performance	58
8.4	Propulsion Performance.....	58
8.5	Flight Testing Results.....	59

Acronyms, Abbreviations, and Symbols

β	Sideslip Angle	KV	Motor RPM per Volt
δ_a	Aileron Deflection Angle	L/D	Lift-to-Drag Ratio
δ_e	Elevator Deflection Angle	M1	Mission One
δ_f	Flap Deflection Angle	M2	Mission Two
δ_r	Rudder Deflection Angle	M3	Mission Three
\S	Section	MDO	Multi-Disciplinary Optimization
AC	Aerodynamic Center	NACA	National Advisory Committee on Aeronautics
AOA	Angle of Attack (also α)	NiCad	Nickel-Cadmium
AVL	Athena Vortex Lattice	NiMH	Nickel-Metal Hydride
CAM	Competition Altimeter for Models	N_{laps}	Number of Laps Completed
C_{d0}	Airfoil Minimum Coefficient of Drag	p	Roll Rate
C_{D0}	Aircraft Parasite Drag Coefficient	PA	Power Available
CG	Center of Gravity	PR	Power Required
C_L	Aircraft Lift Coefficient	psf	Pounds per Square Foot
C_{l0}	Airfoil C _l at Zero Angle of Attack	q	Pitch Rate
C_{lmax}	Airfoil Maximum Lift Coefficient	r	Yaw Rate
C_{Lmax}	Aircraft Maximum Lift Coefficient	RAC	Rated Aircraft Cost
C_l	Aircraft Rolling Coefficient	Re	Reynolds Number
C_{m0}	Airfoil Zero-Lift Pitching Moment Coefficient	t/c_{max}	Maximum Thickness-to-Chord Ratio
C_{M0}	Aircraft Zero-Lift Pitching Moment Coefficient	T/W	Thrust-to-Weight Ratio
C_{mα}	Slope of Airfoil Pitching Moment Curve	T_{climb}	Time of Climb for Mission Three
C_{Mα}	Slope of Aircraft Pitching Moment Curve	T_{avg}	Average Time for Mission Three
Cn	Aircraft Yawing Coefficient	UIUC	University of Illinois Urbana Champaign
CNC	Computer Numerical Control	W/S	Wing Loading
DBF	Design/Build/Fly	W_{flight}	Mission Two Payload Weight
e	Oswald Efficiency Factor	WSU	Wichita State University
ESC	Electronic Speed Control	WTT	Wind Tunnel Test
FOM	Figure of Merit	XPS	Extruded Polystyrene



1.0 Executive Summary

This report summarizes the design efforts of Wichita State University (WSU) for the 2011-2012 AIAA/Cessna Aircraft Company/Raytheon Missile Systems - Student Design/Build/Fly (DBF) Competition. The primary objective of WSU DBF is to develop an aircraft that maximizes the total score according to the competition rules¹. The team's organizational structure takes advantage of team members' respective strengths to accomplish this goal.

DBF rules state that the total competition score consists of the report score, the total flight score, and the Rated Aircraft Cost (RAC). The RAC is the maximum empty flight weight of all 3 missions. The total flight score consists of the sum of individual flight scores for all 3 missions: Ferry Flight, Passenger Flight, and Rate of Climb Flight. The requirement of the first mission is to fly as many laps as possible within a 4 minute time limit, simulating a ferry mission. The second mission consists of flying 3 laps while carrying 8 aluminum blocks, which simulate passengers. The third mission consists of carrying 2L of water to an altitude of 100m (328ft), at which point a Competition Altimeter for Models (CAM-f3q) triggers a servo-operated dump valve to release the water payload. For all missions, the aircraft must takeoff in 100ft or less¹. Overall score is most affected by the RAC, so the selected configuration is designed to minimize empty weight.

The aircraft design is reached by first generating numerous design concepts capable of completing the mission requirements. Figure of Merit (FOM) analyses are completed on each concept to select the final configuration. The selected configuration is comprised of a high-wing monoplane with a tractor motor and a boom fuselage leading to a traditional empennage. Payload is stored in undercarriage pods for M2 and internally in the main spar for M3. Span-loading the payload in this way enables significant reduction in the weight of the wing. The component layout is designed to minimize system weight while maintaining the ability to successfully complete all missions. The final construction consists of a composite structure of balsa wood, extruded polystyrene (XPS) foam, and MicroLite™ covering.

A Multi-Disciplinary Optimization (MDO) tool is created and employed to increase the efficiency of the team through integration of each core engineering discipline. The final design has an RAC of 1.6lb. Expected performance for the 3 missions is as follows:

- Mission 1 (M1): For this mission, speed is optimized to produce a cruise speed of 78ft/s which allows the aircraft to complete 7 laps within the 4 minute time limit.
- Mission 2 (M2): The propulsion and aerodynamics of the aircraft are designed to successfully complete 3 laps while the structure is designed to handle landing loads with the passenger payloads.
- Mission 3 (M3): The design rate of climb (ROC) of 7.3ft/s results in the aircraft climbing to 100m (328ft) in 50 seconds.



2.0 Management Summary

2.1 Team Organization

The team's organizational structure is shown in Figure 1. The leadership responsibilities are divided into two roles, the team leads and the technical lead. The team leads are responsible for overall management which includes scheduling meetings, ensuring that the team meets all deadlines, and resolving communication issues. The technical lead is responsible for overseeing the technical design work on the aircraft. The technical lead must confirm that all systems are compatible and is responsible for managing cross-discipline optimization efforts. Underclassmen are an integral part of the team and must be incorporated into the team effectively to continue the legacy of the WSU DBF program. To this end, an emphasis has been placed on developing the skills and understanding of the team as a whole.

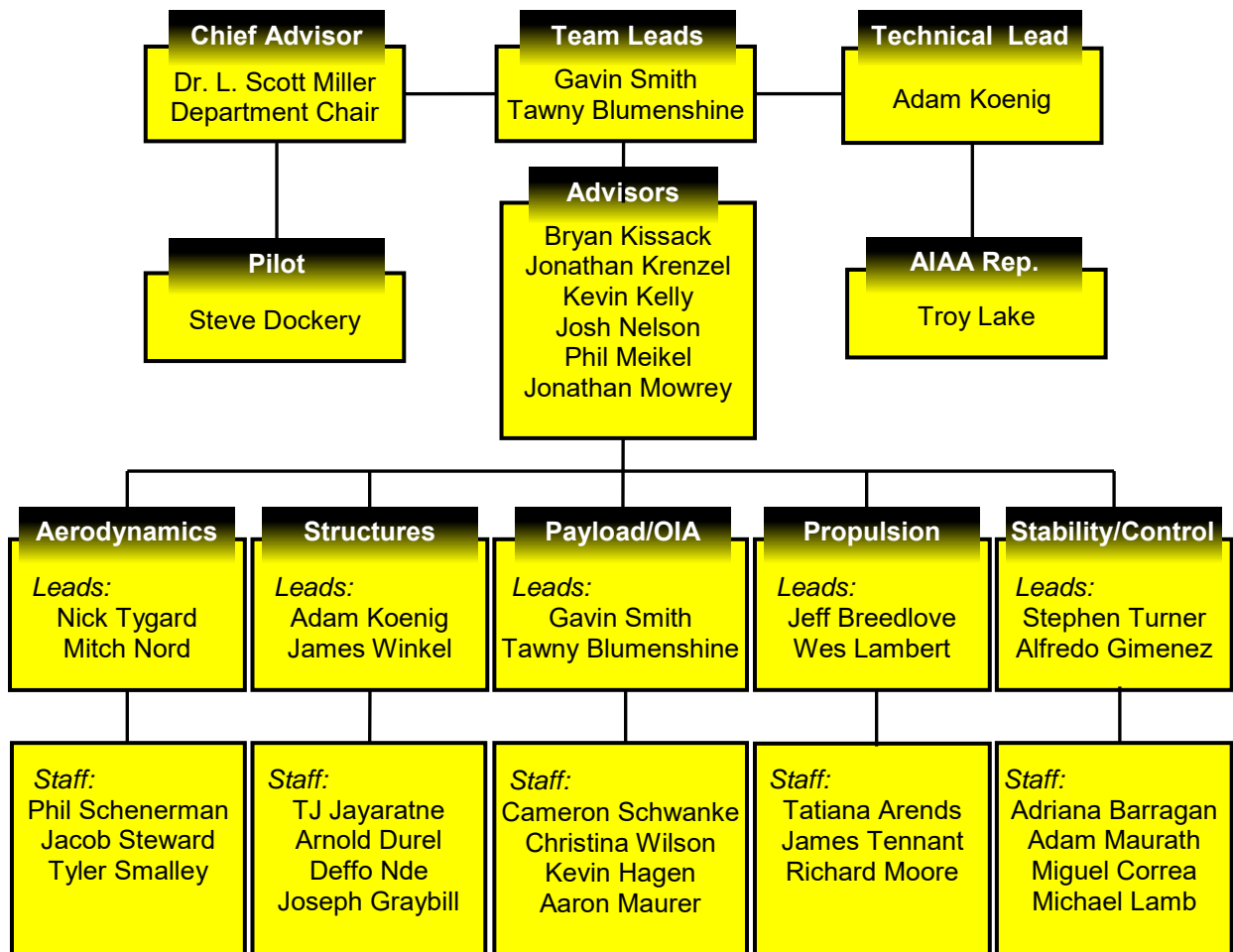


Figure 1: Team Organization Chart



2.2 Design Schedule

An accelerated design schedule is adopted this year due to a WSU internal competition. In order for the internal competition to be effective, the aircraft must be competition ready in February. This schedule also allows more flight testing for the selected aircraft, which allows the pilot to become more comfortable with the competition aircraft. Figure 2 details predicted and actual design progress.

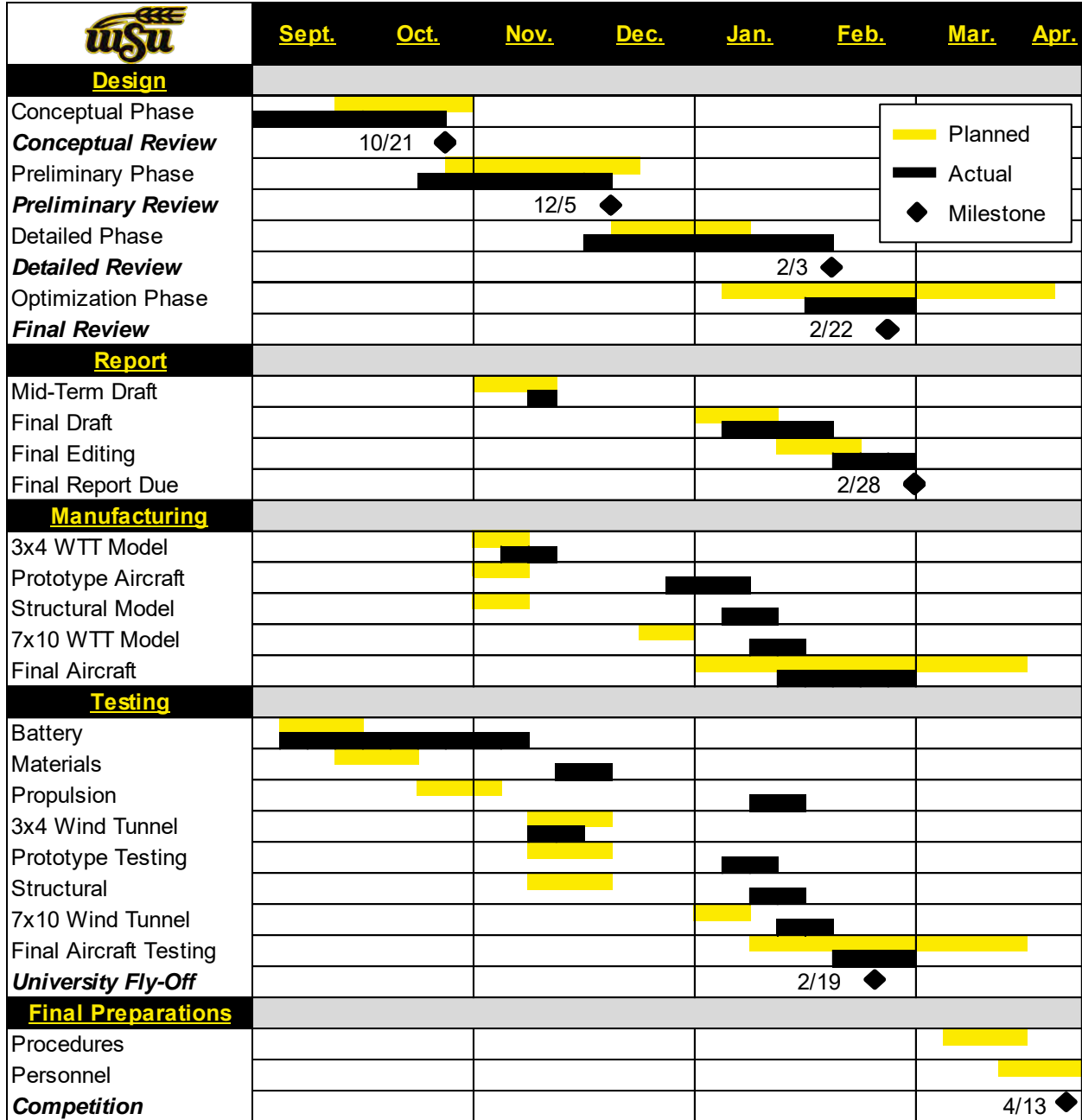


Figure 2: Design Schedule



3.0 Conceptual Design

The 2011-2012 AIAA DBF competition rules detail mission and technical inspection requirements for the aircraft¹. Combining the competition rules with previous WSU DBF experience yields a comprehensive set of design requirements and considerations that drive the design process. To begin determining aircraft configuration, a variety of aircraft concepts are generated. Then a FOM analysis is used to select competitive configurations for further consideration. FOM analysis is also used to select the aircraft sub-systems.

3.1 Mission Requirements

The rules for the AIAA Design/Build/Fly competition for the 2011-2012 academic year specify several requirements for all aircraft¹:

- The aircraft must fly all 3 missions in 1 configuration
- Maximum assembly time of 5 minutes
- Maximum propulsion battery pack weight of 1.5lb
- Maximum takeoff distance of 100ft
- 20A fuse-limited current
- Minimum water capacity of 2L
- The aircraft must be able to hold eight 1×1×5in aluminum blocks oriented vertically in flight

The competition consists of 3 missions¹. The course for the competition is shown in Figure 3. The requirements for each mission are detailed in the following sub-sections.

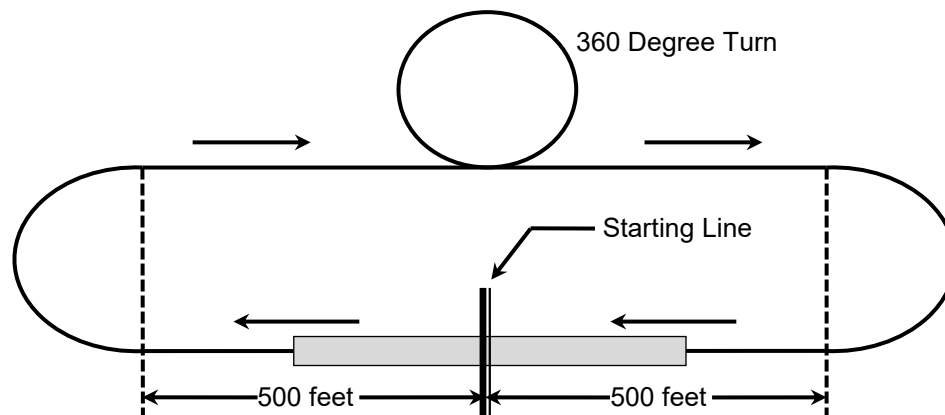


Figure 3: Flight Course

3.1.1 Mission One: Ferry Flight¹

The first mission is a ferry mission requiring the aircraft to complete as many laps as possible in the allotted 4 minutes. Flight time starts when the throttle is advanced for takeoff. The M1 score, defined by Equation 1, depends only on the number of completed laps, N_{LAPS} .



$$M1 \text{ Score} = 1 + \frac{N_{LAPS}}{6} \quad (1)$$

3.1.2 Mission Two: Passenger Flight¹

The second mission requires the aircraft to carry eight simulated passengers represented by 1×1×5in aluminum blocks and weighing a total of at least 3.75lb for 3 laps. The blocks must be oriented vertically during flight and contained within the mold lines of the aircraft. The only variable in the M2 score is the weight of the aircraft after completing the mission, W_{flight} .

$$M2 \text{ Score} = 1.5 + \frac{3.75}{W_{flight}} \quad (2)$$

3.1.3 Mission Three: Time-to-Climb¹

The third mission is a time-to-climb mission. The aircraft must takeoff and climb to an altitude of 100m (328ft) as fast as possible, at which point a CAM-f3q altimeter circuit will open a servo-operated dump “valve,” releasing the water payload. No flight profile is specified other than the implication that the aircraft must complete 1 lap and remain in the competition zone. The flight time starts at throttle up and ends when the judges see the water. The variables in the M3 score are the time-to-climb for WSU, T_{climb} , and the average time-to-climb for all teams successfully completing M3, T_{avg} .

$$M3 \text{ Score} = 2 + \sqrt{\frac{T_{avg}}{T_{climb}}} \quad (3)$$

3.1.4 Total Score¹

The 2012 DBF Competition score is composed of the written report score, the total flight score, and the RAC, as shown in Equation 4.

$$\text{Competition Score} = \frac{\text{Written Report Score} \times \text{Total Flight Score}}{\sqrt{\text{RAC}}} \quad (4)$$

The sum of all 3 mission scores forms the total flight score while the RAC is determined by the maximum empty weight of the aircraft for any mission. This is shown in the equations below:

$$\text{Total Flight Score} = \text{Mission 1} + \text{Mission 2} + \text{Mission 3} \quad (5)$$

$$\text{RAC} = \text{Max Empty Weight (M1, M2, M3)} \quad (6)$$

3.2 Competition Scoring Analysis

Competitive analysis begins with considerations of the scoring equations. These equations show a substantial number of points for completing each mission. The scoring parameters are the number of laps for M1, the flight weight for M2, and the time-to-climb and the average time-to-climb for M3¹.



The next step establishes a limit on possible scores given battery limitations. This analysis assumes the entire weight of the aircraft consists of the battery pack weight. These limitations are established using the energy content of the batteries, the 20A fuse limit, the 1.5lb total battery weight, and the loaded voltage for each cell. The performance characteristics of several common cell sizes of DBF propulsion batteries are considered. The power required (PR) to fly is assumed to be a cubic function of velocity. Maximum possible number of laps is assumed to be the highest number attempted at DBF competition in recent years, 12. For M1, the number of laps achieved is determined using the power available for each battery pack. For M3, assuming no drag, the power available divided by the system weight is the climb rate. Figure 4 shows that the maximum score decreases with increasing battery weight according to this method.

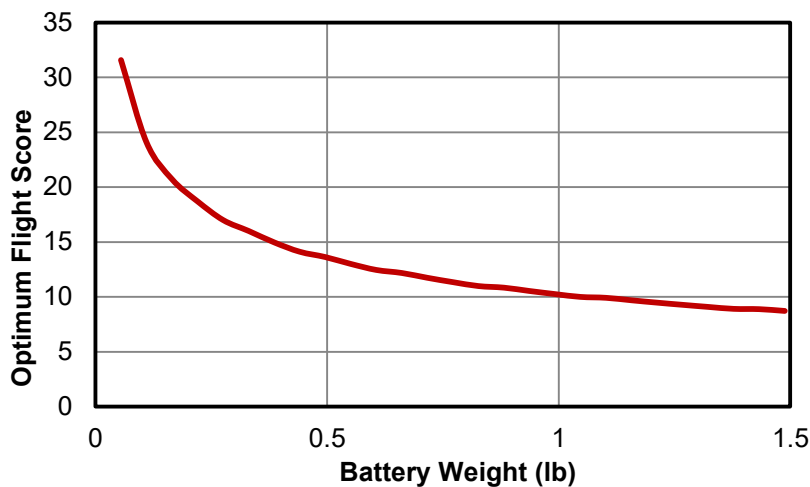


Figure 4: Optimum Flight Score vs Battery Weight

The last step in the scoring analysis is to analyze the equations using a percent perturbation method. The change in score is approximately linear with percent perturbation for any one of the scoring variables. This analysis is performed using various sets of baseline parameters, and the qualitative trends do not change significantly. Figure 5 shows this analysis with a reference of 5 laps, a time-to-climb of 60 seconds, a T_{avg} of 60 seconds, and an empty weight of 1.5lb. The score is plotted against percent change of each variable individually, as shown in Figure 5. The empty weight is the governing variable for the total score. Therefore, for any proposed change to the aircraft that adds weight, if the percent change in the target variable is not at least 5 times greater than the percent change in weight, the trade is not beneficial to the total score.

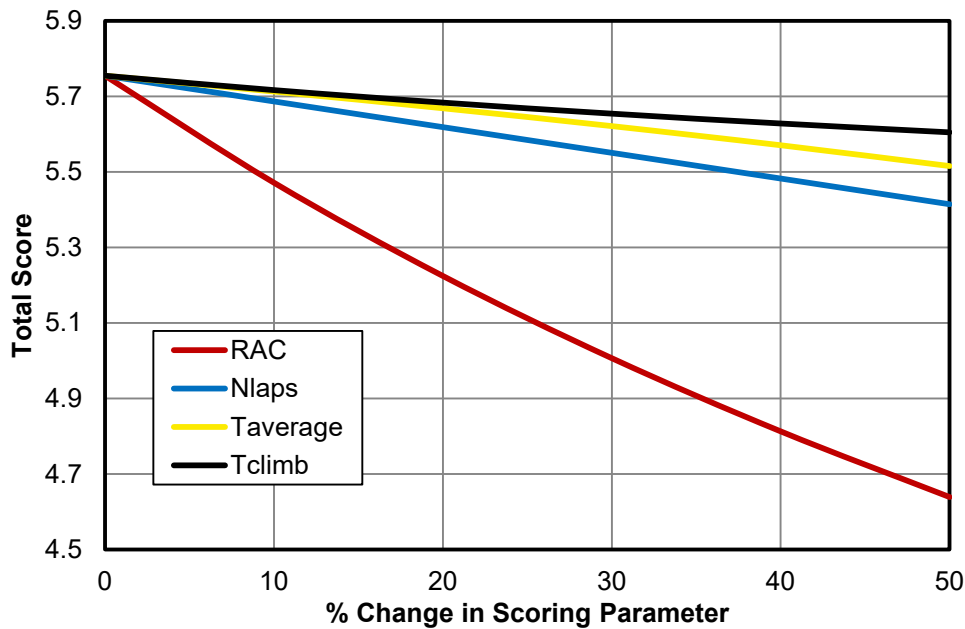


Figure 5: Total Score Sensitivity Analysis

This analysis concludes that the lightest possible aircraft that can successfully complete all 3 missions will win this year's DBF competition. It also provides some basic parameters for trade studies to determine which variables to prioritize in the preliminary design process.

3.3 Translating Mission Requirements into Design Requirements

Besides those explicitly listed in the competition rules, a competitive aircraft will have several other design constraints due to mission profiles, scoring analysis, and experience building remote controlled aircraft. These qualities include:

- *Minimize weight:* Lower weight is synonymous with higher score
- *No sloshing of water payload:* A dynamic CG is difficult to control
- *Maximize flow-rate of water during release:* Higher flow-rate increases visibility
- *Fuse and receiver battery accessibility:* Ease of placement in a fully assembled aircraft
- *Physical connections to be simple and reliable:* A failed connection could result in a crash
- *Minimize part count:* Simplicity provides easier optimization and manufacturing
- *Minimize tool complexity:* Easy manufacturing reduces the possibility of mistakes
- *Max 10 hours build time:* To achieve flight the day after a critical failure
- *Minimize damage in event of crash:* Salvageable parts support a faster rebuild of the aircraft
- *Minimize material cost:* Cheaper materials are more readily available
- *Avoid gearboxes:* Previous experience shows gearboxes tend to increase weight, complexity, and unreliability



3.4 Conceptual Design Selection

The conceptual design selection process involves developing concepts, then performing screening and scoring analysis to determine the most viable options. These concepts are compiled into a list of 24 unique configurations which are screened using a “+” or “-” for each criterion. The top screening concepts are then scored using a refined set of criteria (described below) and a score from 1 to 5 for each criterion with 3 being set to the baseline. The concepts are scored using 8 variations of criterion weights and the criteria are desensitized by increasing each 1 to a 2 and reducing each 5 to a 4. This greatly reduces the possibility of bias in the scoring process. The trend of these 16 scoring attempts is consistent with the original scoring, indicating that the same concepts that have done well initially are still the most viable options. For the purpose of clarity, only the original sampling of the scoring matrix is presented, with the FOM criteria used for the scoring process and their weights are described below used for the scoring process.

- **Multipurpose Structure (30%):** The amount of structure being used for more than one purpose is determined to be a desirable aspect of the concept due to the emphasis on reducing weight for the mission.
- **Solid Flight (20%):** Aircraft that lack a traditional empennage historically tend to be less able to handle the high winds and gusts which are likely during competitions in Wichita, KS².
- **Ease of Water Drop (20%):** Due to M3 involving the release of a water payload at altitude, the ease of water drop is considered during scoring. Concepts with localized water payload with only one dump point scored higher than more complex configurations for payload release. The added weight of the number of servos needed for each concept is also considered in this criterion.
- **Flexibility of Design (15%):** Flexibility refers to the ability to slightly modify the design easily. Greater flexibility enables optimization and testing results to be more fully incorporated.
- **Ease of Manufacturing (10%):** A plane that is simple to build is valuable because it minimizes mistakes in the construction process. Mistakes can add weight and impede aircraft performance. Also, in the event of a crash, easier manufacturing facilitates a faster rebuild.
- **Landing Gear (5%):** Due to the importance of reducing RAC, the amount of landing gear material needed for each concept is considered. Concepts that allow minimal landing gear structure or landing gear structure that can be incorporated in another element of the airframe structure are scored higher.



3.4.1 Configuration Selection

The configuration concepts that pass initial screening are scored against each other using FOM criteria as shown in Figure 6. The conventional concept scores the highest and is used for further development of the aircraft.

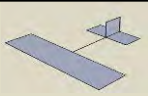
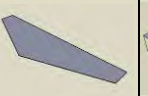
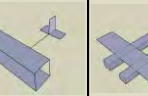
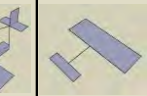
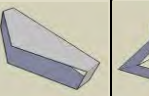
								
Figure of Merit	Weight	Conventional	Flying Wing	Biplane	Twin	Canard	Bi-Wing	Box-Wing
Multipurpose Structure	30	3	5	2	2	3	4	4
Solid Flight	20	3	1	3	3	2	1	1
Ease of Water Drop	20	3	3	3	1	2	1	1
Flexibility of Design	15	3	1	2	2	2	1	1
Ease of Manufacturing	10	3	3	2	2	3	1	1
Landing Gear	5	3	1	3	4	3	4	4
Total	100	3.00	2.80	2.45	2.10	2.45	2.05	2.05

Figure 6: Aircraft Configuration Figure of Merit Analysis

3.5 Component Layout Selection

3.5.1 Propeller Configuration and Location Selection

- **System Weight (50%):** Concepts that involve multiple motors will likely have a higher system weight due to the structure necessary to incorporate each motor.
- **Power (30%):** Two motor concepts will enable a system with greater overall power; thus these concepts score higher than single motor configurations.
- **Thrust-line Reliability (20%):** Motor concepts that result in the thrust-line of the aircraft shifting if one motor were to fail are scored lower than a traditional, reliable design.

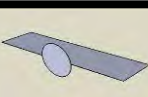
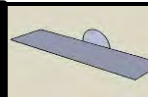
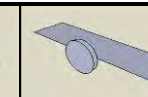
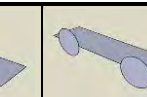
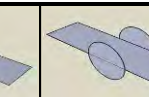
						
Figure of Merit	Weight	Single Tractor	Single Pusher	Contra-rotating	Twin Motor	Tractor-Pusher
System Weight	50	3	2	2	1	1
Power	30	3	3	4	5	5
Thrust-line Reliability	20	3	3	3	1	3
Total	100	3.00	2.50	2.80	2.20	2.60

Figure 7: Propeller Configuration Figure of Merit Analysis

The FOM criteria described above are used to score the propulsion system concepts. Figure 7 shows that the single tractor configuration scores the highest.



3.5.2 Control System Selection

The stability and control system needs to control the aircraft in roll, pitch, and yaw. However, historical data and configurations of previous DBF aircraft³ suggest that full three-axis control through conventional control surfaces (ailerons, elevator, and rudder) is not necessary. The different configurations are scored on their potential weight (50%), drag (15%), and controllability on landing and takeoff (35%). Considering this, these combinations of control surfaces are considered:

- **Conventional Tail with Rudder, Elevator and Ailerons (REA):** This is the most effective and predictable configuration for control; it also requires 3 servos and multiple structural components for control surfaces.
- **Conventional Tail with Elevator and Ailerons (EA):** Forgoing the rudder saves weight by eliminating a servo. This causes a loss in yaw control, hindering takeoff and landing ability.
- **Conventional Tail with Rudder and Elevator (RE):** Without the structural elements and servos required for ailerons, the aircraft will be lighter, but this sacrifices a degree of roll control that is critical for a plane of this size.
- **V-Tail with Ruddervators and Ailerons (RvA):** Joining the horizontal and vertical surfaces of the tail has the potential to reduce drag and weight, however handling characteristics can be sacrificed because of roll and yaw couplings.
- **V-Tail with Ruddervators (Rv):** This has the same advantages of the above V-Tail configuration and also reduces weight by forgoing the ailerons, although this amplifies the control difficulties of a V-Tail because there is no way to counter the adverse pitch and yaw coupling.

Figure of Merit		Weight	Conventional REA	Conventional EA	Conventional RE	V-Tail RvA	V-Tail Rv
Weight	50	3	4	4	3	4	
Drag	15	3	3	3	4	4	
Landing/Takeoff	35	4	2	2	3	2	
Total	100	3.35	3.15	3.15	3.15	3.30	

Figure 8: Control System Figure of Merit Analysis

The conventional tail with all 3 control surfaces is selected because it provides the necessary stability characteristics and does not have the control difficulties of a V-Tail. Also the weight penalty suffered from the extra servos can be partially offset by keeping the surfaces relatively small. Figure 8 shows this FOM analysis.



3.5.3 Payload Configuration and Location Selection

The fact that the payload is the largest contributor to the flight weight for M2 and M3 makes payload configuration selection critically important. Payload configuration has many implications for structural layout and component sizing.

- **Multipurpose Structure (40%):** The amount of structure that is being used for more than one purpose is determined to be a desirable aspect of the concept due to the emphasis on reducing weight for the mission.
- **Payload Distribution (30%):** Distributing the payload over the span of the wing rather than concentrating it at one point greatly reduces the necessary wing structure.
- **Ease of Water Drop (20%):** Due to M3 involving the release of a water payload at altitude, the ease of the water drop is considered during scoring.
- **Flexibility of Design (10%):** Flexibility refers to the ability to slightly modify the design easily. Greater flexibility enables optimization and testing results to be more fully incorporated.

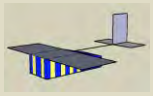
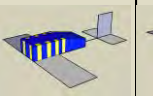
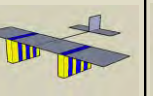
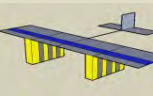
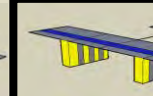
						
Figure of Merit	Weight	Low Tank	High Tank	Discrete Pods	SL & Rigid Pods	SL & Flexible Pods
Multipurpose Structure	40	3	3	2	2	4
Payload Distribution	30	3	3	4	5	5
Ease of Water Drop	20	3	3	1	2	2
Flexibility of Design	10	3	3	3	2	2
Total	100	3.00	3.00	2.50	2.90	3.70

Figure 9: Payload Configuration Figure of Merit Scoring Analysis

The FOM criteria described above are used to score the concepts for payload location. Figure 9 depicts that the configuration with span-loaded water and blocks in flexible pods scores the highest.

3.6 Selected Conceptual Design

The selected conceptual configuration is a high-wing monoplane with a single tractor propulsion system and conventional aileron, rudder, and elevator control surfaces. A small fuselage encloses the CAM-f3q and other electronic components and a boom extends aft to the traditional empennage. The aluminum blocks are carried in pods hung below the wing and the water payload will be span-loaded within the main spar. Span-loading both payloads (discrete distribution for M2 and continuous distribution for M3) minimizes the structural weight of the aircraft. This configuration meets the specified design requirements and has the flexibility for future mission-oriented optimization. This configuration uses a tail dragger landing gear configuration with the front landing gear mounted directly under the pods. This configuration is illustrated in Figure 10.

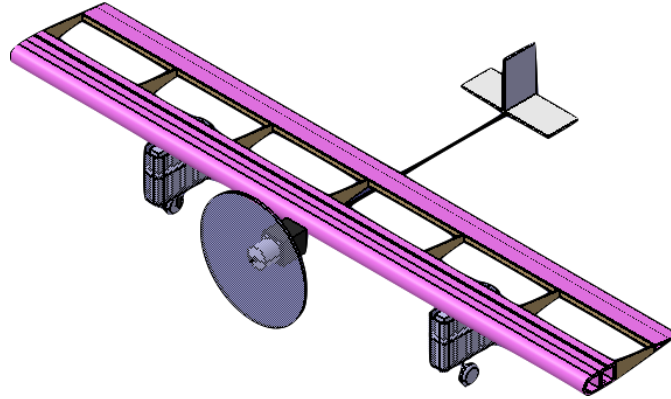


Figure 10: Conceptual Design Rendering

4.0 Preliminary Design

The preliminary design phase identifies critical design variables for each discipline and optimizes them to maximize total flight score. The score sensitivity analysis performed in the conceptual design phase identified empty weight as the critical design variable in order to maximize flight score.

4.1 Design and Analysis Methodology

Preliminary design is accomplished using a multidisciplinary design optimization (MDO) approach. This procedure uses a master module that contains all important parameters and interfaces with the independent analysis modules. The master parameters module contains values for critical aircraft parameters in the current design iteration. This approach streamlines trade studies and design iterations. To perform a trade study, aircraft parameters are changed to improve estimates. The new parameters are tested in the mission analysis problem to determine if there is any potential for score improvement. If score decreases, no further analysis is necessary. If there is improvement potential, the independent analysis modules are analyzed to determine viability of the new design. Analysis modules also identify critical faults in a design change, such as exceeding battery limits. The analysis modules operate independently, which requires efficient communication between design groups, but facilitates comprehensive error checking since all outputs must match with the master parameters module. Figure 11 illustrates the MDO process.

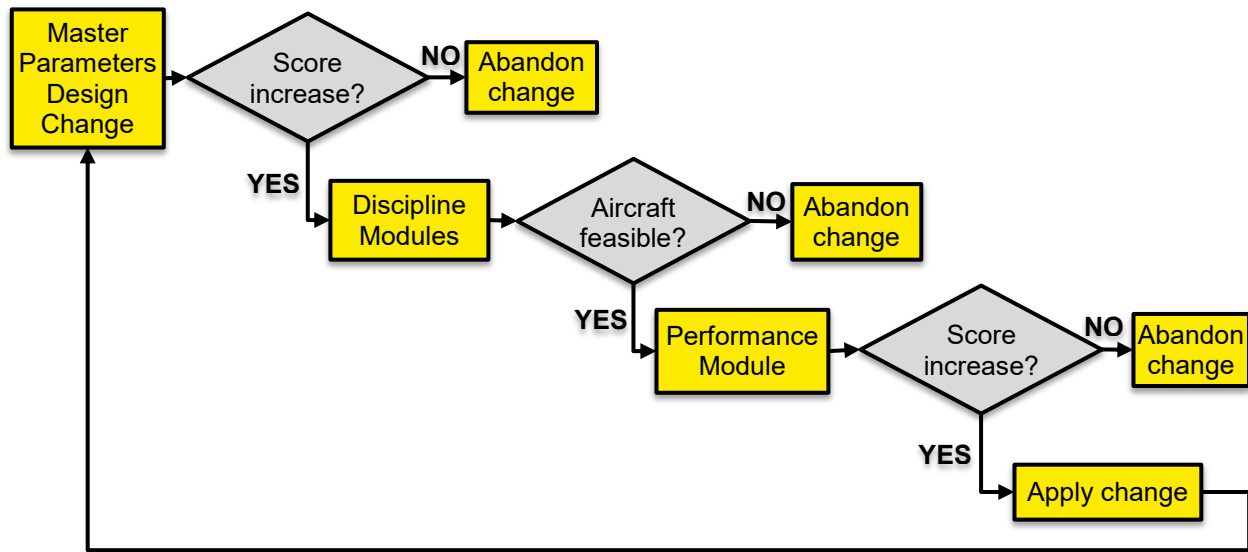


Figure 11: MDO Process

4.2 Mission Model

The mission model is critical to the success of the MDO method. The model simulates all 3 missions to determine number of laps for M1, time-to-climb for M3, and verify that the aircraft can complete M2. This module is used to determine the difference in score for any trade study. The model takes propulsion system specifications from the propulsion module and assumes that the batteries operate at a constant loaded voltage to allow conversion from mAh to Watts. Propulsion system efficiency is estimated from preliminary calculations and historical WSU DBF experience^{3,4,5,6}. The power required in each flight condition is based on estimates of parasitic and induced drag from the aerodynamic analysis module. The mission model identified critical performance parameters for each mission. Propulsion efficiency at high speed is determined to be critical for M1 due to course length and endurance considerations. Energy capacity is critical for M2 as the airplane has to fly 3 laps while heavily loaded. Static thrust is the driving requirement for M3 to satisfy the 100ft takeoff requirement.

4.3 Initial Sizing – Design Method

To size the aircraft, an initial weight estimate is generated from competitive payload fractions from previous DBF aircraft. Next, Raymer's⁷ method is utilized to determine thrust-to-weight ratio (T/W) as a function of wing loading (W/S) for critical design cases. The chosen design point will have a higher T/W than required by all critical cases at the chosen W/S. Minimizing aircraft weight requires minimizing both wing area and propulsion weight, so the selected design point will simultaneously maximize W/S and minimize T/W. Cases are analyzed for stall, takeoff, climb, cruise, and level turn for all missions. The critical cases are determined to be cruise and turn for M1 as well as takeoff and climb for M3. The stall requirement determines maximum allowable wing loading for flight at the stall speed for a given C_{Lmax} ,



assumed to be 1.2. A stall speed of 31ft/sec is selected as a starting point based on past WSU DBF experience in designing aircraft for high payload ratios, which yields a maximum wing loading of 1.25psi^{3,4,5,6}. These values show that a wing area of 4.93ft is required with a takeoff thrust of 1.7lb.

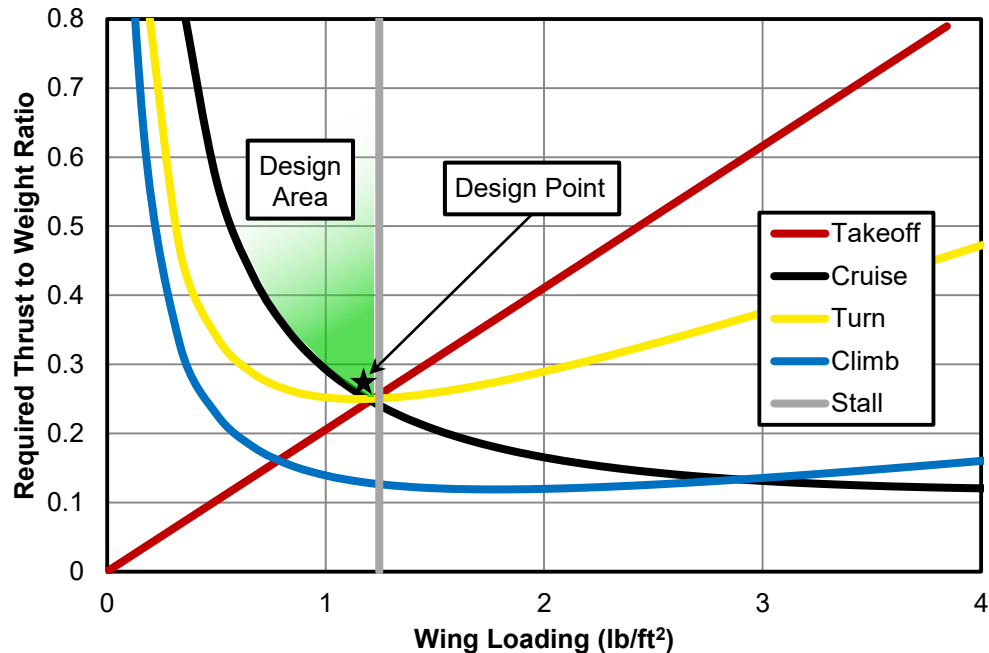


Figure 12: Thrust to Weight vs. Wing Loading

4.4 Aerodynamics

The aerodynamics group is responsible for wing design optimization and drag reduction for the aircraft. An iterative process is used to size aerodynamic components and ensure compatibility with other aircraft subsystems. The process first selects ideal airfoils for aerodynamic surfaces. It then calculates 3D performance characteristics and verifies that the components perform adequately while complying with the design requirements. The aerodynamics group is also responsible for managing wind tunnel testing and confirming preliminary testing data with software including XFOIL⁸ and Athena Vortex Lattice (AVL)⁹.



4.4.1 Aerodynamics Model

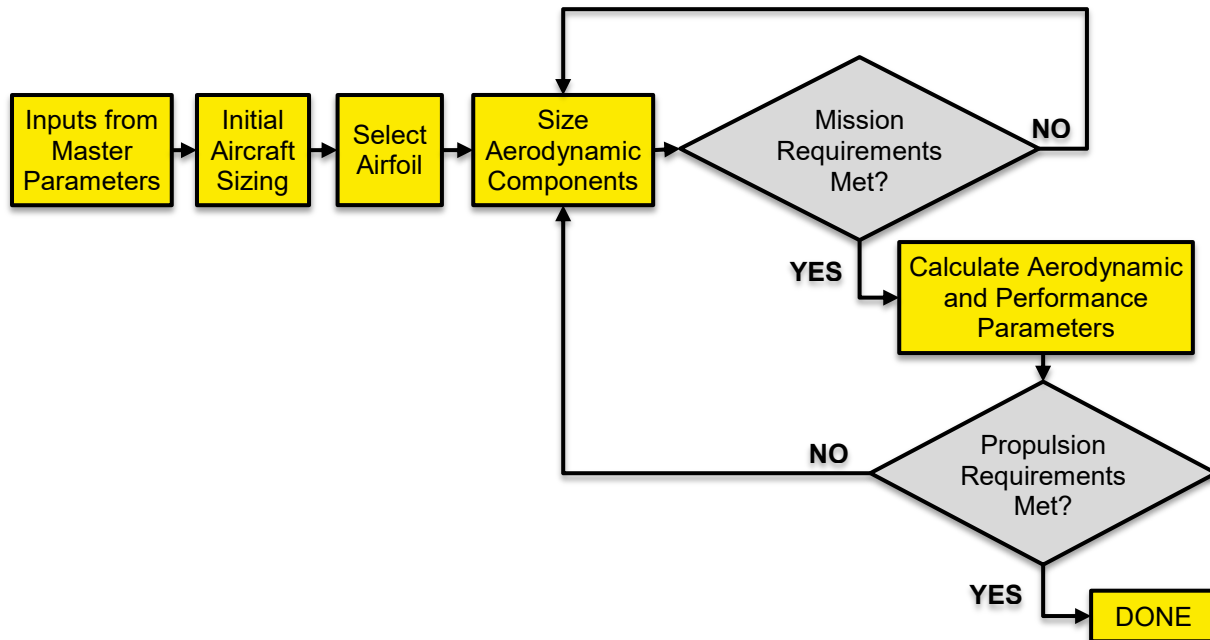


Figure 13: Aerodynamics Design Process

The critical aerodynamic design parameters are listed below:

- **Wing Area:** Wing area is the most important parameter as it is the main source of lift, drag, and payload containment. Although a large wing produces more lift and shortens takeoff distance, it causes an increase in drag which decreases aircraft performance. Wing sizing is driven by the W/S analysis. The wing is sized to the mission profile with the smallest W/S which dictates the minimum size of the wing. The critical mission profile for W/S is takeoff in M3. The final wing area is determined by two factors: the propulsion system and the selected airfoil.
- **Wing Airfoil:** The maximum lift coefficient is dependent on the selected airfoil which is critical for wing sizing at the takeoff condition. The maximum lift coefficient is chosen based on historical data and approximation. Maximum drag coefficients are determined using Raymer's⁷ component buildup method discussed in §4.4.2. These coefficients help provide values of power required for different mission profiles.
- **Aspect Ratio:** The initial aspect ratio is chosen by historical data based on previous DBF planes with similar requirements and concepts^{3,5,6}. Span and chord length are determined based on the value of wing area and aspect ratio. Weight must also be considered when selecting aspect ratio as high aspect ratios incur a structural weight penalty. Aspect ratio may be refined to optimize the performance of the aircraft.



4.4.2 Airfoil Selection

Based on the selected concept, the scoring analysis, and the mission requirements, the critical criteria are determined for the wing airfoil. The criteria are listed below:

- **Maximum lift coefficient, $C_{l_{max}} > 1.3$ (40%).** Having a higher $C_{l_{max}}$ allows for the wing area to be decreased, which decreases the amount of structure. This also ensures that the plane will lift off with maximum payload in the required 100ft takeoff distance.
- **Zero-lift drag coefficient, $C_{d0} \sim 0$ (20%).** The wing produces the majority of the aircraft drag. It is important to reduce drag to improve overall aircraft performance. Reducing parasitic drag increases speed, which reduces wing area.
- **Maximum thickness, $t/c_{max} > 0.1$ (15%).** Thickness must be considered to accommodate a span-loaded concept and to reduce structural material requirements for bending moments. Water payload is stored in the wing; therefore the airfoil must have an appropriate thickness.
- **Pitching moment coefficient, C_{m0} (10%).** A smaller pitching moment coefficient lessens control surface requirements to stabilize and trim the aircraft and reduces torsional loads on the wing structure, both of which help achieve a lightweight design.
- **Stall characteristics (15%).** An airfoil with poor stall characteristics or low stall angle can abruptly lose stability during flight at critical condition. Airfoils with sharp stall characteristics are also more sensitive to flaws in geometry, making manufacturing difficult.

A survey of 85 low Reynolds number airfoils¹⁰ establishes viable options for a satisfactory airfoil. Most of the airfoils are discarded based on the maximum lift coefficient requirement. Manufacturability also plays a significant role in the selection process. If the trailing edge profile is thin, then the airfoil is not considered due to the excessive number of ribs needed to maintain the shape. After the basic screening, 21 airfoils from NACA, Gottingen, Selig, Eppler and CLARK¹⁰ are selected for further consideration. XFOIL⁸, Javafoil¹¹, and published data are used to determine airfoil performance using a takeoff Reynolds number of 200,000. The final 4 airfoils, SD7062, NACA 4415, NACA M24, and CLARK Z are selected for scoring. These final airfoils are further researched to confirm that multiple sources indicate that the airfoil will perform as expected in the proper Reynolds number regime. Based on FOM analysis, shown in Figure 14, the NACA 4415 met all requirements and is selected for the wing airfoil.



					
Figure of Merit	Weight	SD7062	NACA 4415	NACA M24	CLARK Z
$C_{l_{max}}$	40	3	4	2	3
C_{d_0}	20	3	3	2	2
t/c	15	3	3	2	2
C_{m_0}	10	3	2	5	2
Stall Characteristic	15	3	2	2	2
Total	100	3.00	3.15	2.30	2.40

Figure 14: Airfoil Selection

4.4.3 Aerodynamic Performance Predictions

The aerodynamic performance of the aircraft is evaluated at Reynolds numbers of 200,000 to 500,000, matching the predicted stall and cruise velocities. The aircraft lift curve slope is predicted using equations from Anderson¹². Hoerner¹³ and Raymer's⁷ methods are used for establishing drag buildup and utilized for preliminary predictions of drag performance of the selected configuration, as shown in Figure 15. Predicted aircraft lift and drag at a Reynolds number of 200,000 is shown in Figure 16. Flaps are also analyzed, using Etkin's¹³ method, as they help increase lift and decrease wing area. While keeping weight penalty in mind, flaps are optimized for a minimum increase in drag which results in an increase in C_L of .0164 per degree.

Component	C_{D0}	% of Total
Wing	0.0170	37%
Pods (2)	0.0124	27%
Fuselage	0.0088	19%
Stabilizers	0.0036	8%
Landing Gear	0.0025	6%
Doors	0.0015	3%
Total	0.0458	100%

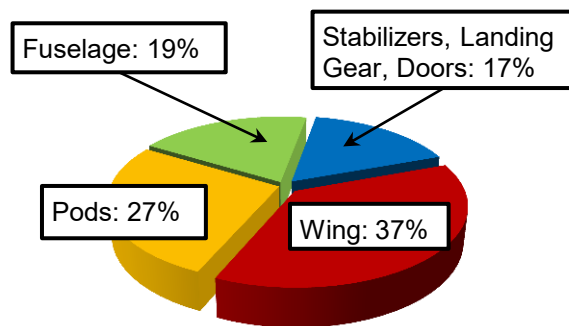


Figure 15: Drag Build Up

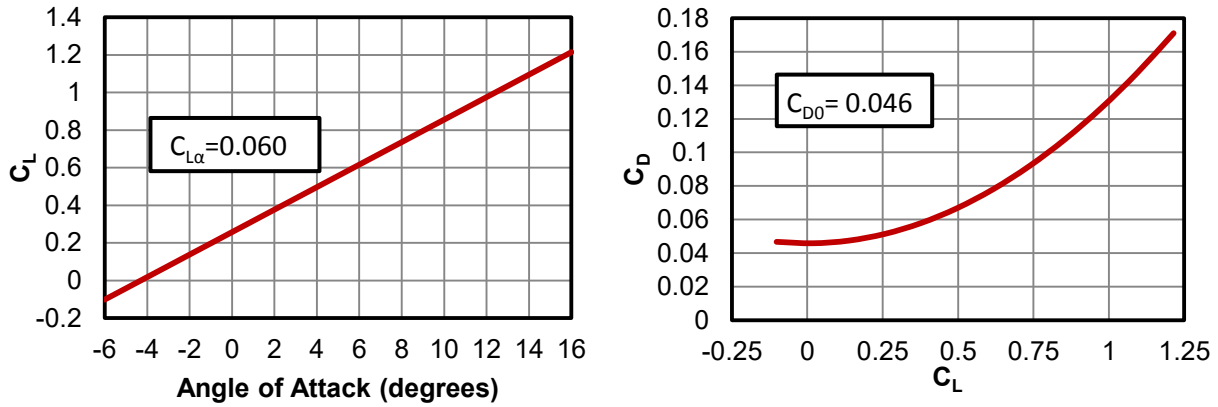


Figure 16: Predicted Lift Curve Slope and Drag Polar

4.5 Stability and Controls

The stability and control group is responsible for ensuring that the aircraft is both stable and controllable in all flight conditions. It is also responsible for ensuring that the aircraft has the control authority to perform all necessary maneuvers and for sizing all servos to actuate the control surfaces.

4.5.1 Stability and Controls Model

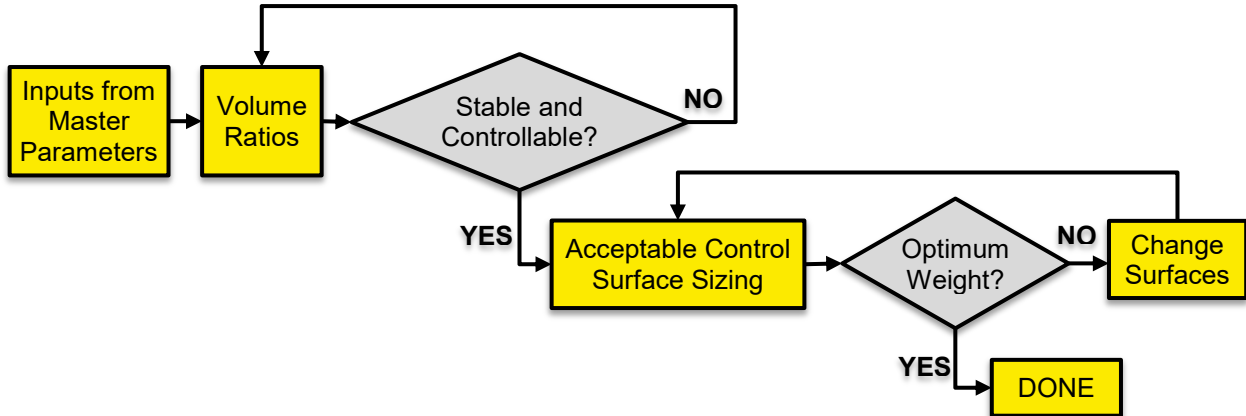


Figure 17: Stability and Control Design Process

The critical stability and control design parameters are listed below:

- **Static Margin:** Past reports show that DBF airplanes have had static margins between 5% and 20%^{3,4,5,6}. Also, having a smaller static margin will make the plane more responsive to elevator deflection, saving weight in servos and hinges. After analysis, a static margin of 6.5% is selected for M1 and 10% for M2 and M3
- **Center of Gravity:** The center of gravity (CG) needs to be placed properly with respect to the neutral point so that the aircraft remains stable. The selected configuration of the aircraft places



the CG close to the aerodynamic center (AC) for all missions. This allows for smaller stability surfaces, as the wing is almost stable on its own.

- **Tail Sizing:** The tail's main purpose is to keep the airplane longitudinally and laterally stable. Also, the surfaces must be large enough to house an effective elevator and rudder.
- **Control Surface Sizing:** The control surfaces are sized to provide enough control on the aircraft, while not being so large that they add unneeded weight or strain on the aircraft.
 - **Elevator:** The elevator must be large enough to trim the aircraft in all flight conditions. Using suggested values from Raymer⁷, the elevator should be 40% of the horizontal tail. However, as the static margin is small, the plane can be controlled with a smaller elevator than suggested. Figure 18 shows the trim plots for the aircraft.

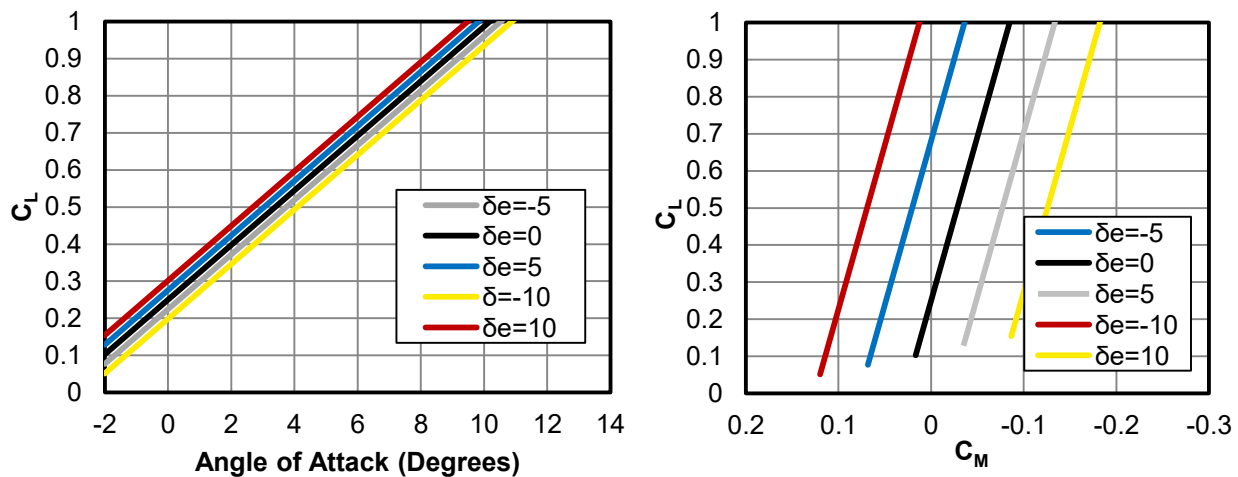


Figure 18: Trim Plots

- **Rudder:** The rudder must have enough authority to keep the aircraft on the runway during takeoff and steer it toward the runway during landing. This is especially critical due to the windy conditions common in Wichita, KS. Using the suggested values from Raymer⁷ while considering the possibility of high crosswinds, the rudder is 40% of the vertical tail.
- **Ailerons:** The ailerons are sized to roll the aircraft in all of the turns and to aid in the water dump if necessary. Using methods from Raymer⁷, the ailerons are sized to approximately 20% of the chord and approximately 40% of the span. This is dependent on the location of the ailerons. As the ailerons are moved outboard they can be made smaller, but this causes heightened risk of aileron reversal from wing twist. Since outboard ailerons are selected, requiring 2 servos, flaps are used with no weight penalty.



4.5.2 Stability and Control Performance Predictions

Stability and control derivatives are calculated using equations from Roskam¹⁴ and Etkin¹⁵ and confirmed using AVL⁹. These parameters are validated in wind tunnel testing and flight testing.

		Wind Angle Derivatives	
		$C_{M\alpha}$	$C_{L\alpha}$
		-0.0083	0.060
Control Surface Derivatives		$C_{n\beta}$	$C_{\xi\beta}$
$C_{\xi\delta a}$	$C_{n\delta a}$	0.031	-0.028
-0.0045	0.00012	Rate Derivatives	
$C_{L\delta f}$	$C_{M\delta f}$	C_{Lq}	C_{Mq}
0.016	-0.0055	0.11	-0.081
$C_{\xi\delta e}$	$C_{M\delta e}$	C_{np}	$C_{\xi r}$
0.0052	-0.010	-0.0003	0.0014
$C_{\xi\delta r}$	$C_{n\delta r}$	$C_{\xi p}$	C_{nr}
-0.00032	-0.0039	-0.0069	-0.00070

Figure 19: Stability and Control Derivatives (per degree)

The dynamic modes of the aircraft are analyzed using the linear approximation from Etkin¹² and checked using AVL⁹, then validated through flight testing. Figure 20 shows that the aircraft is dynamically stable in all modes other than the spiral mode. This mode is slightly unstable but can be corrected with pilot input. Flight testing demonstrated that the aircraft is stable and controllable.

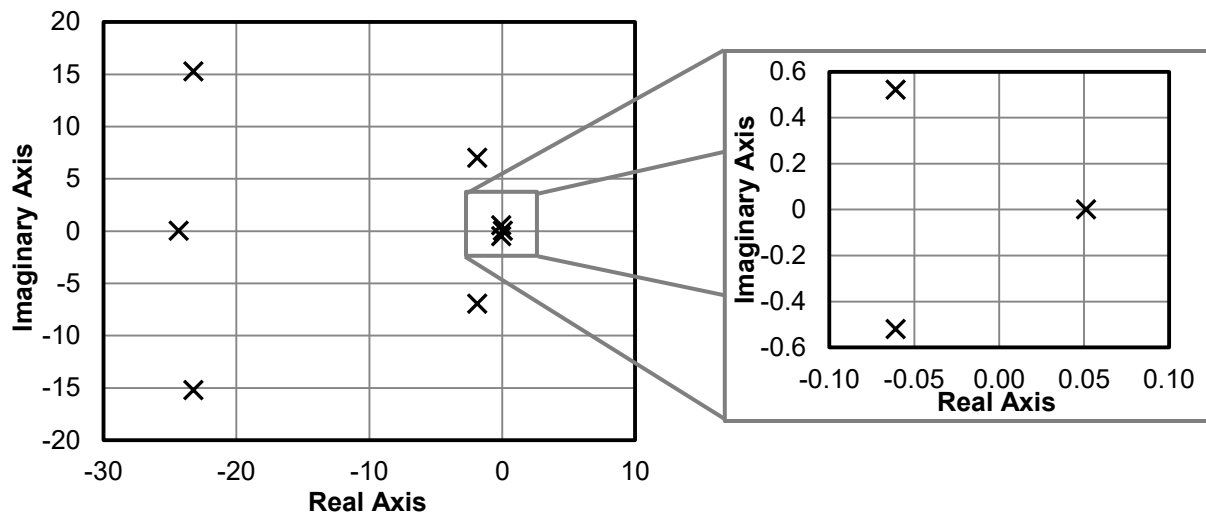


Figure 20: Aircraft Root Locus Plot



4.6 Propulsion

The propulsion group selects the motor, propeller, and battery pack. The group first creates a list of components with desirable performance characteristics from initial estimates. The group then uses analysis methods to find battery packs that yield adequate performance characteristics for each motor and propeller combination. Once these cases are analyzed, the combination resulting in maximum score is selected.

4.6.1 Propulsion Model

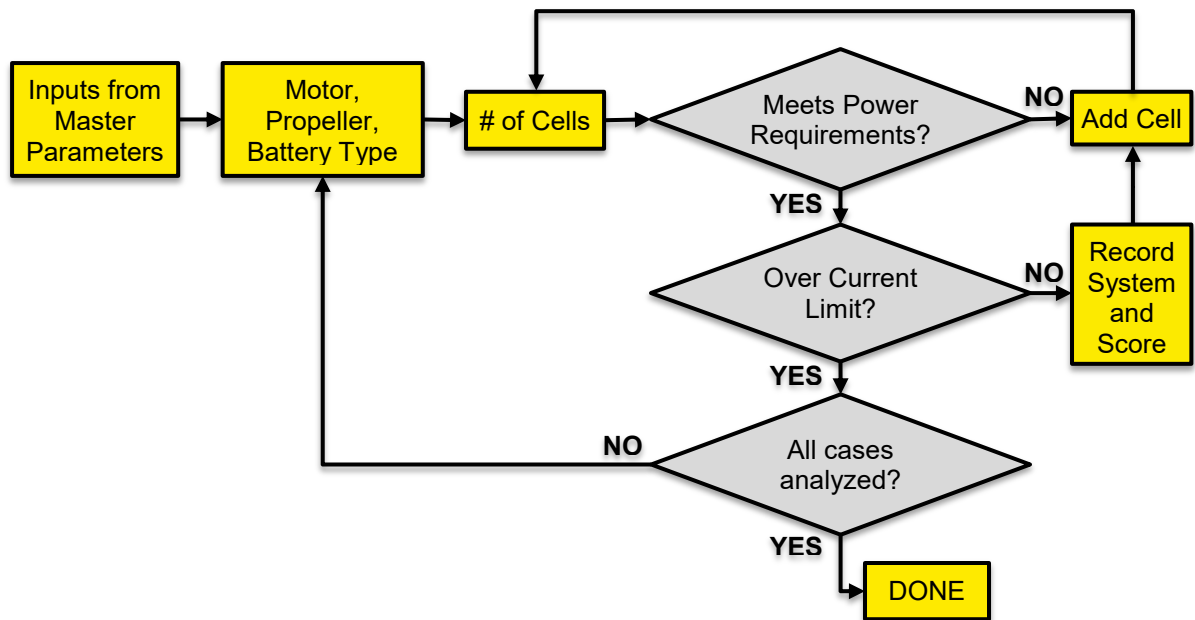


Figure 21: Propulsion Design Process

The mission objectives yield the following propulsion system requirements:

- M2 & M3 – High thrust is required on takeoff to reach takeoff velocity in 100ft
- M3 – High excess power is required to climb to 100m (328ft) altitude at a reasonable rate
- M2 – Low current draw is required at cruise to complete the mission without the need for higher capacity batteries and satisfy the requirement of a 20A fuse
- M1 – Low current draw and high speed at cruise is important, but not at the cost of weight

4.6.2 Propulsion System Constraints

There are several important constraints in the design of the propulsion system. The most important constraint to the system is weight. Using more than necessary increases the RAC. Therefore, it is important to give a high regard to weight for any component of the propulsion system. Using historical weight build ups^{3,4,5,6}, the aircraft has set preliminary limits of 0.16lb for a motor, 0.56lb for the battery



pack, 0.031lb for the propeller, 0.075lb for the ESC, and 0.013lb for the fuse. The entire propulsion system is limited at 0.84lb total.

4.6.3 Propulsion Sizing

First, power required is determined for each part of each flight. The most important power cases are shown to be cruise for each mission and takeoff for M3. The power required for takeoff is a product of thrust required and takeoff velocity as shown by Anderson¹². The power required for cruise is based on the drag at the desired cruise velocity. The power required for each of these cases is shown in Figure 22. The power required for takeoff is considerably higher than the power required for any of the cruise cases. Since the cruise velocities are satisfactory for completing the missions, M3 takeoff becomes the primary driver for system sizing. After the power required values are determined, a typical propeller efficiency of 50% and typical electrical component efficiency of 80% are assumed for a total system efficiency of 40% and the battery power required is determined. The initial battery pack and motor sizing can be completed using this power.

Case	PR Aircraft (W)	PR Batteries (W)
M1 Cruise	23.2	57.9
M2 Cruise	33.4	83.4
M3 Cruise	32.3	80.7
M3 Takeoff	81.4	204

Figure 22: Mission Specific Power Required

4.6.4 Propeller Analysis

The propeller diameter and pitch are selected for each individual mission. For M1, the total flight weight of the aircraft determines that takeoff performance is not problematic, therefore higher pitch propellers are considered in order to maximize cruise velocity. For M2 and M3, the takeoff weights determine that takeoff thrust is the main concern. For this reason, a large diameter, low pitch propeller is ideal. A range of propeller pitches and diameters are analyzed using the JavaProp¹⁶. Using a constant shaft power input, the thrust performance for each propeller are used to model a takeoff roll, and it determines which diameters and pitches had the best takeoff performance. A 12x6 propeller is selected for M2 and M3. The selection based on M1 cruise is a 10x10 propeller. Figure 23 shows the power available (PA) for each propeller as well as the power required (PR) for their appropriate missions.

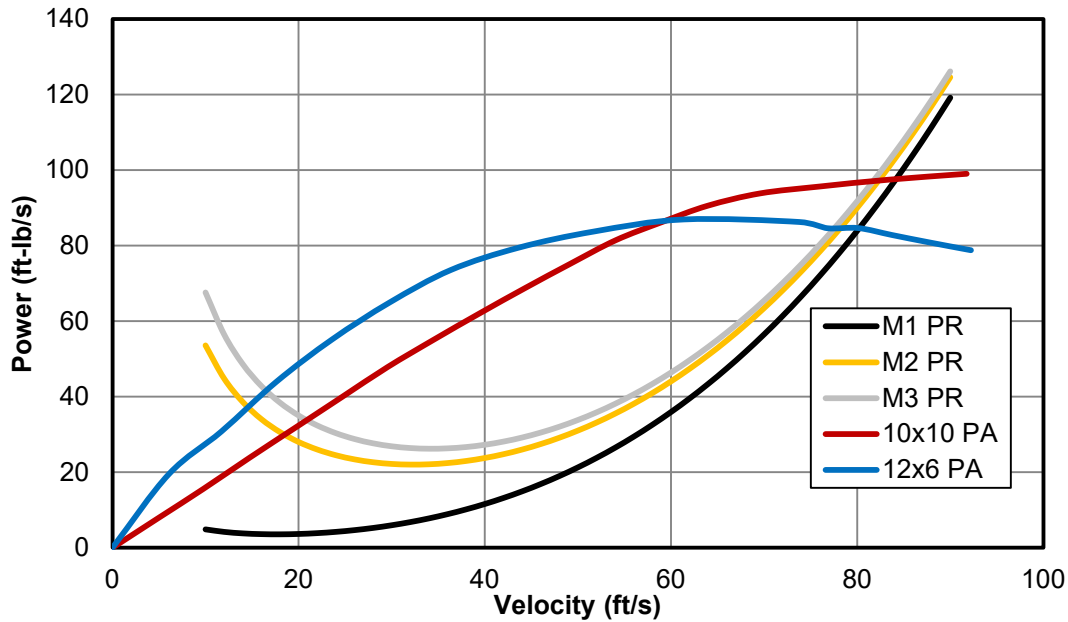


Figure 23: Power Available - Power Required

4.6.5 Battery Analysis

NiMH batteries are chosen over NiCad because they have a higher energy density and they are not prone to suffering the memory effects that can affect NiCad cells. Under demanding current conditions, battery voltage drops below the nominal 1.2V/cell. Thus, the calculations are completed using a value of 1V/cell. The true capacities are also not as high as the rated capacities at high discharge rates. The reduced capacity must be taken into account in mission analysis to ensure that the aircraft can complete the mission without running out of energy. Battery testing shows that the amount of difference between rated capacity and true capacity is not consistent across different manufacturers or even across different cell sizes from the same manufacturer. This is kept in mind during the selection process.

The selected battery pack had to meet several requirements:

- Must provide enough electrical power to the motor to meet the M3 takeoff distance requirement
- Must provide enough capacity to complete each mission
- Must provide the current demanded by the motor without large voltage drop or damage to the batteries

Different battery combinations that can provide the necessary power are shown in Figure 24.



Battery Type	Capacity (mAh)	Weight Per Cell (lb)	Current (A)	# of Cells	Power (W)	Pack Weight (lb)
KAN 400	400	0.017	6	34	204	0.57
Tenergy 1800	1800	0.057	24	9	216	0.51
Elite 1500	1500	0.051	20	10	200	0.51
Elite 2000	2000	0.068	20	10	200	0.68

Figure 24: Battery Pack Configurations

4.6.6 Motor Analysis

The motor is sized at a basic level based on the power required. Assuming that the system has an overall efficiency of 0.4, it shows that the motor must be rated for at least 205W of burst power, and a constant power of at least 85W. Since the propeller is relatively large for the power rating of the motor, a relatively low KV motor must be used keep the current draw low enough. After this, motor weight must be considered and kept to a minimum. There should be a certain correspondence between weight and maximum motor power, but the considered brands have shown a better power-to-weight ratio. Other characteristics of the motor must be kept in mind, such as maximum current and voltage, but they are primarily considered in overall system analysis when a better estimation of current draw is calculated. The motors considered, based on the preliminary analysis, are shown in Figure 25.

Motor Concepts	Continuous Power (W)	KV (rpm/volt)	Weight (lb)	Max Current (A)
Rimfire .10	333	1250	0.16	30
Scorpion 22mm 2215/1131	210	1131	0.14	20
Dualsky XM 3530CA-14	250	1000	0.16	24
Dualsky XM 2834CA-10	260	870	0.15	20

Figure 25: Motor Concepts

4.7 Structures

The structures group is responsible for the design and sizing of all structural components. The structure must be able to withstand all flight loads, landing loads, and the wingtip test, while keeping the RAC low. The structures group works closely with the aerodynamics group to ensure that aerodynamic considerations do not incur large weight penalties. The design process begins by selecting a load-bearing element configuration. Then the structural analysis tool, described in §4.7.7, is used to size the structural elements in order minimize weight and meet strength requirements. Lastly, manufacturing considerations are addressed to ensure that the design is feasible.



4.7.1 Structures Model

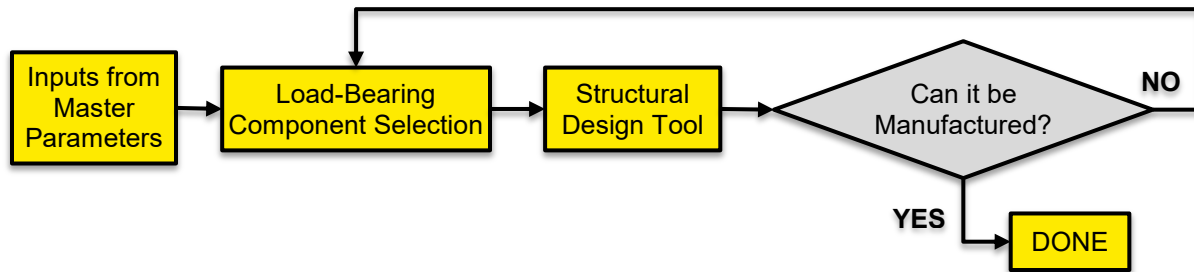


Figure 26: Structural Design Process

Material selection in the layout is driven by a combination of manufacturing and mission requirement concerns. Load-bearing elements are sized using an advanced structural analysis tool developed by WSU's DBF team.

The critical structural design parameters are listed below:

- **Part Count:** Minimizing part count reduces additional weight from the adhesives required to assemble the structure. Minimizing part count also lessens the number of joints, which are typically areas of structural weakness in aircraft designs.
- **Material Selection:** Materials with high specific strength are essential for a competitive aircraft design. However, manufacturing concerns with small or delicate pieces must be considered.
- **Multipurpose Structural Elements:** Designing structural elements to serve multiple purposes also serves to minimize weight by decreasing part count and reducing the size of non-structural components.

4.7.2 Structural Layout and Load Paths

The layout of the aircraft must accommodate the span-loaded water and passenger restraints in outboard portions of the wing. Furthermore, the number of joints in the water-bearing portion of the wing must be minimized in order to keep the structure watertight. The primary load paths of the chosen design are a composite front spar assembly, a balsa aft spar, and a wrapped carbon fiber composite tail boom. The selected layout with load paths is shown in Figure 27.

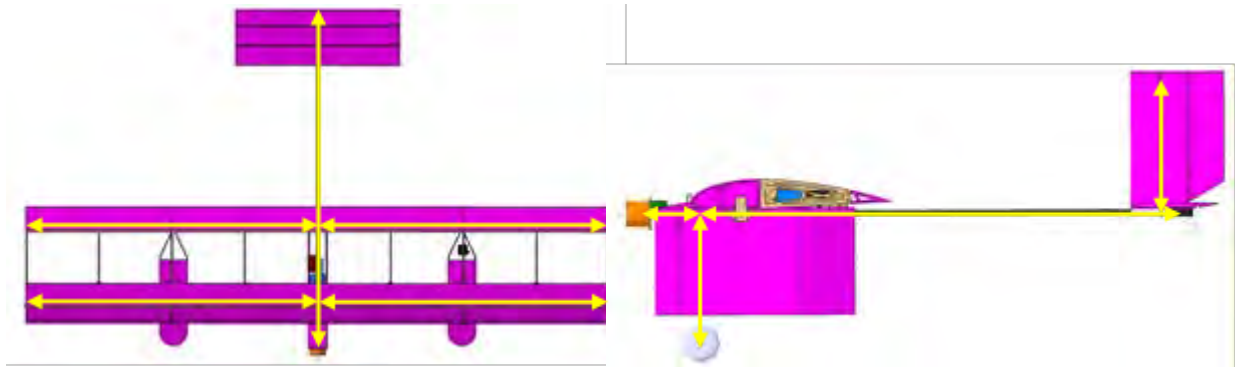


Figure 27: Structural Load Path

4.7.3 Material Selection

The majority of the aircraft structure consists of balsa and extruded polystyrene foam. These materials have desirable characteristics for aircraft construction on this scale and have well-documented properties. Most of these material properties are confirmed by basic testing in the material selection process. Balsa wood has high specific strength and keeps component sizes reasonable. Foam does not have the best axial strength properties, but is strong enough to resist shear loads, maintain spar cap separation, and airfoil geometry. Carbon fiber composite is the material of choice for the landing gear and tail boom due to its excellent specific strength and rigidity.

4.7.4 Wing Design

The wing design consists of 3 distinct sections. The first section consists of a two-cell front spar assembly reinforced with 2 balsa spar caps on the ends of the center shear web. The configuration choice to span-load the water requires a box spar to contain the water without incurring a large weight penalty. The foam cells serve to contain the water, resist transverse shear loads, and constrain deflection of the spar caps. The second section consists of traditional balsa and MicroLite™ cover construction. There is a balsa aft spar at the 80% chord location. This design has reduced coverage with MicroLite™, which decreases the risk of sagging. With the desired placement of the block payload structures, ribs at the quarter span points are necessary. Nine total ribs are used, giving a rib spacing of 6.7in. The ribs are fitted with large lightening holes to reduce weight since the ribs' primary function is to maintain airfoil geometry. The center section is fitted with cross struts to prevent the aft spar from translating with respect to the front assembly. The final section forms the trailing edge and consists of a hollow foam shell attached to the aft spar. The ailerons consist of hollow foam pieces secured to the aft spar by tape hinges. The layout of wing structural elements is illustrated in Figure 28.

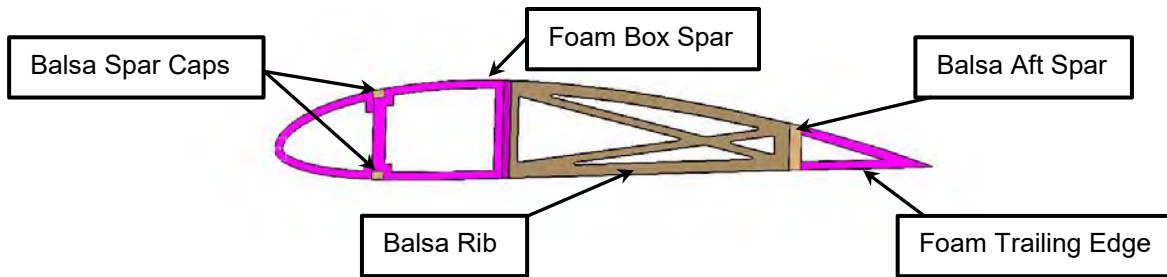


Figure 28: Wing Structural Cross Section

4.7.5 Fuselage Design

Span-loading is only effective in reducing structural loads if all payloads are span-loaded. To accomplish this, the two pods on the outboard sections of the wing are substituted for the traditional fuselage in order to reduce loads due to the blocks. The water payload is span-loaded in the wing.

The center fuselage only serves to hold the electronics. The pods are constructed of a balsa framework with XPS foam shells to contain the blocks in the mold lines of the aircraft. The cradle assembly consists of several balsa beams fitted together with dovetail joints to maximize strength by optimizing the grain direction of the balsa.

4.7.6 Boom, Tail, and Landing Gear Design

The aircraft design uses a carbon fiber composite rod to connect the center fuselage to the traditional empennage and the motor. The traditional empennage consists of symmetric NACA 0006 airfoils cut from XPS foam reinforced with thin carbon fiber spars for bending rigidity.

The landing gear has been a significant contributor to structural weight in past years. This weight must be kept to a bare minimum for a competitive aircraft. The landing gear consists of light weight carbon fiber rods attached to the pods and lightweight wheels on the end. The gear is mounted to the wing with a breakaway joint in order to minimize damage to the wing in the event of a crash. The axle for the wheels is made of thin aluminum tube that serves as a connection to the carbon fiber rods. The tail has an aluminum skid to raise the tail off the ground and set the desired angle of attack for takeoff.

4.7.7 Critical Load Analysis

The critical design loads for the aircraft are calculated using Schrenk's approximation¹⁷ for the lift distribution and the estimated weight distribution in each flight condition of the aircraft to determine which conditions exert the most stress on the airframe. The shear and bending moment distributions can be found using methods described in Hibbeler¹⁸ by integrating the distributed load to find the shear load, then integrating the shear load to find the bending moment. Analysis also includes the effects of torsion moments. These results are then combined with the loads from the wingtip test and landing loads to determine the design loads. The wingtip test and the landing loads for M2 define the critical loads for the



design process. The landing loads largely depend on pilot skill and wind conditions, so some allowance must be made for landing inconsistencies.

The structure is sized to the wingtip test loads because they are the largest static loads on the aircraft. These loads are used to establish maximum load factors for turning and landing maneuvers. This leads to maximum load factors of 6 for M1 turning, 2.6 from M2 turning, 6 for M3 turning, and 4 for M2 landing. These are consistent with the load factor requirement for M1 turn performance. The limiting factor for these load cases is the shear load for all missions because the bending moment does not exceed the wingtip test. When the structure is sized to these loads, the safety factor is 1.25 or greater in bending for the wing tip test and flight conditions. The maximum wing tip deflection for the wing tip test is 1.35in. This figure is calculated using Castigliano's Theorem¹⁹.

The shear and bending moment load profiles for critical conditions are shown in Figures 29 and 30.

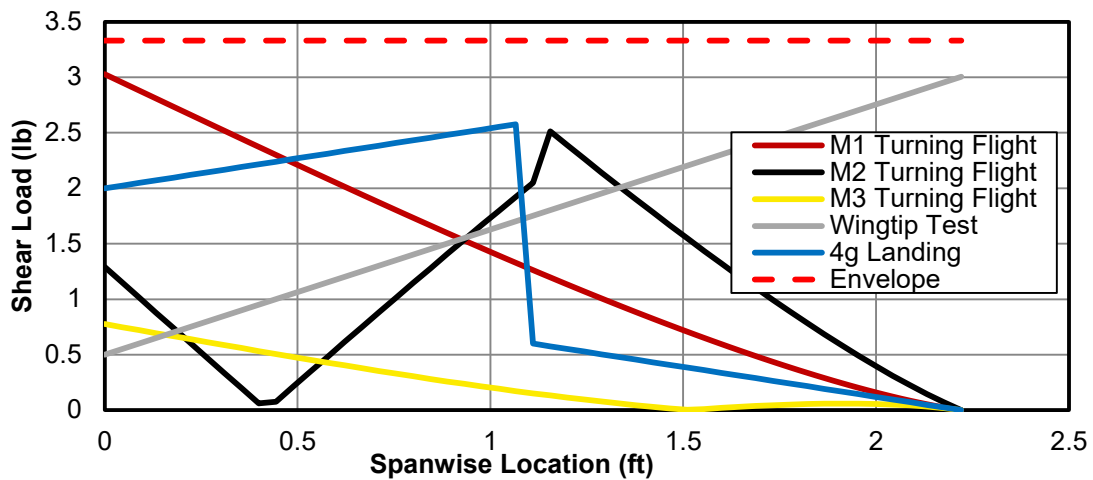


Figure 29: Shear Load Envelope

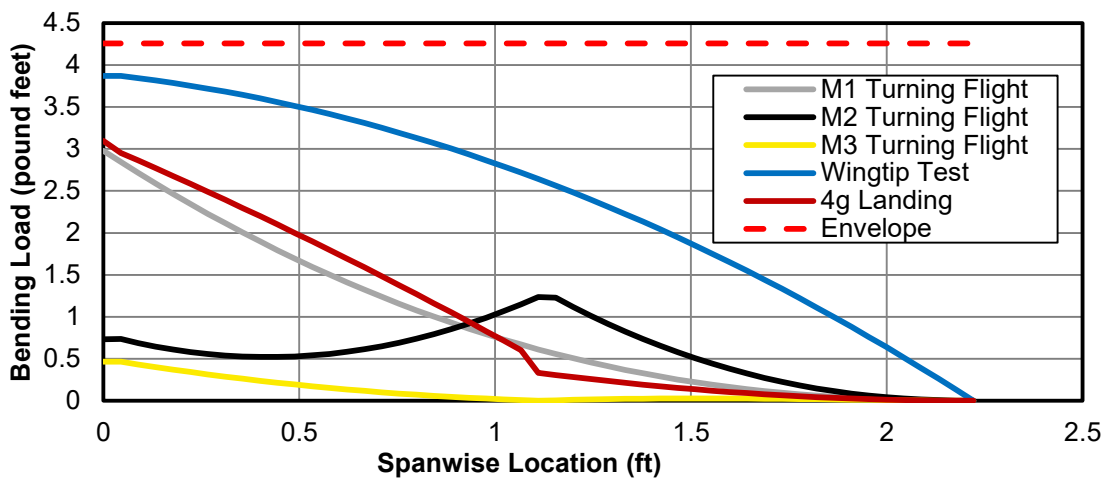


Figure 30: Bending Moment Load Envelope



In order to size the load-bearing elements to these load profiles, the WSU DBF team develops an advanced structural analysis tool to analyze stresses in load-bearing elements and optimize the structural design. The analysis tool is based on methods described in Allen¹⁹ with small modifications. It allows the load-bearing elements to be treated as independent elements with bending and torsional rigidity. The elements are allowed to deform independently, while the torsional rigidity contribution is taken from the difference in the deflection slopes and the torsional rigidity of all elements. The bending and torsional rigidity are entered as functions of span wise location for each element. For each element, the solver then imposes compatibility equations on the loads applied to each element that the sum of the shear, bending, and torsion loads are equal to the loads applied on the wing. The solver identifies the loads on each spar by solving the nonlinear compatibility equations. This solver is utilized in all flight conditions to determine maximum stress in each element. The elements are then sized to maximum allowable stress with a small safety margin, which saves a considerable amount of weight in the spar caps and aft spar. This analysis also allows the use of thinner walls for the box spar and leading edge than initially expected. The accuracy of the structural test predictions outlined in §7.4 validates the structural analysis tool.

4.7.8 Landing Analysis

The unconventional nature of the configuration requires specific analysis of landing loads. The landing gear is located next to the pods in order to minimize landing loads transmitted to the wing. The gear is also located as far aft on the chord line while still maintaining acceptable ground handling stability to minimize torsion loads. A dynamic model of the landing loads shows that the shear and torsion moments exceed all flight and wingtip test loads in the event of a rough landing, so the wing components are sized to a landing load factor of 4.

4.7.9 Weight Buildup

The weight of the aircraft is calculated using the density of the involved materials. The current wing design aims to minimize weight by maximizing simplicity. These estimates allow for 20% adhesive weight in the wing and 10% adhesive weight throughout the rest of the aircraft. The estimates for the major components of the aircraft are shown in Figure 31.



Component	Weight (lb)
Wing	0.388
Boom	0.056
Fuselage	0.013
Pods	0.050
Tail	0.031
Gear	0.063
Motor Mount	0.031
Dump Valves	0.063
Total	0.693

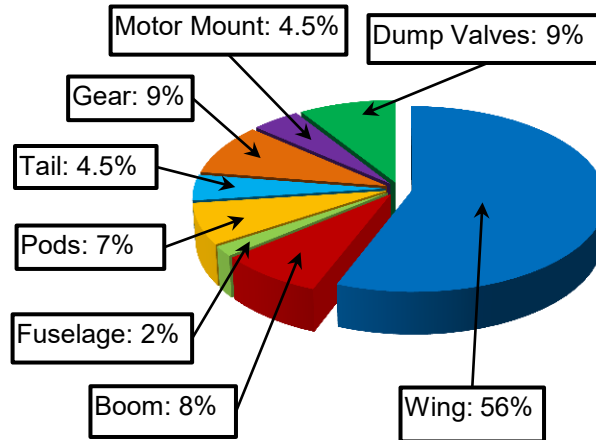


Figure 31: Weight Build Up

4.8 Aircraft Flight Performance

Performance Parameter	M1	M2	M3
$C_{L_{cruise}}$	0.059	0.21	0.24
$C_{L_{max}}$	1.1	1.1	1.1
$C_{L_{takeoff}}$	0.81	0.82	0.82
e	0.75	0.75	0.75
C_{D0}	0.046	0.046	0.046
L/D_{cruise}	1.3	4.2	4.8
L/D_{max}	8.0	8.0	8.0
Climb Rate (ft/s)	24	8.4	7.3
W/S	0.40	1.4	1.5
Cruise Speed (ft/s)	78	64	64
Stall Speed (ft/s)	17	32	36
Maximum Endurance (s)	276	336	252
Empty Aircraft Weight (lb)	1.6	1.6	1.6
Gross Weight (lb)	1.6	5.35	6
Total Flight Score	2.2	2.2	3.1

Figure 32: Aircraft Flight Performance

5.0 Detail Design

Following completion of preliminary design, focus shifts to system integration and optimization. Electrical components are selected, component connections are finalized, and assembly considerations are addressed.



5.1 Dimensional Parameters

The figure below shows the dimensional parameters of the aerodynamic system and control surfaces.

		Horizontal Stabilizer		Aileron	
		Span	15.0in	Span	13.3in
Wing		Chord	5.04in	% of Chord	20.0%
Span	53.3in	Area	75.6in ²	Max δ_a	25°
Chord	10.7in	Airfoil	NACA 0006	Rudder	
Aspect Ratio	5	Incidence	-3°	Span	6.96in
Wing Area	569in ²	Vertical Stabilizer		% of Chord	40.0%
Airfoil	NACA 4415	Span	6.96in	Max δ_r	25°
Static Margin M1	6.50%	Chord	5.04in	Elevator	
Static Margin M2/M3	10.0%	Area	35.1in ²	Span	15.0in
Incidence	0°	Airfoil	NACA 0006	% of Chord	30%
Fuselage		Pod		Max δ_e	25°
Length	10.7in	Length	10.7in		
Width	1.80in	Width	0.24in		
Height	1.80in	Height	5.76in		

Figure 33: Dimensional Parameters

5.2 Structural Characteristics

Aircraft weight must be minimized in order to be competitive. To that end, the detail design phase focuses on removing excess material. This effort focuses on the wing, pods, and landing gear since they are the largest contributors to structural weight.

5.2.1 Wing

The wing structure is designed to withstand the load profiles outlined in §4.7.7. WSU DBF's structural analysis tool is used to size load-bearing elements and stresses in these elements. Figure 34 shows the maximum stress experienced by each component along the wingspan normalized by the maximum allowable stress.

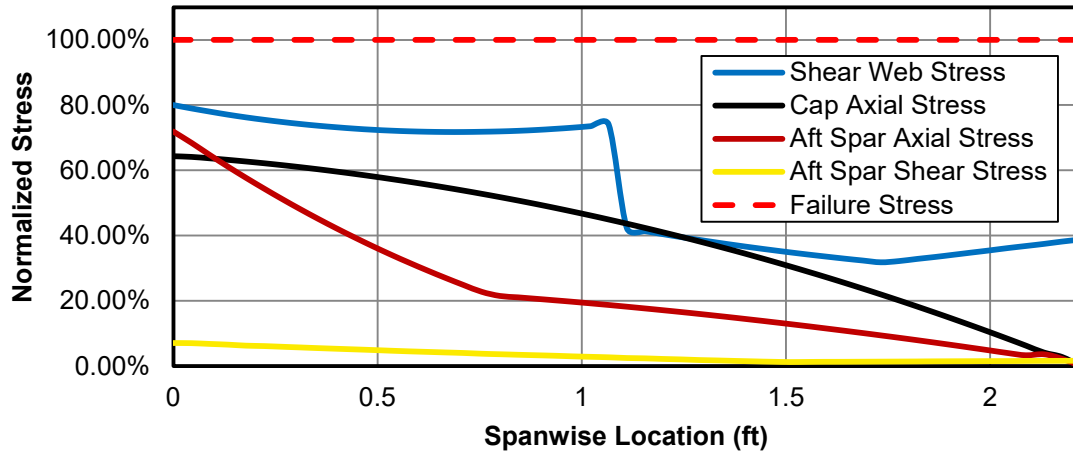


Figure 34: Normalized Stress Plot

For the wing tip test and flight loads, maximum stresses do not exceed 80% of the maximum allowable stress, leaving a small margin of safety. The uncertainty in the structural design is from the landing loads.

5.3 System Design, Component Selection and Integration

5.3.1 Payload Systems

For M2, the aluminum block payload will be stored in pods located under the wings next to the landing gear. The blocks are contained by a balsa framework which resists all loads induced by the blocks. This framework is initially covered in MicroLite™ to minimize weight, but this method has undesirable drag characteristics. The balsa framework is now assisted by foam shells that prevent the blocks from translating while simultaneously reducing drag.

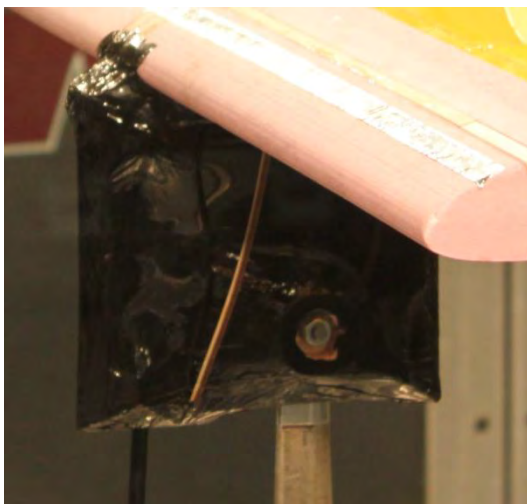


Figure 35: Comparison of Pod Designs



The rules outline requirements for how the block payload may be restrained within the aircraft. These requirements are summarized in Figure 36. The 1/4in tall contact points of balsa and foam that restrain the movement of the blocks, along with maintaining the required spacing are shown in Figure 37.

Spacing Requirements	Restraint Requirements
1/2in fore/aft around/between	Carried internally
1in side-to-side between rows of passengers	No more than 2in x 1/4in tall contact points between the passenger and the restraints
Not required to have space between outside passenger and aircraft body	Passenger may sit on the floor
1in on one side if passengers in a single row	Reasonable provisions for restraints may protrude within the required open space

Figure 36: M2 Payload Mission Requirements

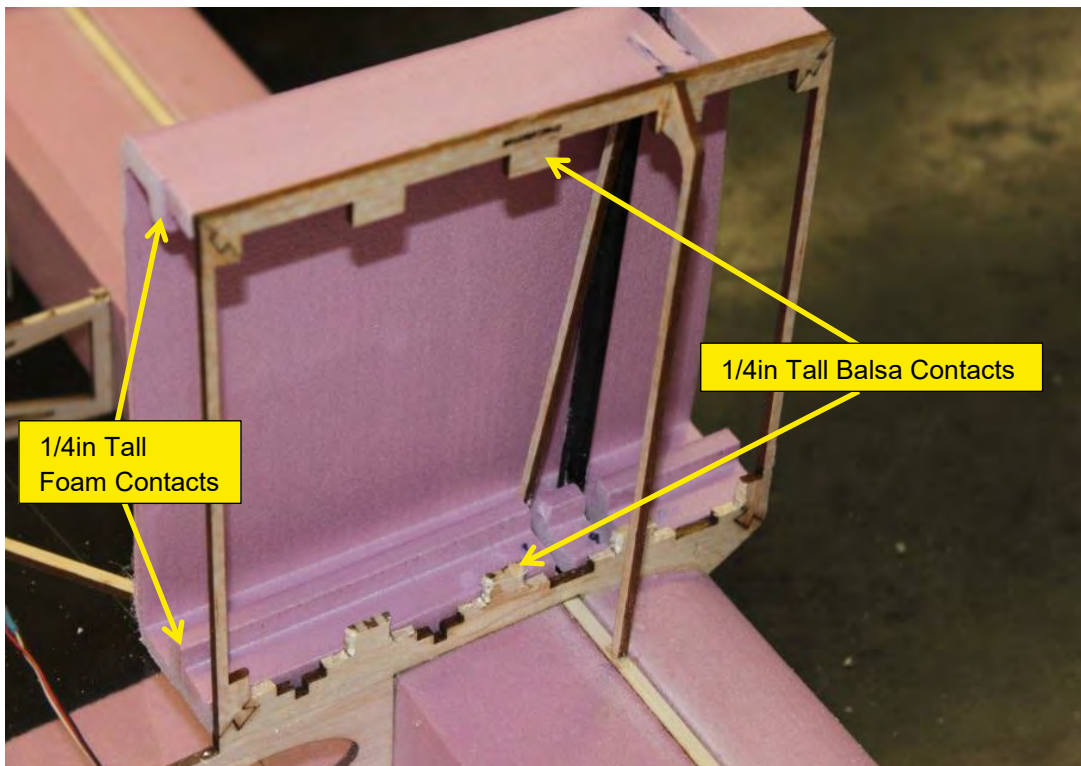


Figure 37: Pod Shown Inverted and Without Fairings

In addition to the spacing and restraint requirements for the M2 payload, the blocks must also be loaded into the aircraft by one person within a 5 minute time limit. In order to accomplish this, the internal payload bay of each pod is accessed by opening the external panel of the pod fairing.



For M3, the water payload is span-loaded in the main box spar in the wing, similar to fuel storage in the wing of full-scale aircraft. The spar is made of a single piece of foam in order to maintain the integrity of the container. The drop mechanism consists of a single servo which, when activated, pulls pins that open two dump valves located on the wingtips. Placement of one dump valve on each wingtip prevents water from becoming trapped in the wing during flight. Several dump valve designs are considered and tested. The chosen dump valves consist of balsa plates lined with weather stripping to prevent leakage. The pins are balsa sticks that fix the dump valves to end plates on the wing. When the altimeter circuit detects that the aircraft has reached 100m (328ft), the servo mounted on the center rib of the wing pulls the pins via two braided monofilament cords running through the ribs in the wing. The valve design and weather stripping sealant is shown in Figure 38.

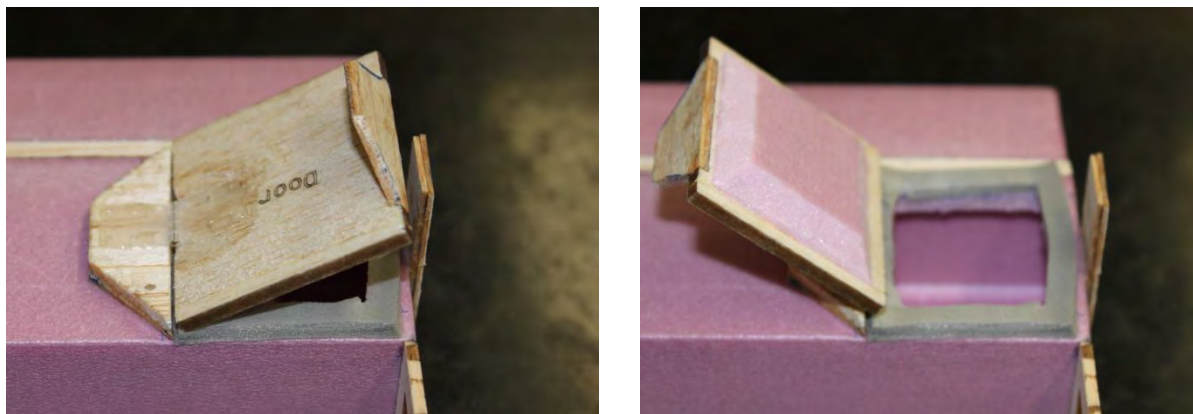


Figure 38: Dump Valve Showing Foam-to-Weather Stripping Seal

5.3.2 Propulsion System Integration

Once an initial sizing is done for each component of the propulsion system, the best components are evaluated using a total system analysis tool. The propulsion parameters are combined with aerodynamic power required data to predict flight velocities and climb rates. This data can then be used to predict flight scores. Competitive components identified in the preliminary search are evaluated in this tool based on the process outline in §4.6.1.

In this process, each successful system is recorded along with its score. Some systems are seen to require a higher ratio of current-to-voltage than is typical, suggesting that the motor is trying to spin too large of a propeller. When spinning the manufacturer's largest recommended propeller, most motors draw a current of approximately 3 times the voltage. When the motor is running outside its typical range of current-to-voltage, there are concerns about the system's ability to perform as predicted. For this reason, systems drawing over a current-to-voltage ratio of 3 are not considered. Motors operating in a ratio less than 3 tend to be far enough below their maximum current that an additional battery cell could be added safely to increase flight performance. Selected combinations are shown in Figure 39.



Motor	Motor KV	Prop M1	Prop M2, M3	Battery	Cells	Predicted Score
Dualsky XM2834CA-10	870	APC E 10x10	APC E 12x6	Elite 1500	10	5.47
Rimfire .10	1250	APC E 10x10	APC E 11x6	Tenergy 1800	9	5.46
Scorpion 2215-1121	1121	APC E 10x10	APC E 12x6	Tenergy 1800	9	5.22
Dualsky XM3530CA-14	1000	APC E 10x10	APC E 12x6	Elite 1500	9	5.51

Figure 39: Propulsion Scoring

During detailed design, the selected propulsion system is tested in the WSU 3x4ft wind tunnel. The tested system draws a lower current than expected, so the battery power provided to the motor is less than necessary. Two options are considered to increase power. Use a higher KV motor, and increase the voltage supplied from the batteries. An ideal replacement motor in the desired weight range is not readily available, so 2 battery cells are added to provide the necessary voltage increase.

The new propulsion system consists of a Dualsky XM3530CA-14 1000KV motor, an 11 cell Elite 1500mAh battery pack, an APC-E 10x10 propeller, and an APC-E 12x6 propeller. This motor weighs 0.16lb and is rated at 250W max power. The battery pack weighs 0.56lb and supplies a maximum current of up to 20A. A 10x10 propeller is selected for high speed performance in M1, while a 12x6 propeller is selected for high takeoff and climb thrust in M2 and M3.

5.3.3 Electronic Component Selection

Weight is the driving factor in all electronic component selection. Figure 40 compares 4 options of potential servos, with the Futaba S3114 selected as the lightest weight servo that meets the maximum expected hinge moment of 15.72oz-in. A Spektrum AR600 is chosen as the receiver because it is the lightest option that has 6 channels and is compatible with DBF fail safe requirements. The receiver battery pack is 4 KAN 180mAh cells, which provides the desired voltage with sufficient capacity while remaining lightweight. A Castle Creations Phoenix 25 ESC is the lightest model satisfying the current-draw requirement.

Servos	Weight (lb)	Torque @ 4.8v (oz-in)	Speed @ 4.8v (s/60°)
BMS-306	0.014	12	0.11
S3114	0.018	21	0.1
HS-65 HB	0.024	25	0.14
HS-81	0.036	36	0.11

Figure 40: Servo Selection



5.4 Aircraft Component Weight and CG Buildup

The weight and location of each component of the aircraft is shown in Figure 41.

Component	Weight (lb)	X (in)	Y (in)	Z (in)
Wing	0.284	3.56	0.00	0.372
Fuselage	0.019	0.504	0.00	-0.696
Motor Assembly	0.284	-2.60	0.00	0.00
Boom	0.041	11.6	0.00	-0.696
Pods	0.053	2.66	0.00	-5.30
Landing Gear	0.028	-0.873	0.00	-3.47
Empennage	0.084	25.6	0.00	0.828
Electronics	0.122	2.99	0.00	-0.420
Batteries	0.613	2.40	0.00	-0.996
Wire and Linkages	0.044	3.00	0.00	-0.384
Altimeter	0.013	-1.74	0.00	-0.120
Blocks	3.75	2.66	0.00	-3.47
Water	4.41	2.66	0.00	0.396
M1	1.58	3.16	0.00	-0.516
M2	5.33	2.81	0.00	-2.59
M3	5.99	2.80	0.00	0.156

Figure 41: CG and Weight Build Up

5.5 Flight Performance Summary

Figure 42 lists applicable performance parameters for each mission as determined by the design analysis. These parameters are compared to flight testing.

Performance Parameter	Mission 1	Mission 2	Mission 3
$C_{L_{cruise}}$	0.059	0.21	0.24
$C_{L_{max}}$	1.1	1.1	1.1
$C_{L_{Takeoff}}$	0.81	0.82	0.82
e	0.75	0.75	0.75
C_{D0}	0.046	0.046	0.046
L/D_{cruise}	1.3	4.2	4.8
L/D_{max}	8.0	8.0	8.0
Climb Rate (ft/s)	24	8.4	7.3
W/S	0.40	1.4	1.5
Cruise Speed (ft/s)	78	64	64
Stall Speed (ft/s)	17	32	36
Total Flight Time (s)	280	340	250
Empty Aircraft Weight (lb)	1.6	1.6	1.6
Gross Weight (lb)	1.6	5.35	6.0

Figure 42: Flight Performance Parameters



5.6 Mission Performance Summary

The figure below details the propulsion system performance for each portion of each mission. In the most demanding mission, a maximum of 1100mAh capacity is consumed, while testing has shown that the batteries have a usable capacity of 1200mAh, which leaves a reasonable excess for safety. Figure 43 shows the predicted scores for each mission and Figure 44 shows the total predicted competition score assuming a T_{avg} of 60 seconds.

M1	# of Segments	Velocity (ft/s)	Distance (ft)	Time (sec)	Current (mA)	Capacity Used (mAh)
<i>Takeoff</i>	1	16	90	5.8	25	40
<i>Climb</i>	1	47	77	1.6	22	10
<i>Cruise</i>	14	85	1000	160	17	760
<i>Turn 1eight0</i>	14	44	76	24	22	150
<i>Turn 360</i>	7	44	150	24	22	150
Total				220		1100
M2	# of Segments	Velocity (ft/s)	Distance (ft)	Time (sec)	Current (mA)	Capacity Used (mAh)
<i>Takeoff</i>	1	16	90	5.8	23	37
<i>Climb</i>	1	41	240	5.8	18	29
<i>Cruise</i>	6	71	1000	85	10	250
<i>Turn 1eight0</i>	6	44	120	16	19	83
<i>Turn 360</i>	3	44	249	16	19	83
Total				130		480
M3	# of Segments	Velocity (ft/s)	Distance (ft)	Time (sec)	Current (mA)	Capacity Used (mAh)
<i>Takeoff</i>	1	17	90	5.3	22	30
<i>Climb</i>	1	41	1800	45	19	240
Total				50		270

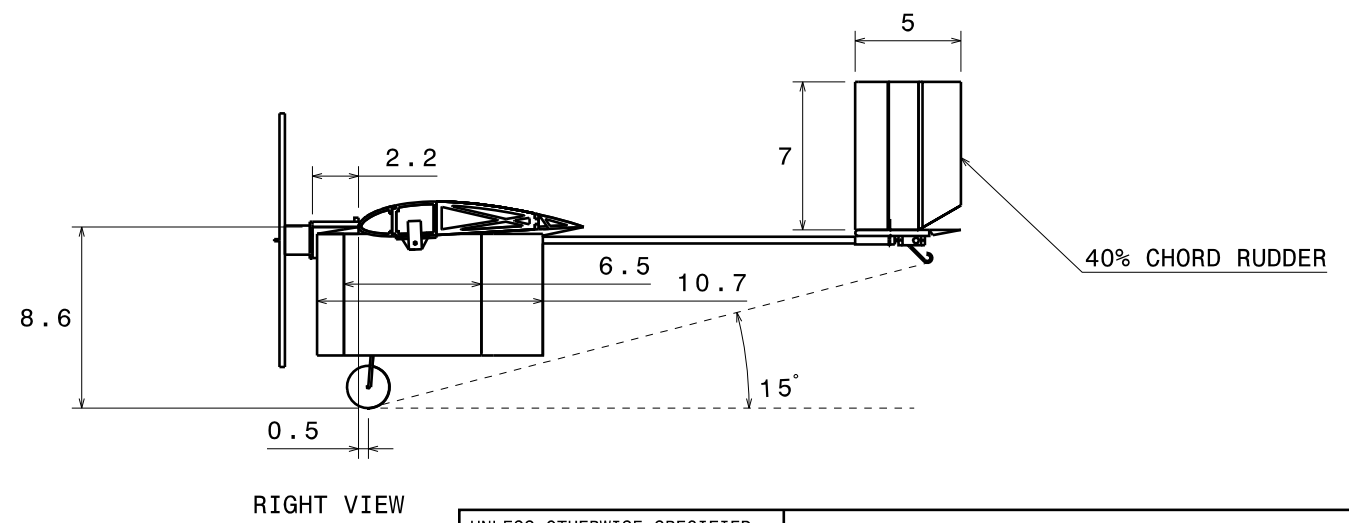
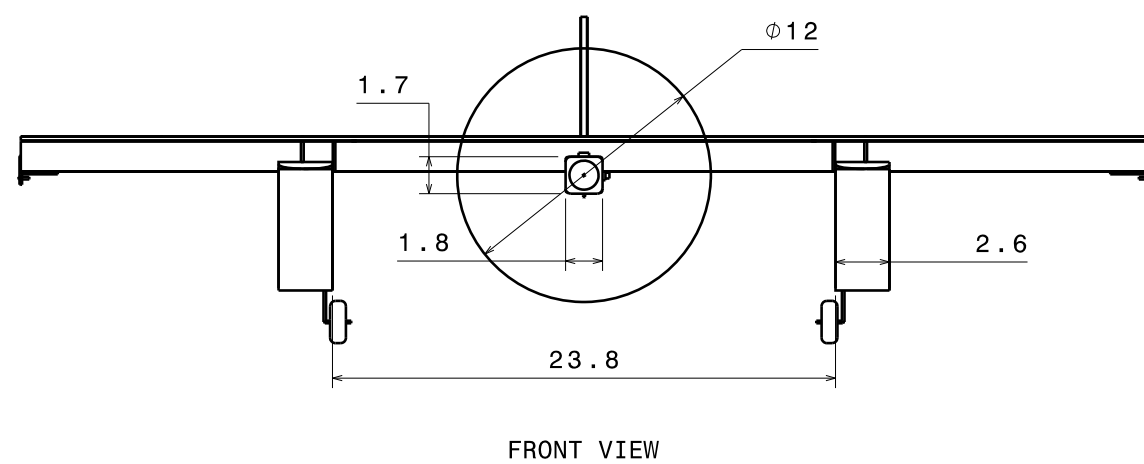
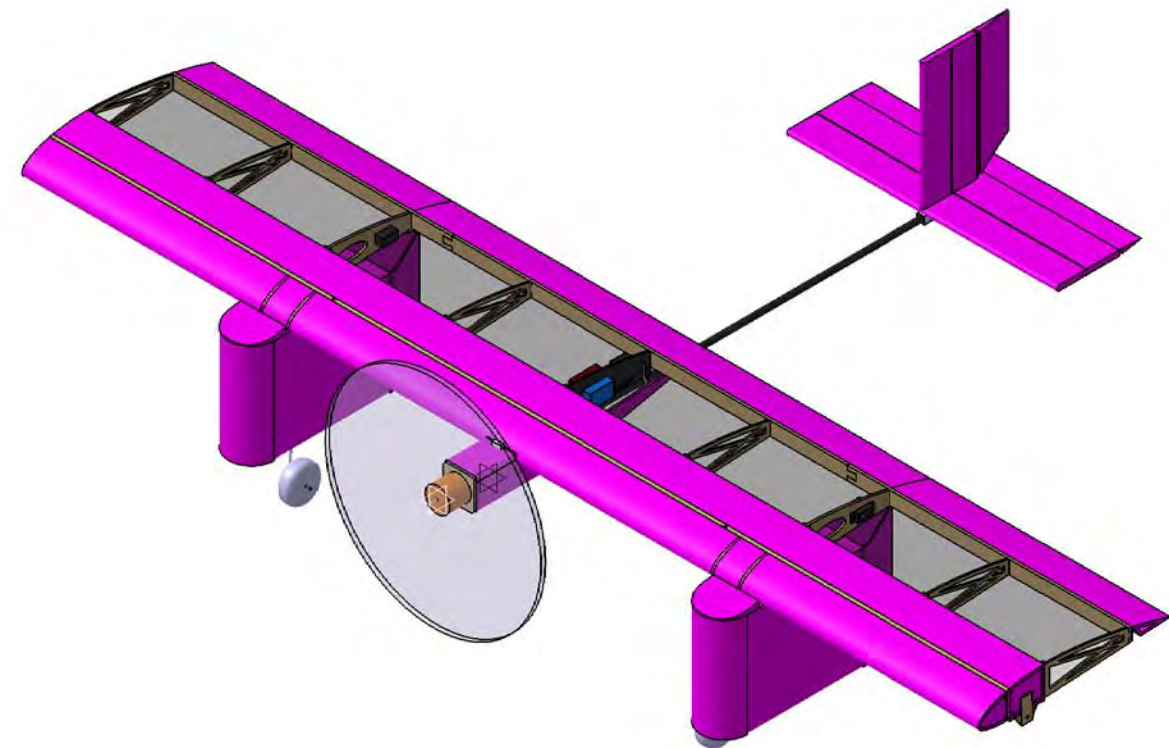
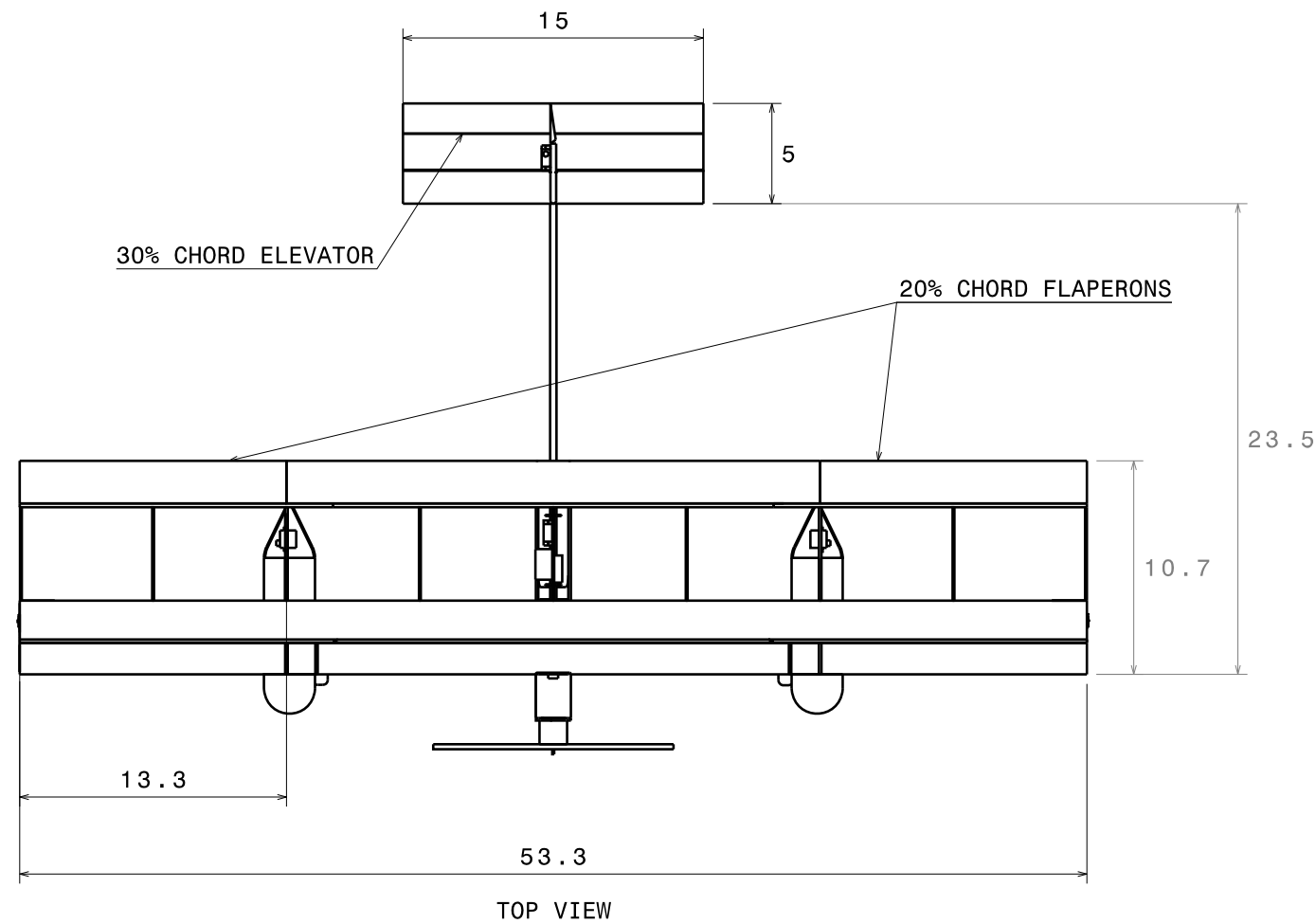
Figure 43: Mission Performance

M1	M2	M3	Flight	Report	Score
2.17	2.18	3.10	7.45	0.98	5.54

Figure 44: Total Competition Score

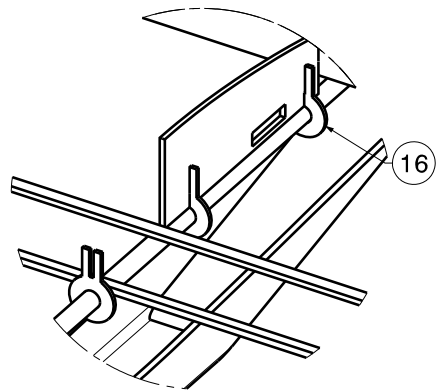
5.7 Drawing Package

The following drawing package includes dimensioned 3-view, structural arrangement, aircraft systems layout, and mission configuration drawings. All drawings are made using CATIA²⁰.

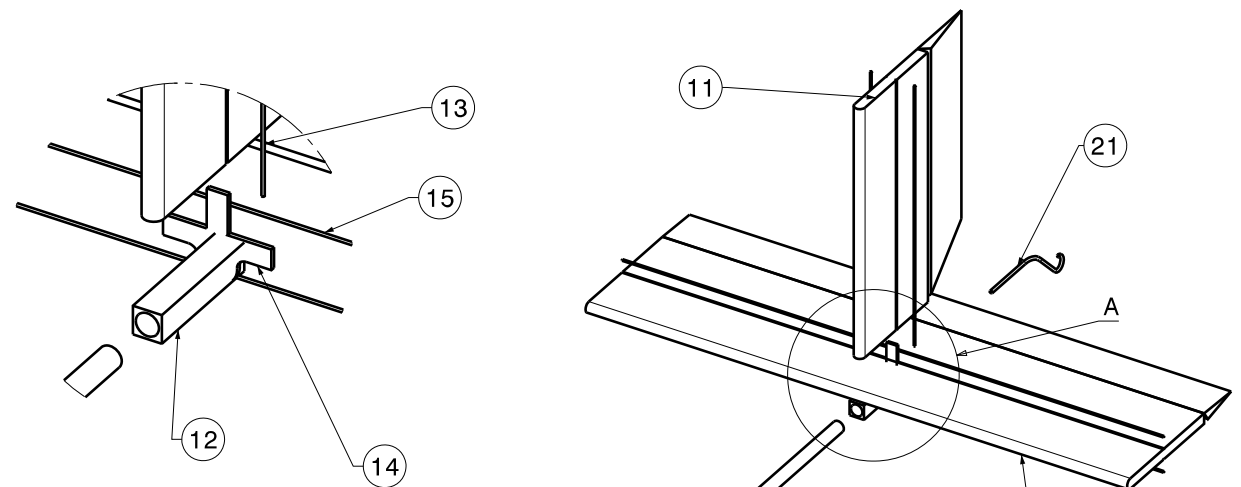


UNLESS OTHERWISE SPECIFIED ALL DIMENSIONS ARE IN INCHES TOLERANCES FOR: DECIMALS: .XX = ±.03 ANGLES: .X = ±.1		WICHITA STATE UNIVERSITY DBF TEAM 2011-2012		
DRAWN BY J. BREEDLOVE		DRAWING TITLE AIRCRAFT 3 VIEW		
DATE 2/28/2012		SIZE B	DRAWING NUMBER 2012-001	REV B
CHECKED BY G. SMITH	DATE 2/28/2012	SCALE NONE	PAGE 42 of 60	SHEET 1/4
DESIGNED BY WSU DBF	DATE 2/28/2012			

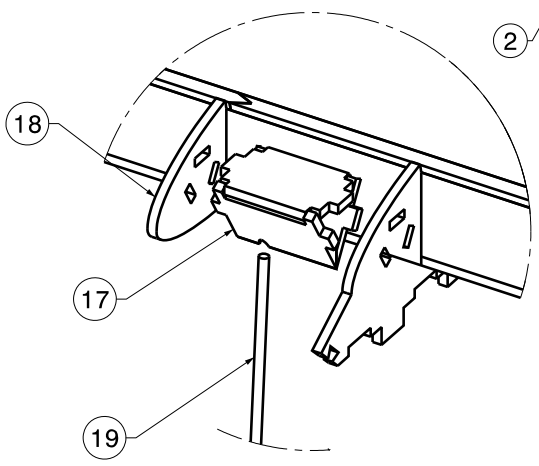
DETAIL B
BOOM TO FUSELAGE JOINT
 SPAR & LEADING EDGE
 HIDDEN FOR CLARITY



DETAIL A
TAIL JOINT ASSY EXPLODED VIEW
 HORIZONTAL STABILIZER HIDDEN FOR CLARITY



DETAIL C
LANDING GEAR JOINT ASSY
 EXPLODED VIEW
 LEADING EDGE HIDDEN
 FOR CLARITY



ENGINEERING BILL OF MATERIALS			
Part Number	Item	Qty	Material
1	FUSELAGE	1	XPS FOAM
2	MOTOR MOUNT	1	1/8 PLYWOOD
3	SPAR & LEADING EDGE	1	XPS FOAM
4	SPAR CAP ASSY	2	1/8 x 3/16 BALS
5	RIB	6	3/32 BALS
6	CENTRAL RIB	1	3/32 BALS
7	PAYLOAD SUPPORT RIB	2	1/8 BALS
8	AFT SPAR ASSY	1	3/16 BALS
9	TAIL BOOM	1	φ .30 HOLLOW CARBON FIBER
10	HORIZONTAL STABILIZER	1	XPS FOAM
11	VERTICAL STABILIZER	1	XPS FOAM
12	TAIL JOINT	1	XPS FOAM
13	VERTICAL STABILIZER SPAR	2	φ 1mm CARBON FIBER
14	TAIL JOINT PLATE	1	1/16 PLYWOOD
15	HORIZONTAL STABILIZER SPAR	2	φ 1mm CARBON FIBER
16	BOOM TO WING JOINT	3	1/16 PLYWOOD
17	LANDING GEAR JOINT ASSY	2	1/8 BALS
18	LANDING GEAR RIB	2	1/8 BALS
19	LANDING GEAR ROD	2	φ .28 HOLLOW CARBON FIBER
20	PAYLOAD CRADLE ASSY	2	1/8 BALS
21	TAIL SKID	1	φ 1/8 ALUMINUM
22	PAYLOAD POD FAIRING ASSY	2	XPS FOAM
23	PAYLOAD LATERAL SUPPORT	2	1/8 BALS
24	WHEEL	2	φ 1.25 FOAM

UNLESS OTHERWISE SPECIFIED
 ALL DIMENSIONS ARE IN INCHES
 TOLERANCES FOR:
 DECIMALS: .XX = ±.03
 ANGLES: .X = ±.1

DRAWN BY
J. BREEDLOVE
 DATE
 2/28/2011

CHECKED BY
G. SMITH
 DATE
 2/28/2011

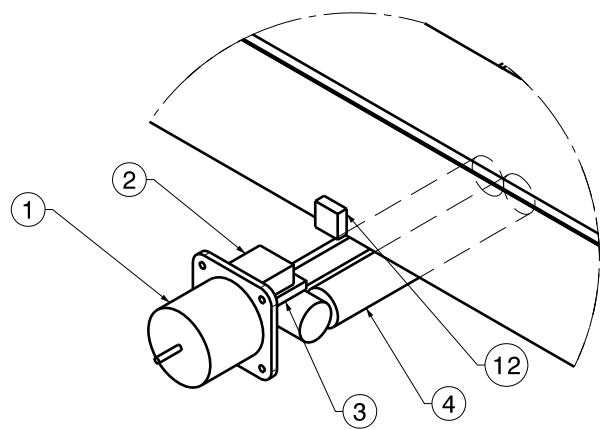
DESIGNED BY
WSU DBF
 DATE
 2/28/2011

WICHITA STATE UNIVERSITY
DBF TEAM 2011-2012

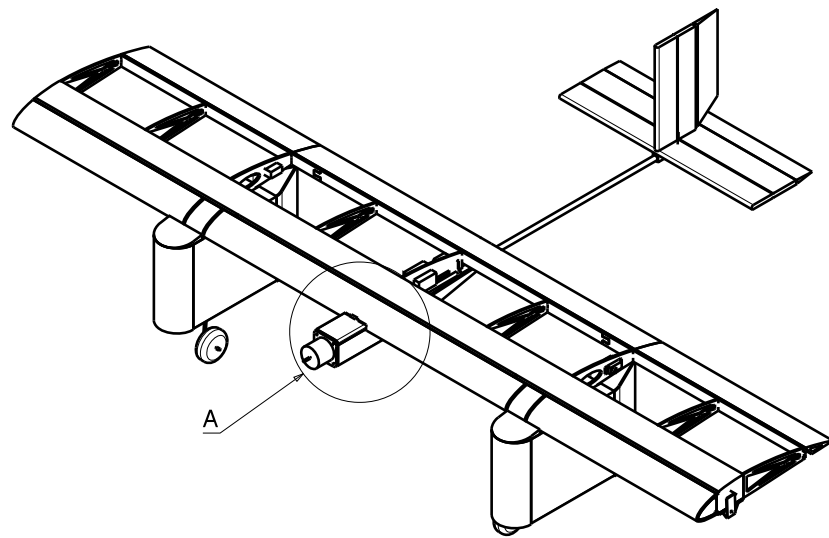
DRAWING TITLE
STRUCTURAL ARRANGEMENT

SIZE **B** DRAWING NUMBER **2012-002** REV **B**

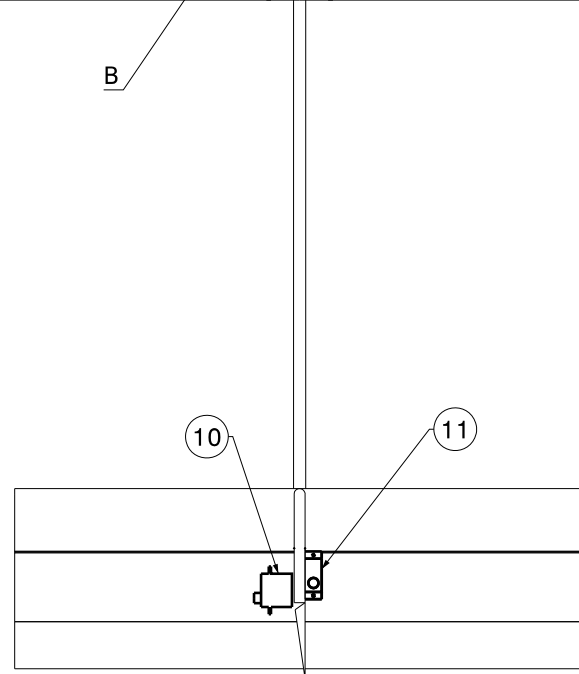
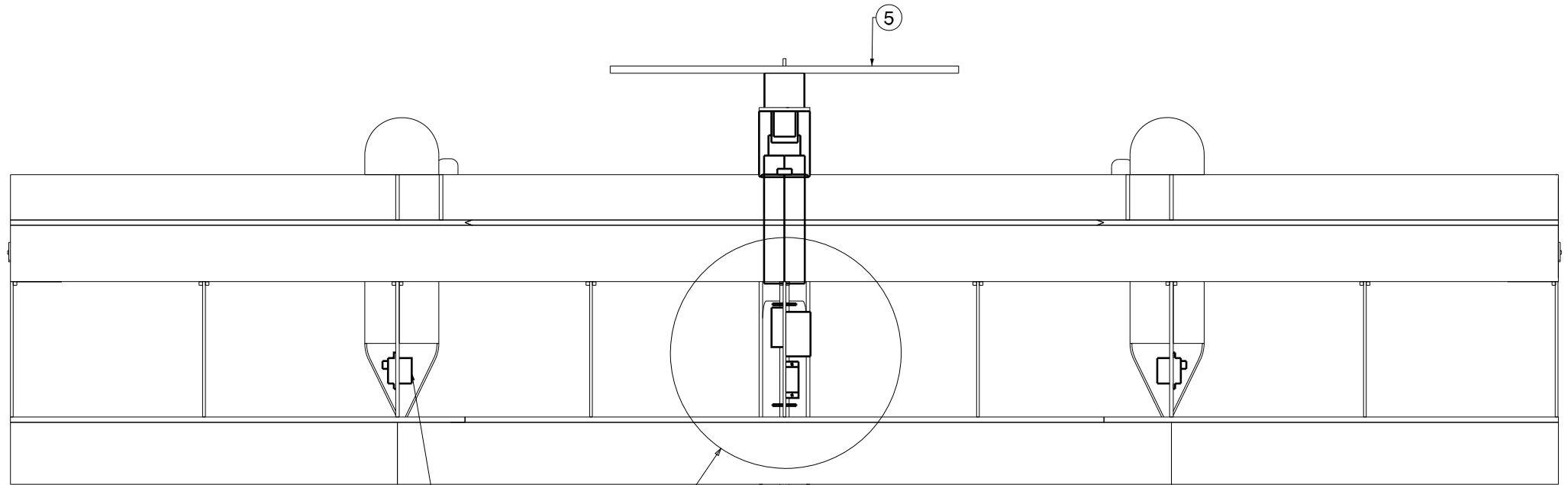
SCALE NONE PAGE 43 of 60 SHEET 2/4



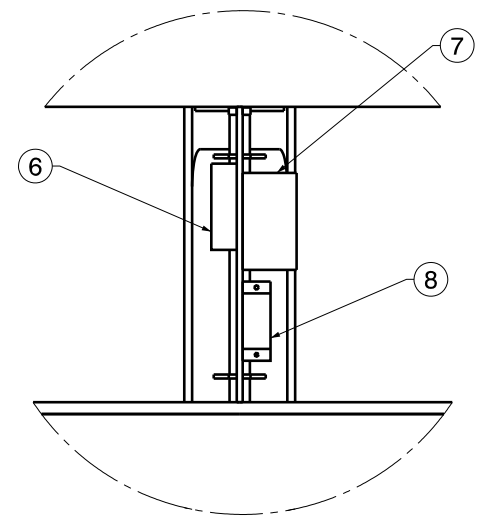
DETAIL A
PROPELLER AND FOAM FUSELAGE
HIDDEN FOR CLARITY



ISOMETRIC VIEW



TOP VIEW

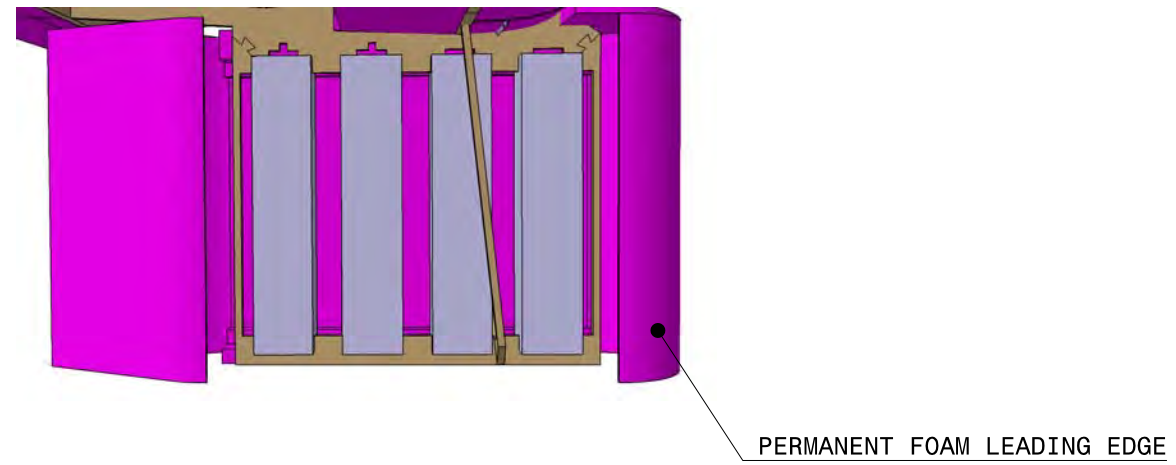


DETAIL B

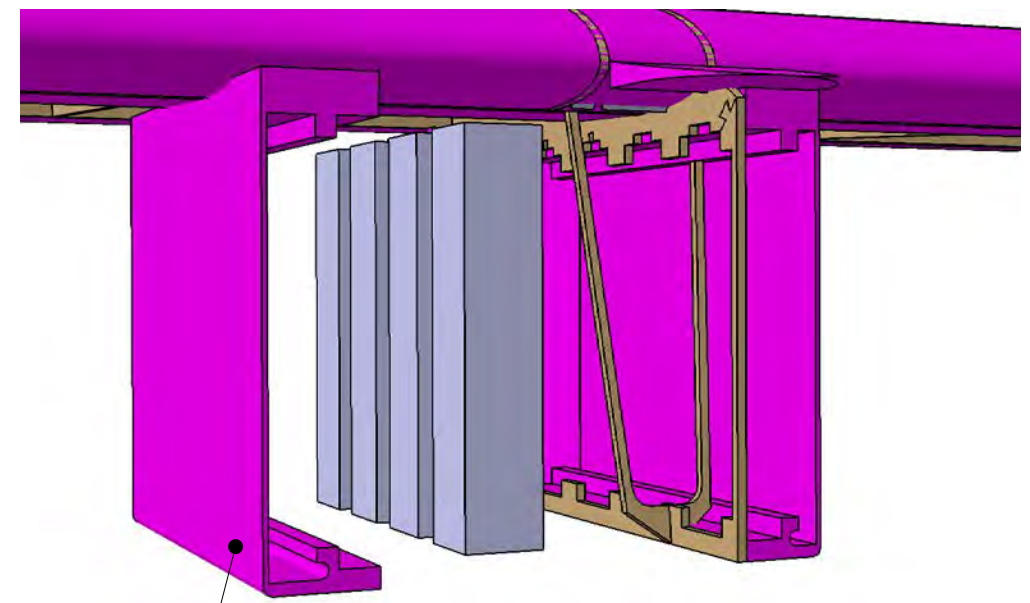
System Component List			
Part Number	Item	Source	Qty
1	MOTOR	DUALSKY XM3530CA-14	1
2	ALTIMETER CIRCUIT	SOARING CIRCUITS CAM-f3q	1
3	ESC	CASTLE CREATIONS PHOENIX 25	1
4	BATTERY	11X ELITE 1500mAh	1
5	PROPELLER	APC-E 12x6	1
6	RECEIVER BATTERY	4X KAN 250mAh	1
7	RECEIVER	SPEKTRUM AR600	1
8	PAYLOAD SERVO	FUTABA S3114	1
9	AILERON SERVO	FUTABA S3114	2
10	ELEVATOR SERVO	FUTABA S3114	1
11	RUDDER SERVO	FUTABA S3114	1
12	FUSE	20A LOW PROFILE MINI FUSE	1

UNLESS OTHERWISE SPECIFIED ALL DIMENSIONS ARE IN INCHES TOLERANCES FOR: DECIMALS: .XX = ±.03 ANGLES: .X = ±.1		WICHITA STATE UNIVERSITY DBF TEAM 2011-2012	
DRAWN BY J. BREEDLOVE		DATE 2/28/2012	
CHECKED BY G. SMITH		DATE 2/28/2012	
DESIGNED BY WSU DBF		DATE 2/28/2012	
DRAWING TITLE SYSTEMS LAYOUT		SIZE B	DRAWING NUMBER 2012-003
SCALE NONE		PAGE 44 of 60	REV B
SHEET 3/4			

M2 PAYLOAD ACCOMMODATION
ALUMINUM BARS



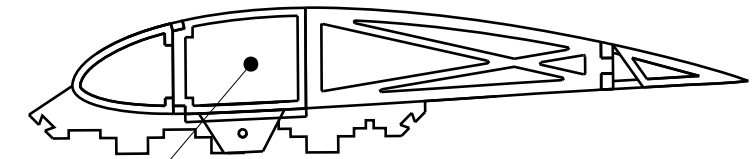
BLOCK PAYLOAD INSTALLED
VIEW FACING INBOARD
REMOVABLE FOAM OUTBOARD COVER NOT SHOWN



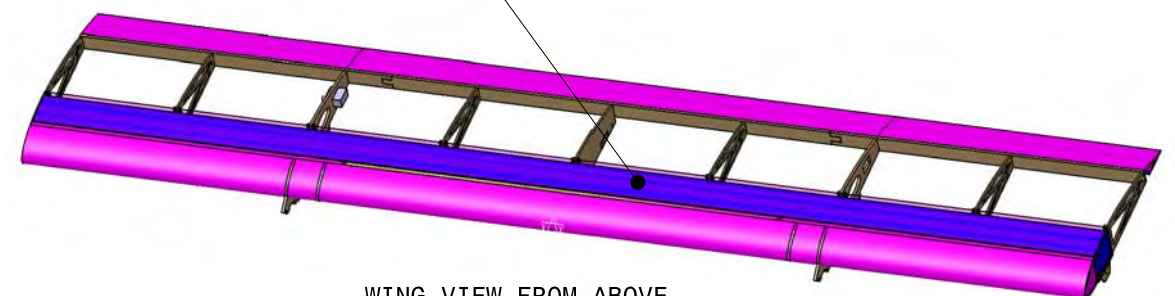
REMOVABLE FOAM COVER

BLOCK PAYLOAD EXPLODED
FRONT VIEW WITH REMOVABLE OUTBOARD COVER PULLED AWAY
PERMANENT FOAM LEADING EDGE NOT SHOWN

M3 PAYLOAD ACCOMMODATION
2L WATER



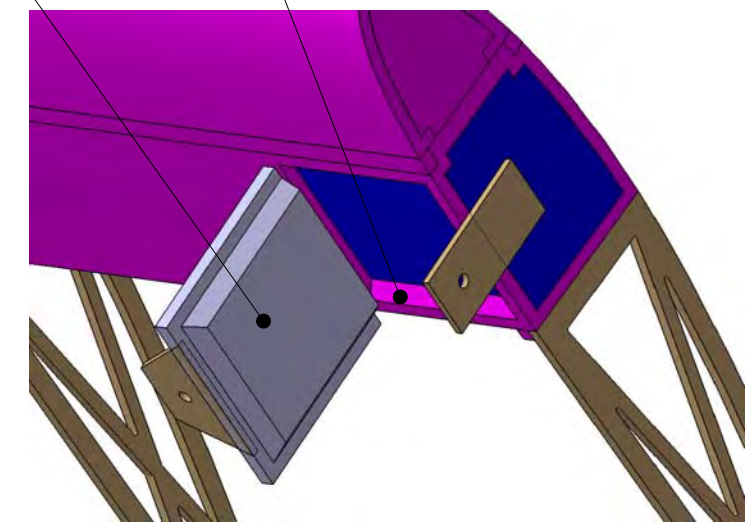
2L WATER PAYLOAD IN HOLLOW BOX SPAR WING SIDE VIEW



WING VIEW FROM ABOVE

WEATHER STRIPPING SEAL

WATER DROP DOOR OPEN



WATER DROP DOOR DETAIL VIEW

UNLESS OTHERWISE SPECIFIED
ALL DIMENSIONS ARE IN INCHES
TOLERANCES FOR:
DECIMALS: .XX = ±.03
ANGLES: .X = ±.1

WICHITA STATE UNIVERSITY
DBF TEAM 2011-2012

DRAWN BY J. BREEDLOVE		DATE 2/28/2012		DRAWING TITLE PAYLOAD ACCOMODATION	
CHECKED BY G. SMITH		DATE 2/28/2012		SIZE B	DRAWING NUMBER 2012-004
DESIGNED BY WSU DBF		DATE 2/28/2012		SCALE NONE	PAGE 45 of 60
				SHEET 4/4	REV B



6.0 Manufacturing Plan and Processes

For each aircraft prototype, a model is created in CATIA²⁰ prior to starting the manufacturing process. Drawings from this model are used as templates during manufacturing of the prototypes.

6.1 Manufacturing and Material Selection

To keep the aircraft as light as possible, choosing the best material and manufacturing method is of primary importance. These materials are compared with a FOM.

- **Solid Foam:** A solid foam block cut to shape with a CNC hot wire foam cutter. Non-essential material is removed by cutting out excess material from the center. This method has the benefit of having no joints, but suffers from excessive weight due to foam's relatively low specific strength
- **Balsa construction:** A balsa framework covered in MicroLiteTM in order to maintain external geometry. Pieces defining the shape of the component are cut from a balsa sheet with a laser cutter and are held together with thin balsa beams that maintain spacing between components. This method suffers in weight due to the number of joints, but is historically proven to be simple and reliable.
- **Carbon Fiber Composite:** Carbon fiber cloth laid over a mold, permeated with resin, and cured. Carbon fiber composite is strong. However, it is difficult to manufacture on a scale that does not make it too strong for this application. The manufacturing process is also difficult and time consuming.
- **Hybrid Composite:** Several pieces consisting of foam and balsa or carbon fiber. The foam is used to maintain geometry while balsa or carbon fiber is used to resist axial and bending loads. This can also be combined with elements of balsa and MicroLiteTM construction. WSU DBF incorporated the combined use of balsa and foam last year with significant success³.

The FOM criteria for material selection are detailed below:

- **Weight:** Weight is the primary scoring variable; therefore keeping weight down is of high importance.
- **Strength:** All structural elements are designed to resist loads.
- **Skill/Material requirements:** The available facilities are ill-suited for some build up methods.
- **Time to Build:** With the time constraint of the competition, the aircraft must be able to be rebuilt overnight.



6.1.1 Material Selection

The hybrid composite buildup method is most suitable for the aircraft. The box spar is made of a single piece of XPS foam with balsa spar caps. The ribs and aft spar are made of balsa. The tail boom is made of carbon rod and the empennage is comprised of foam and small carbon rods for rigidity.

Figure of Merit	Weight	Solid Foam	Balsa Construction	Carbon Fiber Composite	Hybrid Composite
Weight	40	2	3	2	4
Watertightness	25	4	2	4	4
Strength	15	2	3	5	4
Skill/Material Requirements	10	4	4	2	3
Time to Build	10	4	3	2	3
Total	100%	2.90	2.80	2.95	3.80

Figure 45: Material Selection

6.2 Manufacturing Schedule

Design validation and testing relies heavily on the timeliness of prototype manufacturing, thus a manufacturing schedule is used to track the progress of each prototype during the fabrication process. Figure 46 summarizes the timeline of manufacturing the aircraft prototypes for both ground and flight testing.

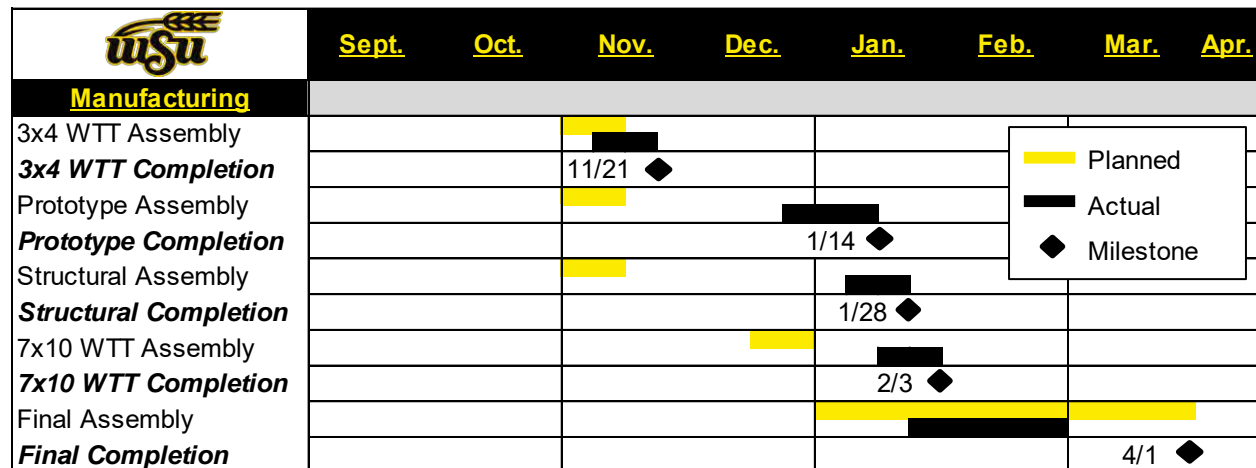


Figure 46: Manufacturing Schedule

6.3 Aircraft Manufacturing Process

Since most of the aircraft is made of a composite structure, the aircraft has a large number of parts that must be assembled quickly and accurately to satisfy design requirements. Several tooling jigs are designed in order to expedite the assembly process and improve build quality.



First, the ribs are secured to the spars by means of an assembly jig that ensures that the ribs are kept in line. This also increases the efficiency of adhesive use since the joints are held in their proper position. Once forward spar assembly and aft spar are secured to the ribs, the ribs are broken off the jig along perforated cuts. The rib jig is shown below in Figure 47.

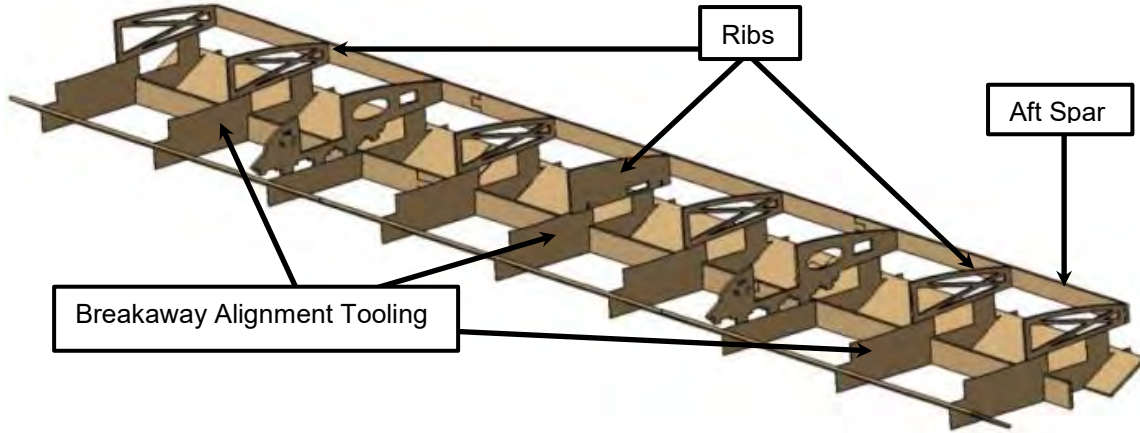


Figure 47: Breakaway Rib Jig

The trailing edge jig is used to expedite attaching the foam trailing edge to the aft spar. The jig consists of balsa ribs lined with foam to prevent damaging the foam piece. The trailing edge piece is inserted into the jig and the jig is pressed to the aft spar.

7.0 Testing Plan

All aircraft systems are tested independently to validate performance predictions and generate experimental data for further refinement of the design. Following completion of sub-system tests, prototypes are developed for flight testing to validate full system.

	<u>Sept.</u>	<u>Oct.</u>	<u>Nov.</u>	<u>Dec.</u>	<u>Jan.</u>	<u>Feb.</u>	<u>Mar.</u>	<u>Apr.</u>
Testing								
Battery	Planned		Actual					
Materials	Planned		Actual					
Propulsion		Planned		Actual				
3x4 Wind Tunnel			Planned		Actual			
Prototype Flight Test			Planned		Actual			
Structural			Planned		Actual			
7x10 Wind Tunnel				Planned		Actual		
Final Flight Test				Planned		Actual		
University Fly-Off						2/19	Milestone	

Figure 48: Testing Schedule



7.1 Aerodynamic Testing

7.1.1 50% Scaled Wind Tunnel Model Test

The aerodynamic system is first tested during the preliminary design phase in the 3x4ft wind tunnel at Wichita State University. This test is used to evaluate C_L , C_D , and C_M performance at various angles of attack and airspeeds. The test facility is shown in Figure 49.



Figure 49: Pictures of the 3x4ft WSU Wind Tunnel Test

7.1.2 Full Scale Wind Tunnel Model

The full scale wind tunnel model is built to emulate the external geometry of the competition model. This prototype is tested in the 7x10ft Walter H. Beech Memorial Wind Tunnel at Wichita State University in order to validate the final aerodynamic and stability and controls analysis. This model verifies C_L , C_D , and C_M like the previous test as well as verifying stability derivatives and control surface effectiveness. Fairings and varying fuselage geometries are also utilized in order to reduce overall drag. This test matrix is shown in Figure 50. Different flow visualization methods, including yarn tufts and smoke, are used to investigate flow behavior. The yarn tufts identify laminar, turbulent, and separated flow on the aircraft; while smoke is used investigate the flow behavior around the pods and fuselage.



Run	Speed	AoA	Beta	δ_f	δ_e	δ_r	δ_a	Comments
1	M1cruise	A1	0	0	0	0	0	Baseline
2	M3takeoff	A1	0	0	0	0	0	Baseline
3	M3climb	A1	0	0	0	0	0	Baseline
4-6	M3takeoff	A1	0	X	0	0	0	Baseline/10°,20°,30° Flaps
8-12	M1cruise	A1	0	0	X	0	0	Baseline/-25°,-15°,-5°,5°,10° Elevator
13-16	M3takeoff	13	B1	0	0	X	0	Baseline/35°,25°,15°,5° Rudder
17-20	M1cruise	A1	0	0	0	0	X	Baseline/20°,15°,10°,5° Aileron
21	M3climb	A1	0	0	0	0	0	Propeller Run
22-23	M1cruise	A1	0	0	0	0	0	Baseline/Rear Pod Fairings #1,#2
24	M1cruise	A1	0	0	0	0	0	Baseline/Best Rear and Front Fairings
25	M1cruise	A1	0	0	0	0	0	Baseline/Pod Fairings and Fuselage 2
26-28	M1cruise	A1	0	0	0	0	0	Baseline/Trip Strips/0°,10°,20° Flaps
29+	Secondary Runs and Flow Visualization							
A1 = -6° to 16° by 2°								
B1 = 0° to 30° by 5								

Figure 50: Wind Tunnel Test Matrix

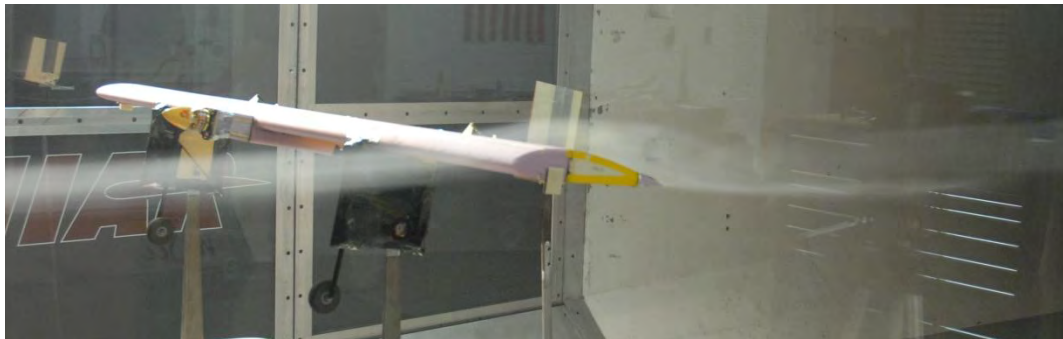


Figure 51: Smoke Visualization in the 7x10ft Walter H. Beech Wind Tunnel Test

7.2 Propulsion System Testing

7.2.1 Battery Testing

Due to the importance of battery performance in the propulsion system an assortment of battery types are acquired and tested. This test includes capacity, maximum current draw, and loaded voltage, on KAN 400, Elite 1500, and Elite 2000. The data obtained in this test is used to limit battery performance capabilities. Due to poor performance during a cold day of flight testing, a test is conducted comparing room temperature batteries to batteries cooled in a freezer. The test shows that the cold batteries



provided approximately 0.15V/cell lower voltage compared to the room temperature batteries until they warmed up.

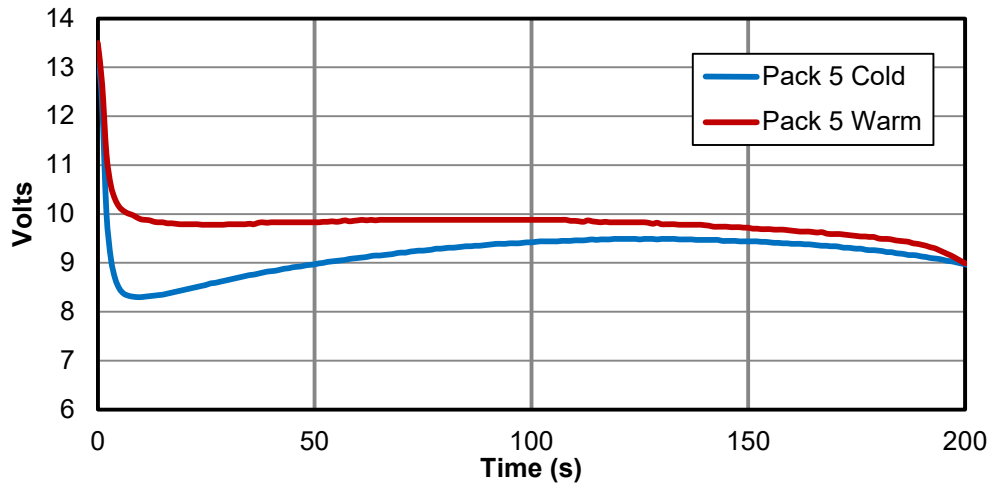


Figure 52: Cold Battery 20A Discharge Test

7.2.2 Propulsion System Testing

The full propulsion system is tested in the 3x4ft Wind Tunnel at Wichita State University. The purpose of this test is to validate the thrust performance and electrical power consumption estimations for the entire system. Several propeller and battery pack combinations are tested through dynamic airspeed sweeps to generate a comprehensive set of data. This is used in conjunction with aerodynamic test data to confirm predictions for flight velocities. The propulsion test plan is shown in Figure 53.

Run	Propeller	Power Input	Velocity (ft/s)	Recorded Data
1	12x6	9V Power Supply	0-100	Current, Thrust, RPM
2	12x6	10V Power Supply	0-100	Current, Thrust, RPM
3	11x7	9V Power Supply	0-100	Current, Thrust, RPM
4	11x7	10V Power Supply	0-100	Current, Thrust, RPM
5	12x6	9-cell Elite 1500	0-100	Current, Voltage, Thrust, RPM
6	12x6	10-cell Elite 1500	0-100	Current, Voltage, Thrust, RPM

Figure 53: Propulsion Test Plan

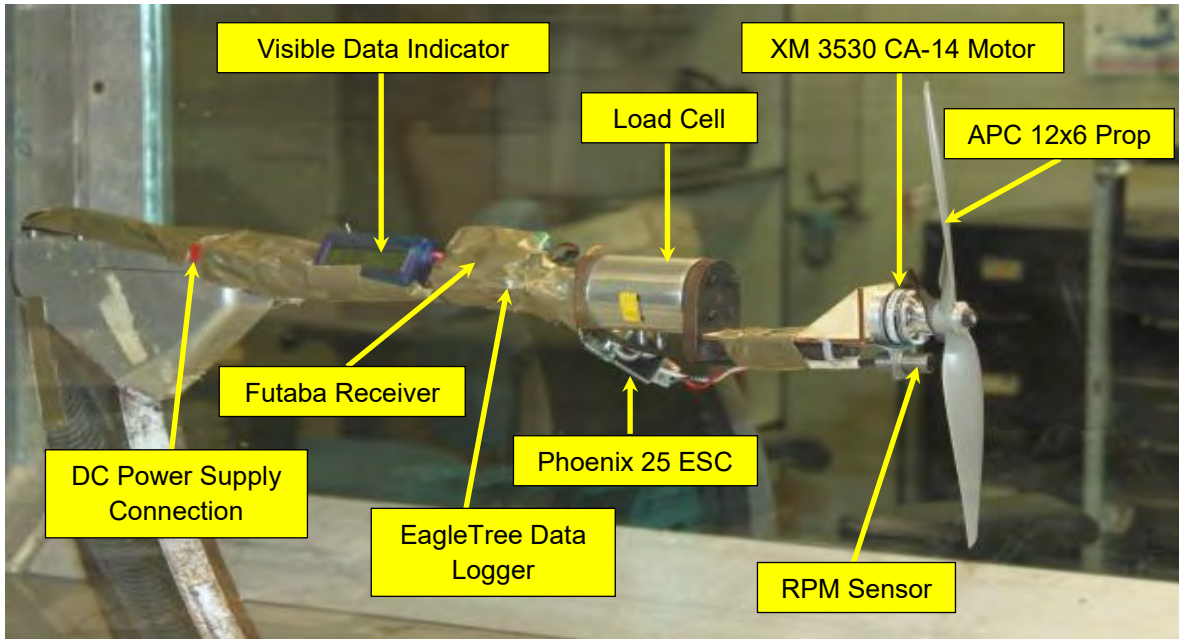


Figure 54: Picture of Propulsion Wind Tunnel Test

7.3 Structural Testing

7.3.1 XPS Foam Material Properties Validation

Testing was conducted last year by WSU Team Mini Wheat³ to verify that XPS foam has the strength the manufacturer reports in the technical data sheet. This year, tension testing is performed on the tension test machines at WSU and confirmed the reported technical data. The stress and strain plot for the XPS foam is shown in Figure 55.

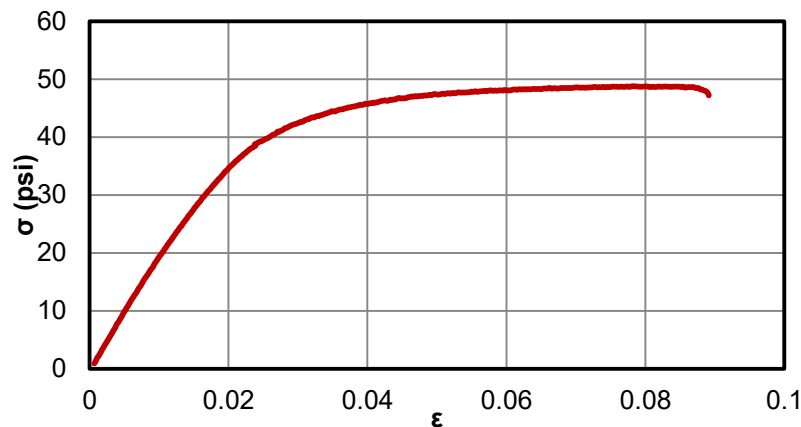


Figure 55: XPS Foam Stress and Strain Plot



XPS foam has a limited range of Hookean behavior, but foam components are not designed to withstand large loads under any condition, so analysis assuming Hookean behavior yields reasonable results.

7.3.2 Wing Testing

The wing structure is subjected to a simulated wingtip test and loaded to failure to confirm accuracy of the advanced structural analysis tool. The wing is loaded with 2L of water to simulate the wing tip test. After this, the wing is loaded with sand bags at the center until failure. Throughout this process, the deflection profile is measured at 3 points along the span. The structural test rig is shown below in Figure 56.



Figure 56: Structural Deflection Test

7.4 Flight Testing

A series of flight tests are conducted to verify the performance of the aircraft. These tests include water drop, initial foam prototype, and final prototype testing.

7.4.1 Initial Flight Testing

Initial flight testing consists of water visibility and foam prototype testing. Water visibility testing is conducted using an existing model aircraft and a 2L bottle. The plane is flown to 100m (328ft) where the altimeter circuit opens a drop valve. This test demonstrated that with a relatively low flow-rate the water is visible from 100m (328ft). The first flying prototype (Aircraft #1) is intended to be aerodynamically identical to the competition design but structurally stronger and easier to manufacture. This model is constructed from solid foam with the capability of carrying simulated competition payloads. The purpose of the prototype is to demonstrate that the design concept is capable of completing all of the mission requirements. Figure 57 shows each prototype during testing.



a) Water Visibility With Existing Aircraft



b) Initial Foam Prototype During Takeoff

Figure 57: Initial Flight Testing Pictures

Flight testing of the initial foam prototype identifies the wide range of external factors that influence the results of flight testing. A process for flight testing is developed and utilized to evaluate the system performance of each subsequent prototype. Figure 58 shows an example of the data that is recorded during testing.

Flight Description				Pre-Flight Check List			
Date:	2/19/12	Time:	16:45	Transmitter Check	X	Control Surfaces Check	X
Aircraft #:	2	Location:	Chapin	Secure Batteries	X	Range Check	X
Flight #:	7	Flight Time:	3:25 min	Altimeter Check	X	Static Check	X
Mission Objectives:	Complete M1 and record flight speeds using data logger			Wheel Check	X	Door Check	X
Configuration				CG Check	X	Shake Test	X
Weight (lb):	1.6	Propulsion #:	2	Weather Conditions			
Payload:	None	Receiver #:	1	Wind mph:	14 SW	Temperature:	45 F
CG Location:	3.16in	Propeller:	10x10	Humidity:	25%	Cloud Cover:	Clear
Post Flight Comments:	Increase in rudder size effective for crosswind, 10x10 slightly improved flight speeds						

Figure 58: Sample Flight Test Check List



7.4.2 Competition Prototype

The second flying prototype (Aircraft #2) is constructed to the specifications of the design for competition, and is used for performance validation during the WSU internal fly-off. This aircraft also demonstrates the manufacturing methods and validates the accuracy of the weight estimates, by having an empty flight weight of 1.53lb. Figure 59 depicts the competition prototype during flight. The test plan for flight testing of the initial two prototypes is shown in Figure 60.



Figure 59: Competition Prototype

Aircraft	Configuration	Purpose
#1	M1 Empty	Set empty trim of aircraft
#1	M1 Empty	Execute maneuvers
#1	M2 Sand	Set loaded trim of aircraft and demonstrate landing capability
#1	M3 Water	Demonstrate takeoff capability and test altimeter circuit
#1	M3 Water	Test altimeter circuit
#1	M1 Empty	Obtain a simulated M1 score
#1	M2 Sand	Obtain a simulated M2 score
#1	M3 Water	Obtain a simulated M3 score
#2	M1 Empty	Set empty trim of aircraft
#2	M1 Empty	Execute maneuvers
#2	M2 Passengers	Set loaded trim of aircraft
#2	M3 Water	Demonstrate takeoff capability and test altimeter circuit
#2	M1 Empty	Complete M1 for University Fly-Off
#2	M2 Passengers	Complete M2 for University Fly-Off
#2	M3 Water	Complete M3 for University Fly-Off

Figure 60: Initial Flight Test Plan



8.0 Performance Results

The aircraft sub-system and flight testing outlined in §7.4 is used to compare preliminary analysis methods to actual aircraft performance. This data is incorporated into the final design and optimization of the aircraft.

8.1 Aerodynamic Performance

The aerodynamic system is subjected to a comprehensive set of wind tunnel tests to evaluate lift and drag performance. The aircraft is tested at Reynolds numbers from 220,000 to 420,000, encompassing the full range from M3 takeoff velocity of 40.3ft/sec to M1 cruise at 77.3ft/sec. Figure 61 shows a comparison of lift data from the wind tunnel tests and theoretical predictions. The evident difference between the data obtained during the 7x10 wind tunnel test (WTT) is not a concern as it only exists at low angles of attack. At angles of attack below 5, all C_L values provide sufficient lift for all flight cases. The results from both WTT match the predicted values at high angles of attack but fail to achieve the predicted maximum values beyond 14 degrees angle of attack.

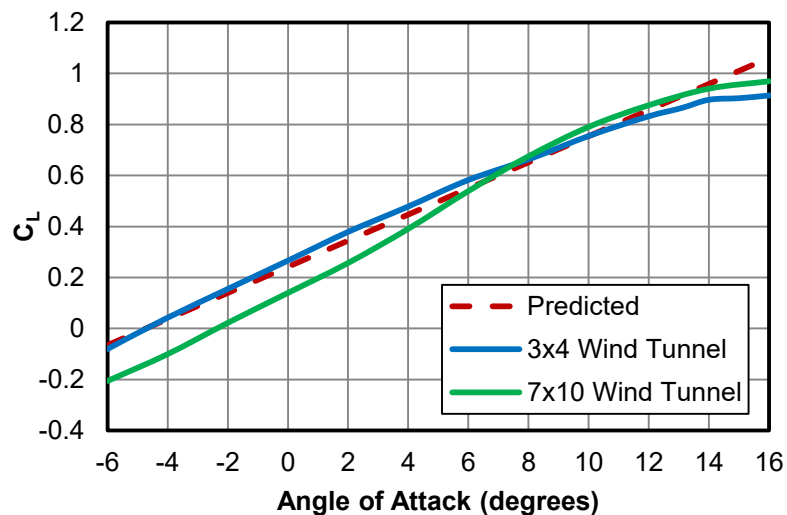


Figure 61: Lift Curve Slope Comparison

The drag behavior is also measured and compared to theoretical analysis in the wind tunnel tests. The theoretical and measured drag polars are shown in Figure 62.

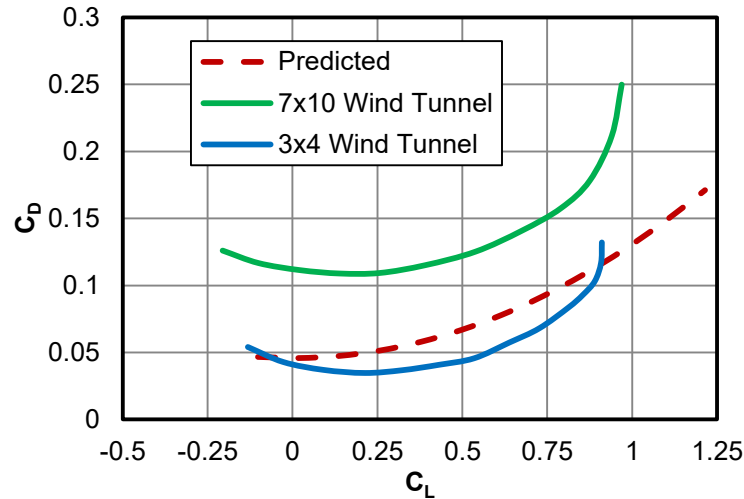


Figure 62: Drag Polar Comparison

The 7x10ft Beech Wind Tunnel test shows the drag to be consistently higher than predicted over the entire scope of the test. This is due to interference drag between the pods, landing gear, and wing. The pods also exhibited asymmetric drag behavior, which necessitated the fairings on the final design. The high drag data obtained during the 7x10 testing is not consistent with the performance that flight testing demonstrates. This indicates a flaw in the test which yields inaccurate data.

8.2 Stability and Controls Performance

The stability and control characteristics are verified in the 7x10ft Beech Wind Tunnel test. The aircraft can be trimmed within 8 degrees of elevator deflection. Confirmation on the performance of the elevator is shown in Figure 63. The unexpected significant drag from the pods accounts for the slight difference in pitching moments.

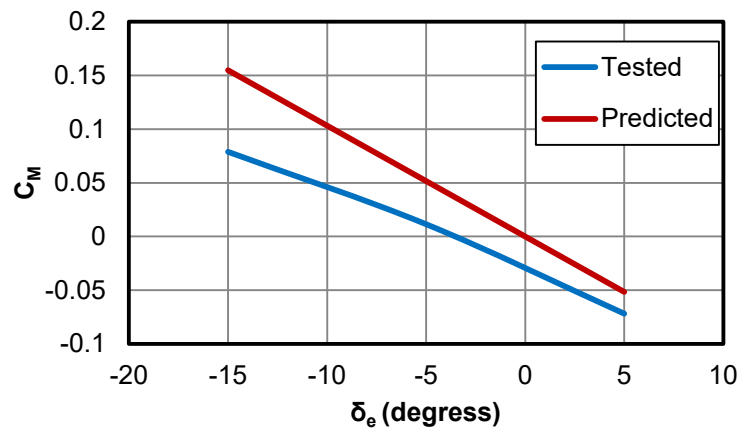


Figure 63: Pitching Moment Comparison



Accurate yaw and rolling data is not collected in the wind tunnel tests due to erratic behavior caused by the pods. It was found that the pods were not manufactured symmetrically and they caused large rolling and yawing moments that do not appear after the pod re-design. This was confirmed during initial flight testing as demonstrated by completion of the mission profiles.

8.3 Structures Performance

The structural wing tip test is used to validate performance characteristics of the wing and the structural analysis tool discusses in §5.2.1. The wing structure is subjected to a simulated wing tip test and then loaded to failure as described in §7.4. The wing holds 4.2lb of water span-loaded in the spar and 3.25lb of the sand in the center for 20 seconds before failure. Calculating the loads from this profile yields an ultimate bending strength of between 5.6 and 5.96lb-ft. The structural analysis tool predicts an ultimate strength of 5.77lb-ft, differing from experimental data by less than 4%. Figure 64 compares theoretical deflections with experimental data.

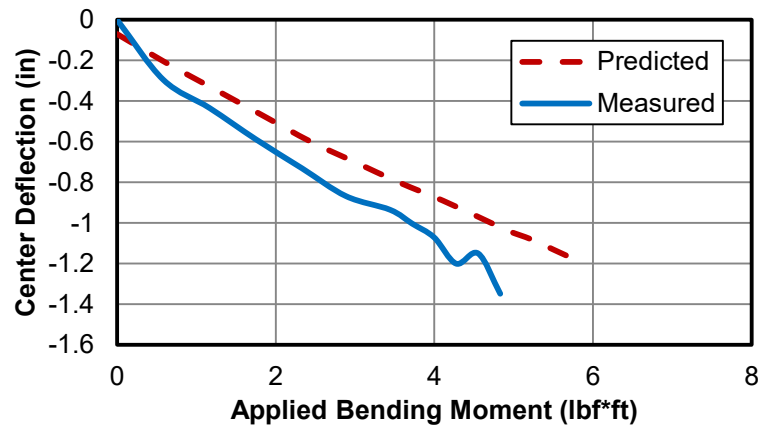


Figure 64: Structural Deflection Comparison

The deflection could not be measured until failure because the sand on the center interfered with the measurement apparatus. Over the measured range, the structural analysis tool consistently underestimates the deflection by 0.2in. This can be attributed to non-Hookean behavior of the foam. While the difference in deflection is significant, the ultimate strength of the structure is close to predicted value. The results of the structural test successfully validate performance estimates from the structural analysis tool for design purposes.

8.4 Propulsion Performance

The propulsion system is tested to compare actual thrust profiles with analysis methods. Figure 65 shows a comparison of experimental data for a 12x6 propeller on a Dualsky XM3530CA-14 motor using a DC power supply voltage of 10V. This test is representative of an 11 cell pack of Elite 1500 batteries. This test is conducted as a baseline test to compare motor performance to predictions. The motor provides



less thrust than expected while also pulling less current than expected. As a result of this test, the expected battery pack of 9 cells of Elite 1500s is changed to a pack of 11 cells of Elite 1500s. This is done to meet the M3 takeoff thrust requirements, but with further flight testing, the possibility of decreasing the pack to 10 cells will be evaluated in an attempt to reduce the RAC.

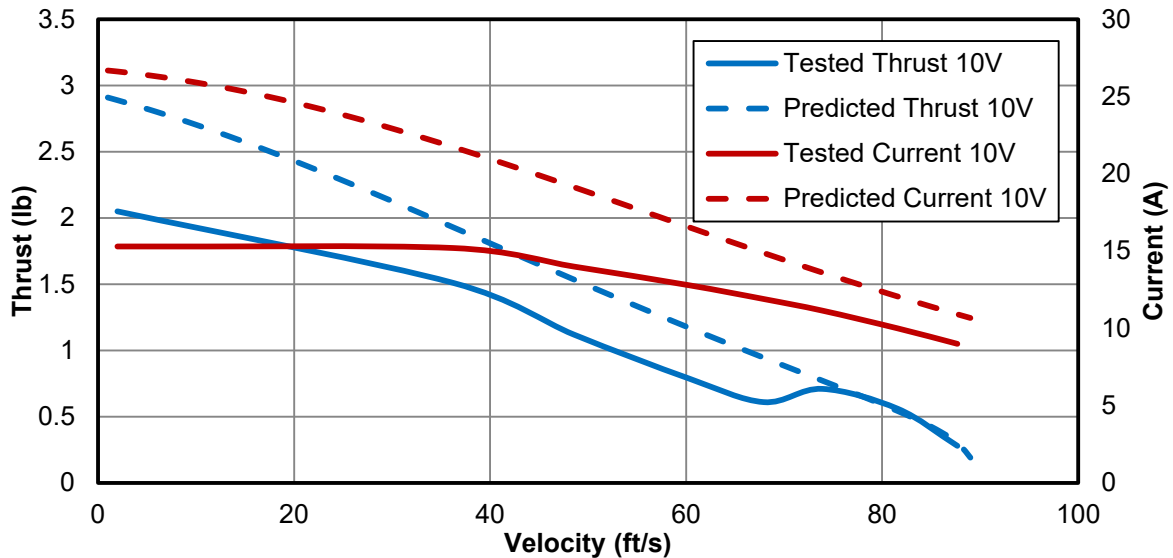


Figure 65: Thrust profile comparison

8.5 Flight Testing Results

The flight testing results of the first two prototypes indicate issues with the design that must be addressed to ensure the success of subsequent prototypes. These issues are outlined in Figure 66 along with the corresponding actions and design improvements

Aircraft	Issue	Action
#1	Difficulty tracking during crosswind takeoff	Increase rudder from 30% of vertical to 40%
#1	Loss of battery power in cold conditions	Conduct cold battery testing
#1	Altimeter does not release water	Test alternate transmitter and servo settings
#1	Elevator ineffectiveness due to boom flex	Use a more rigid carbon boom for tail
#2	Loss of receiver battery connection	Revise location of receiver battery
#2	Microlite™ separation during flight	Glue Microlite™ to the top of the spar cap
#2	Difficulty ground tracking	Increase wheel diameter and redesign axle
#2	Difficulty with 100ft takeoff distance loaded	Analyze increase in wing size
#2	Undesired roll immediately after takeoff	Incrementally test and trim flaps at altitude until full deflection is trimmed and stable
#2	Crash during M2 landing	Redesign breakaway joint and increase pilot familiarity with landing approach

Figure 66: Results of Initial Flight Testing



References

- ¹AIAA. (2011 04-October). 2011/12 Rules and Vehicle Design. Retrieved 2011 04-Oct. from AIAA DBF: [http://www.aiaadb.org/2012_files/2012_rules.htm]
- ²Blumenshine T., Gimenez A., Lambert W., Nord W., Winkel J. (February 2012). Shockin Stingray Design Report AIAA/Cessna/Raytheon Design Build Fly. Wichita State University
- ³Bottom, A., Bird, J., Broodryk, I., Fast, P., Herbert, A., (2011, February). Team Mini Wheat Design Report AIAA/Cessna/RMS Design Build Fly. Wichita State University
- ⁴Kelly, K., Krenzle, J., Hinson, B., Lemon, K., & Staab, L. (2009). Team sUAVe Design Report AIAA/Cessna/RMS Design Build Fly. Wichita State University.
- ⁵Oorebeek J., Orr D., Reader B., Yaberg T., Yang S., (2009) Turbo Encabulator Design Report AIAA/Cessna/RMS Design Build Fly. University of Southern California.
- ⁶Beavers M., Carver M., Keatling F., Paul R., Still A. (2010) OSU team Black Design Report AIAA/Cessna/RMS Design Build Fly. Oklahoma State University.
- ⁷Raymer, D. (2008). Aircraft Design: A Conceptual Approach. Reston, Virginia: American Institute of Aeronautics and Astronautics.
- ⁸Drela, M., & Youngren, H. (2008, 04 07). XFOIL. Retrieved 09 05 2011, from Subsonic Airfoil Development System: [http://web.mit.edu/drela/Public/web/xfoil/]
- ⁹Drela, M., & Youngren, H. (2008, 08 04). AVL. Retrieved 11 30, 2011, from [http://web.mit.edu/drela/Public/web/avl/]
- ¹⁰UIUC Airfoil Coordinate Database." 29 Oct, 2008. <http://www.ae.uiuc.edu/m-selig/ads/coord_database.html>
- ¹¹Hepperle, M. (2007, 27 01). JavaFoil Retrieved 09 05, 2011, from [www.mh-aerotoools.de/airfoils/javafoil.htm]
- ¹²Anderson, J. (2008). Introduction to Flight Sixth Edition. Hoboken, New Jersey: John Wiley and Sons.
- ¹³Hoerner, S.F. Fluid Dynamic Lift. 2nd ed. Bakersfield, CA: Hoerner, 1992.
- ¹⁴Roskam, J. (2007). Airplane Flight Dynamics and Automatic Flight Controls. Lawrence, KS, United States of America: DAR Corporation.
- ¹⁵Etkin, B., & Reid, L. D. (1996). Dynamics of Flight Stability and Control Third Ed. Hoboken, New Jersey: John Wiley and Sons.
- ¹⁶Hepperle, M. (2003, 08 09). JavaProp Retrieved 09 10, 2011, from [http://www.mh-aerotoools.de/airfoils/javaprop.htm]
- ¹⁷Schrenk "A Simple Approximation Method for Obtaining the Spanwise Lift Distribution" NACA TM 948, 1940.
- ¹⁸Hibbeler, R. C., Mechanics of Materials, 7th ed, Prentice Hall, Upper Saddle River, NJ, 2008.
- ¹⁹Allen, D. & Haisler, W. (1985). Introduction to Aerospace Structural Analysis. Hoboken, NJ. Wiley
- ²⁰Dassault Systems (2008, October), CATIA v5r19

San Jose State University

AIAA Design/Build/Fly 2011-2012
Design Report



University of California, Irvine

2011-2012

Aircraft Design Report



Cessna/Raytheon AIAA Design/Build/Fly
Competition



Table of Contents

1.0	Executive Summary	3
2.0	Management Summary	4
2.1	Team Organization	4
2.2	Project Milestone Chart	6
3.0	Conceptual Design	6
3.1	Design Constraints	6
3.2	Scoring Formula	7
3.3	Mission Sequence – Small Passenger Aircraft.....	7
3.4	Sensitivity Analysis	8
3.5	Configuration Selection	10
3.6	Sub-systems Selection	12
3.7	Conceptual Design Summary.....	17
4.0	Preliminary Design	18
4.1	Design and Analysis Methodology	18
4.2	Mission Model.....	20
4.3	Design and Sizing Trades	21
4.4	Lift, Drag and Stability Characteristics.....	25
4.5	Predicted Mission Performance.....	27
5.0	Detail Design	29
5.1	Dimensional Parameters	29
5.2	Structural Characteristics and Capabilities.....	30
5.3	System Design and Component Selection/Integration	31
5.4	Weight and Balance	37
5.5	Flight Performance Parameters.....	39
5.6	Predicted Mission Performance.....	40
5.7	Drawing Package	41
6.0	Manufacturing Plan and processes:	47
6.1	Wing and Tail.....	47
6.2	Landing Gear.....	48
6.3	Fuselage Fairing.....	48
6.4	Water Tank.....	49
6.5	Water Tank Release.....	49
6.6	Milestone Chart	50
7.0	Testing Plan	50
7.1	Objectives.....	50
7.2	Master Test Schedule.....	52
7.3	Preflight check list.....	52
7.4	Flight test plan	53
8.0	Performance Results	53
8.1	Performance of Key Subsystems	53
8.2	Flight Test Performance	56
9.0	References	58



1.0 Executive Summary

This report documents the design, manufacturing processes, and testing conducted by the University of California, Irvine (UCI), Team Angel of Attack for their aircraft entry in the 2011-2012 AIAA/Cessna/Raytheon Design/Build/Fly competition. The objective of the competition is to produce an electric remote controlled aircraft that will receive the highest total score; a combination of the written report score, total flight score, and rated aircraft cost (RAC).

The theme for this year's competition is the small passenger aircraft [1]. The goal of the aircraft is to be as light as possible while carrying 8 aluminum bars simulating passengers. The aircraft must be capable of completing three missions that will test its performance extremes: first, is to fly the greatest number of laps under a four minute period without payload; second, is to maximize the payload-to-flight weight ratio; and third, is to minimize the time to climb 100 meters with a fully loaded aircraft. The major challenge is being able to takeoff during the payload missions given the propulsion limitations imposed by a 20 amp fuse and 1.5-lb maximum battery weight.

Team Angel of Attack determined that the winning aircraft would be one built to complete all three missions with the lightest possible empty weight. There was no way that focusing completely on one mission or empty weight alone could win the competition. In addition, for mission 3, the aircraft must release 2 liters of water once it has climbed to 100 meters, which adds another level of complexity to the design. To address the challenges posed by each mission, the team designed an aircraft that could balance the mission requirements, primarily high speed for mission 1, low flight weight for mission 2, and high thrust for mission 3.

The 20 amp fuse forced the team to chose a low Kv motor and increase the voltage and propeller diameter in order to gain enough thrust for takeoff during the payload missions. Because the third mission had the heaviest payload (4.41-lbs), the aircraft's wing was sized specifically for the takeoff portion of that mission. This meant that the wing was overbuilt to fly mission 1, which allowed it to pull high G turns to reduce turn radius and lap time.

Mission 2, flown at the aircraft's speed for best range, needed to complete the mission with the lightest combination of structure and propulsion weight. The energy requirement for this mission was the highest, so efforts were taken to make sure that the selected battery pack would provide enough energy without penalizing weight.

The key to success at the competition is being able to complete all missions, but empty weight is a significant factor as well. A lot of effort was put into reducing structural weight. Wing weight correlated strongly with propulsion weight and manufacturing methods were improved to create as light a wing as possible.

Constraints on how to position the passengers within the aircraft drove the fuselage design. They were arranged in a 2x4 configuration. The fuselage featured a thin foam/fiberglass fairing surrounding a central carbon rod that ran from the motor to the tail. Stress was transmitted from the wing spar to the landing gear through the wing-box. The aluminum passenger payload was supported within a



foam/carbon-fiber structure bonded to the wing-box that doubled as the water tank for mission 3. Water was ejected by unfolding the latex joint of a bent carbon tube connected to the tank. This method of releasing water proved to be very light and reliable.

The team's optimization program ran thousands of plane designs through a mission model and converged on an aircraft with the highest competition score. This aircraft came in at a predicted empty weight of 2.49-lbs using the team's weight calculations tied to the optimization program. Details on all the subsystem selections made to arrive to this aircraft solution are explained in the following sections. The predicted outcome of mission 1 was 6 laps and the mission 3 climb was clocked at 31.3 seconds, all very competitive values resulting in a maximum competition score of 448. The team proceeded to build and test fly a prototype to confirm the predictions and calibrate the optimization code. The predictions were very close to actual values, but deviations occurred due to difficulties in drag estimation. Nonetheless, the team's pilot is getting the needed practice and taking the prototype to its performance limits as preparation for the competition, all while the rest of the team is fine-tuning the design to improve future test flight results. Team Angel of Attack is well on its way to bringing a competitive aircraft to this year's DBF competition.

2.0 Management Summary

The UCI team implemented an organizational structure and design timeline that focused on maximizing efficiency and team collaboration. With 38 dedicated members, the team benefits from a wide range of interests and capabilities.

2.1 Team Organization

The team follows a hierarchical structure similar to industry, which places responsibility on members to perform their required tasks. Figure 2.1 shows the team's organizational chart.

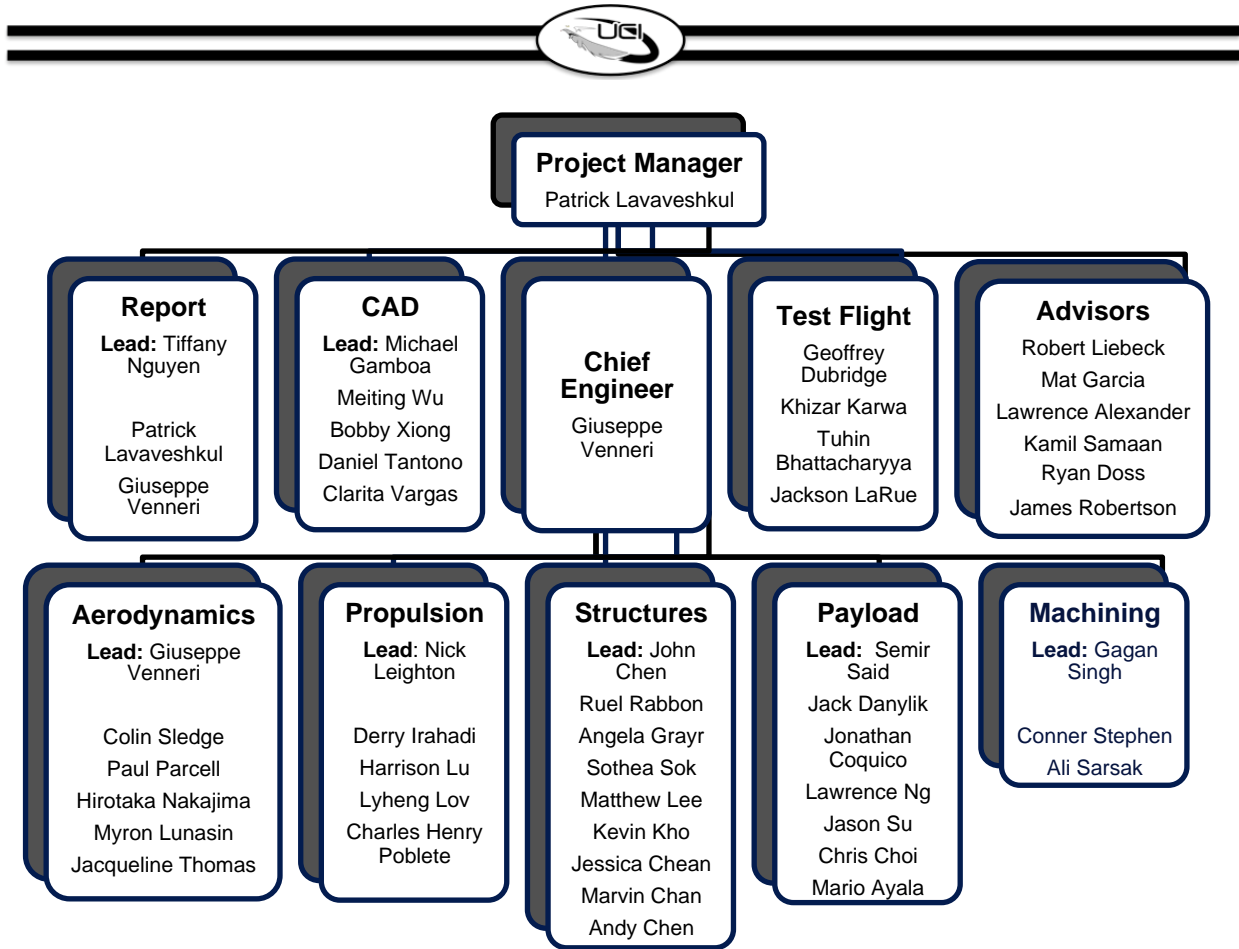


Figure 2.1 Team Organization

The Project Manager is responsible for facilitating productivity in all areas of the project. He monitors budget, material procurement, scheduling, and leads team meetings. The Chief Engineer steers the design effort and facilitates the communication between design groups. These two individuals lead the project, which is further supported by the following individuals and teams:

- **Test Flight** maintains the flight checklist. Organizes and conducts the test flights.
- **CAD** creates detailed drawings of every component of the aircraft system and aids in the rapid visualization of possible aircraft solutions.
- **Report** collects, formats, and verifies the work done by the design groups and flight test crew for inclusion into the design report.
- **Aerodynamics** computes the flight characteristics and necessary wing dimensions. This team also ensures that the aircraft meets certain control and stability standards, and uses numerical modeling to predict flight performance.
- **Propulsion** analyzes the propulsion system to find the best motor, propeller, and battery combination for the aircraft.
- **Structures** optimizes the load-bearing components of the aircraft and maintains a weight build-up.

- **Payload** designs and experiments with different payload restraint mechanisms, including the water release system.
- **Machining** manufactures fuselage molds using CNC foam cutting equipment and also manufactures the payload to be used in testing and the competition.

2.2 Project Milestone Chart

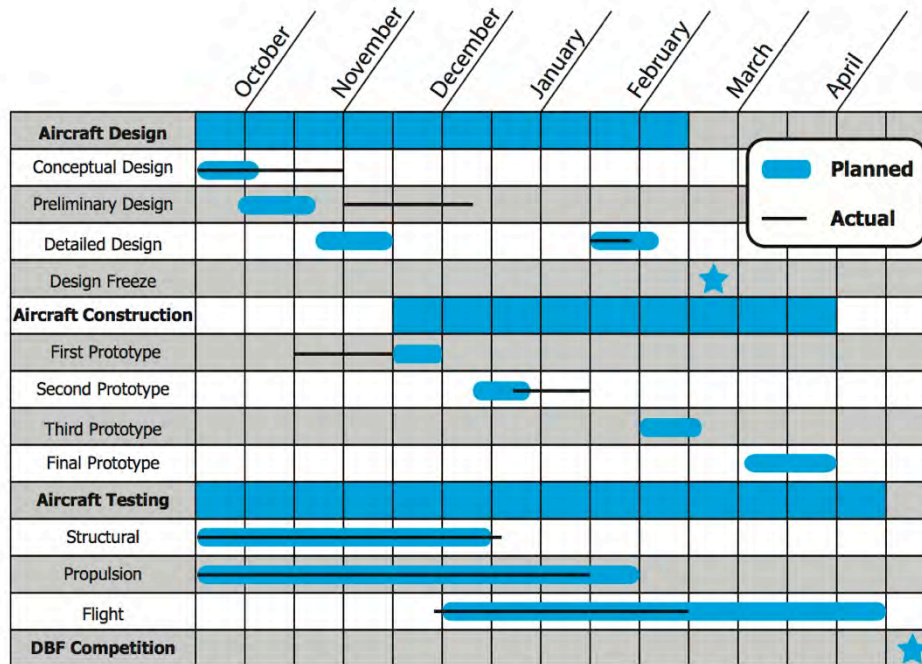


Figure 2.2: Master Schedule

The demand for a competitive aircraft requires an aggressive schedule. The Project Manager maintains a master schedule that tracks the various phases of the design, testing, and important milestones. The planned and actual schedules are shown in Figure 2.2.

3.0 Conceptual Design

The objective of the conceptual design process is to extract a set of figures of merit (FOM) from the analysis of mission goals, requirements, and the design constraints set out in the contest rules. During this process, different design concepts are chosen using the FOM. The end result of this was a high-performance design that maximizes the overall flight score.

3.1 Design Constraints

The team analyzed the contest rules to determine the important design limitations set by the contest. Listed below are the requirements for the Design/Build/Fly competition for this year.



- The weight of the propulsion battery must not exceed 1.5 pounds.
- Maximum drawn current supplied by the battery pack(s) or received by the motor(s) is limited to 20 amps by means of a 20 amp fuse.
- All payloads must be secured sufficiently to assure safe flight without possible variation of aircraft's center of gravity (CG) during flight.
- All payloads must be carried fully internal to the aircraft mold lines.
- The aircraft must be designed to fly all three missions.
- The ground rolling takeoff distance is a maximum of 100 ft.

3.2 Scoring Formula

The AIAA Design/Build/Fly Competition for 2012 consists of three missions and the design report. The total score is contingent on a combination of the scores received along with the rated aircraft cost (RAC). The formula to determine a team's total score is:

$$Total\ Score = \frac{Report\ Score \times Total\ Flight\ Score}{\sqrt{Rated\ Aircraft\ Cost}} \quad (Equation\ 3.1)$$

$$Total\ flight\ Score = M_1 + M_2 + M_3 \quad (Equation\ 3.2)$$

Where M_n is the flight score for that mission.

$$Rated\ Aircraft\ Cost\ (RAC) = Max(EW_1, EW_2, EW_3) \quad (Equation\ 3.3)$$

Where EW_n is the empty weight, including batteries, measured after the flight with the payload removed.

3.3 Mission Sequence – Small Passenger Aircraft

The team will have a maximum of four flight attempts with five minutes to install payload and check control surfaces before each flight. The assembly/flight line crew is limited to only the pilot, observer, and one ground crew member. The course consists of a 1000-foot course with two 180° turns and one 360° turn (Figure 3.1). To receive a score for a mission, the plane must land on the runway without significant damage (as determined by the judges).

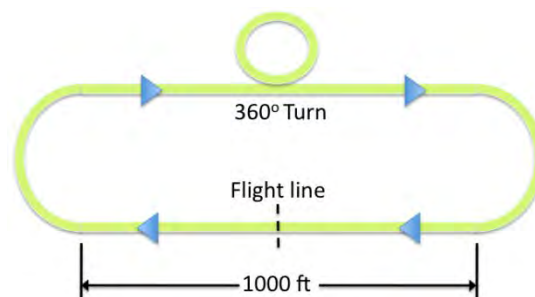


Figure 3.1: Course Layout shown to scale



3.3.1 Mission 1 – Ferry Flight

The goal of mission 1 is to complete as many laps as possible within a four-minute period. Mission 1 is an empty flight mission. The score for mission one is given by the equation:

$$M_1 = 1 + \frac{N_{laps}}{6} \quad \text{(Equation 3.4)}$$

where N_{laps} is the number of complete laps flown by the team for a successful mission 1 flight. The flight time begins when the throttle is advanced for the first takeoff or attempt. Only complete laps are counted in the score.

3.3.2 Mission 2 – Passenger Flight

Mission 2 is a three-lap payload flight with no time limit. The goal of this mission is to maximize the payload to flight weight ratio. The payload consists of eight simulated passengers. The simulated passengers are 1"x1"x5" aluminum blocks. The team will supply the aluminum payload, which must not weigh less than 3.75 lbs. They must be situated with the long dimension vertical and each have ½" open space fore and aft with 1" aisles separating columns of passengers. The flight score for this mission is given by the equation:

$$M_2 = 1.5 + \frac{3.75}{\text{Flight Weight (lbs)}} \quad \text{(Equation 3.5)}$$

The flight weight of the aircraft will be obtained immediately after completion of the mission by weighing the plane with the payload installed.

3.3.3 Mission 3 – Time to climb

Mission 3 is a single takeoff and climb to 100 m altitude. The payload will be a team supplied "Time End Indicating System" (TEIS). It consists of a team designed and fabricated water tank with a capacity of two liters fitted with a servo operated dump valve. A soaring circuit will actuate the dump valve at 100 meters from the ground. This will signal to the judges that the altitude has been reached. The objective of mission 3 is to climb as fast as possible. The flight score for this mission is given by the equation:

$$M_3 = 2 + \sqrt{\frac{T_{avg}}{T_{team}}} \quad \text{(Equation 3.6)}$$

where T_{team} is the time from advancing throttle for the initial takeoff to altitude and T_{avg} is the average time to climb for all teams getting a successful score for mission 3.

3.4 Sensitivity Analysis

The score equations were used to perform an analysis and determine the level of impact each score parameter had on the total score. In the first stage of this analysis the team considered the extreme cases to determine if the score equations can have unusual behavior in these conditions. Following this step, an analysis was done using MATLAB to determine the sensitivity of the score parameters. To perform this analysis, the scores were estimated using past years' competition data. The estimated values for an average team were 3-lb empty weight, 6 laps, and a 30 sec climb time.

3.4.1 Extreme cases

The score equations were analyzed for extreme behavior by considering the extreme cases for every score variable. The score variables consist of N_{laps} , EW_{max} , and T_{team} . Figure 3.2 shows the extreme cases considered.

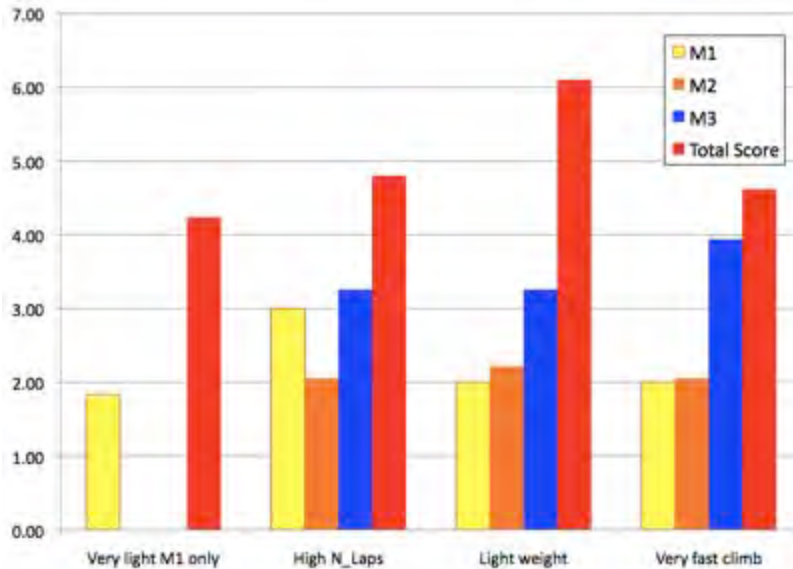


Figure 3.2: Flight Score Analysis

The first case represents the smallest aircraft that can complete mission 1. The weight of this aircraft can be as low as 4 oz and can complete 5 laps. This design will have the best RAC, however, due to its size, it will not be able to complete mission 2 and 3. The second design is a faster design that can complete 12 laps, but has the penalty of a heavier propulsion system. The third design is the lightest design that can complete all three missions. The final design is one that can climb very quickly. As seen in this figure, none of the extreme cases produce a significant change in the total score except for a lightweight aircraft that can complete all three missions.

3.4.2 Sensitivity analysis

A sensitivity analysis was conducted to determine the effects of each score parameter on the total score. This study uses the same average design as the last score study. The impact of each score parameter on the total score was determined by varying one parameter at a time while holding the others constant.

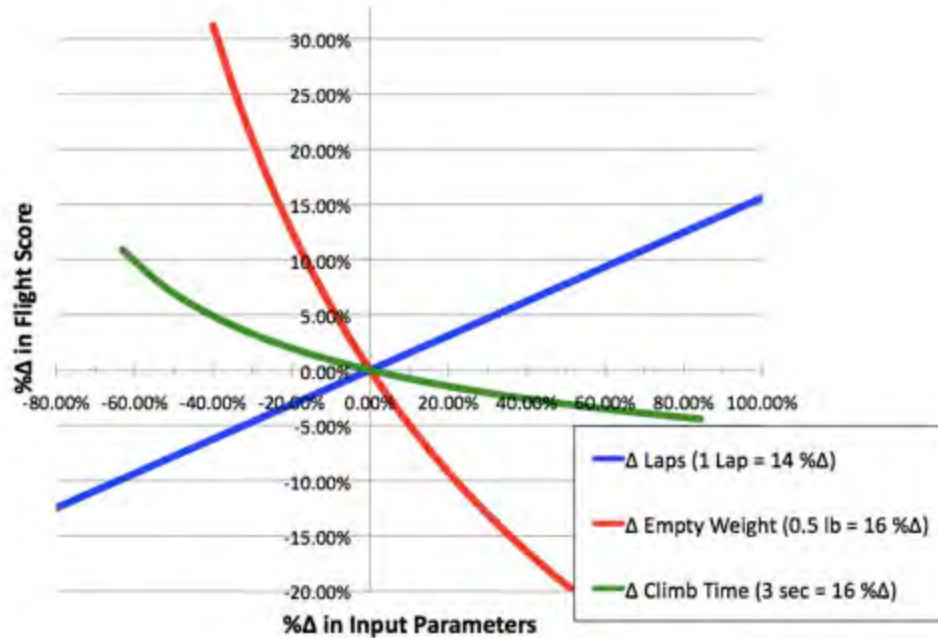


Figure 3.3: Impact of change in parameters on the total score

Figure 3.3 shows the effects of the change in each score parameter on the total score. This figure shows that the empty weight (EW_{max}) has the largest impact on the total score followed by the number of laps then by the climb time.

3.5 Configuration Selection

The design process was initiated by selecting an aircraft configuration that was favored by the results of the scoring analysis.

3.5.1 Configuration Figures of Merit

During the configuration selection process, each configuration was scored independently using a set of scoring parameters in order to find the best configuration for this year's competition. Based on the scoring analysis, more weight was given to specific areas. The scoring parameters were:

- **System Weight (45%):** The first and most important characteristic evaluated was system weight. This consists of the empty aircraft weight without motor, servos, or payload. Because a lighter aircraft will score higher, this area was given the most weight in determining the aircraft configuration.
- **L/D (30%):** The lift to drag ratio was given the second highest weight. L/D is a basic function of all aircraft and can be used to evaluate the flight performance. Choosing a configuration to maximize L/D ensures an aircraft that can travel longer distances for a given battery pack and can achieve high climb rates, both of which factor into the score to reduce weight and climb time.

- **Low Speed/Ground Handling (15%):** Some configurations offer problems in these areas where good handling is critical to the completion of the mission. Longer takeoff rolls and instability at low speeds are examples.
- **Manufacturability (10%):** The ease with which the aircraft can be manufactured was a consideration in the design process. The ability to design and build a specific configuration is determined by the experience of the members and more difficult configurations would require more time to build.

3.5.2 Configuration Selection

A few basic configurations were evaluated as possible options for this year's design. The aircraft configurations were evaluated according to how well they could accomplish the tasks of the missions as dictated by the sensitivity analysis, with the conventional configuration acting as the baseline for comparison. Configurations considered were:

- **Conventional:** The benefits of a conventional aircraft are that it is proven and relatively easy to design and build. Each component of the plane is entirely single-purpose and it would not be the most efficient design when it comes to weight and materials. However, without a span limit, a composite wing can easily match a flying wing's lightweight and flight performance without the drawbacks of reduced stability.
- **Flying Wing:** This type of aircraft offers a lightweight design by minimizing the material necessary to build, while having a greater L/D than the conventional. The body acts as both the payload storage as well as the lifting surface. With less wetted area than other configurations and a full streamlined body, drag is greatly reduced. They are also generally less stable due to the lack of a horizontal tail with a long moment arm, which also results in an increased takeoff distance.
- **Biplane:** The biplane configuration is a great solution for a short span constraint. However, they generally produce more drag than conventional due to interference between the wings. They also require additional structure to connect the wings together, which adds weight and drag.



Figure 3.4: Aircraft Configurations



FOM	Weight	Conventional Aircraft	Flying Wing	Biplane
Aircraft Weight	45	0	0	-1
L/D	30	0	1	-1
Handling	15	0	-2	0
Manufacturability	10	0	-1	0
<i>Total</i>	<i>100</i>	<i>0</i>	<i>-10</i>	<i>-75</i>

Table 3.1: Aircraft configuration figures of merit

The conclusion reached is that for this year's competition a conventional configuration would offer the best combination of a lightweight aircraft with good L/D and reliability.

3.6 Sub-systems Selection

After a conventional configuration was selected, the major sub-system components were analyzed using a figure of merit analysis to determine the best options. The main sub-systems were motor, tail, landing gear, payload, water tank, and water release configuration.

3.6.1 Motor configuration

The team investigated the placement and number of motors, which would affect the aircraft's efficiency and ability to carry payload. The 20 amp fuse places significant limitations on the capabilities of the propulsion system which will affect the thrust output and system weight. A scoring sheet was used to gauge the different propulsion methods, using the single tractor configuration as the baseline for comparison.

- **Single Tractor:** This configuration is lightweight and less likely to have propeller strikes on landing than a pusher configuration. Forward-mounted propellers have high efficiency because they act on undisturbed air. If high thrust is desired, a geared motor is the only way to not go over 20 amps, and this increases system weight.
- **Single Pusher:** Mounting a single motor aft of the aircraft will allow better air flow around the fuselage, improving stall characteristics and reducing drag. For clearance against a fuselage, it must be mounted on a pylon, thereby increasing weight.
- **Double Tractor:** Two motors of reduced size can use smaller propellers to attain takeoff speed. This system's weight is more than the single motor system for the same amount of thrust. The increased forward mass can make it difficult to balance the aircraft properly during the empty mission.
- **Push-Pull:** The system weight is similar to the double tractor, and places a motor at the front and rear of the aircraft. This demands additional structure from the fuselage to support the large moments from the separated motors. Balancing the aircraft can be a problem.

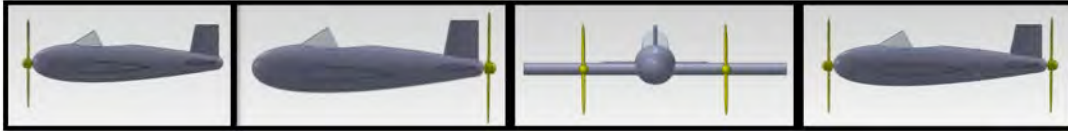


Figure 3.5: Motor Configurations

FOM	Weight	Single Tractor	Single Pusher	Double Tractor	Push-Pull
Aircraft Weight	45	0	-1	0	-1
System Weight	30	0	0	-1	-1
Efficiency	15	0	1	0	-2
Clearance	10	0	-1	1	-2
<i>Total</i>	<i>100</i>	<i>0</i>	<i>-40</i>	<i>-20</i>	<i>-130</i>

Table 3.2: Motor Configuration Figures of Merit

The single tractor configuration was selected from the FOM chart because it resulted in an overall lighter aircraft.

3.6.2 Landing Gear Configuration

Takeoff and landing are very critical for the successful completion of the missions. The challenge at takeoff is to maintain sufficient control during the ground roll till the aircraft attains sufficient speed. During the landing portion, the landing gear must take the load from the ground impact. A scoring sheet was used to gauge the different landing methods, using tricycle as the baseline for comparison.

- **Tricycle:** Two main gear wheels are under the wing and one smaller wheel is under the nose of the aircraft. This configuration has good ground handling, but will have more weight and drag than a tail dragger configuration.
- **Bicycle:** This configuration has two centerline wheels and two wing tip skids. It is heavier than the other options but suffers in ground handling because it cannot rotate on takeoff.
- **Tail Dragger:** Two main gear wheels are under the wing and one smaller wheel is under the tail of the aircraft. This configuration does not have good ground handling in the presence of crosswind, but has less drag than a tricycle configuration.

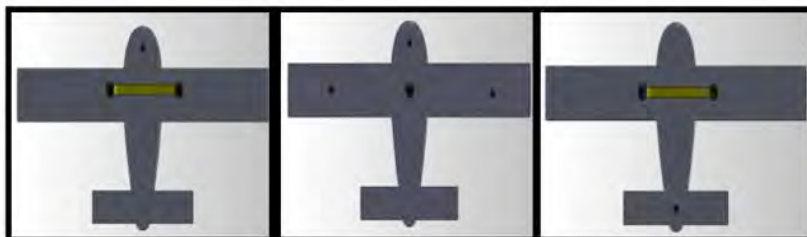


Figure 3.6: Landing Gear



FOM	Weight	Tricycle	Bicycle	Tail Dragger
Aircraft Weight	40	0	-1	1
Handling	40	0	-1	-2
Drag	10	0	-1	1
Durability	10	0	-1	0
<i>Total</i>	<i>100</i>	<i>0</i>	<i>-100</i>	<i>-30</i>

Table 3.3: Landing Gear Configuration Figures of Merit

The tricycle configuration was selected due to its reliability and superior ground handling.

3.6.3 Tail Configuration

The tail provides stability and allows the aircraft to make high performance turns. Three configurations were considered with conventional used as the baseline.

- **Conventional:** This configuration is simple to install and provides sufficient stability
- **T-Tail:** It is effective at high angles of attack, but placing the horizontal stabilizer on top of the vertical will increase its structural weight.
- **V-Tail:** Two surfaces form a “V” with the tail boom and provide both elevator and rudder control. Control authority is reduced in both yaw and pitch.



Figure 3.7: Tail Configuration

FOM	Weight	Conventional	T-Tail	V-Tail
System Weight	50	0	-1	0
Drag	30	0	0	0
Stability	20	0	1	-2
<i>Total</i>	<i>100</i>	<i>0</i>	<i>-35</i>	<i>-40</i>

Table 3.4: Tail Figures of Merit

The conventional tail was selected for its simplicity of design and robust stability behavior.

3.6.4 Payload Configuration

Two payload configurations were considered for mission 2 that would influence the shape of the aircraft fuselage: a single 1x8 row and a 2x4 configuration of aluminum passengers. Both choices affected fuselage frontal and side area, and therefore structural weight and drag. The minimum clearance requirements specified in the rules were used in the comparison. 2x4 was used as the baseline.

- **1x8:** This configuration had the largest side area. The rules required that a 1" aisle follow along one side of the passengers, making them off-center unless another 1" aisle were also on their other side. This effectively gave the 1x8 configuration the same frontal area as the 2x4 configuration. The main structure, needed for supporting the payload, could not run lengthwise, central to the fuselage, but had to go around the payload, potentially increasing structural weight.
- **2x4:** With a smaller side area, this configuration is less susceptible to crosswinds. The enclosed volume is also less. A smaller fuselage is less destabilizing which allows for smaller tail surfaces. This configuration also allows for a single main support structure to pass lengthwise through the middle of the payload and fuselage, reducing weight and complexity.

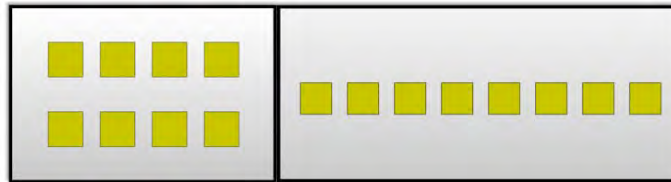


Figure 3.8: Payload configurations

FOM	Weight	2 x 4	1 x 8
System Weight	50	0	-1
Drag	30	0	-1
Stability	20	0	-1
<i>Total</i>	<i>100</i>	<i>0</i>	<i>-100</i>

Table 3.5: Payload Figures of Merit

The 2x4 payload configuration was selected because it was lighter and had less drag.

3.6.5 Water Tank Configuration

The rules specify that the water tank must be sealed using non-collapsible material and be internal to the aircraft mold lines. Because the water gets ejected mid-flight, it is important to keep the CG from moving in order to maintain stability throughout the entire flight. The water plume must also be visible for the judges to see. As water gets released, the water slosh in the tank might be destabilizing if allowed to shift for long distances. Two tank configurations were considered, a center tank housed in the fuselage and a tank housed in the wing.

- **Center Tank:** This water tank combines with the structure used to hold the aluminum passenger payload for mission 2. Water has less room to shift, and the tank walls take up less area, reducing the number of places where leaks in the tank can form.
- **Wing Tank:** This configuration was initially investigated because of perceived weight savings. The load is distributed over the wing, reducing stress in the wing spar during flight. As water gets released, residual water may shift back and forth making it difficult to stabilize in roll. A gyro will



help keep the aircraft laterally stable during the water release. The larger surface area of the wing tank increases the number of places where a leak may occur.

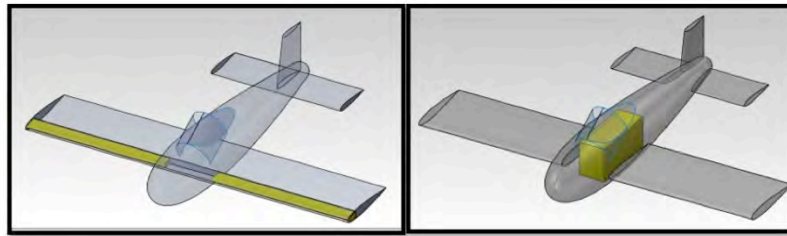


Figure 3.9: Water Tank configurations

FOM	Weight	Center Tank	Wing Tank
System Weight	50	0	0
Stability	30	0	0
Reliability	20	0	-1
<i>Total</i>	<i>100</i>	<i>0</i>	<i>-20</i>

Table 3.6: Water Tank Figures of Merit

A center fuselage tank was selected because it provided less surface area for the water and minimized CG shift during the water release.

3.6.6 Water Release Configuration

It is important that the release system stays sealed and does not leak before reaching the 100-meter altitude. The servo actuated release system must work every time and provide a sufficiently visible plume for the judges. Three different configurations were analyzed and tested to observe how well they stayed sealed when not actuated.

- **Plug release:** A servo would pull up a plug that was fitted to a hole at the bottom of the tank. The weight of the water would keep the plug sealed, however, a lot of torque was required from the servo to release the water. The edges of the exit had to precisely conform with the plug in order to not let any water leak.
- **Door release:** The back end of the tank was fitted with a door hinged from the top that was prevented from opening by use of a pin that would be removed by a servo. The door and doorframe were heavy, and the sealing material used between the locking interfaces was difficult to make completely watertight.
- **Boom release:** An exit pipe connected to a latex tube that was kept in a bent upward position by a servo arm. This kink in the latex tube was enough to prevent water from flowing out of the tank.

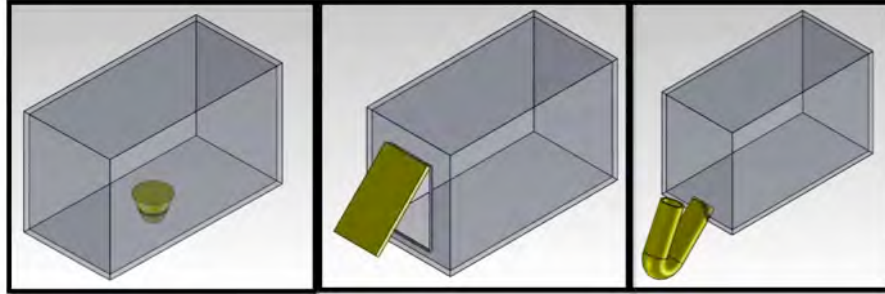


Figure 3.10: Water release configurations

FOM	Weight	Plug	Door	Boom
System Weight	40	0	-1	1
Watertight	30	0	-1	1
Reliability	15	0	-1	1
Manufacturability	15	0	0	1
<i>Total</i>	<i>100</i>	<i>0</i>	<i>-85</i>	<i>100</i>

Table 3.7: Water Release Figures of Merit

The boom release method offered a simple and very reliable way of releasing the water less susceptible to errors in manufacturing.

3.7 Conceptual Design Summary

The finalized conceptual design is a conventional aircraft, powered by a single tractor propeller, and features a tricycle landing gear configuration that will take the landing loads during touchdown. The water tank and aluminum payload share the same space and the water release system includes a bent latex tube that prevents water from flowing until let loose by a servo arm. This final concept reflects the qualities that the team deemed important in order to obtain a high score at the competition.



Figure 3.11: Final conceptual design sketch



4.0 Preliminary Design

Preliminary design took the configuration proposed during the conceptual design phase and applied it to a mission model that would output several aircraft. This section shows how the sizing and optimization of each subsystem was done to converge on an aircraft that would score the highest at the competition.

4.1 Design and Analysis Methodology

From a set motor, battery type, fuselage dimension, landing gear configuration, tail volume, wing airfoil, and chord, the optimization program started the sizing process with a simulation of mission 3 since it carried the heaviest payload of all missions (4.41-lbs of water). This mission would set the required wing area for the aircraft. It cycled through a large number of propulsion systems with varying numbers of battery cells and propeller types. The aircraft increased its wingspan, as the chord was kept constant, until it was able to take off within 90-ft (a 10-ft safety margin was imposed). After speeding up to its best climb speed, the aircraft went up to a 100-m altitude, at which point time to climb (T_{team}) and energy required were recorded. If the energy available in the batteries was less than that required, then the aircraft was discarded. This was repeated again for different propulsion systems and resulted in a list of successful aircraft.

The list of aircraft were then passed through a simulation of mission 2 where the propulsion system was varied, but this time only the lightest system with enough energy to complete three laps with the 3.75-lb aluminum passenger payload was kept for each aircraft. These aircraft were then passed through a simulation of mission 1 with their propulsion weight not to exceed mission 2 or 3 to keep empty weight at a minimum. The aircraft flew the course at their maximum level flight speed for four minutes and only the propulsion systems that completed the most laps were kept. The chart below shows how the optimization program works.

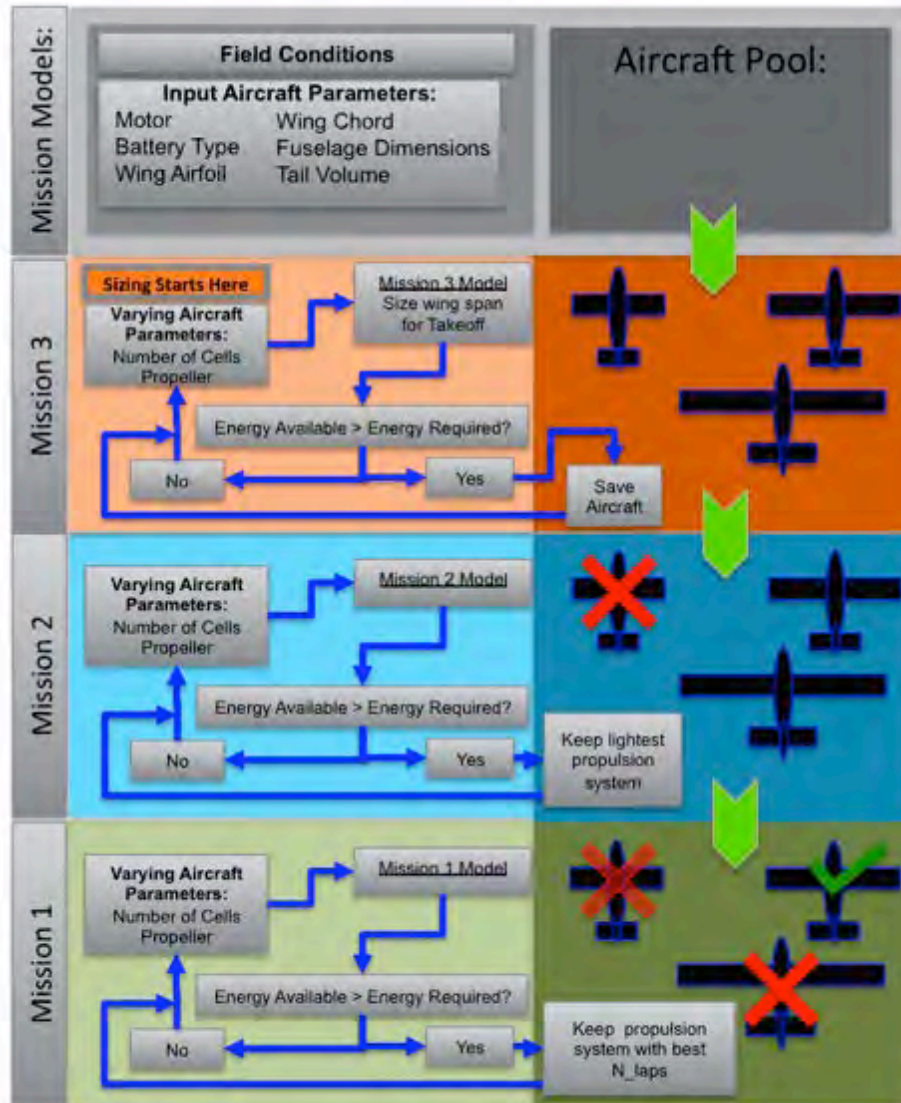


Figure 4.1: Optimization program flow chart

Out of the aircraft that completed mission 3, those with small spans tended not to complete mission 2 because of the endurance requirement with a heavy payload and increased induced drag. The aircraft with large spans were not ideal for mission 1 because, when flown at their max velocity, their large parasite drag from the wings drained a considerable amount of their small battery packs.

The list of aircraft that were able to complete all three missions were then entered into the score equation and plotted with respect to span. This process was repeated for different airfoil, motor, and battery type options, one at a time, to see their effect on the total score.

Optimization Analysis

The optimization code made use of structures, drag, propulsion, and energy models. An accurate weights build-up and drag model were crucial to the sizing program because they strongly affected flight velocities and energy consumption. Safety factors on thrust and power were applied to make up for



uncertainties in the calculations, which were later readjusted using flight data from the first prototype to calibrate the code.

- **Wing Chord:** The competition rules did not put any limit on wingspan. Aerodynamics says that increasing aspect ratio will improve range and overall flight efficiency, which could allow the aircraft to reduce battery weight. To maximize range, $C_D/C_L^{1/2}$ must be minimized and aspect ratio is present in the denominator [2].

$$\frac{C_D}{C_L^{1/2}} = \frac{C_{Dp}}{C_L^{1/2}} + \frac{C_L^{3/2}}{\pi \cdot AR \cdot e} \quad \text{(Equation 4.1)}$$

For a given wing area, this will reduce the needed chord. Laminar flow at low Reynolds numbers can have devastating effects on airfoil drag as it can separate more easily. Drag starts to significantly deteriorate airfoil performance below a Reynolds number of 200,000, which corresponds to takeoff speeds of around 35 ft/s for 9-inch chords. Thus this set a minimum chord length of 9 inches.

- **Wing Airfoil:** Early in the design process, thin airfoils below 10% t/c were eliminated due to their susceptibility to laminar flow separation. Comparisons were made between different high lift low Reynolds number airfoils to see which would result in a higher score. They were of varying thickness, Cl max, and drag bucket behavior.
- **Tail volume:** Using historical aircraft data on tail volumes, an initial estimate for horizontal and vertical tail volume was made ($C_h = 0.5$, $C_v = 0.035$). Due to the small fuselage, tail surface size could be reduced and still maintain lateral and longitudinal stability.
- **Motor type:** Motors with a 300 watt output provided good thrust for their weight while larger watt motors started getting too heavy (more than 8oz). Smaller watt motors provide insufficient thrust to takeoff with a max payload weight of 4.41-lbs of water. To be able to output sufficient power and still remain below 20 amps, a low Kv motor is required. Motors in the 300-600 Kv range were investigated and from the start it was seen that outrunners were heavier than geared inrunners in the 300 watt class.
- **Battery type:** The optimization study looked at the effect of different battery cells as they come with different weight, capacity, and cell resistance, all of which strongly affect mission performance.
- **Cell count and propeller choice:** Successful combinations of these two parameters were an output of the optimization code to satisfy takeoff, energy, and flight requirements.

4.2 Mission Model

The mission model was used to estimate power and energy requirements for each mission. Its capabilities are shown below:

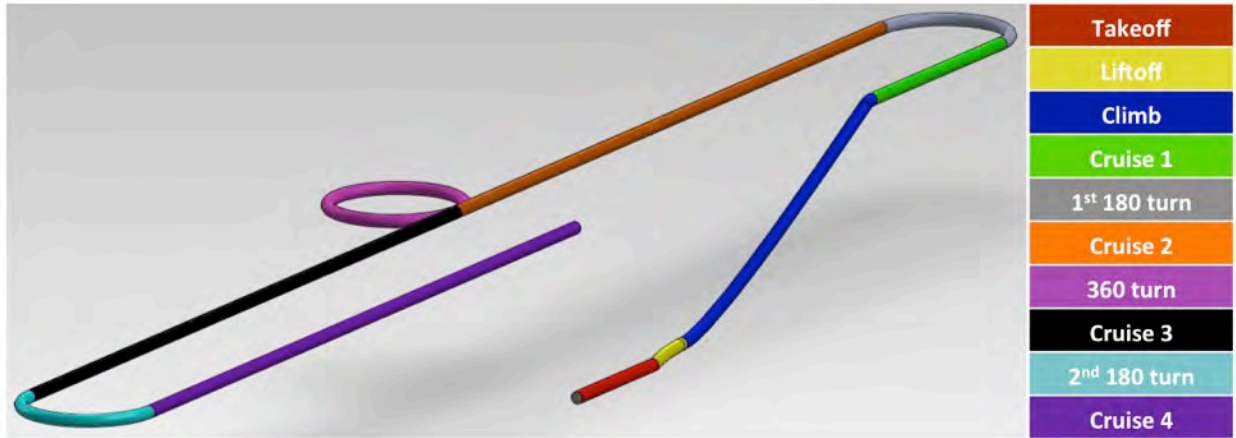


Figure 4.2: Mission model

Takeoff: This starts from a still position on the ground, and sees the aircraft accelerate to takeoff speed at full throttle.

Liftoff: After takeoff, the aircraft will reach its best climb speed before climbing up to pattern altitude.

Climb: The aircraft will arrive to a specified altitude while flying at its best climb speed.

Cruise: This is done at pattern altitude at max speed for mission 1, and at best range for mission 2.

Turn: Turns take up a significant part of the total flight time, so making them as short as possible is important. What limits the radius of the turn is the structural loading and L/D max of the wing. Turns were made at an equivalent load factor of 3 using the weight from mission 3. Since the wings are sized for mission 3, which has the heaviest payload, structural loading for mission 1 can be significantly increased since it flies empty.

Assumptions: The mission model assumes no headwind or crosswind conditions.

4.3 Design and Sizing Trades

To understand the influence of certain design choices on the total score, the optimization program was run with one characteristic changing at a time. A baseline aircraft was needed to make the comparisons. Its characteristics are shown below.

Airfoil	Motor	Battery
Eppler 214	Hacker B40-14L	Elite 1500

Table 4.1: Baseline aircraft specifications

4.3.1 Aerodynamic Trade-offs

The airfoils considered were high performance low Reynolds number airfoils. The most significant contribution to aircraft performance/score is how compatible the airfoil is with the speed and lift requirements of the aircraft. A heavy payload will favor airfoils with a high $C_{l_{max}}$. Also, the airfoil's drag at cruise conditions should be minimal. The airfoils shown in Figure 4.3 differ in best L/D, and CL_{max} , but have about the same low C_L behavior. The plots were obtained through Xfoil [3].

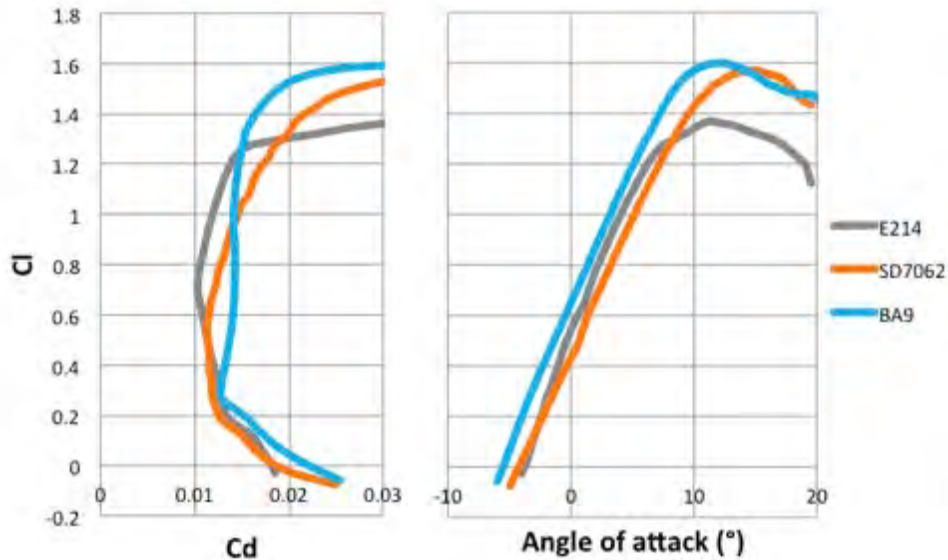


Figure 4.3: Aerodynamic characteristics of airfoils considered

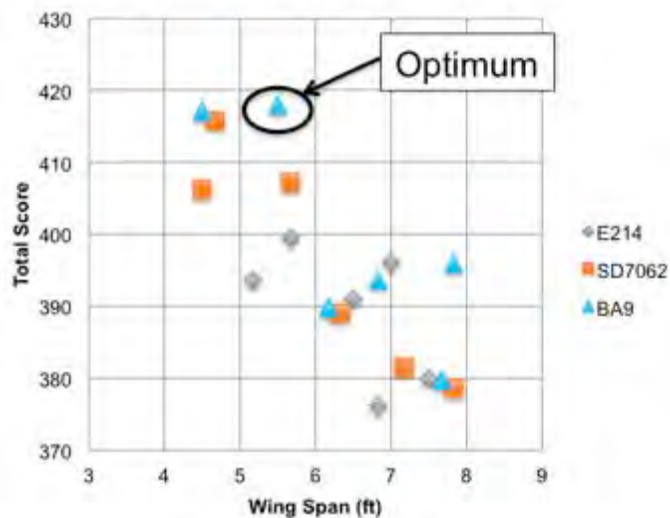


Figure 4.4: Effect of airfoil selection and span on total score

After taking each airfoil through the optimization program, it was seen that the BA-9 scored above the other airfoils. Its steep drag bucket and higher Cl_{max} were a contributing factor.

4.3.2 Propulsion System Trade-offs

Motor Selection

Inrunner motors with a Maxon 4.4 gear drive reduction were considered. A 6.7 gear reduction, which was heavier, would have brought down effective K_v to a point where RPM was too low, making it difficult to have decent prop pitch speed, and increasing the battery voltage to make up for RPM loss would have resulted in a heavier battery pack. Every motor was run in the optimization code with different sets of props and battery combinations.



Motor	Kv	Wt. (oz.)	Rm(ohms)	Idle Amps	Continuous Watts
Neu 1107 2.5Y + 4.4	557	5.0	0.033	0.75	300
Neu 1107 6D + 4.4	432	5.0	0.058	0.45	300
Hacker B40-14L + 4.4	487	7.34	0.035	0.86	300
Hacker B40-21L + 4.4	325	7.34	0.078	0.42	300

Table 4.2: List of motors considered

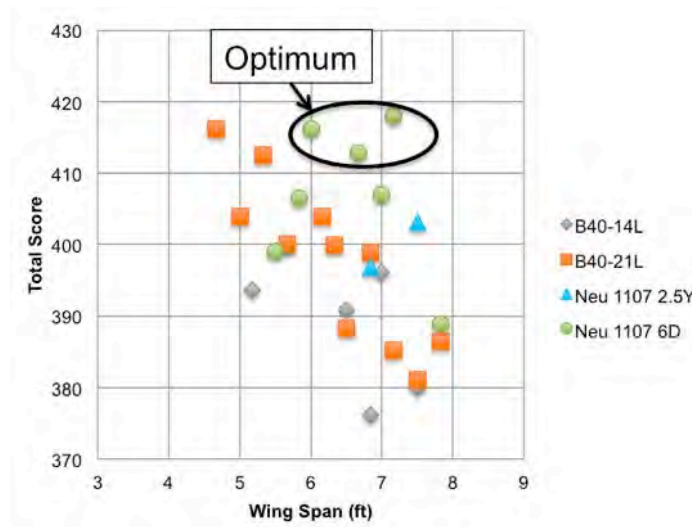


Figure 4.5: Effects of motor selection and span on total score

According to the optimization study, the Neu 1107 6D resulted in the highest total score. It needed less battery cells than its immediate competition, and weighed less. Its good performance at higher wing-spans shows how it uses the energy from each cell more efficiently.

Battery Selection

A low Kv motor should be accompanied by a high voltage battery pack in order to maximize motor RPM. Depending on the energy demands of the mission, a high voltage battery pack can be composed of cells with less mAh than a smaller battery pack. Cells with less capacity also weigh less. They come with the disadvantage of increased resistance, but the optimization program will show if it nullifies the effect of their weight loss. Elite 1500 battery cells have the most capacity for their weight, while the KAN 650 provide a little less than half the capacity at half the weight.

Battery	Capacity (mAh)	Resistance (ohms)	Weight (oz.)	Energy density
Elite 1500	1500	0.009	0.81	1852
Elite 2000	2000	0.009	1.16	1724
KR1400	1400	0.013	1.2	1167
KR500N	500	0.019	0.6	833
KAN650	650	0.014	0.49	1327

Table 4.3: List of batteries considered

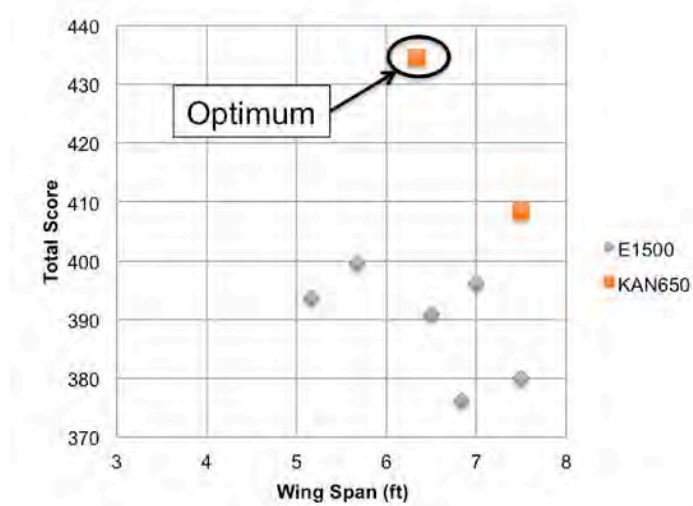


Figure 4.6: Effects of battery selection and span on total score

The KAN650 cells show that a sacrifice in mAh is necessary in order to gain a significant advantage in weight.

4.3.3 Final Optimized Aircraft

Airfoil	Motor	Battery
BA-9	Neu 1107 6D 4.4:1	KAN 650

Table 4.4: Specifications of the optimized aircraft

The selection of these three features for the aircraft subsystems through an investigation of their effect on the competition score was the result of the first step in the aircraft preliminary design. The BA-9 brought down the stall speed, the Neu 1107 6D allowed the aircraft to perform at high voltage and high prop pitch speed, which in turn made the use of low capacity, lower weight KAN650 cells more possible. Below is the optimization run for the selected subsystems with a peak score occurring at a span of 4'10".

	Mission 1	Mission 2	Mission 3
Prop	8x7	12x6	14x7
Number of cells	21	21	21

Table 4.5: Optimized propulsion systems for all missions

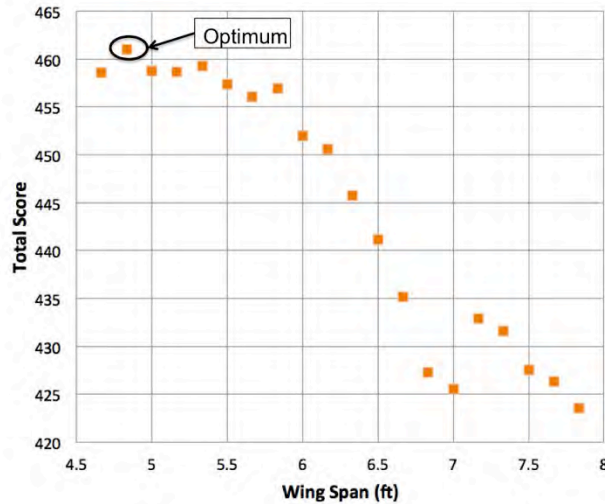


Figure 4.7: Effects of span on total score for final plane design

4.4 Lift, Drag and Stability Characteristics

This section details the flight characteristics of the optimized design. The drag polar and L/D curve for the entire aircraft are shown below. Each mission is flown with a different C_L . Mission 1 is a fast mission, so the aircraft will fly at the C_L that will give it its max flight speed and minimum induced drag. Mission 2 is flown at the C_L for best range. Mission 3 is a climbing mission, so its C_L is that for max L/D.

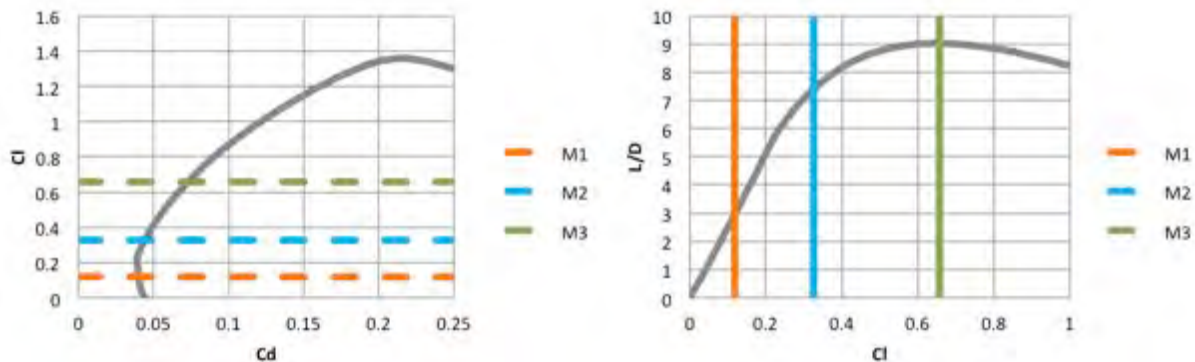


Figure 4.8: Left: Drag polar of the entire plane. Right: Lift to drag ratio of the entire plane

Drag

The drag buildup for each mission, Figure 4.9, shows the relative contributions of friction and induced drag. Drag calculations were done as prescribed by Mark Page [4]. Mission 1 has minimum induced drag and is dominated by friction forces as seen from its low cruise C_L . Mission 2, flown at the speed for best range, is still friction drag dominated since the speed for best range is high. In order to maximize rate of climb, Mission 3 must be flown at max L/D where friction drag equals induced drag.



Figure 4.9: Drag profile for all missions

Stability and Control

The aircraft's flight C_L is highest for mission 3. A Trefftz plot, shown in Figure 4.10, was created, with the geometry input in Figure 4.11, with the Athena Vortex Lattice (AVL) program, which was developed by Mark Drela and Harold Youngren at MIT [5]. This plot verified that peak C_L occurred within 50% of the semi-span and that section C_L 's did not exceed $C_{L\text{max}}$ at any point.

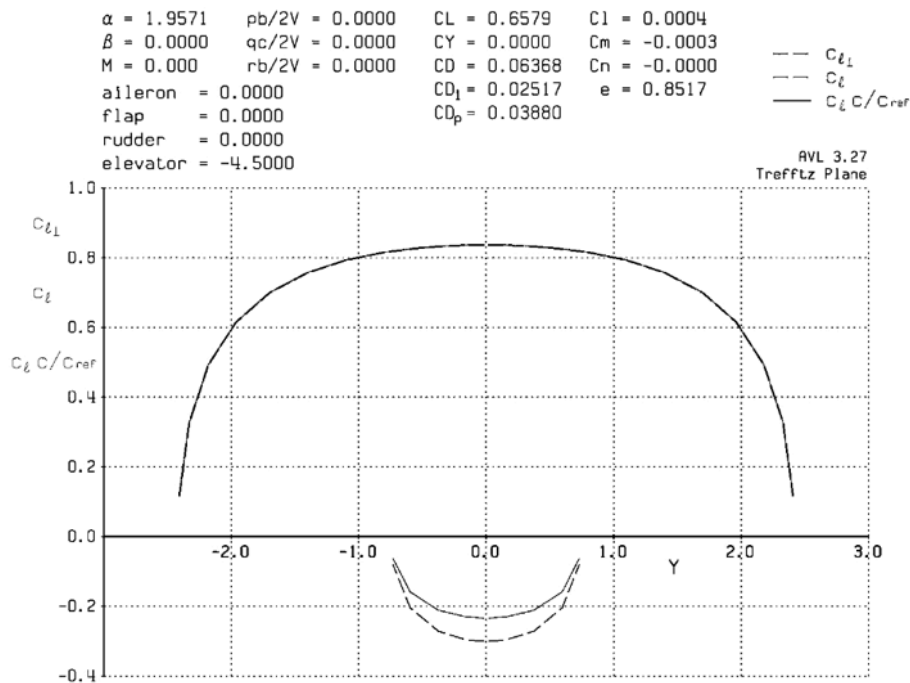


Figure 4.10: Trefftz plot

In order to evaluate the effects of the high climb rate and slow speed of mission 3, its flight conditions were simulated in the AVL program. The geometry input model is shown in Figure 4.11. The weights and drag build-up previously performed were included in the model by specifying an estimated C_{Dp} for the various components as well as mass properties for each.

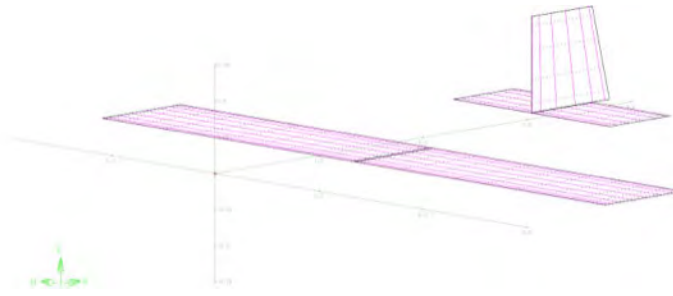


Figure 4.11: Geometry input model

AVL takes the input geometry and uses an extended vortex lattice method to calculate the stability and control derivatives and the open loop transfer functions for the control surfaces. Figure 4.12 shows the resulting pole-zero map of the eigenvalues calculated by the program.



Figure 4.12: Pole-zero map

All modes achieve level 1 criteria for a class I plane per MIL-SPEC 8785C [6] with two exceptions. The only unstable mode was a slight spiral divergence. But with a time-to-double of 5.54 seconds, it falls under level 3 specifications. In addition, the Control Anticipation Parameter falls within level 2 criteria, having an n/α of 10.59 g's/rad at a short period natural frequency of 9.99 rad/sec. Upon conducting further research, it was found that these are very common values for small-scale UAVs as discussed by Tyler Foster of Brigham Young University [7].

4.5 Predicted Mission Performance

An output from the mission model was the time and energy consumption for each mission. The aircraft uses at most 70% of the available energy leaving 30% of the energy as a factor of safety.



	M1	Time track (s)	Energy (KJ)
1 st Lap	Takeoff	1.9	0.39
	Liftoff	3.4	0.71
	Climb	11	2.22
	Cruise 1	11.1	2.24
	1st 180 turn	12.7	2.52
	Cruise 2	20.6	3.75
	360 turn	23.3	3.82
	Cruise 3	31.6	4.95
	2nd 180 turn	33	5.02
	Cruise 4	41.2	6.13
2 nd through 6 th Lap
	Cruise 4	230.2	30.79
7 th Lap attempt	1st 180 turn	239.1	32.25

	Cruise 4	268	35.72
Landing	End of mission	280.5	36.37

Table 4.6: Mission 1 profile

	M2	Time track (s)	Energy (KJ)
1 st Lap	Takeoff	4.0	1.92
	Liftoff	5.1	2.41
	Climb	11.8	5.06
	Cruise 1	11.9	5.10
	1st 180 turn	16.3	6.56
	Cruise 2	24.2	8.31
	360 turn	32	10.16
	Cruise 3	39.6	11.84
	2nd 180 turn	43.5	12.76
	Cruise 4	51	14.41
2 nd and 3 rd Lap
	Cruise 4	142.9	35.18
Landing	End of mission	156.9	38.43

Table 4.7: Mission 2 profile



	M3	Time track (s)	Energy (KJ)
1 st Lap	Takeoff	3.8	2.46
	Liftoff	4.8	3.06
	Climb	31.3	18.07

Table 4.8: Mission 3 profile

5.0 Detail Design

Following the optimization process and mission profile predictions, the aircraft dimensions were finalized. The prototype of the final design was then built and tested to confirm the mission profile predictions.

5.1 Dimensional Parameters

Table 5.1 details the dimensions, propulsion system and electronics of the final design.

Wing		Horizontal Stabilizer		Vertical Stabilizer	
Span	58"	Airfoil	SD8020	Airfoil	SD8020
Chord	9"	Span	18"	Span	8"
Aspect Ratio	6.44	Chord	7"	Root Cord	9"
Wing Area	522 in ²	Area	126 in ²	Tip Chord	7"
Airfoil	BA9	Incidence	0	Rudder	
Static Margin	31.3%	Elevator		Span	8"
Aileron		Span	18"	Root Cord	3.375"
Span	26.5"	Chord	2"	Tip Chord	2"
Chord	2.25"	Deflection	±15°	Deflection	±20°
Deflection	±10°	Motor		Batteries	
Fuselage		Type	Neu 1107-6D	Type	KAN650
Length	34"	Kv	1900 rpm/v	Capacity	650 mAh
Width	6"	Gear Box	Maxon 4.4:1	R	0.014 Ω
Height	6.5"	RPM _{max}	60,000	V	1.2 V
Electrical System		I _o	0.45 A	I _{max}	30 A
Speed Controller	Phoenix ICE Lite 50	R _m	0.058 Ω	Number of Cells	21
Radio Receiver	Spektrum AR7000	P _m	300 watt	Pack Energy	43 KJ
Number of Servos	6	Propellers	8x7, 12x6, 14x7	R _{pack}	.294 Ω
Servo Type	HS-65 MG			V _{pack}	25.2 V

Table 5.1: Dimensional parameters

5.2 Structural Characteristics and Capabilities

This section describes the structural characteristics and capabilities, as well as the advantages that each component adds to the overall design. The sensitivity analysis determined that weight was the most important parameter, so the biggest focus was made on making the aircraft as light as possible. Before a formal detailed design could be finalized, an analysis of the aircraft loads along the wing and fuselage was made in both flight and landing scenarios.

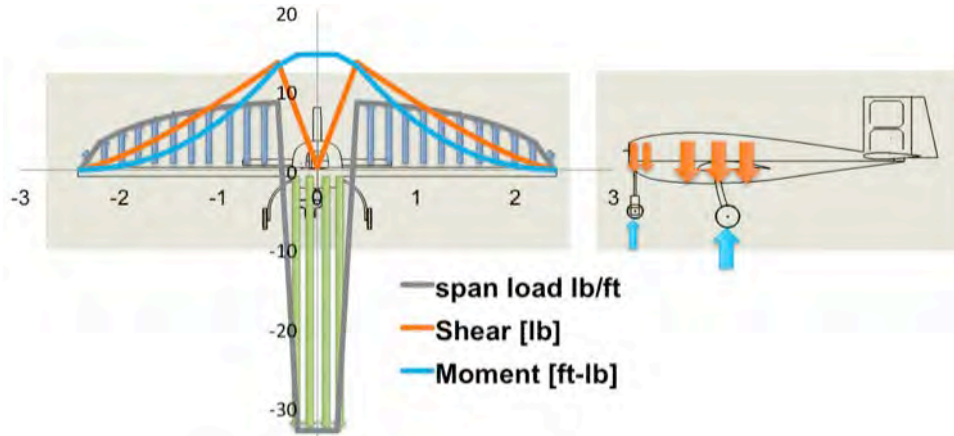


Figure 5.1: Shear and moment diagram

The wing was designed to take on a 3 G load for mission 3 and therefore an 8.7 G load for mission 1. Using the max load, lift and speeds for each mission, the operational flight envelope was created (see the V-n diagram below). Mission 3 is note worthy for its higher max velocity compared to missions 1 and 2. Its propulsion system is meant to maximize thrust and obtain as high a climb rate as possible, to the point where half the battery is used up in the 30 seconds that it takes to climb 100 meters.

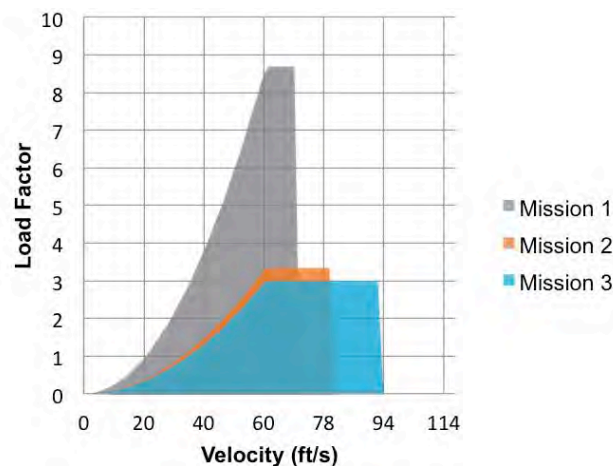


Figure 5.2: V-n diagram

The fuselage structure is comprised of a structural central carbon rod and non load-bearing foam-fiberglass composite fairing. All loads during landing would be transmitted through the spar-rod connection (wing-box) down to the landing gear. The passenger and water payload were supported by a



basket-type structure that hung from the wing-box. The water tank featured a latex tube situated at the tank exit that was bent by a servo until the water needed to be released. This system proved to be lighter and more reliable than other release systems considered. The wings had a square carbon spar and foam ribs with carbon rims to provide rigidity. So-lite[®] that covered the spar and ribs completed the wing structure in what resulted in a very light and strong wing. All the components combined to make a lightweight aircraft that could effectively compete for the highest score.

5.3 System Design and Component Selection/Integration

The following subsystem components were analyzed with more detail to finalize the aircraft design.

5.3.1 Passenger Payload Accommodation

The 2x4 passenger layout had to follow strict clearance requirements set by the competition rules. There needed to be at least a 0.5" clearance fore/aft and around/between each passenger except along the outside walls. Also, an aisle of 1" minimum width had to run between the columns of passengers. Structure within the space between the payloads is allowed as long as it does not become a significant obstruction. The payload support structure consisted of the spar, fuselage rod, and water tank walls. The water tank, hanging from the wing-box, yielded a very light support structure because it eliminated the need to have rigid members to hold up the payload. Precautions had to be taken to ensure that all clearance requirements were met and there would be enough volume for two liters of water. The payloads were held in place on the floor and at mid-height with thin foam plates with holes in them to insert the payload.

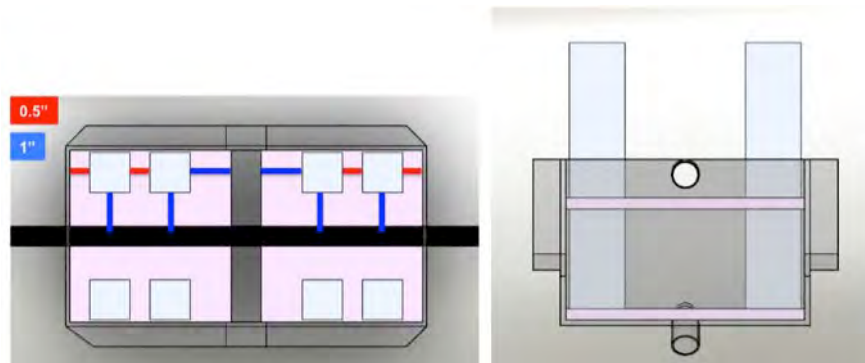


Figure 5.3: Payload accommodation

5.3.2 Water Tank

The water tank needed to provide support for the aluminum payload and be sealed to hold the water. The aircraft also could not shift its center of gravity in flight after releasing the water. The tank walls for the prototype were made of a carbon/foam composite which gave it enough rigidity to hold the water or aluminum payload. The water stayed isolated while the tank was kept very light. On the first prototype, the tank walls needed to be sealed with silicone where the landing gear pierced the tank. On subsequent designs this flaw was corrected by having the landing gear follow the edge of the spar until it came out of

the tank. The water release system consists of a 0.75" diameter carbon fiber tube joined to a nozzle at the back of the tank using a latex tube. The latex tube allows the two-section carbon fiber tube to bend and produce a kink, which seals the water tank. A servo mounted on the tank keeps the carbon tube bent shut. The servo swings its arm down when the 100 meter altitude has been reached releasing the carbon tube and the water. A baffle was used to reduce sloshing effects. Flight tests showed that during the discharge time (~15 seconds) water shifting in the tank did not affect the ability of the pilot to control the aircraft, so the horizontal tail volume of 0.5 proved to be adequate to control the aircraft during the water discharge.

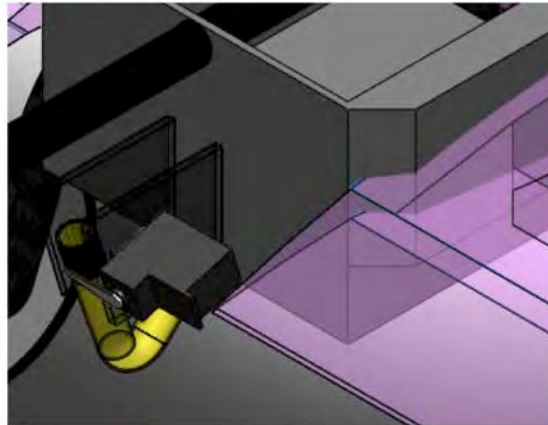


Figure 5.4: Water tank release system

5.3.3 Wing-box

The wing-box is the central structure co-cured to the wing spar that directs the wing loads to the landing gear on landing. This structure also connects the wing spar to the fuselage rod and payload holder.

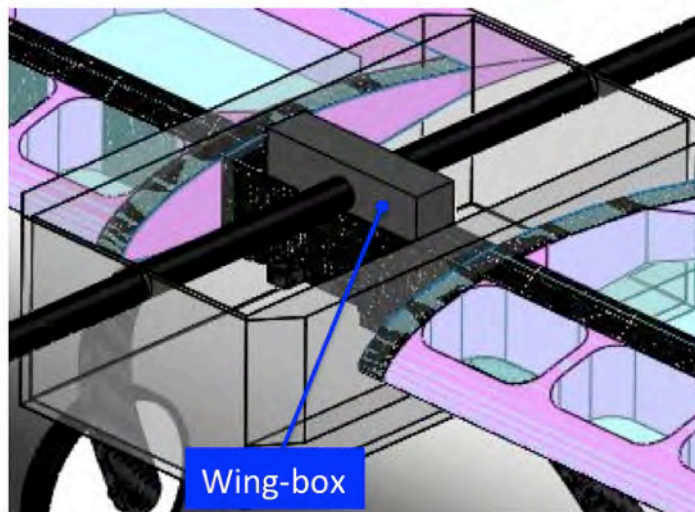


Figure 5.5: Wing-box placement

5.3.4 Wings/tails

The objective of the wing and tail design was to reduce weight as much as possible while still being sufficiently strong. Several wing-manufacturing methods were explored that are explained in section 6. The wing was created using a carbon spar with carbon reinforced foam ribs, which was then covered in So-lite[®] material. This wing design eliminated most of foam core that comprised most of the wing's initial weight. The same manufacturing technique was also used for the tails.

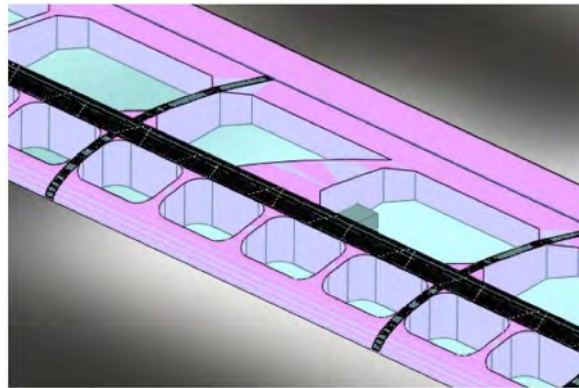


Figure 5.6: Hollow foam and carbon fiber wing

The number and distribution of carbon fiber layers used in the spar was dependent on the cap width, which was varied in order to find the spar with minimum weight. Figure 5.7 shows the spar cap width vs. weight for the wing.

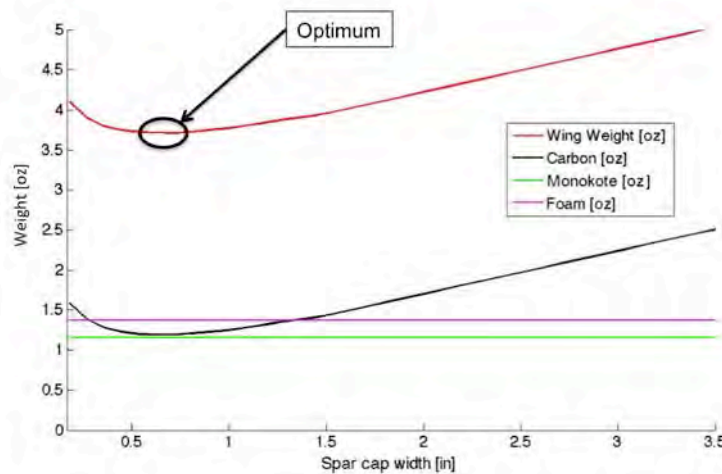


Figure 5.7: Effect of spar cap width on the total wing weight

Modeling was done in MSC Nastran to determine if the carbon fiber spar cap was enough to prevent compression buckling of the wing.



Figure 5.8: Compressive stress (psi) on the wing spar due to a 5 G load

5.3.5 Fuselage

The fuselage was made non-structural in an effort to make it as light as possible. The payload was the biggest shape constraint for the fuselage. The molded fuselage fairing, made of 1/16" foam and fiberglass, had a very rapid taper from the payload section to the tail (more than 7°) which caused concern that flow would separate and not flow nicely over the tail. MSC flow simulation software was used to model the flow over the fuselage at the flight conditions resulting from the high angle of attack required during the climb for mission 3. Flow stayed attached according to the simulation. The removable top hatch used for battery and payload access was made from the same mold used for the fuselage.

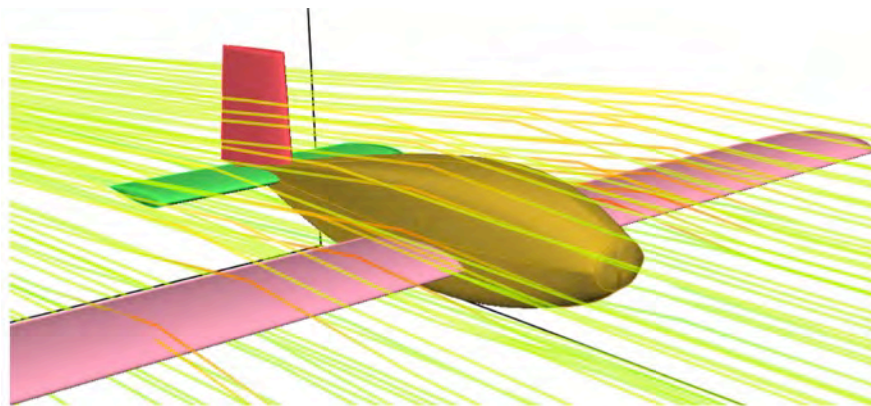


Figure 5.9: Flow simulation results

5.3.6 Tail-boom

A tail-sizing model varied the tail boom length and sized the tails using a prescribed tail volume, and determined the tail moment arm that resulted in the lightest weight of the tails and tail boom. The choice of a carbon laminated foam tail boom allowed for longer moment arms that reduced tail wetted area and helped in tapering of the fuselage.

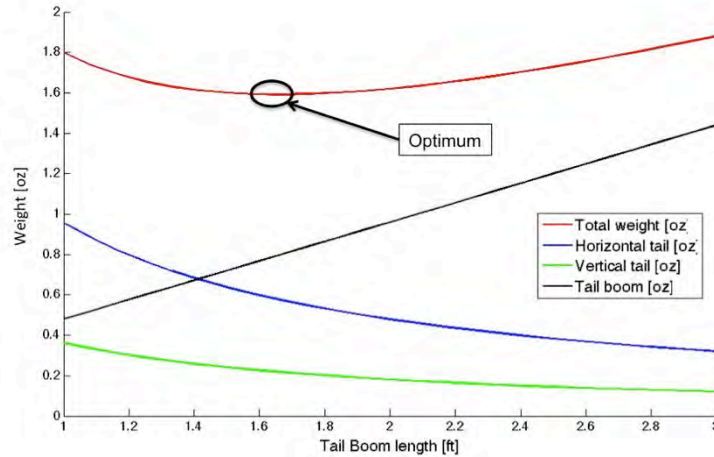


Figure 5.10: Effects of tail boom length on the total weight of tails and tail boom

5.3.7 Motor mount

The motor mount was designed with the motor offset to the side of the rod. This allowed for the attachment of a nose gear to the motor mount. Pre-trimming the rudder could counterbalance the yawing moment that the off-center motor created.

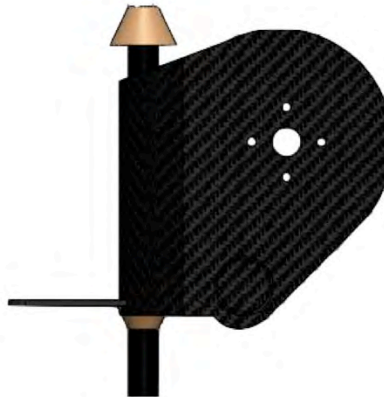


Figure 5.11: Off set motor mount with nose gear attachment included

5.3.8 Landing gear

The Tricycle configuration was chosen for its ground handling. Two different types of main gears were considered: one-piece inverted-U shape and a two piece wing-spar mounted landing gear. The inverted-U shape landing gear was chosen due to its modularity and ability to be mounted to the wing box. The nose gear was created in-house. A carbon rod was used as the strut and a carbon fiber mushroom axle mount at the bottom absorbed 20 percent of the landing force. The nose gear height was limited by the maximum prop diameter (14"). The optimum angle from the CG to the main gear was 14° for a tricycle gear. The main gear height was constrained by a -6° rake angle to minimize induced drag on the initial takeoff roll. The tread width of the landing gear was determined to be 12" in order to meet tip-forward requirements. Euler-Bernoulli beam theory was applied to determine the core thickness, width, and

number of layers of uni-carbon fiber that were needed to prevent buckling. The landing scenario assumed a 5G symmetrical landing with a safety factor of 3.0. This was assumed sufficient in conjunction with the nose gear. Simple finite element calculations were done assuming no taper on the gear and symmetrical sections. The initial calculations were done using MATLAB.

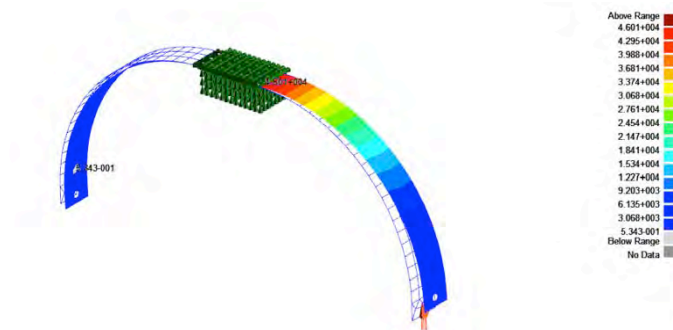


Figure 5.12: Compressive stress (psi) for one wheel landing

5.3.9 Electronics

Servo Selection

The most important factor when selecting a servo is proficient torque during flight. They were selected by analyzing hinge-moments for each control surface using AVL and then finding servos that had sufficient control power to handle the calculated moments, with the lightest weight possible. Five Hitec servos were considered: HS-225BB, HS-311, HS-85 MG (Metal Gear), HS-65 MG and HS-81 MG. These were compared according to their stall torque, weight and dimensions.

Servo	Stall Torque 4.8v (in-oz)	Stall Torque 6v (in-oz)	Weight (oz)	Dimensions (in)
HS-225BB	54.15	66.65	0.95	1.27" x 0.66" x 1.22"
HS-311	42	48.6	1.51	1.57" x 0.78" x 1.43"
HS-85 MG	41.66	48.6	0.77	1.14" x 0.51" x 1.18"
HS-81 MG	36.1	41.66	0.62	1.17" x 0.47" x 1.16"
HS-65 MG	24.99	30.55	0.42	0.92" x 0.45" x 0.94"

Table 5.2: List of servo considered

All of the servos considered had sufficient torque to move the parts; however, since weight and size were important factors in production, the HS-311 and HS-85 MG were deemed too heavy. While the HS-81 provided more than ample torque, the HS-65 was chosen because it provided the required torque in the smallest volume and lightest assembly.

Speed Controller Selection

The competition regulations limit the motor current with a 20 amp slow blow fuse. During motor testing it was discovered that when the motor was running full throttle at takeoff, the fuse would allow 20-25 amps to pass through it for a short time. This meant that higher than 20 amps would be needed for the peak value of any electronic speed controller (ESC) chosen. In addition, the high pack voltage (25.2v) necessitated that an ESC rated for high enough voltage be used.



ESC	Max (amps)	Max (volts)	Dimensions (in)	Weight (oz)
Phoenix 25	25	19.2	1.08 x 0.91 x 0.16	0.6
Phoenix Ice2 HV 40	40	50	1.8 x 1.7 x 0.8	2.2
Phoenix Ice Lite 50	50	25	1.6 x 1.00 x 0.67	1.7
Phoenix Ice 50	50	34	1.8 x 1.7 x 0.8	2.3

Table 5.3: List of speed controllers considered

The speed controller chosen was the Castle Creations Phoenix Ice Lite 50. Representatives from Castle Creations confirmed that the max voltage limit could be slightly surpassed as long as it was for a short period of time. It met the minimum specifications required while also being among the lightest of the speed controllers available.

Electronics Integration

All electronics except for the wing, tail, and release servos were housed in the compartment in the nose section in front of the payload. 4 KAN180 cells powered the receiver. An external switch was used to easily turn on/off the receiver to conserve energy while waiting in the flight line without opening up the aircraft. The fuse was mounted to the side of the fuselage in front of the payload. The altimeter circuit was located in the nose section in front of the wing as per the contest rules.

5.4 Weight and Balance

Aircraft weight, without payload, was estimated to be 2.49-lbs. A weight and balance table was computed for each mission based on weight estimates for the aircraft components. All measurements were made from a point 22 inches in front of the wing's center of gravity. Components were placed so that the aircraft's center of gravity would fall on the wing's quarter chord or slightly in front of it. The Payload was placed at the aircraft's quarter chord.



	Component	Weight (oz)	Arm (in)	Moment (oz-in)
Structure	Fuselage	6.1	22.0	134.9
	Wing	7.3	22.0	160.6
	Horizontal Tail	1.1	42.0	44.1
	Vertical Tail	0.8	42.0	31.5
Propulsion	Motor/Gearbox	5.0	11.0	55
	Speed Controller	1.7	15.0	25.5
	Battery	11.2	18.3	204.4
	Propeller	1.0	9.5	9.5
	Fuse/Holder	0.4	16.0	5.6
Avionics	Receiver / Rec. Battery / Rec. Switch	1.0	15.0	15
	Altimeter Circuit	0.1	15.0	1.2
	Nose Gear Servo	0.4	14.0	5.6
	Water Release Servo	0.4	27.0	10.8
Landing Gear	Nose Gear	1.0	11.0	11
	Main Gear	2.5	21.3	53.1
Total	Aircraft	39.9	---	767.8
	Center of Gravity (in)		19.26	

Table 5.4: Mission 1 weight and balance

	Component	Weight (oz)	Arm (in)	Moment (oz-in)
Aircraft	w/o Battery	28.7	19.7	563.4
	Battery	11.2	15.0	168.0
Payload	Eight Aluminum Passengers	60.0	19.8	1185.0
Total	Aircraft	99.9	---	1916.4
	Center of Gravity (in)		19.19	

Table 5.5: Mission 2 weight and balance



Component		Weight (oz)	Arm (in)	Moment (oz-in)
Aircraft	w/o Battery	28.7	19.7	563.4
	Battery	11.2	18.3	204.4
Payload	2 Liters of Water	70.6	19.8	1393.4
Total	Aircraft	110.4	---	2161.2
Center of Gravity BEFORE water release (in)			19.57	
Center of Gravity AFTER water release (in)			19.26	

Table 5.6: Mission 3 weight and balance

5.5 Flight Performance Parameters

The table below details the flight performance parameters for all three missions that were predicted by the mission model. These predictions were later compared to actual parameters obtained at the test flights.

C_{Lmax}	e	L/D_{max}	Available Energy (KJ)	Empty Weight (lbs)
1.36	0.89	9.05	43	2.49

	Mission 1	Mission 2	Mission 3
$C_{Lcruise}$	0.118*	0.3261	0.6575**
C_{Do}	0.0388	0.0349	0.0375
L/D_{cruise}	2.94*	7.49	8.763**
ROC_{max} (ft/min)	851	655	750
W/S (oz/ft ²)	11.0	27.6	30.5
V_{cruise} (ft/s)	70.6*	67.7	50**
V_{stall} (ft/s)	20.4	33	35
T/O distance (ft)	27	92	93
T/W (static)	0.55	0.54	0.63
Flight time (s)	240	142.9	31.3
Max G Load	8.70	3.35	3.00
V_{max} (ft/s)	70.6	80.6	93.5
Turn rate (deg/s)	138	46	40
Energy required (KJ)	36.4	38.4	18.1
TOGW (lbs)	2.49	6.24	6.90
Cruise current (amps)	6	8	19.5
*Cruise for Mission 1 is flown at V_{max}			
**Cruise for Mission 3 is flown at $V_{L/D_{max}}$			

Table 5.7: Flight performance parameters



5.6 Predicted Mission Performance

Aircraft parameters and mission outcomes from the mission model were used to predict the final competition score.

	Mission 1	Mission 2	Mission 3
Empty Weight	2.49	2.49	2.49
N_{laps}	6	---	---
FW_2	---	6.24	---
T_{team}	---	---	31.3
Flight Score	2.00	2.10	2.98
RAC	1.58		
Competition Score	100 x Flight Score / RAC = 448.1		

Table 5.8: Predicted mission performance

Mission 1 – Ferry Flight

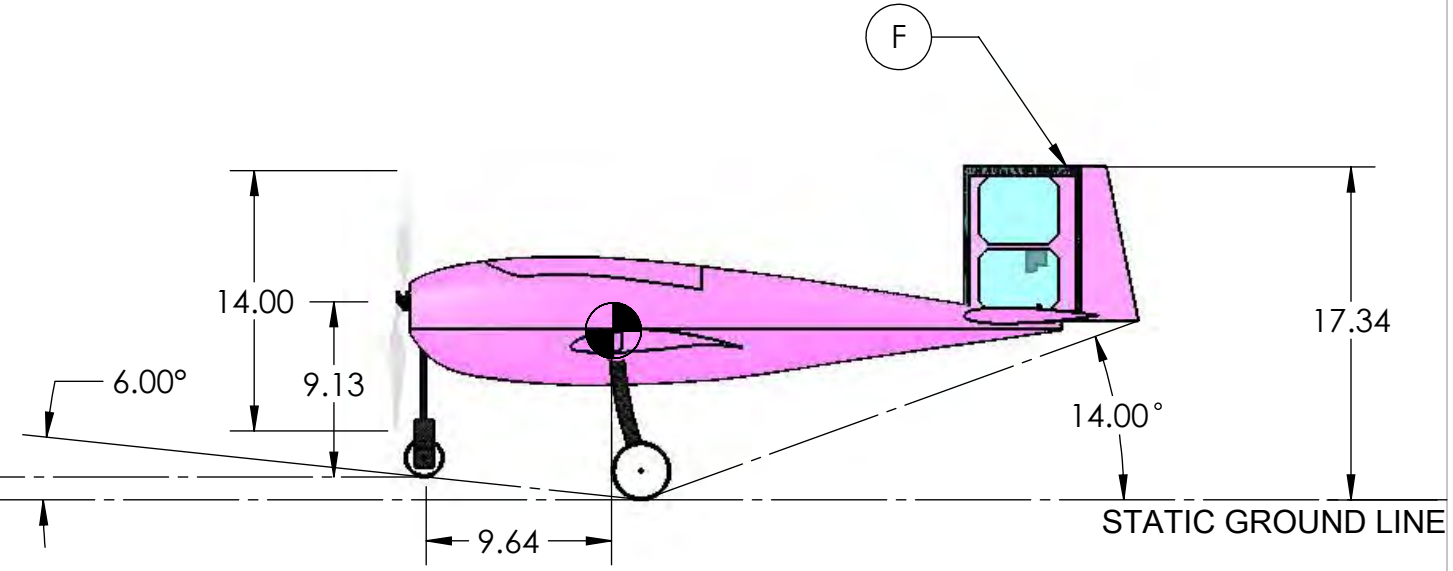
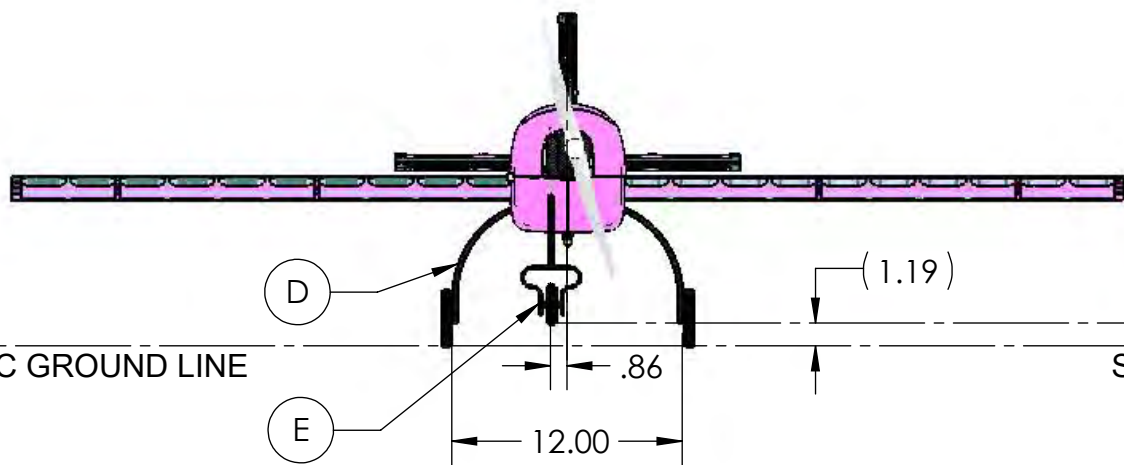
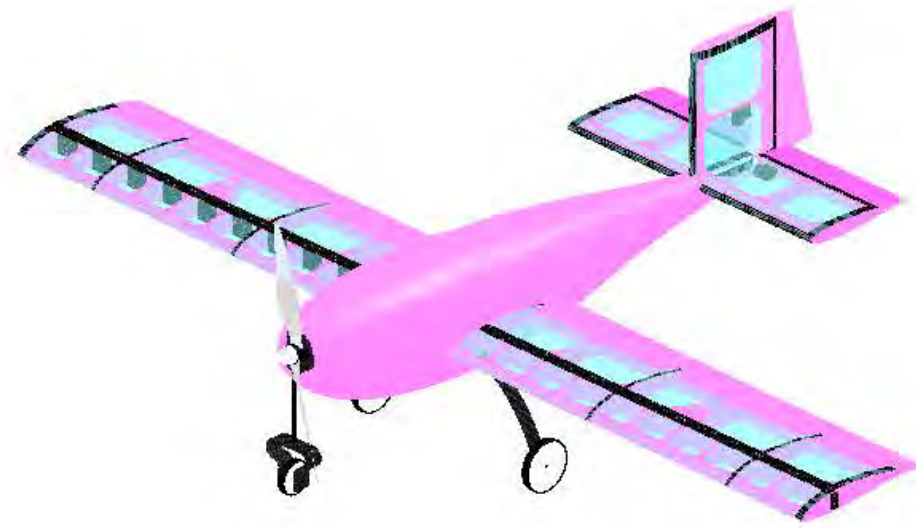
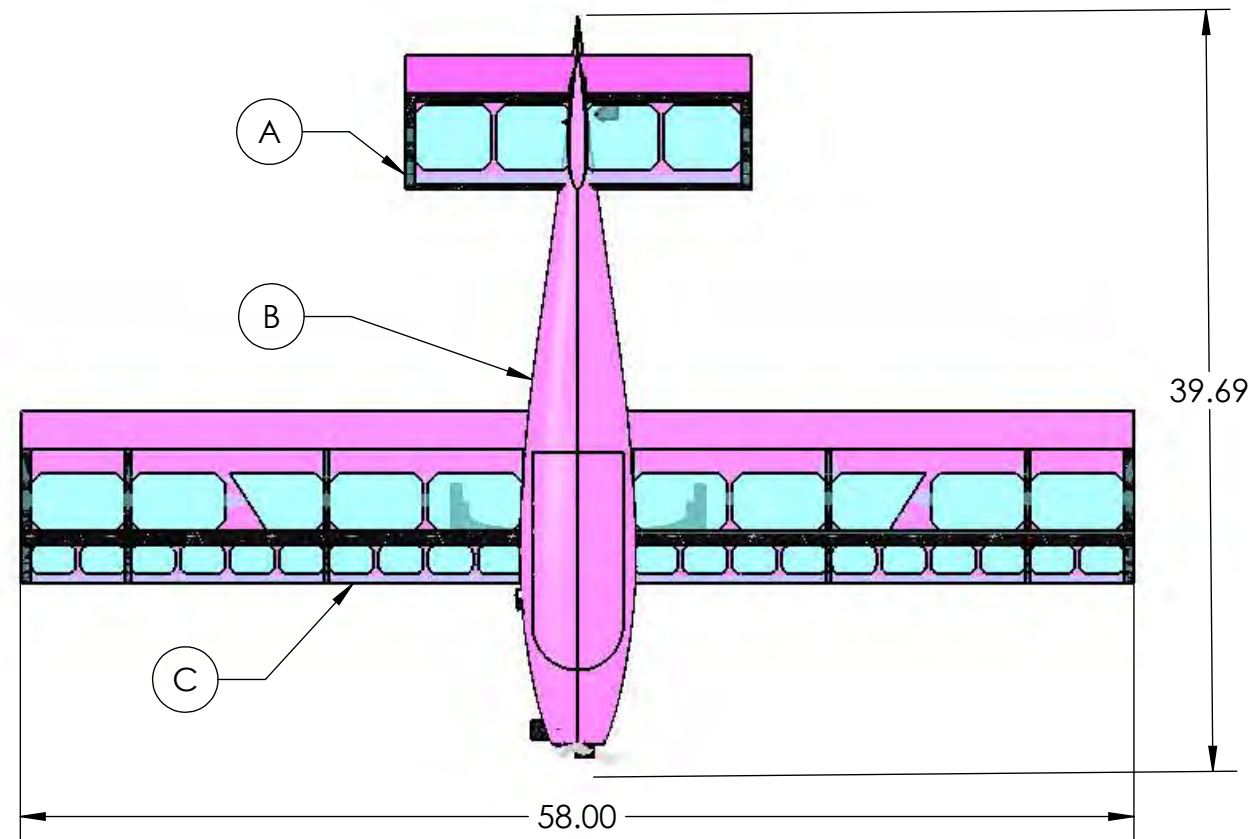
The main focus of this mission is to perform as many laps as possible within four minutes. This is an empty mission, so takeoff field distance is short and the aircraft lacks no power for climb. It will be able to fly at its max speed and make tight turns constrained only by its structural load limit. The aircraft is predicted to fly 6 laps within those four minutes. Flight tests will determine actual energy use and fine-tune the propulsion system to maximize the number of laps.

Mission 2 – Passenger Flight

The aircraft must provide enough thrust and energy to takeoff within 100-ft and complete three laps with the aluminum passenger payload. The flight is made at the aircraft's speed for max range to conserve energy. Critical to the success of the mission is the battery's ability to provide the energy required. Propulsion tests with the expected propulsion system will confirm the energy consumption. Flight weight factored into the score for mission 2, so battery weight was kept at a minimum, resulting in a takeoff weight of 6.24-lbs.

Mission 3 – Time to Climb

To minimize climb time for this heavy mission, thrust had to be maximized. The climb was made at the aircraft's best L/D. Due to the high thrust demand, energy consumption was high. The climb to 100 meters was predicted to be 31.3 seconds. Critical to the success of the mission, other than being able to release the water, was the ability to pull a high number of amps through the battery during the entire flight without damaging it. Flight tests will more accurately correlate the current draw with expected thrust and fine-tune the propulsion system such that climb time can be minimized without taking it beyond rated performance maximums.



STATIC GROUND LINE

STATIC GROUND LINE

STATIC GROUND LINE

PRIMARY COMPONENTS	
A	HORIZONTAL STABILIZER
B	FUSELAGE
C	WING
D	MAIN GEAR
E	NOSE GEAR
F	VERTICAL STABILIZER

NOTE:
 DIMENSIONS ARE IN INCHES
 TOLERANCES:
 ANGULAR: $\pm .5^\circ$
 ONE PLACE DECIMAL $\pm .100$
 TWO PLACE DECIMAL $\pm .030$
 THREE PLACE DECIMAL $\pm .005$

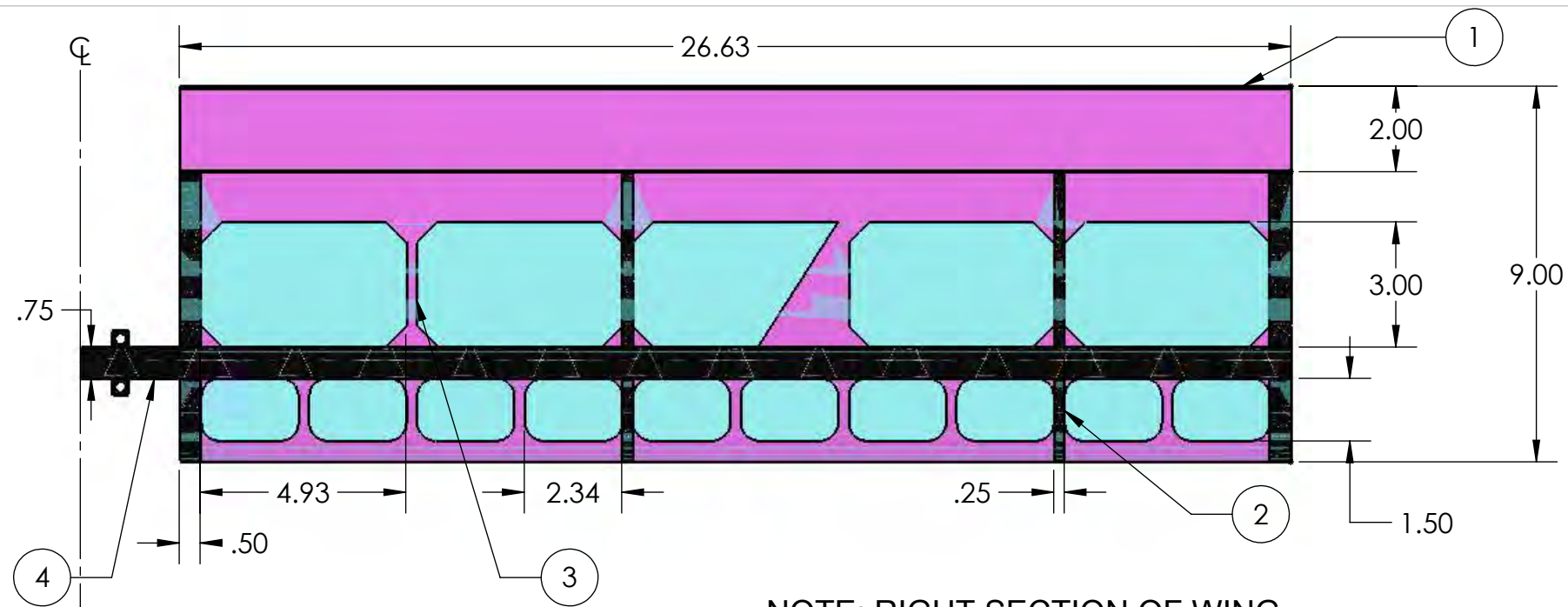


UNIVERSITY OF CALIFORNIA, IRVINE
 ANGEL OF ATTACK

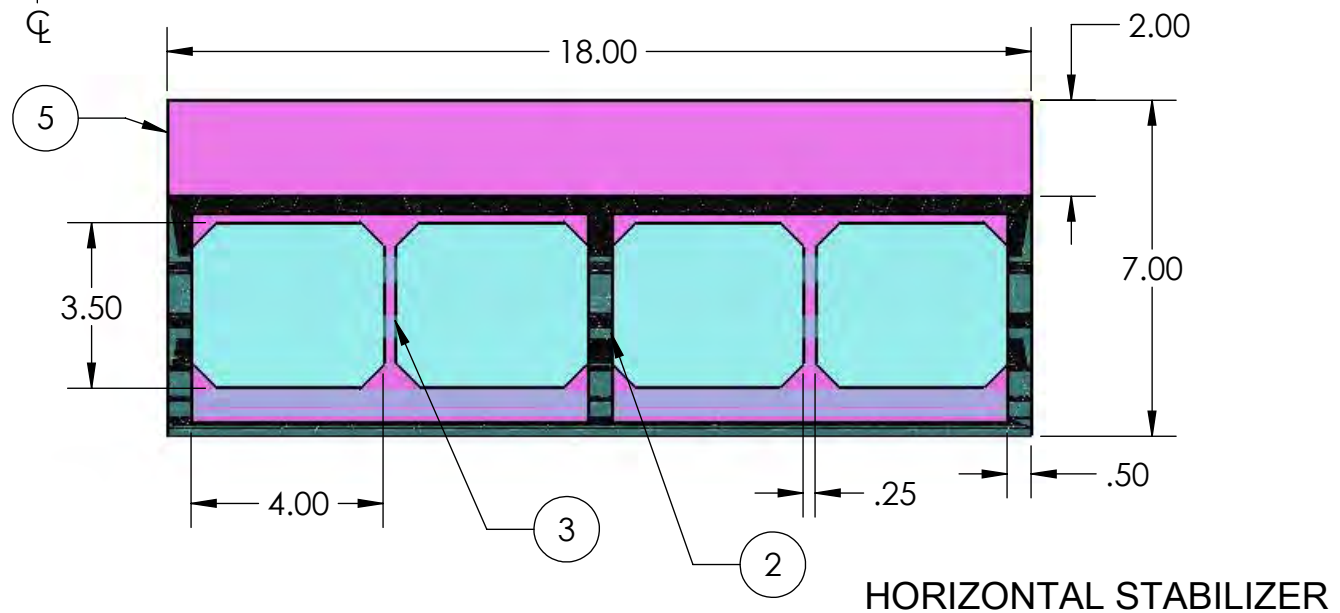
CESSNA-RAYTHEON-AIAA-DESIGN/BUILD/FLY 2012

DOCUMENT TITLE:
AIRCRAFT 3 - VIEW

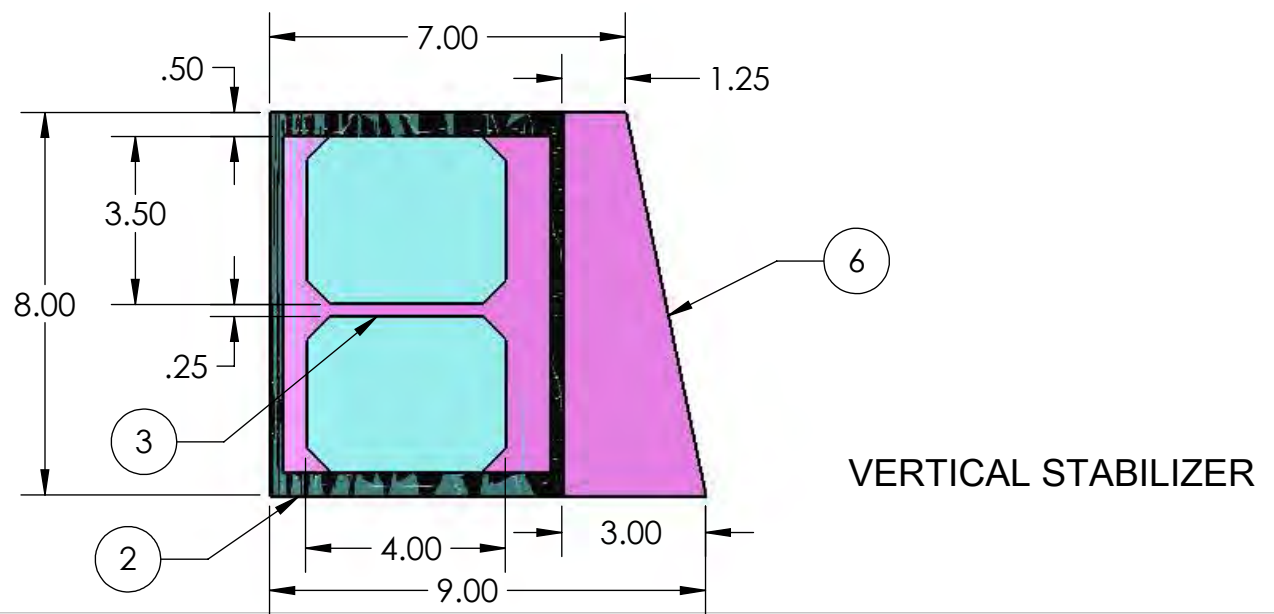
	NAME	DATE	SIZE	APPROVAL DATE:	REPORT TITLE:	REV
DRAWN BY:	J. HO	2012-02-04	B	2012-02-15	DRAWING PACKAGE	NC
CHECKED BY:	M.C. GAMBOA	2012-02-12				
ENG APPR.	G. VENNERI	2012-02-15				
				SCALE: 1:10	PAGE 1 OF 6	



NOTE: RIGHT SECTION OF WING



HORIZONTAL STABILIZER

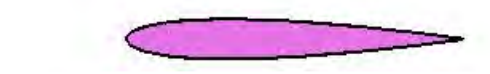


VERTICAL STABILIZER

ITEM NO.	NAME	MATERIAL
1	RIGHT AILERON	FOAM - FIBERGLASS
2	STRUCTURAL RIB	CARBON FIBER-FOAM
3	NON-STRUCTURAL RIB	FOAM
4	WING SPAR	CARBONFIBER - FIBERGLASS
5	ELEVATOR	FOAM - FIBERGLASS
6	RUDDER	FOAM - FIBERGLASS



BA-9 AIRFOIL (MAIN WING)



SD 8020 AIRFOIL (HORIZONTAL STABILIZER AND VERTICAL STABILIZER)

NOTE:
 DIMENSIONS ARE IN INCHES
 TOLERANCES:
 ANGULAR: $\pm .5^\circ$
 ONE PLACE DECIMAL $\pm .100$
 TWO PLACE DECIMAL $\pm .030$
 THREE PLACE DECIMAL $\pm .005$



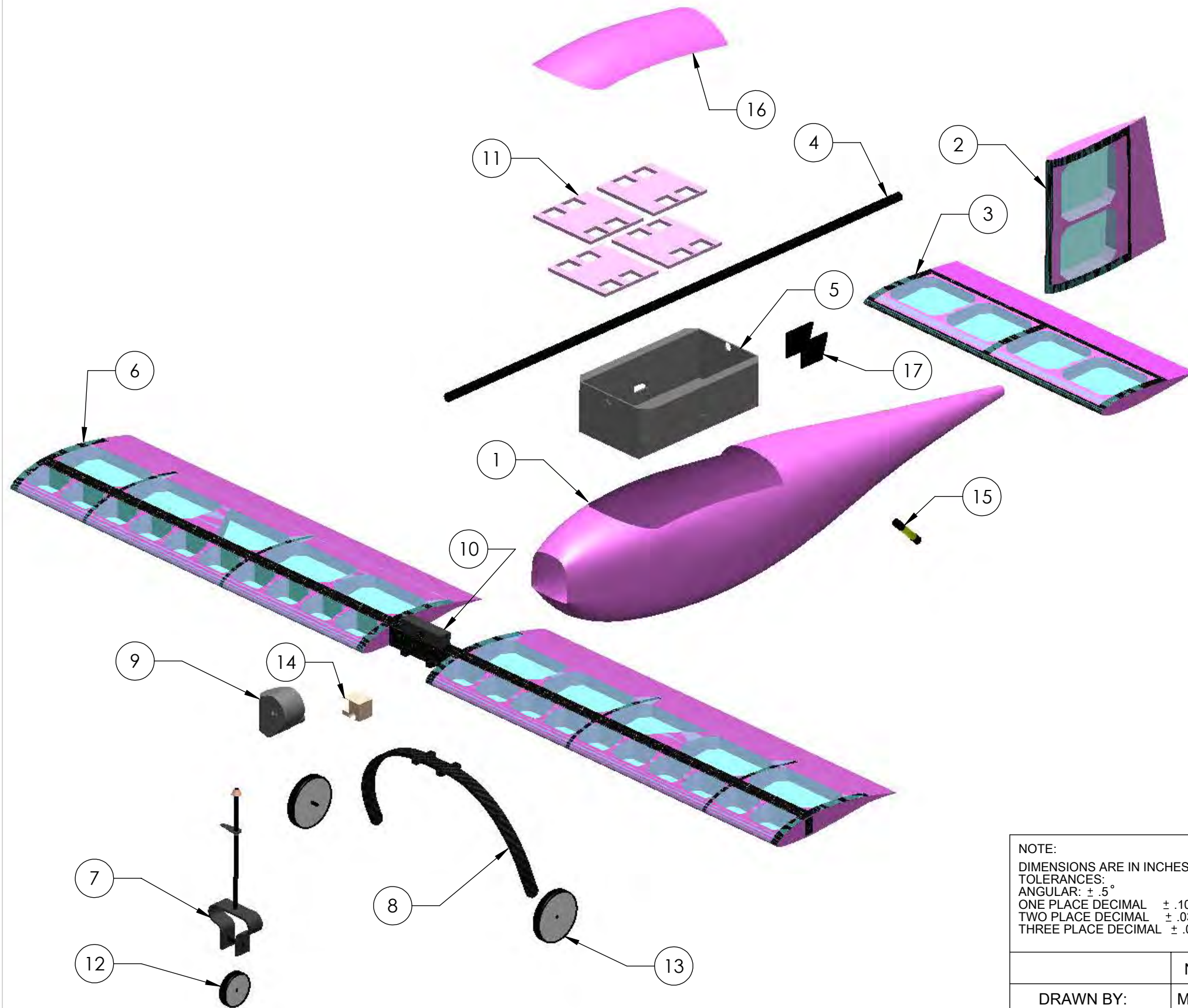
UNIVERSITY OF CALIFORNIA, IRVINE
 ANGEL OF ATTACK

CESSNA-RAYTHEON-AIAA-DESIGN/BUILD/FLY 2012

DOCUMENT TITLE:
COMPONENTS LAYOUT

NAME	DATE	SIZE	APPROVAL DATE:	REPORT TITLE:	REV
DRAWN BY: E. JUAREZ	2012-02-04	B	2012-02-15	DRAWING PACKAGE	NC
CHECKED BY: M.C. GAMBOA	2012-02-12				
ENG APPR. G. VENNERI	2012-02-15				

SCALE: 1:4 PAGE 2 OF 6



ITEM NO.	NAME	MATERIAL	QTY.
1	FUSELAGE	FOAM - FIBERGLASS	1
2	VERTICAL TAIL	FOAM - FIBERGLASS - CARBON FIBER - SO-LITE®	1
3	HORIZONTAL TAIL	FOAM - FIBERGLASS - CARBON FIBER - SO-LITE®	1
4	TAIL BOOM	FIBERGLASS - CARBON FIBER	1
5	WATER TANK	FOAM - CARBON FIBER	1
6	WING	FOAM - CARBON FIBER - FIBERGLASS - SO-LITE®	1
7	NOSE GEAR	BALSA - CARBON FIBER	1
8	MAIN GEAR	BALSA - CARBON FIBER	1
9	MOTOR MOUNT	FOAM - CARBON FIBER - PLYWOOD	1
10	WING BOX	CARBON FIBER - FOAM	1
11	PAYLOAD HOLDERS	FOAM	4
12	NOSE GEAR WHEEL	PLASTIC - RUBBER	1
13	MAIN GEAR WHEEL	PLASTIC - RUBBER	2
14	NOSE GEAR SERVO ATTACHMENT	BALSA	1
15	RELEASE TUBE	CARBON FIBER - FIBERGLASS - LATEX RUBBER	1
16	HATCH	FOAM - FIBERGLASS	1
17	RELEASE TUBE SERVO HOLDERS	CARBON FIBER-FIBERGLASS	2

NOTE:
 DIMENSIONS ARE IN INCHES
 TOLERANCES:
 ANGULAR: $\pm .5^\circ$
 ONE PLACE DECIMAL $\pm .100$
 TWO PLACE DECIMAL $\pm .030$
 THREE PLACE DECIMAL $\pm .005$

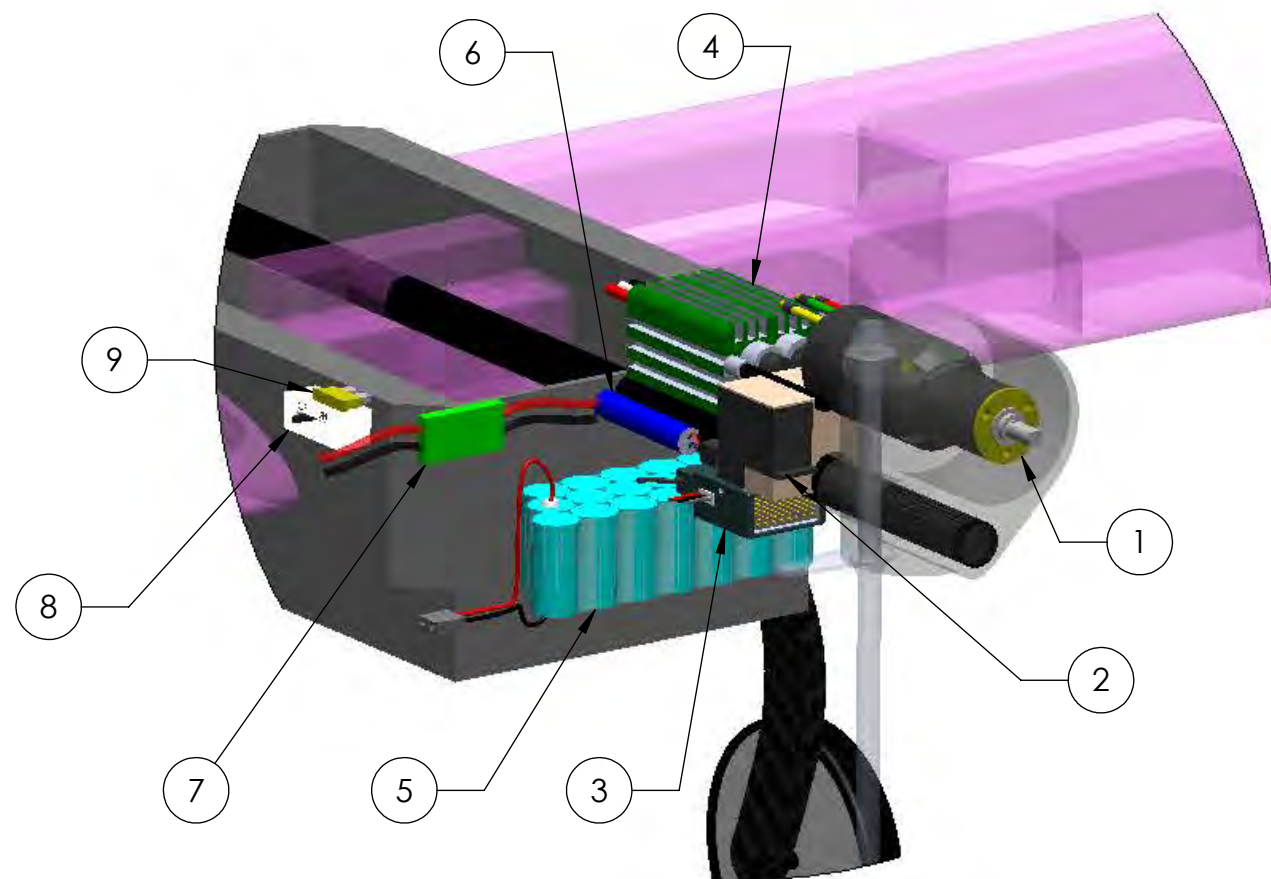
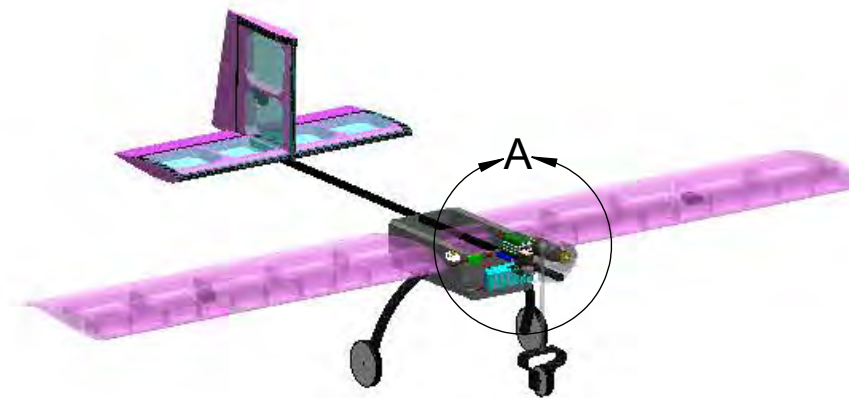
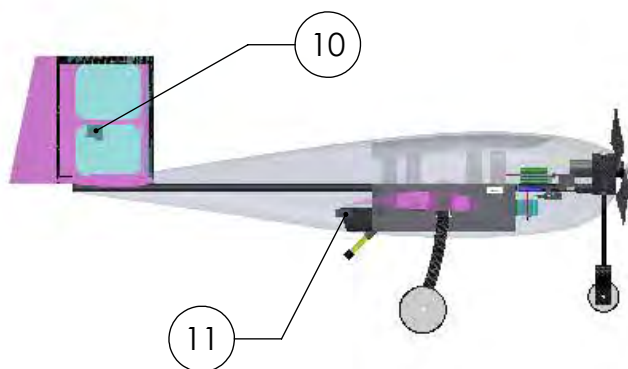
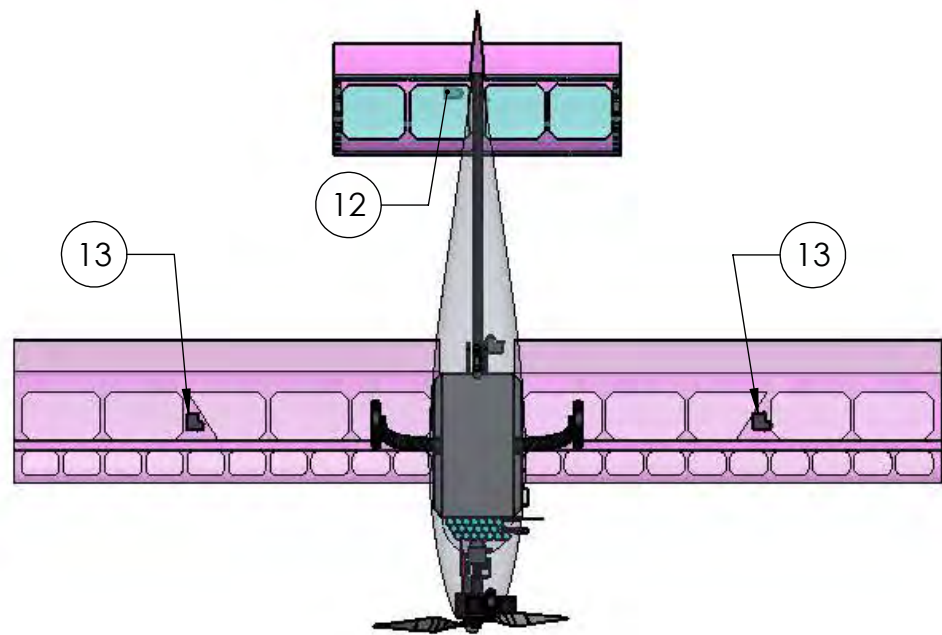


UNIVERSITY OF CALIFORNIA, IRVINE
 ANGEL OF ATTACK

CESSNA-RAYTHEON-AIAA-DESIGN/BUILD/FLY 2012

DOCUMENT TITLE:
STRUCTURAL ARRANGEMENT

	NAME	DATE	SIZE	APPROVAL DATE:	REPORT TITLE:	REV
DRAWN BY:	M. WU	2012-02-04	B	2012-02-15	DRAWING PACKAGE	NC
CHECKED BY:	M.C. GAMBOA	2012-02-12				
ENG APPR.	G. VENNERI	2012-02-15				
				SCALE: 1:6	PAGE 3 OF 6	



DETAIL A
SCALE 1 : 2

ITEM NO.	NAME	MANUFACTURER	MODEL
1	MOTOR	NEUTRONICS	1107 6D
2	NOSE GEAR SERVO	HITEC	65 MG
3	RECEIVER	SPECTRUM	AR7000
4	SPEED CONTROLLER	CASTLE CREATION	PHOENIX ICE LITE 50
5	BATTERY PACK	KAN	650 MAH
6	RECEIVER BATTERY	KAN	180 MAH
7	ALTIMETER CIRCUIT	SOARING CIRCUITS	CAM 3
8	SWITCH	EFLITE	N/A
9	FUSE	ATO	BLADE FUSE 20A
10	VERTICAL TAIL SERVO	HITEC	55 MG
11	WATER RELEASE SERVO	HITEC	55 MG
12	HORIZONTAL TAIL SERVO	HITEC	55 MG
13	WING SERVOS	HITEC	65 MG

NOTE:
DIMENSIONS ARE IN INCHES
TOLERANCES:
ANGULAR: $\pm .5^\circ$
ONE PLACE DECIMAL $\pm .100$
TWO PLACE DECIMAL $\pm .030$
THREE PLACE DECIMAL $\pm .005$

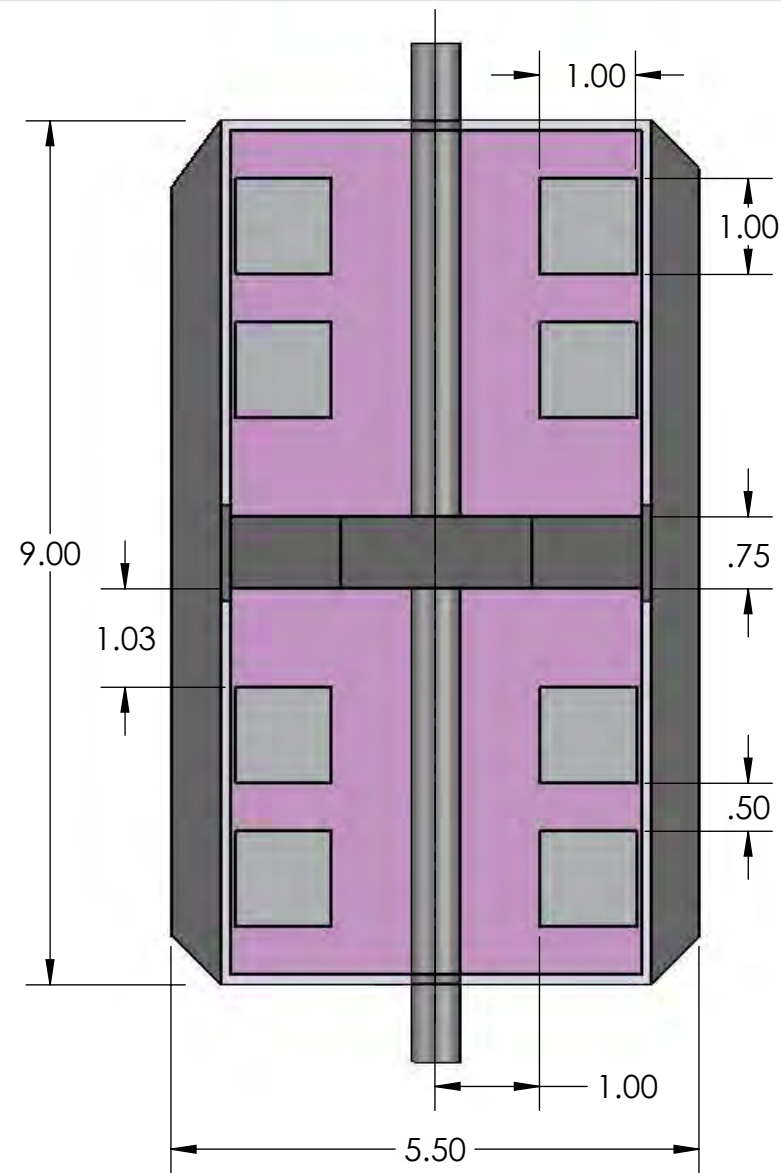


UNIVERSITY OF CALIFORNIA, IRVINE
ANGEL OF ATTACK

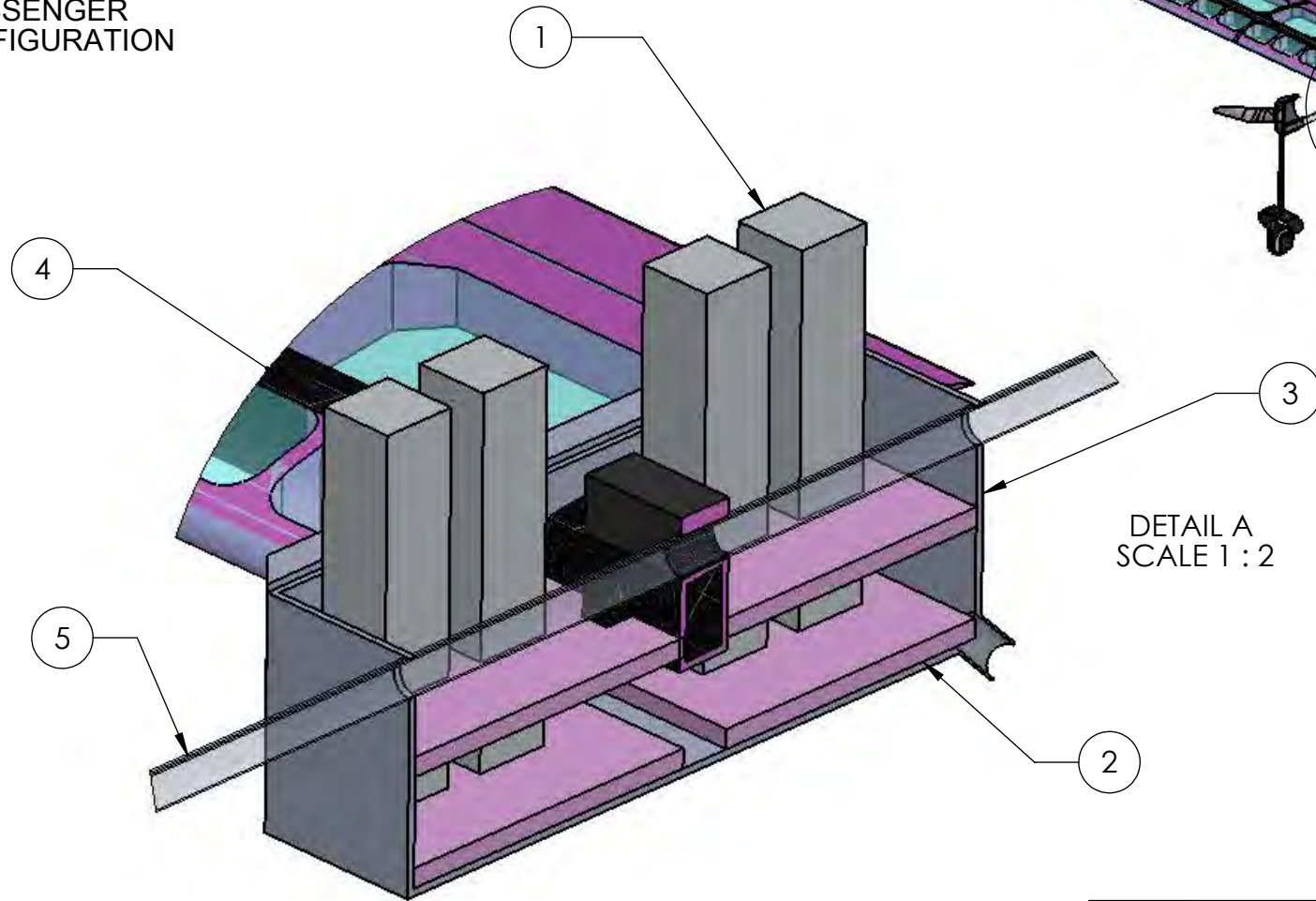
CESSNA-RAYTHEON-AIAA-DESIGN/BUILD/FLY 2012

DOCUMENT TITLE:
SYSTEMS LAYOUT

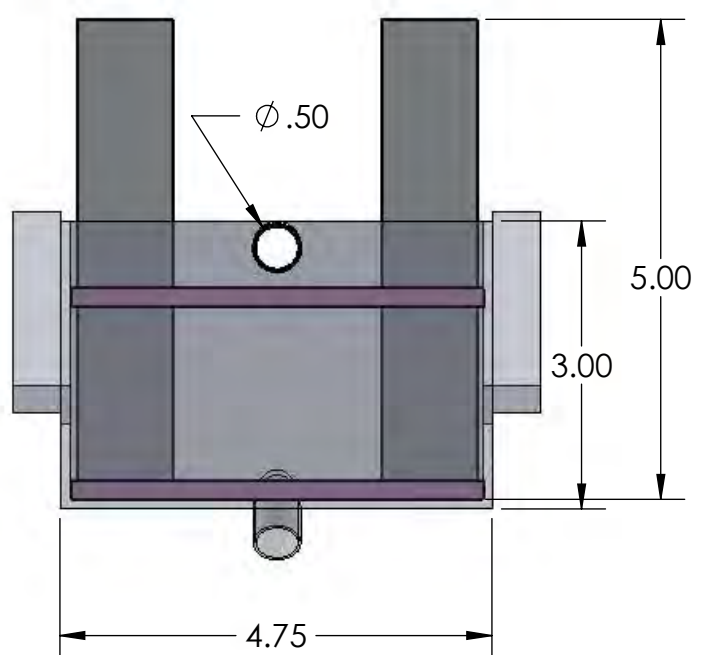
	NAME	DATE	SIZE	APPROVAL DATE:	REPORT TITLE:	REV
DRAWN BY:	D. TANTONO	2012-02-04	B	2012-02-15	DRAWING PACKAGE	NC
CHECKED BY:	M.C. GAMBOA	2012-02-12				
ENG APPR.	G. VENNERI	2012-02-15				
				SCALE: 1:12	PAGE 4 OF 6	



ALUMINUM PASSENGER PAYLOAD CONFIGURATION



DETAIL A
SCALE 1 : 2



NOTE: WATER TANK USED TO CARRY PASSENGERS

ITEM NO.	NAME	QTY.
1	PAYLOAD	8
2	PAYLOAD HOLDER	4
3	WATER TANK	1
4	WING SPAR	1
5	TAIL BOOM	1

NOTE:
DIMENSIONS ARE IN INCHES
TOLERANCES:
ANGULAR: ± .5°
ONE PLACE DECIMAL ± .100
TWO PLACE DECIMAL ± .030
THREE PLACE DECIMAL ± .005

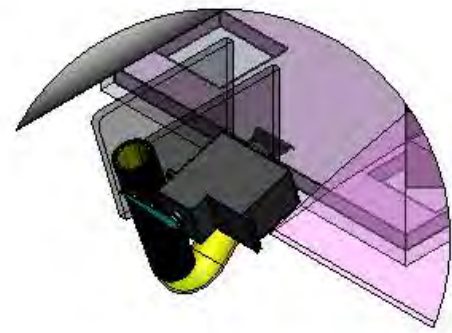


UNIVERSITY OF CALIFORNIA, IRVINE
ANGEL OF ATTACK

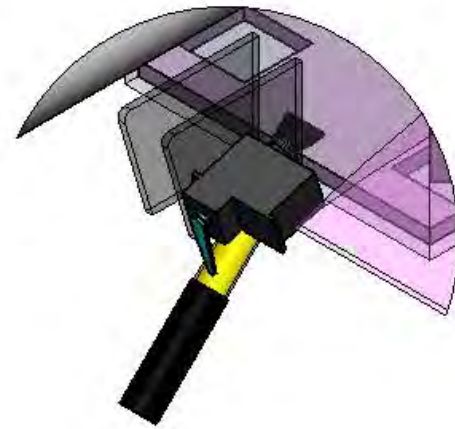
CESSNA-RAYTHEON-AIAA-DESIGN/BUILD/FLY 2012

DOCUMENT TITLE:
PAYLOAD ACCOMMODATION-1

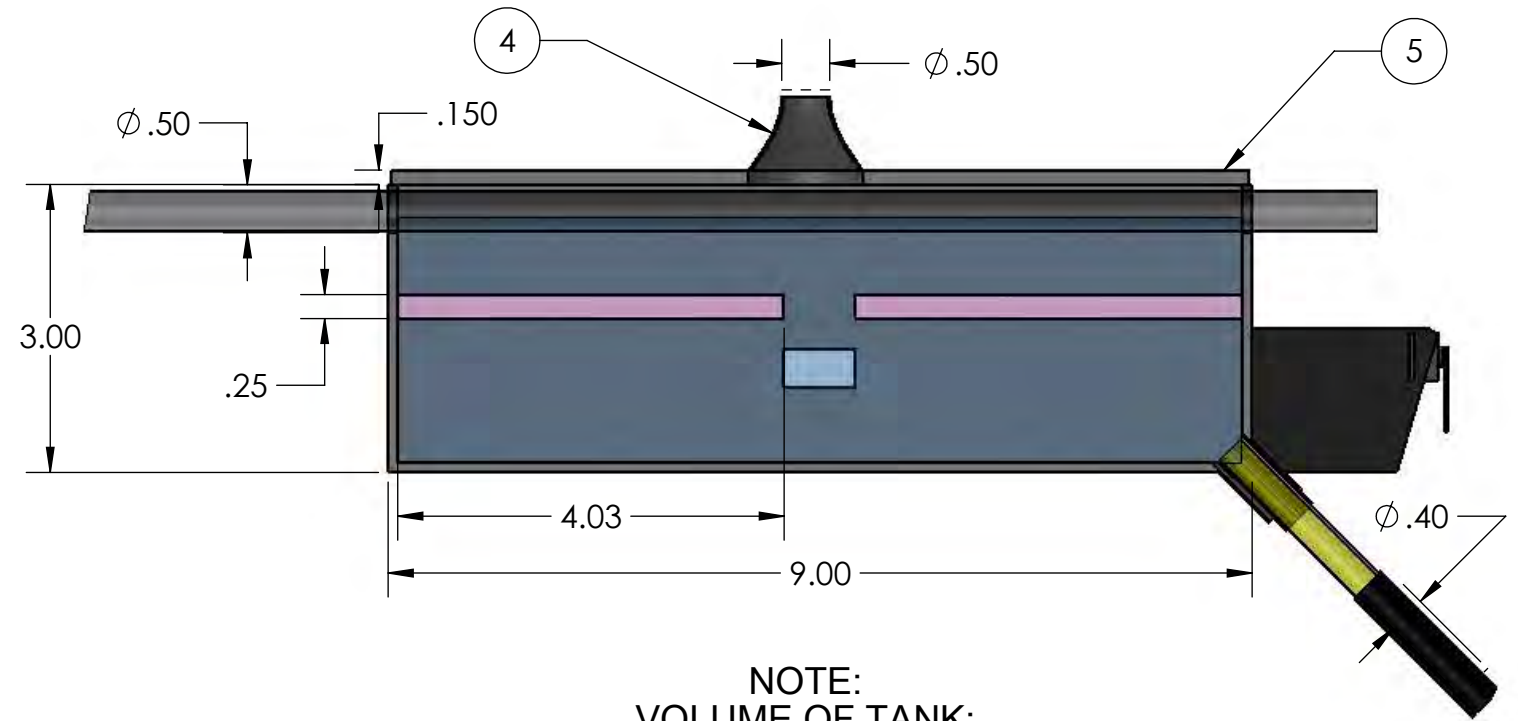
	NAME	DATE	SIZE	APPROVAL DATE:	REPORT TITLE:	REV
DRAWN BY:	B. XIONG	2012-02-04	B	2012-02-15	DRAWING PACKAGE	NC
CHECKED BY:	M.C. GAMBOA	2012-02-12				
ENG APPR.	G. VENNERI	2012-02-15				
				SCALE: 1:2	PAGE 5 OF 6	



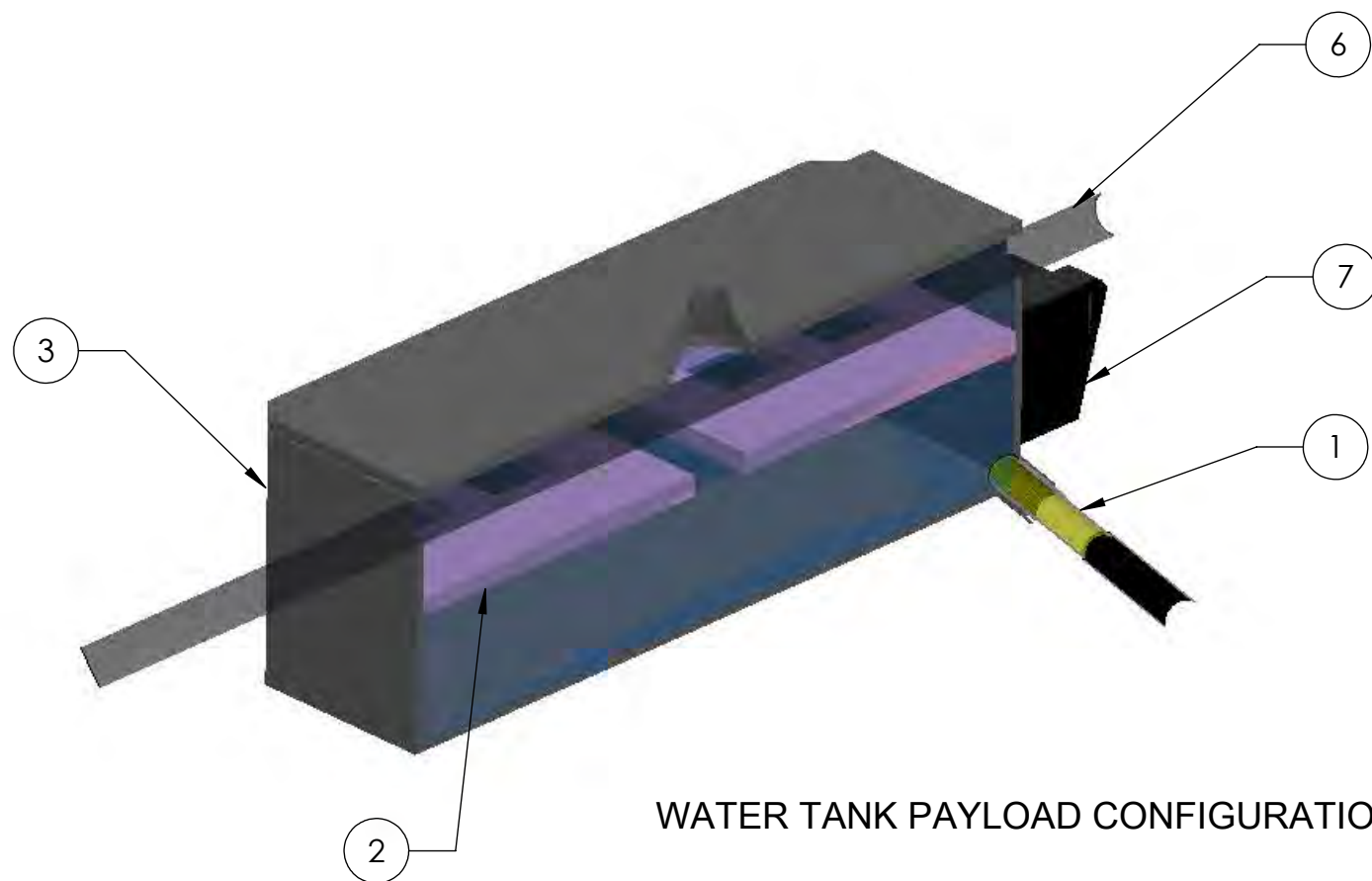
NOTE: RELEASE TUBE RETRACTED



NOTE : RELEASE TUBE OPENED



NOTE:
VOLUME OF TANK:
9 X 3 X 4.75 = 128.25 IN³



WATER TANK PAYLOAD CONFIGURATION

ITEM NO.	NAME	QTY.
1	RELEASE TUBE	1
2	BAFFLE	2
3	WATER TANK	1
4	PITOT VENT	1
5	WATER TANK LID	1
6	TAIL BOOM	1
7	WATER RELEASE SERVO HOLDER	2

NOTE:
DIMENSIONS ARE IN INCHES
TOLERANCES:
ANGULAR: ± .5°
ONE PLACE DECIMAL ± .100
TWO PLACE DECIMAL ± .030
THREE PLACE DECIMAL ± .005



UNIVERSITY OF CALIFORNIA, IRVINE
ANGEL OF ATTACK

CESSNA-RAYTHEON-AIAA-DESIGN/BUILD/FLY 2012

DOCUMENT TITLE:
PAYLOAD ACCOMMODATION-2

	NAME	DATE	SIZE	APPROVAL DATE:	REPORT TITLE:	REV
DRAWN BY:	C. VARGAS	2012-02-04	B	2012-02-15	DRAWING PACKAGE	NC
CHECKED BY:	M.C. GAMBOA	2012-02-12				
ENG APPR.	G. VENNERI	2012-02-15				
				SCALE: 1: 2	PAGE 6 OF 6	

6.0 Manufacturing Plan and processes:

Although the aircraft was sized to be as light as possible, multiple manufacturing methods were experimented with to conserve weight. Our manufacturing plan focused on the production of four main components: Wings and tail, landing gear, fuselage, and the water tank system.

6.1 Wing and Tail

The wings and tail are large volume components where manufacturing methods have a strong impact on weight reduction. Three methods were considered for manufacturing the wing and tail:

- **Foam core** – The foam core method consists of foam cut by hot wire into the proper airfoil shape. The foam is then supported with carbon fiber spars and fiberglass.
- **Balsa built-up** – This built up method consists of laser cut balsa ribs that would attach to a spar. Stringers create a frame that could be coated with a light material to preserve the airfoil shape.
- **Carbon ribbed** – A foam wing is cut via hot wire and lined with thin carbon fiber strips as ribs. Excess foam would be cut out using a hot wire and the wing would be coated with a light material.

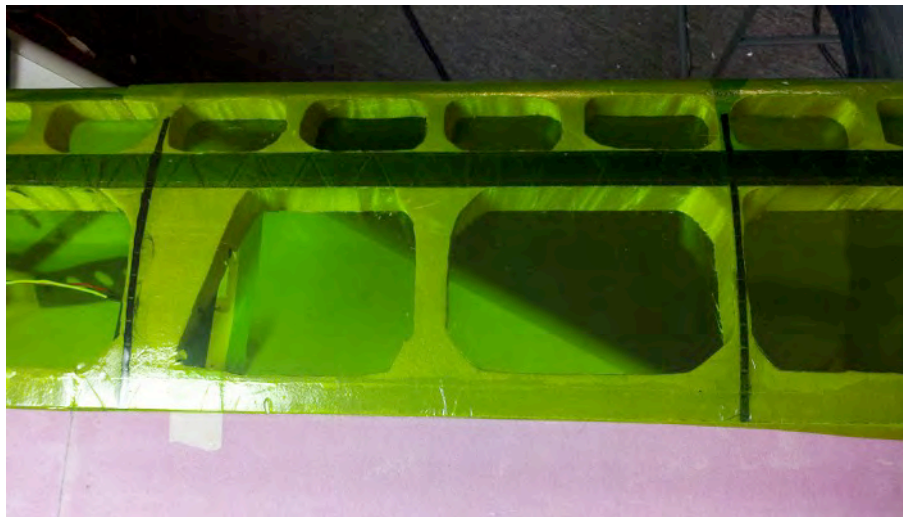


Figure 6.1: The wing of the second prototype

The foam wing has carbon ribs spaced 6 inches along the span to maintain structure. Foam sections were cut out leaving foam in areas that needed more surface area for the coating material to preserve the airfoil shape. The wing was cut into three sections before bagging it, and the center section was wrapped in carbon fiber to act as a spar along the maximum thickness of the airfoil.

Covering materials for the built up wings were also evaluated based on their weight and application method. Table 6.1 shows So-lite[®] film as the ideal material choice since it is the lightest and can be ironed on to the surface whereas the dope for Japanese tissue paper would deteriorate the foam. So-lite[®] was eventually selected over MonoKote[®].



Covering Material	Weight (oz/yd)	Application Method	Description
Japanese Tissue	0.21	Dope	Light tissue paper that requires adhesive to apply to the airframe and doping.
So-lite film	0.62	Iron-on	Extremely light plastic film that can be ironed on to the wing surface. Typically clear coated.
Solarfilm	1.70	Iron-on	Plastic film covering that comes in various colors.
Monokote	2.07	Iron-on	Heavy but durable plastic film covering material.

Table 6.1: List of covering materials considered

6.2 Landing Gear

Different landing gear methods were used based on what the design called for:

- **Balsa / carbon fiber sheets** – Balsa sheets were sandwiched by carbon fiber. The sheets were cut out to accept a rib section of the wing for attachment on one end and holes were drilled for the wheels on the other end.
- **U-shaped gear** – Balsa sheets were soaked in water and bent to take the shape of a foam mold. After the wood dried into shape, it was sanded to a round shape then laid up with fiberglass, unidirectional carbon fiber, and another layer of fiberglass.
- **Mushroom Nose Gear** – A mushroom-like foam mold was cut and taped on all sides. The tape allowed the carbon fiber lay-up to take its shape without the epoxy ruining the foam mold.

6.3 Fuselage Fairing

Methods were investigated to create a fuselage that was large enough to house the payload, yet would still preserve a smooth outer surface to reduce skin friction.

- **Clay molding** – A male mold was constructed using chloroplast templates that were cut and spaced out to loft the shape of the fuselage. The gaps between the templates were then filled with clay and smoothed out. Perfection proved to be hard to achieve since small bumps were hard to identify and smooth out.
- **Foam CNC** – a male fuselage mold was cut using a computer numerical controlled (CNC) milling machine. High density foam was used to maintain an even surface. The mold was coated with two layers of polyester paint to reassure that the surface would remain smooth.
- **Female molding** – Both the clay and foam male mold methods were preceding steps to making a female mold. Once the male molds were acceptably sanded, several layers of tooling gel coated the male mold and fiberglass was laid up on it to provide structure. Once dry, the tooling gel could be removed as a female mold that reflects the same shape of the male mold. Any dents that were



in the male mold showed up in the female mold, so male molding techniques played a key role in the quality of the female mold.

Composites were then laid up in the female mold to adhere to the shape and smoothness that the mold provided.



Figure 6.2: CNC cut fuselage molds (Left), tooling gel mold making (Right)

6.4 Water Tank

The water tank structure was designed to be load bearing and hold the aluminum payload while staying waterproof. Several materials were considered for manufacturing this tank including balsa wood, plywood, fiberglass, carbon fiber and foam. Weight build up estimations showed that the lightest method to manufacture the tank was a single layer of bi-directional carbon fiber and one layer of bi-directional fiberglass. The carbon fiber provided rigidity while the fiberglass insured a waterproof seal.

The tank was manufactured using the lost foam method. A foam mold covered with tape and wax was used to shape the carbon fiber and fiberglass layer in the desired shape of the tank. The vacuum bagging process insured smooth surfaces and no leaks at the corners. The drain tube at the bottom of the water tank where the water is released from was part of the mold. The tank was made in one piece and glued to the wing and tail boom after the lost foam process was completed.

6.5 Water Tank Release

The water release system was designed as a drain that could be attached to a bendable tube. The tank was fabricated and a foam male mold was created for the tank to have a drain that could accept the diameter of a designated latex tube.

6.6 Milestone Chart

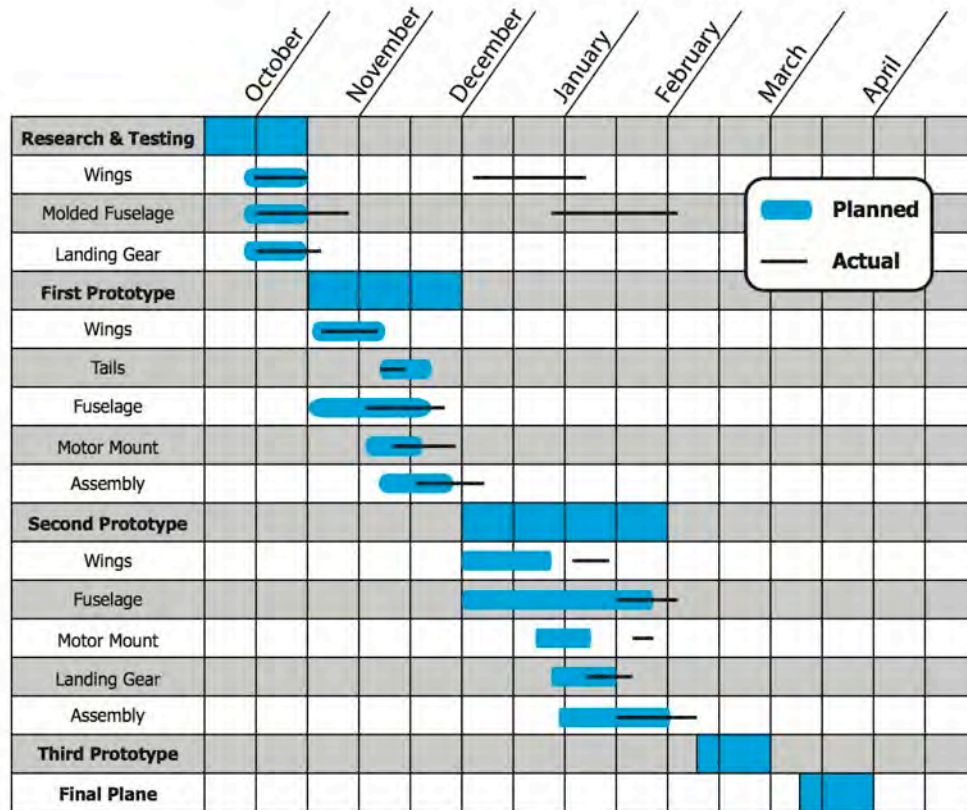


Figure 6.3: Milestone chart

7.0 Testing Plan

Tests were performed to guarantee that components, subsystems, and the assemblies were competition ready. Tests involved structural testing, propulsion tests, visual evaluations, and flight testing.

7.1 Objectives

Test objectives were defined for components that were critical or new to the team's manufacturing experience. Components were compared against other manufacturing methods or they verified modeling calculations.

7.1.1 Components

Wings

The wing spars were designed and tested to handle a certain bending stress. Maximum load tests were conducted on the wings through a three point bending test. The wings were supported on their tips while loaded with weights distributed along their spar. Wings were tested till they exceeded their maximum predicted bending stress.



Landing Gear

The landing gear must withstand the impact of the aircraft upon landing. Multiple bow landing gears were made to verify the modeled calculations. The gear was first loaded statically by supporting weights on top of it. Once it passed bending tests, the gear was mounted to a vertical rail and dropped from various heights with different weights to simulate impact landing.

Water Release

The water tank needed to seal and release water efficiently and reliably. Every manufacturing method for the water tank was tested to see how well they could hold two liters of water without leaking. Any water that did not leave the tank would be counted in the empty weight of the aircraft. Systems were weighed “dry” before and after containing water. Once the most effective method of containment and release was chosen, it was implemented into a test plane to verify that the release was visible when the aircraft was at the proper altitude.

7.1.2 Propulsion

To validate the rated performance of the motors, batteries, and propellers, static thrust tests were conducted with various systems. Holding two components of the system constant, the third component was varied for comparison against the other types of that component as well as its listed performance.

Battery

Battery testing was performed to ensure that good cells were used and soldered properly. Battery packs were cycled through charging and discharging a sufficient number of times so that they could reach their optimum state. The batteries were then tested using a certain propeller and motor as a control system. The voltage and endurance was monitored while maintaining a fixed current. The best battery packs were marked so that they could be used for test flights.

Propeller

Various propellers were tested on the static thrust stand while holding the motor and power supply constant. The thrust, RPM, and power outputs were recorded. The propeller tests verified the performance and selection of the optimal propeller.

Motor

Motors were tested on the static thrust stand holding the propeller and power supply constant. Tests were mainly done to verify estimated calculations and search for any unexpected problems.

Propulsion System

Once all three components of the propulsion system were tested and chosen, the entire system was put together to verify performance on the static thrust stand. After passing static thrust testing, the system would be used in the test flights, first with a higher capacity battery supply, then with the optimum battery during a later flight.



7.1.3 Flight Tests

To evaluate the overall performance of the aircraft, flight tests were performed with a telemetry system on board. Flight test objectives were outlined prior to test flight dates. These objectives included trimming the plane, pilot control feedback, completing all three missions, visibility of the water release in the air, verifying that the altimeter circuit worked, and monitoring the propulsion performance.

7.2 Master Test Schedule

Test	Objective	Start Date	End Date
Wing Spar	Verify spar meets bending stress requirements	10/3	10/17
Reduced Wing	Repeat wing spar tests with reduced foam wing	12/19	1/16
Landing Gear Testing	Impact Testing to simulate hard landing	10/10	10/17
Water Release Systems	Ensure no leakage, reliability, and ease of release	10/3	11/21
Propulsion System	Static thrust performance tests with motor, prop, and battery packs	10/17	1/16
Flight Testing	Compare flight measurements to calculated model	12/12	4/11

Table 7.1: Master test schedule

7.3 Preflight check list

Pre-Flight checklist	
Structural Integrity – Visual inspection for damaged components	
<input type="checkbox"/> Wing	<input type="checkbox"/> Boom
<input type="checkbox"/> Control Surfaces / Linkages	<input type="checkbox"/> Landing Gear
<input type="checkbox"/> Wing Box	<input type="checkbox"/> Nose Gear
<input type="checkbox"/> Water Release System	<input type="checkbox"/> Fuselage
<input type="checkbox"/> Propeller	<input type="checkbox"/> Motor Mount
Avionics – Ensure all wires and electrical components are connected and performing properly	
<input type="checkbox"/> Servo Wiring	<input type="checkbox"/> Receiver Properly Connected
<input type="checkbox"/> Avionic Power Test	<input type="checkbox"/> Receiver Battery Peaked
<input type="checkbox"/> Range Test	<input type="checkbox"/> Main Battery Peaked
<input type="checkbox"/> Servo Test	<input type="checkbox"/> Failsafe
Propulsion – System should perform as desired	
<input type="checkbox"/> Motor Wiring	<input type="checkbox"/> Prop Clearance
<input type="checkbox"/> Battery Connected	<input type="checkbox"/> Motor Test
Final Inspection – Ensure safe, successful flight	
<input type="checkbox"/> Correct Control Surface Movement	<input type="checkbox"/> Ground Crew Clear
<input type="checkbox"/> Mission / Objective Restated	<input type="checkbox"/> Pilot and Spotter Ready

Table 7.2: Pre-flight check list



7.4 Flight test plan

Flight test plan 02/05/2012 Prototype 2: XGF	
<input type="checkbox"/> Acquire telemetry for all flights <input type="checkbox"/> Keep track in live time of mAh, speed, current and altitude <input type="checkbox"/> Ramp throttle to 100% before each flight on the ground	
First flight: Trim flight Battery: 21 cells 650 mAh, Propeller: 12x6	Second flight: Mission 2 simulation Battery: 21 cells 650 mAh, Propeller: 12x6
<input type="checkbox"/> Trim plane	<input type="checkbox"/> Takeoff weight: 6.25 lb
<input type="checkbox"/> Understand behavior in straightaways and turns	<input type="checkbox"/> Cruise speed: 60-65 ft/s <input type="checkbox"/> Stall speed: 30 ft/s
<input type="checkbox"/> Try flap settings in takeoff/landing normal and running	<input type="checkbox"/> Flight duration 3 minutes
<input type="checkbox"/> Switch pilots and repeat	<input type="checkbox"/> Fly the course with spotters
Third flight: Mission 3 simulation Battery pack: 21 cells 650 mAh, Propeller: 14x7	Fourth flight: Mission 1 simulation Battery: 21 cells 650 mAh, Propeller: 8x7
<input type="checkbox"/> Takeoff weight 7 lb	<input type="checkbox"/> Takeoff weight 2.49 lb
<input type="checkbox"/> Climb speed: 45-50 ft/s <input type="checkbox"/> Stall speed: 35 ft/s	<input type="checkbox"/> Climb speed: 65-70 ft/s <input type="checkbox"/> Stall speed: 22 ft/s
<input type="checkbox"/> Flight duration 1 minute	<input type="checkbox"/> Flight duration 4 minute
<input type="checkbox"/> Fly the course with spotters	<input type="checkbox"/> Fly the course with spotters

Table 7.3: Flight test plan

8.0 Performance Results

All of the aircraft systems were tested extensively to insure the measured performance matched the model predictions. The results of these tests were used to calibrate the system models and factors of safety.

8.1 Performance of Key Subsystems

8.1.1 Component Performance

Wing performance

The wing spar strength was tested with a 5 G loading test, which accounted for turning loads. Every wing was span-loaded after manufacturing before use on aircraft as see in Figure 8.1.

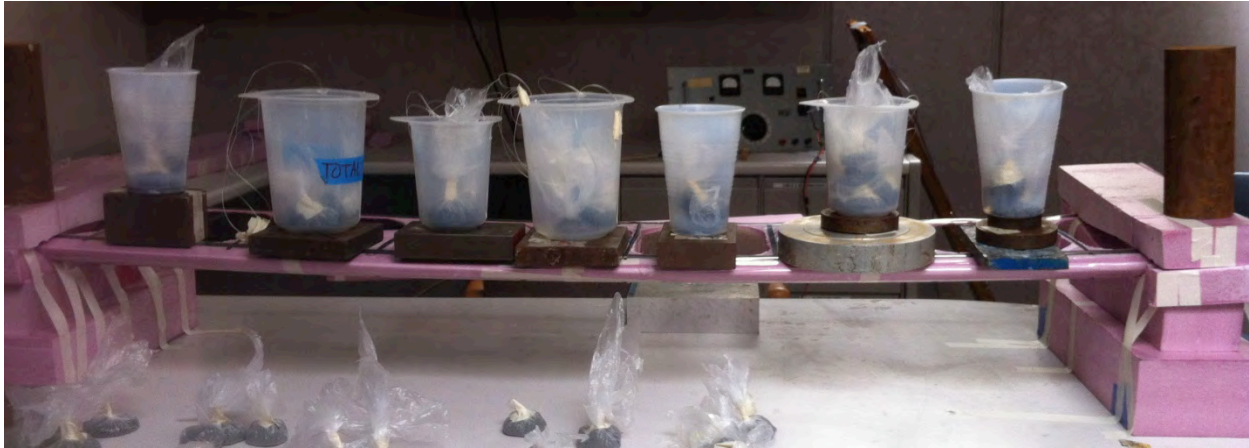


Figure 8.1: Wing load test

Results from testing the first two wings were utilized to calibrate the wing-spar sizing program that was used to size the wing-spar of the final plane.

Landing Gear Performance

The main landing gear was subject to two tests that ensured its reliability: a static loading test and a dynamic drop test. The static loading test consisted of loading the main gear statically up to the design load. The main gear is designed to support 5 times the maximum predicted takeoff weight, which was 35 lbs.



Figure 8.2: Main gear static load test

Trial	Design load (lb)	Displacement (in)	Failure load (lb)
1	35	2.4	21
2	35	1.7	29
3	35	0.9	36

Table 8.1: Landing gear static test results

Table 8.1 shows the results of three prototype main gear. These results were used to calibrate the landing gear sizing program. Once the landing gear survived the static test, it was brought over to a drop



stand where it was secured at the top in place of the connection to the plane, and dropped from various heights. The dynamic test consisted of a 2-ft free fall drop with a 7-lb load. This test simulated a stall landing where the plane falls 2-ft above the runway.

Water Release

The selected water release system was implemented on to a test plane. The CAM 3 circuit was used on the test plane to drop the water at 100 meters. The latex tube release method proved to be reliable and visible from that altitude. The optimization code predicted the climb time to be 31.3 seconds and the measured climb time at the test flight was 35 seconds.



Figure 8.3: Water released at 100 m altitude using CAM 3 circuit and the boom release method

8.1.2 Propulsion Performance

Batteries

Several tests were carried out to measure the performance and determine the capacity of the KAN 650 and the Elite 1500 batteries. In the first test, the loose cells were cycled, and the voltage and charge retained and discharged were monitored. The cells with the best performance are used to manufacture high performance battery packs. These packs are then cycled and rated based on the voltage and charge retained. The packs were then tested on the thrust test stand to measure the voltage drop due to the internal resistance of each battery pack. These test results were used to rate the battery packs and determine their capabilities.

Propulsion system

The propulsion predictions that were made by the propulsion model in the optimization code were tested to further calibrate the model. Static test results in Table 8.2 show that the model predictions were accurately modeling the propulsion system.

Propeller	Thrust (lb)		Current (amps)	
	Predicted	Measured	Predicted	Measured
12x6	3.65	3.52	14.6	13.9
12x8	3.86	3.79	16.9	16.1
12x10	3.74	3.67	21.4	20.7

Table 8.2: Static thrust test results for the Nue 6D and a 21 cell battery pack

The propulsion model was also confirmed in flight-testing as the current, voltage and motor RPM values are logged using a wireless data logging system.

8.2 Flight Test Performance

Flight tests were performed to accurately simulate the missions. The course was measured and spotters were set at both ends of the flight path. An Eagle Tree Telemetry data collection system was used and it compared data against the performance model code that was generated in MATLAB. The following plot compares the predicted current drawn by the motor verses the measured value for the second mission.

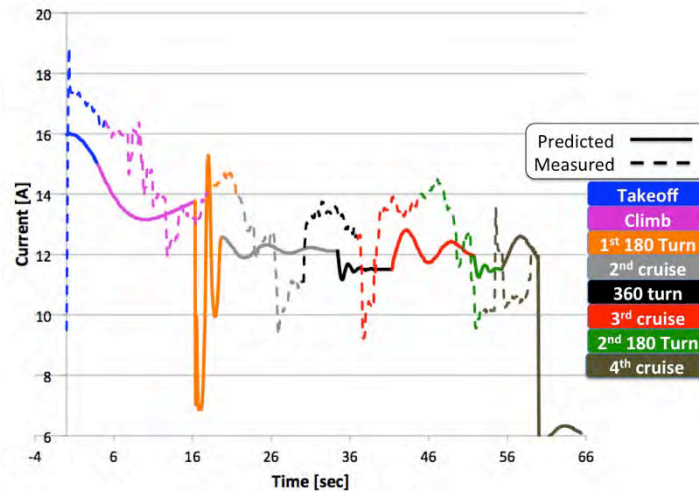


Figure 8.4: Predicted and measured current for mission 2 lap 1

Figure 8.4 shows that the predictions made by the propulsion model in the optimization code were accurate to ± 2 amps. The measured current was on average 1 to 2 amps higher than the prediction. This is due to the added drag caused by mounting the telemetry equipment that was not accounted for in the model. This plot also shows that the period of completing a task such as takeoff or climb was also modeled reasonably well.

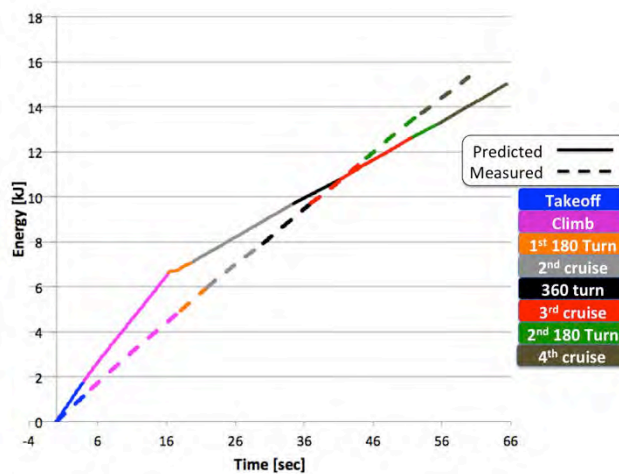


Figure 8.5: Predicted and measured energy for mission 2 lap 1

Figure 8.5 compares the modeled energy consumption and measured values. It shows a close correlation between these values with some deviation.

All missions were simulated in the flight tests performed. Following a trim flight, mission 2 was flown; the pilot flew the plane at the desired cruise speed with the help of live telemetry data recording. The plane performed as expected with great turning performance. Mission 3 was flown next with 2 liters of water and the altimeter circuit. The water plume was very visible and there were no noted CG shifts during the water release period of 15 seconds. Mission 1 was flown last. In this flight the pilot was instructed to push the plane to its limits. The plane reached a maximum speed of 68 ft/s, where the predicted value was 70 ft/s. The plane was able to complete six laps as predicted in this flight.

The results of these test flights show that some of the measured performance parameters were lower than the predicted values. This is due to the difficulty in predicting the drag very accurately. In some cases the measured performance parameters were better than predicted such as takeoff field length, which was on average 10 ft shorter than predicted. This is due to the factor of safety implemented in the optimization code. In the upcoming month, the team will focus on flight-testing to practice and promote consistency in the performance. The span will be shortened by two inches increments on the second prototype and it will be tested to see if it still makes the takeoff field length. Having a shorter span will reduce the wing area and that may help in reducing skin friction drag. This may help add one more lap in mission 1.



Figure 8.6: Prototype 2 taking off



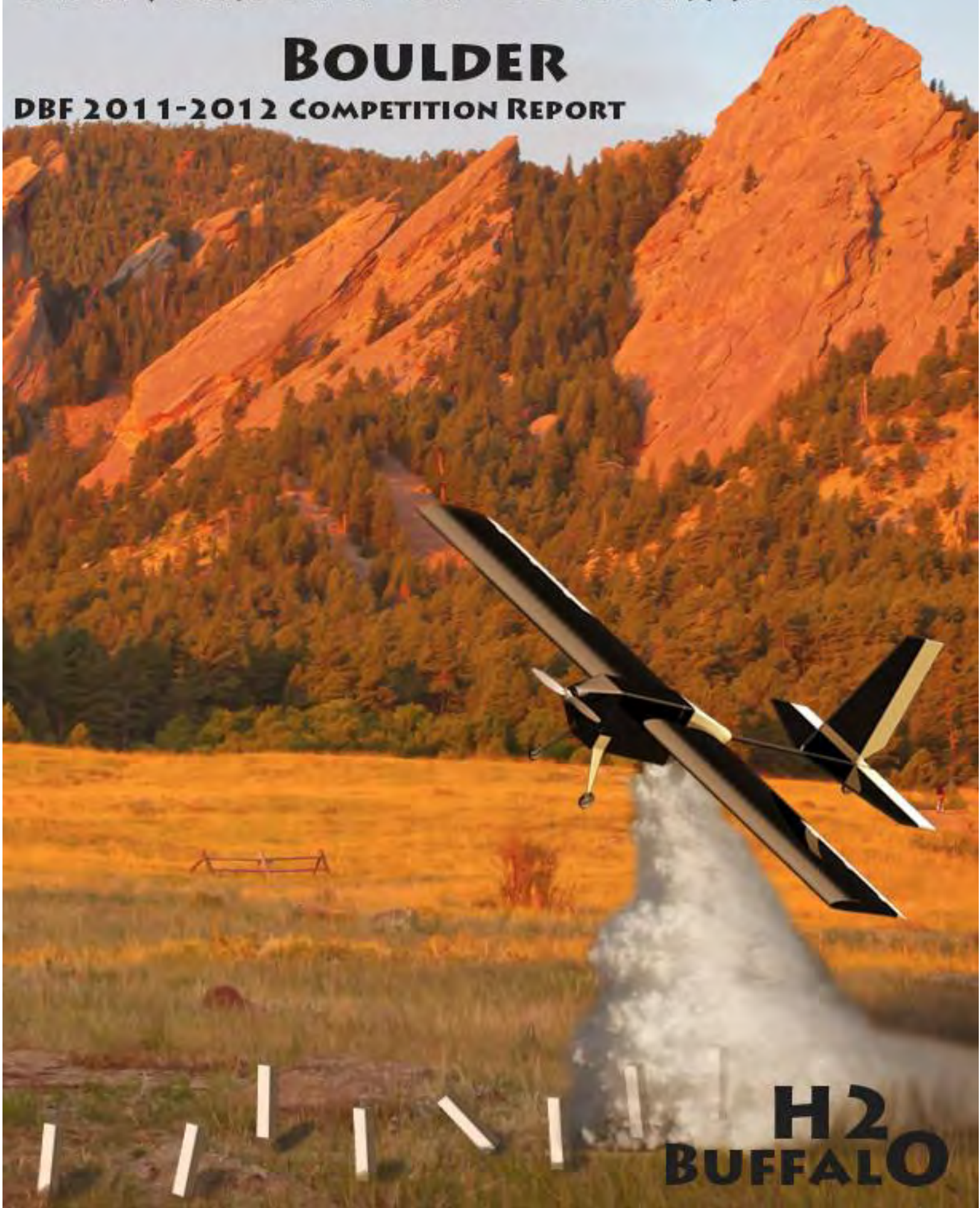
9.0 References

- [1] "AIAA Design/Build/Fly Competition - 2011/2012 Rules", 10 Nov. 2011, <<http://www.aiaadbf.org/>>.
- [2] Shevell, Richard. Fundamentals of Flight. 2nd Edition. Prentice Hall. 1988.
- [3] Drela, Mark. XFOIL Subsonic Airfoil Development System. 28 January. 2012
- [4] Page, Mark. Airplane Design. 2nd Edition. 2002
- [5] Drela, Mark & Harold Youngren. Athena Vortex Lattice, v. 3.27. Computer Software. MIT, 2008.
- [6] MIL-F-8785C. Military Specification: Flying Qualities of Piloted Airplanes, November 1980.
- [7] Foster, Tyler M. Dynamic Stability and Handling Qualities of Small Unmanned-Aerial-Vehicles, Brigham Young University, April 2005.

UNIVERSITY OF COLORADO

BOULDER

DBF 2011-2012 COMPETITION REPORT



**H2
BUFFALO**



Table of Contents

- 1.0 Executive Summary 6
 - 1.1 Design Summary..... 6
 - 1.2 Mission Requirements and Design Solutions 6
 - 1.3 Performance and Capabilities 7
- 2.0 Management Summary 7
 - 2.1 CUDBF Organization 7
 - 2.2 Design and Fabrication Schedule 8
- 3.0 Conceptual Design 9
 - 3.1 Mission Requirements 9
 - 3.1.1 Mission 1: Ferry Flight..... 10
 - 3.1.2 Mission 2: Passenger Transport 10
 - 3.1.3 Mission 3: Time to Climb 10
 - 3.2 Design Requirements..... 10
 - 3.2.1 Sensitivity Analysis..... 11
 - 3.2.2 Mission Driven Design Requirements 12
 - 3.3 Aircraft Configurations..... 13
 - 3.4 Concept Weighting and Results 13
 - 3.4.1 Aircraft Configurations..... 13
 - 3.4.2 Empennage Configuration 14
 - 3.4.3 Fuselage and Payload Layout..... 15
 - 3.4.4 Landing Gear..... 15
 - 3.4.5 Motor Configuration..... 16
- 4.0 Preliminary Design 16
 - 4.1 Design Analysis/Methodology 16
 - 4.1.1 Fuselage Shape 16
 - 4.1.2 Weight Prediction 16
 - 4.1.3 Wing Area..... 16
 - 4.1.4 Airfoil Selection..... 16
 - 4.1.5 Empennage/Tail 17
 - 4.1.6 Battery Type and Quantity 17
 - 4.1.7 Speed Controller 17
 - 4.1.8 Motor Selection 17
 - 4.1.9 Propeller Diameter and Pitch 17
 - 4.2 Design/Sizing Trades 18
 - 4.2.1 Fuselage Shape 18
 - 4.2.2 Weight Prediction 18
 - 4.2.3 Wing Area..... 19
 - 4.2.4 Airfoil Selection..... 20
 - 4.2.5 Empennage/Tail 21
 - 4.2.6 Battery Selection and Cell Quantity 23
 - 4.2.7 Speed Controller 24
 - 4.2.8 Motor Selection 24
 - 4.2.10 Propeller Diameter and Pitch 27
 - 4.3 Mission Model 27
 - 4.3.1 Ferry Flight 27
 - 4.3.2 Passenger Transport..... 28
 - 4.3.3 Time to Climb 28
 - 4.4 Lift, Drag and Stability Characteristics 28
 - 4.4.1 Control Surface Sizing 28
 - 4.4.2 Lift and Drag..... 28
 - 4.4.3 Stability..... 30
 - 4.5 Aircraft Mission Performance Estimation 32
 - 4.5.1 Ferry Flight 32
 - 4.5.2 Passenger Transport..... 33





- 4.5.3 Time to Climb 33
- 5.0 Detailed Design 33
 - 5.1 Dimensional Parameters 33
 - 5.2 Structural Characteristics: Component Selection, Integration, and Architecture 34
 - 5.2.1 Wings Sections and Securement 34
 - 5.2.2 Water Tank, Fuselage and Airframe 35
 - 5.2.3 Nose Cone 35
 - 5.2.4 Empennage Attachment 36
 - 5.2.5 Tail Boom Attachment 36
 - 5.2.6 Water Release Mechanism 37
 - 5.2.7 Passenger Restraint 38
 - 5.2.8 Electronics 38
 - 5.2.9 Propulsion 38
 - 5.3 Weight and Balance 39
 - 5.4 Flight Performance 41
 - 5.5 Mission Performance 41
 - 5.6 Drawing Package 41
- 6.0 Manufacturing Plan 46
 - 6.1 Manufacturing Processes 46
 - 6.1.1 Wing Structure 47
 - 6.1.2 Fuselage Structure 47
 - 6.1.3 Tail Boom Structure 48
 - 6.1.4 Empennage Structure 48
- 7.0 Testing Plan 48
 - 7.1 Testing Objectives 48
 - 7.1.1 Wing Testing 48
 - 7.1.2 Fuselage Testing 49
 - 7.1.3 Static Propulsion Test 49
 - 7.1.4 Aerodynamic Prototype Flight Testing 50
 - 7.1.5 Water Release Testing 51
 - 7.1.6 Pitot Probe Testing 53
 - 7.2 Testing Schedule 54
 - 7.3 Testing Checklists 54
- 8.0 Performance Results 56
 - 8.1 Structures 56
 - 8.1.1 Wing 56
 - 8.1.2 Tail Boom 56
 - 8.2 Aerodynamics 56
 - 8.3 Propulsion 57
 - 8.3.1 Batteries 57
 - 8.3.2 Propeller 57
 - 8.3.3 Motor 57
 - 8.4 System Performance 58
 - 8.4.1 Unloaded Performance 58
 - 8.4.2 Loaded Performance 58
- 9.0 References 58





Acknowledgements:

The 2011-2012 University of Colorado Design Build Fly Team would like to thank our advisors, Dr. Donna Gerren and Dr. Brian Argrow, and our talented pilot, James Mack. We would also like to thank the graduate advisors who have continued to support the team.

This year's team would not have been able to compete if it were not for our gracious sponsors:

University of Colorado Engineering Dean's Office, Engineering Excellence Fund, University Research Opportunity Program, SolidWorks, and MaxAmps.

We would also like to thank the Research and Engineering Center for Unmanned Vehicles for the use of the fabrication lab and manufacturing facilities.



**Acronyms and Symbols**

Acronyms	
AGL	Above Ground Level
AIAA	American Institute of Aeronautics and Astronautics
CAD	Computer Aided Design
CUDBF	University of Colorado Design/Build/Fly
FOM	Figure of Merit
IAS	Indicated Airspeed
RAC	Rated Aircraft Cost
TIES	Time End Indicating System
Variables and Symbols	
AR	Aspect Ratio
C_D	Coefficient of Drag
CG	Center of Gravity
C_L	Coefficient of Lift
C_M	Coefficient of Moment
EW1	Mission 1 Empty Weight
EW2	Mission 2 Empty Weight
EW3	Mission 3 Empty Weight
M1	Mission 1 Score
M2	Mission 2 Score
M3	Mission 3 Score
N_{laps}	Mission 2 Number of Laps
T_{avg}	Average Mission 3 Time to Climb
T_{team}	Mission 3 Time to Climb
W/P	Weight to Power Ratio
W/S	Wing Loading
W_{tot}	Mission 2 Total Aircraft and Payload Weight
X_{CG}	CG Distance From Leading Edge
α	Angle of Attack





1.0 Executive Summary

The objective of the University of Colorado Design Build Fly (CUDBF) team is to design a remote controlled aircraft to compete in the 2011-2012 American Institute of Aeronautics and Astronautics (AIAA), Cessna Aircraft and Raytheon Missile Systems Design Build Fly competition. The presented design, the H₂BuffalO, has been created for optimal performance under the provided competition rules and restraints. The H₂BuffalO will be designed to complete the three missions of this year's competition so as to maximize points earned.

The two payloads consist of eight aluminum block simulated passengers, and a Time End Indicating System (TEIS). This document presents the detailed design, analysis, testing, manufacturing, aircraft performance and management plan employed to ensure a successful flight system.

1.1 Design Summary

Several aircraft configurations were considered for the design of the H₂BuffalO including conventional monoplane, flying wing, canard, and dual wing. The conventional monoplane configuration was ultimately selected due to the available wealth of knowledge about the design and manufacturing processes, as well as the high volume payload capacity. The conventional design also allowed for a high wing placement, allowing less structural interference with the internal payload volume. A conventional tail layout was also selected for its longitudinal stability and simplicity. The structure weight of the aircraft is critical to the scoring for each mission. Therefore, the aircraft was designed with lightweight construction in mind. In order to decrease the maximum flight weight of the aircraft, the fuselage was designed to be waterproof, thus eliminating the need for extra component and weight for mission three.

1.2 Mission Requirements and Design Solutions

The ferry flight and loaded missions require that the system allow for set up and loading in a five minute time period. The aircraft must also carry the aluminum passengers or TEIS payload while withstanding a 2.5 g load maneuver, and must land on the runway after completing each flight. Mission two requires the aircraft to complete three laps while carrying eight aluminum passengers. The payload restraint system for the aluminum passengers was designed to securely hold the passengers while allowing for the installment of the TEIS payload. Aluminum block passengers will be held in place by a light foam insert. In mission three, the water payload must be released upon reaching 100 meters in altitude as indicated by a CAM-f3q altimeter which will actuate a servo operated dump valve. Following these requirements, in addition to constraints imposed by the 1.5 lb battery limitation, the aircraft was designed to have a low stall speed of 24.7 ft/s and a cruise speed of 86.5 ft/s at maximum gross take-off weight.





A sensitivity analysis was performed on the mission scoring equations. It was determined that the most sensitive parameter of this competition is the maximum total mission weight of the aircraft. The time to climb is the second most important parameter.

1.3 Performance and Capabilities

The aircraft is designed to have the lowest possible structure weight while remaining sufficiently rigid to endure the stresses of flight. Because the aircraft must carry 2 liters of water during mission three, the internal payload compartment of the fuselage is waterproofed so that no water is released before reaching 100 meters and no electrical components are subjected to moisture. Since the payload compartment must also serve as a passenger cabin, the access hatch and restraints accommodate aluminum blocks.

The estimated flight weight of the aircraft for Mission 1 is 3.44 lb. For Mission 2 and Mission 3 it is 7.34 and 7.85 lb, respectively. Mission 1 consists of an empty aircraft. The Mission 2 weight includes the weight of the passengers, and the Mission 3 weight includes the weight of the Time End Indicating System.

2.0 Management Summary

2.1 CUDBF Organization

CUDBF consists of approximately 25 undergraduate students. Of these students, 11 are juniors and of these, 7 are veteran CUDBF participants. There are two veteran sophomore participants. The 7 veteran juniors are fulfilling leadership roles within the team as shown in Figure 1 below. The team is advised and supported by two faculty advisors and several alum advisors.

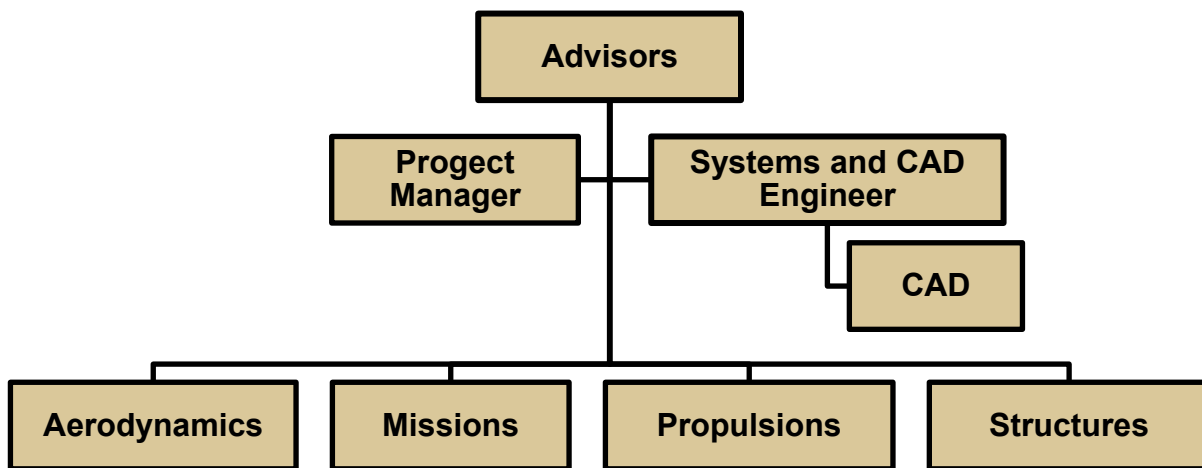


Figure 1: CUDBF Hierarchy Chart





At the administrative level, CUDBF is organized with a Project Manager and Systems Engineer:

- **Project Manager:** Garrett Hennig
 - Represents the team through correspondence with DBF officials.
 - Organizes team meetings and keeps communication flowing among team members
 - Procures funding for the team
- **Systems and CAD Engineer:** Grant Boerhave
 - Organizes interfacing among sub-teams.
 - Maintains CAD model and presides over the CAD Sub-Team

Five technical sub-team leaders support the administration of CUDBF and preside over their respective sub-teams:

- **Aerodynamics:** Jacob Varhus
 - Wing and empennage design
 - Determination of external configuration
 - Conducts analysis of stability, flight characteristics
- **Missions:** Matthew Zeigler
 - Score analysis and strategy optimization
 - Payload design and configuration
- **Propulsions:** Cameron Trussell
 - Optimizes aircraft propulsion based on competition requirements
 - Selects motor, propeller, and electronic components
- **Structures:** Dominique Gaudyn
 - Optimizes structure material and configuration for competition missions

2.2 Design and Fabrication Schedule

The design and fabrication of the H₂Buffalo was a complex iteration process. Many of the tasks along the design process are interdependent and occur simultaneously. The project schedule was designed to keep the design and fabrication process at an appropriate pace in order to deliver a final aircraft on time.

The design phase of the H₂Buffalo was broken into three distinct phases: Conceptual Design, Preliminary Design, and Detailed Design. Manufacturing is also divided into three phases: Aerodynamic Prototype, Manufacturing Prototype, and Competition Aircraft. Testing will occur throughout the design and manufacturing phases. Shown in Figure 2, below, is a Gantt chart illustrating the flow of the aircraft design.



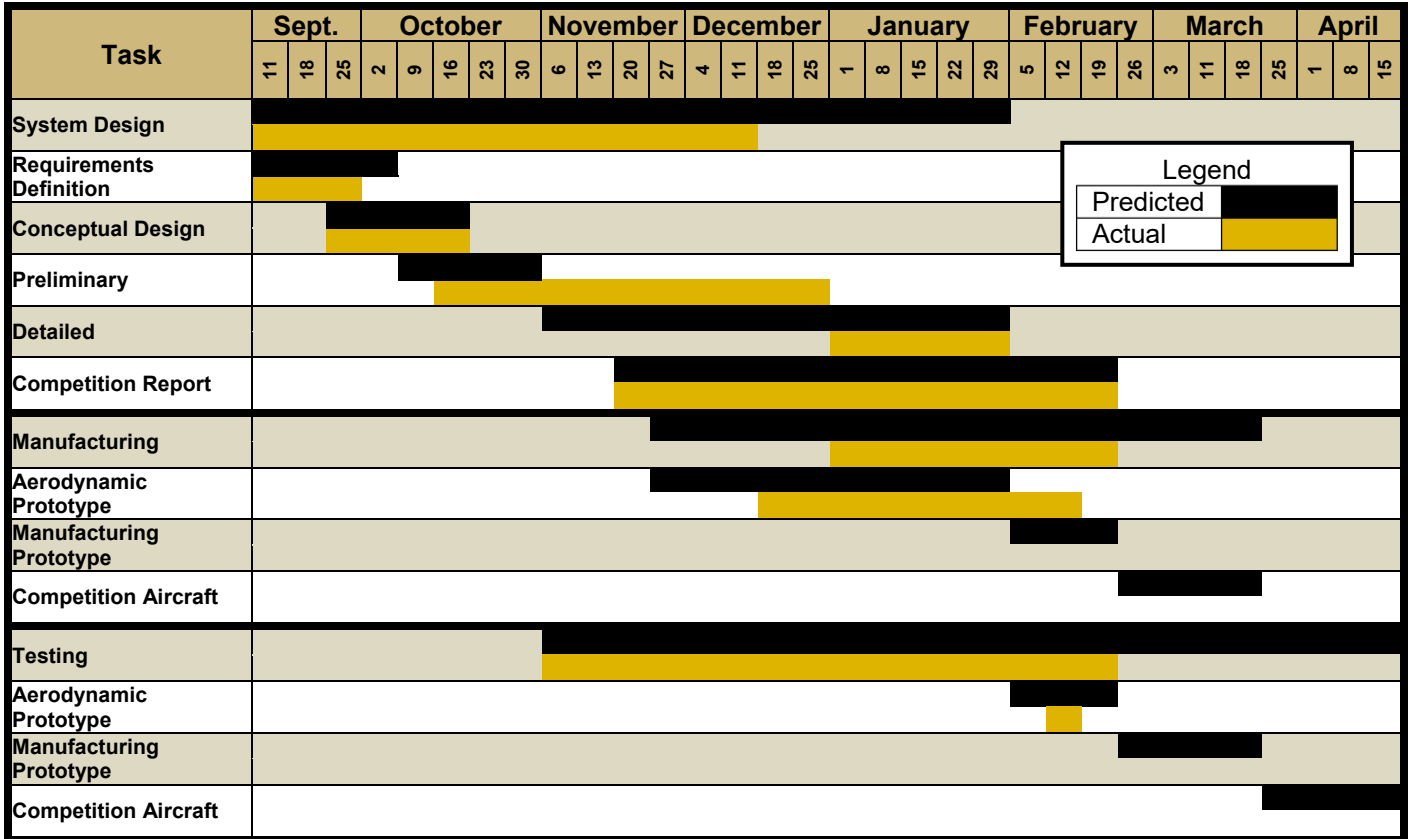


Figure 2: Project Schedule Gantt Chart

3.0 Conceptual Design

During the conceptual design phase, the team considered competition requirements along with the mission scoring formulas to guide general understanding of how to maximize the overall score. By analyzing each mission score independently then calculating the total score, the relative sensitivity of various aircraft characteristics on score were determined.

3.1 Mission Requirements

This year's aircraft is required to successfully complete three unique missions in order to complete the competition. After completing each mission, the team will receive a score based on the performance of the aircraft during that mission. The final score is calculated using the following formula:

$$Score = \frac{Written\ Report\ Score * Total\ Flight\ Score}{\sqrt{RAC}}$$

Total flight score is the sum of the three mission scores as shown below:

$$Total\ Flight\ Score = M1 + M2 + M3$$





The final score is inversely proportional to the rated aircraft cost (RAC), which is equal to the maximum empty weight of the aircraft as measured following each of the three missions.:

$$RAC = \text{Max}(EW1, EW2, EW3)$$

3.1.1 Mission 1: Ferry Flight

In mission 1, the aircraft must demonstrate superior straightaway speed and maneuverability. The aircraft flies along a designated flight course and attempts to complete as many laps as possible within four minutes of initial throttle-up. Mission one flight score is linearly dependent on the number of laps completed as shown in the equation below:

$$M1 = 1 + \frac{N_{Laps}}{6}$$

3.1.2 Mission 2: Passenger Transport

The second mission is an exercise in construction of aircraft with low structure to payload weight ratio. In order to successfully complete the mission, the aircraft must carry eight simulated passengers represented by 1"x1"x5" aluminum blocks. The total weight of the passengers must be no less than 3.75 lb. The score for this mission is inversely proportional to the total weight of the aircraft including the structure, batteries, and the simulated passengers. An aircraft with high mission 2 score must have a low structure to payload weight ratio:

$$M2 = 1.5 + \frac{3.75}{W_{tot}}$$

3.1.3 Mission 3: Time to Climb

Mission three is a demonstration of both engineering creativity and high aircraft performance. Teams begin mission 3 by loading 2 liters of water into the aircraft's Time End Indicating System (TEIS). Judges will measure the time from initial throttle-up to the aircraft's release of the water payload upon reaching 100 meters in altitude. The TEIS will use a CAM-f3q altimeter to automatically actuate a servo-operated dump valve at 100 meters above ground level. The challenge of mission three is in the nature of the payload. The water must not leak between loading and staging which may take 20 minutes or more. The score for mission two is normalized by the average time to climb of all the teams that successfully complete the mission. To do well in mission three, the aircraft performance must minimize time to climb:

$$M3 = 2 + \text{sqrt}\left(\frac{T_{avg}}{T_{team}}\right)$$

3.2 Design Requirements

Using the scoring criteria of each mission, the most sensitive design parameters were determined. The aircraft design as well as each of the subsystems design was optimized within the other design system constraints of the competition.





3.2.1 Sensitivity Analysis

In order to optimize the design on the aircraft for the highest possible final score, a sensitivity analysis was performed. This analysis evaluated the increase of each mission parameter and its effect on the total competition score. In order to accomplish this, a baseline model was chosen and a final score for the model was calculated. Then, for each mission, the baseline model's characteristics were varied and the resulting percent change in total score was plotted. Figure 3 displays the results of this analysis.

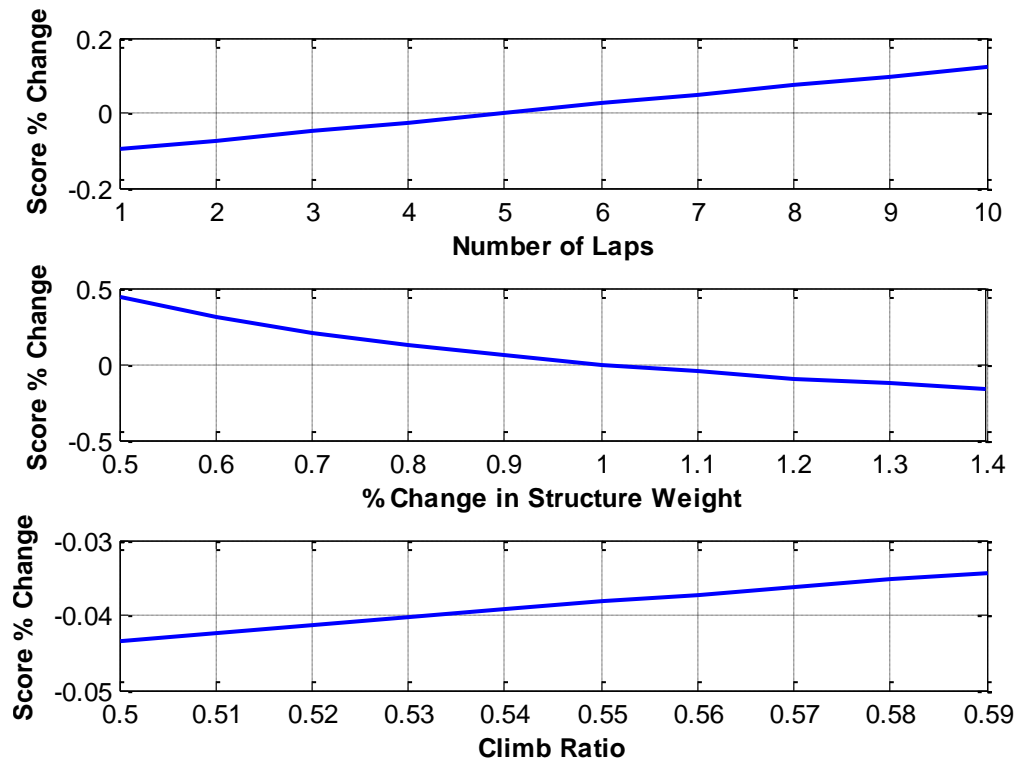


Figure 3: Mission Score Sensitivity Plots

The baseline model's mission characteristics used for this analysis as well as a description of why each one was chosen can be found in Table 1.

Table 1: Description of Baseline Model Used in Sensitivity Analysis

Mission Characteristic	Baseline Value	Description
Number of Laps	5	Chosen because it was the number of laps obtained by last year's CU DBF team with similar aircraft design and payload weight
Structure Weight	4.4 lbs.	Same weight as maximum payload, resulting in competitive structure weight to payload ratio of 1
Climb Ratio	1	Represents the value equivalent to a climb time equal to average climb time of all teams





From the sensitivity analysis it was determined that structure weight was the most sensitive parameter. This makes sense as the weight of the aircraft affects both the Mission 2 score, as well as the RAC which affects the total score.

The number of laps and time to climb parameters were thus deemed less sensitive and therefore less important than structure weight. However, in order to obtain a competitive score, these parameters could not be ignored. Figure 4 , given below, illustrates this fact.

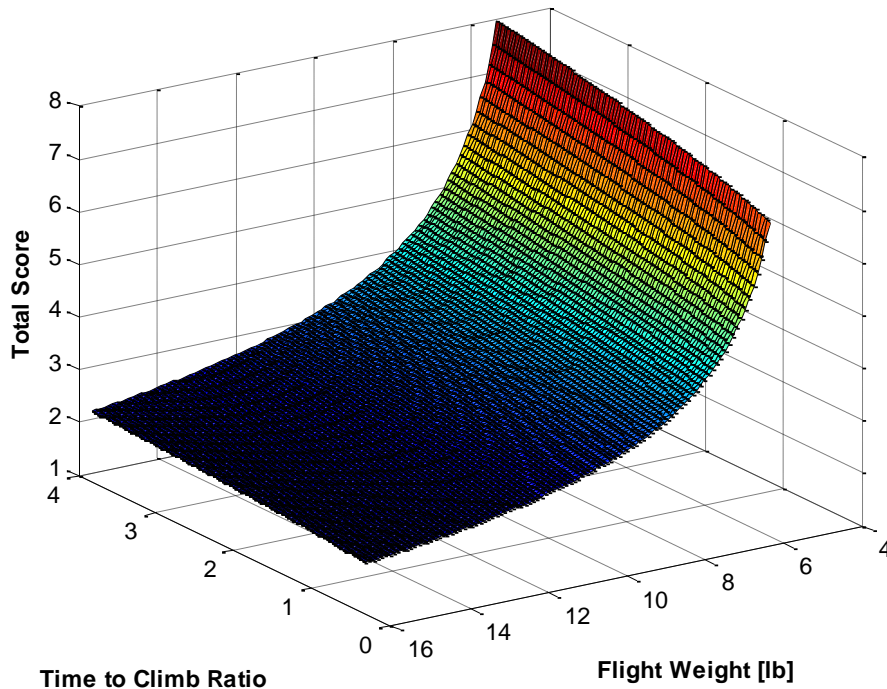


Figure 4: Effect of Time to Climb Ratio and Flight Weight on Total Score

As shown in Figure 4, though decreasing flight weight increases total score most effectively, the effect of time to climb ratio on total score cannot be ignored. Also, it is important to note that due to time to climb's dependence on velocity, the time to climb and the number of laps completed by the aircraft is coupled, meaning a faster climb time should result in more possible laps.

For these reasons the team designed an aircraft that would be the lightest possible while still remaining competitive in the ferry flight and time to climb missions.

3.2.2 Mission Driven Design Requirements

From the competition rules and previous year's DBF results, more design requirements were derived which include the following:

- The fuselage must be internally waterproofed.
- The water payload release mechanism must be servo-operated.
- The aluminum passengers must be fully secured during flight.





- All mission specific payloads must be secured in a fashion such that the center of gravity of the aircraft is unchanged with the addition and removal of each respective payload.
- All payloads must be carried fully internal to the aircraft mold lines.

3.3 Aircraft Configurations

In order to design the mission optimizing aircraft that provided the potential for the maximum achievable mission score, a variety of generic aircraft configurations were compared and contrasted against one another in the form of a trade study. A basic description of the advantages and disadvantages provided by each aircraft configuration is described below:

- **Conventional:** Often used in large payload applications, an extensive knowledge base is available, and the configuration of such an aircraft involves simple and reliable fabrication techniques.
- **Canard:** Employs a horizontal stabilizer forward of the aircraft's main wing. The canard may be designed to provide positive lift in trimmed flight, however, canard designs can be less stable.
- **Flying Wing:** Without a fuselage, this configuration has little potential to carry a high-volume internal payload. There is a limited knowledge-base for this configuration, and the manufacturing is complex.
- **Dual Wing:** This configuration places a lifting wing section both above and below the aircraft's fuselage, allowing for a shorter wingspan at the expense of increased drag.

3.4 Concept Weighting and Results

As described previously, a series of trade studies were performed to decide on the overall configuration of the aircraft. The most important configuration considerations that were analyzed were quantified in terms of a Figure of Merit (FOM). The FOM's employed in these trade studies were chosen based on their relevance to the mission, the knowledge-base surrounding each proposed configuration, and the benefits to the aerodynamic performance of the aircraft. As such, each FOM was weighted based on relative importance to the mission requirements and to give each possible aircraft configuration an overall score.

3.4.1 Aircraft Configurations

It should be noted that of the four aircraft designs proposed, only three were actually considered for trade study: the conventional, the canard, and the dual wing. Flying wing was eliminated because of payload sizing requirements. The categories chosen to weight the overall effectiveness and feasibility of each configurations were: knowledge-base surrounding the aircraft with regards to ease of design and manufacturing; maximum internal payload volume; aircraft structure weight; and lift-to-drag ratio. These categories were weighted individually at 15, 15, 50, and 20 percent, respectively. Each considered





configuration was given a figure of merit on a scale from 1-10 in each of the four categories considered, relative to the comparative advantage or disadvantage of all known aircraft configurations. These FOM's were then weighted and summed to ultimately score each aircraft configuration, also on a scale of 1-10. The results of the performed trade studies are seen in Table 2.

Table 2: Aircraft Wing Configuration Trade Study

Attribute	Weight	Conventional		Canard		Dual Wing	
		Score	Weighted Score	Score	Weighted Score	Score	Weighted Score
Knowledge Base	15	10	1.5	5	0.8	8	1.2
Payload Volume	15	9	1.4	8	1.2	9	1.4
Aircraft Weight	50	7	3.5	6	3	5	2.5
Lift vs. Drag Ratio	20	7	1.4	7	1.4	5	1
Total	100		7.8		6.4		6.1

As seen above, the conventional monoplane has the largest knowledge base, making the design and manufacture of this configuration more reliable and less complex. The conventional design also allows for a large payload volume in the fuselage and good payload accessibility. The wings are placed above the longitudinal axis, and the avionics may be easily placed in the nose of the aircraft to aid in optimizing the center of gravity location of the aircraft without the use of ballast. The conventional design also scored highest in terms of aircraft weight. This was ultimately the most important factor in choosing the conventional configuration, as weight is explicitly factored twice into the mission and overall score of the competition aircraft.

3.4.2 Empennage Configuration

The aircraft's tail assembly configuration was weighted on three characteristics: weight at 50%; ground clearance at 25%; and complexity of manufacturing at 25%. Because of the mission scoring scheme, weight of the empennage was determined to be the most critical attribute. The configurations considered for the empennage included H-tail, T-tail and V-tail configurations. Table 3 shows the weighted and total score of each empennage design; all scores are on scale of 1-3.

Table 3: Aircraft Tail Configuration Trade Study

Attribute	Weight	Conventional		Cross Tail		V Tail		T Tail	
		Score	Weighted Score	Score	Weighted Score	Score	Weighted Score	Score	Weighted Score
Weight	50	3	150	2	100	3	150	1	50
Clearance	25	3	75	1	25	3	75	3	75
Complexity	25	3	75	2	50	1	25	2	50
Total:	100		300		175		250		175





From the weighted scores, it was determined that the conventional empennage assembly provided the best combination of low weight, clearance, and ease of manufacturing out of the three configurations.

3.4.3 Fuselage and Payload Layout

The design and layout for the fuselage was driven almost entirely by the need to carry rectangular blocks in mission 2 as well as water in Mission 3. The payload was designed such that the loading and dumping of water was efficient, reliable, and fool-proof while allowing for passenger constraints. The requirement of the use of a servo to operate a hatch mechanism that releases the water motivated a fuselage design which is rectangular with planar sides. The need to secure all passengers for Mission 2, while adhering to the spatial requirements listed in the rules for that mission, also justified the need for a rectangular, block shaped fuselage.

3.4.4 Landing Gear

Three landing gear configurations were considered for the H₂Buffalo: tricycle gear, bicycle gear, and tail dragger. The description of each and encompassing trade study are seen below:

- **Tricycle Gear:** This configuration has predictable ground behavior, but having three landing gear components in the free stream increases the total drag on the aircraft.
- **Bicycle Gear:** This gear configuration provides a lightweight solution, and the wheels could easily be recessed into the fuselage to reduce drag.
- **Tail Dragger:** By having only two wheels in the free stream, the drag on the aircraft is reduced and increased ground clearance allows for the use of a larger diameter propeller

Table 4: Landing Gear Configuration Trade Study

Attribute	Weighting	Tricycle		Tail Dragger		Bicycle	
		Score	Weighted Score	Score	Weighted Score	Score	Weighted Score
Weight	35	1	35	3	105	2	70
Drag	20	1	20	2	40	2	40
Complexity	10	1	10	3	30	1	10
Stability	20	3	60	1	20	2	40
Prop Clearance	15	2	30	3	45	1	15
Total:	100		155		240		175

The tail dragger configuration was selected as the best option for the H₂Buffalo for several reasons. It requires the least amount of structure weight on an aircraft, it is the simplest to manufacture, and allows for the greatest amount of propeller clearance and, in turn, the greatest amount of available thrust.





3.4.5 Motor Configuration

The initial considerations for the design of the propulsion system were the location and quantity of the motors. Single- and multi-motor configurations were explored. A two-motor configuration inherently includes two speed controllers, additional wiring, and two structural attachment points. A two-motor configuration would allow the motors to be placed on the wings, and would allow for the use of smaller diameter propellers. These factors all contribute to an increased aircraft empty weight. A single-motor configuration limits the placement of the power plant. Primarily, the payload of the aircraft drove the placement of the motor. Ground clearance was not a design constraint as the estimated power output of the weight-limited battery size capped the propeller diameter at approximately 16".

As the empty weight of the aircraft is the most sensitive element of the scoring matrix, a single motor in a tractor configuration was selected to reduce overall propulsion system weight and keep electronic components out of the water plume.

4.0 Preliminary Design

4.1 Design Analysis/Methodology

4.1.1 Fuselage Shape

The fuselage was required to endure multiple takeoffs and landings, restrain passengers, as well as contain two liters of water without leaking. Given these parameters and the arrangement of the passengers in the fuselage, a rectangular, conventional fuselage was chosen. It was found that the best passenger layout was to have two rows of four passengers running longitudinally through the fuselage. This brought the center of gravity within the required envelope and the configuration also made the fuselage the right size for the two liter water mission.

4.1.2 Weight Prediction

A comparison of payload-to-weight ratios of previous CUBDF aircraft as well as competitive aircraft placing fifth and above at the DBF competition was used to estimate the structure weight based on maximum payload weight. This weight estimate was then used to determine a wing area and power required estimate.

4.1.3 Wing Area

Performance constraint plots were created to determine the required wing area given thrust and weight predictions. Wings were sized to produce the required lift with minimum induced drag. Minimizing wing area both decreases weight and drag of the aircraft. Minimizing weight is paramount since weight is the most sensitive scoring parameter. Decreasing drag will increase the rate of climb.

4.1.4 Airfoil Selection

Selection of an airfoil for the wing emphasized two main requirements. The first requirement was for an airfoil that had a high coefficient of lift. This was the most important parameter as the most sensitive





score factor was weight. By having a high coefficient of lift the wing size can be reduced, decreasing the overall weight. The second most sensitive parameter was the lift-to-drag ratio. A high lift-to-drag ratio decreases the drag produced by the aircraft for the same lift. This allows the aircraft to fly faster for the first mission, increasing the amount of laps that can be completed, and for the third mission a decrease in drag allows the aircraft to climb faster, increasing the overall score. A number of airfoils were examined based on the aerodynamic characteristics stated above and analyzed to determine which provided the optimal combination of high lift-to-drag and coefficient of lift.

4.1.5 Empennage/Tail

The required tail volume was calculated in order to achieve the desired stability and control authority. Since weight was determined to be the most sensitive score parameter linear density of the tail boom and area density of the horizontal and vertical tail surfaces were taken into account to determine the lightest combination of tail length and surface area to achieve the necessary tail volume. The center of gravity (CG) of the tail was also taken into account as it played a major role in the longitudinal CG location of the entire aircraft. Optimum tail dimensions were chosen considering tail weight, CG location and tail volume.

4.1.6 Battery Type and Quantity

With the third mission of the competition being dependent on quick time-to-climb, the rate of climb had to be maximized. The largest factors contributing to the aircraft's climb rate are thrust, weight, and drag. Therefore, cells were chosen to maximize power output while minimizing weight. The cell's ability to draw high current for a large time interval, as well as maintain a nominally constant output voltage, were all major design constraints. The quantity of cells was optimized through static testing for endurance and power output.

4.1.7 Speed Controller

The speed controller selection was primarily driven by the operational characteristics of the other components of the propulsion subsystem, taking into account the battery voltage and estimated current draw. After satisfying these requirements, a lightweight, reliable programmable speed controller was selected.

4.1.8 Motor Selection

The selection of a motor is extremely important as to the overall performance of the aircraft. The motor selection was primarily based on the efficiency of the motor, as well as the weight and electrical output of the system. The motor was selected to fit the power ratings, efficiency, and weight restrictions to optimize the cruise speed and time-to-climb performance variables.

4.1.9 Propeller Diameter and Pitch

The propeller is one of the most inefficient elements of a propulsion system. The pitch and diameter of the propeller were selected to meet the needs of the mission requirements. A highly pitched propeller





is ideally suited for improved efficiency at higher speeds, while a lower pitch is ideal for maximizing static thrust. A larger diameter propeller effectively displaces more air, but requires additional power from the system. Current limitations and battery weight constrained the selection of a propeller; therefore, the selection was based primarily on current draw of the system, in addition to the estimated output voltage of the battery pack.

4.2 Design/Sizing Trades

4.2.1 Fuselage Shape

The first thing to be considered while designing the fuselage was its payload volume capacity. As the payload bay had to be able to hold both 2L of water as well as accommodate the eight passengers and their spatial restrictions, a two by four passenger configuration was chosen. This configuration constrained the inner dimensions of the fuselage to 3 "x 5 "x 8.5". The shape of the payload bay was left rectangular to better hold the rectangular blocks. In order to internally contain the batteries as well as the CAM-f3q altitude sensor, a second smaller payload compartment was designed and placed directly above the payload chamber with a foam plate of thickness 0.5 inches. With both chambers, the preliminary outer dimensions of the fuselage were 4 "x 6.5" x 10".

The material chosen for the fuselage construction was medium-density insulation foam as it was both light-weight and structurally stable if reinforced with a front firewall and rear bulkhead. Further support was added by using balsa/plywood blocks to support the landing gear and wing spar. These additional blocks were implemented to keep the foam from deflecting due to flight and landing forces. The outer surfaces of the fuselage were coated with Monokote™ in order to reduce skin friction drag.

There are a number of advantages that come from this design. First, the foam chosen for manufacturing allows for easy construction using a template and a hot wire. Also, the landing and wing blocks along with the front and back bulkheads provides a structure able to handle all aerodynamic forces from flight as well as the impulse forces from landing. One slight disadvantage of these materials was the difficulty waterproofing the internal payload bay.

4.2.2 Weight Prediction

The CUDBF final competition aircraft from last year is in many ways comparable to this year's design. The materials and payload weight are remarkably similar and therefore the weight properties of that aircraft can be used to estimate the weight of this year's aircraft. Last year, the heaviest payload weighed 4 lb while the empty aircraft weighed 3.13 lb, making the empty weight to payload weight ratio 0.78. This weight ratio is compared to historic averages and is shown to be on the lower end of these ratios. The results of this comparison are shown in Table 5, below.





Table 5: Historic Aircraft Weight Ratios

	W_E/W_{PL} Ratio	Empty Aircraft Weight (lb)
Mean	1.12	7.0
Lower Limit	0.78	3.13
Upper Limit	1.35	8.44

The heaviest payload that the H₂Buffalo will have to carry is the water at a total of 4.4 lb. Using the empty weight to payload weight ratio from last year, the empty aircraft is predicted to be 3.44 lb. The aerodynamic prototype was found to weigh 4.4 lb. Ideally, further prototypes will significantly decrease this ratio as the manufacturing processes are perfected.

4.2.3 Wing Area

Figure 5 shows a constraint tradeoff plot to find the optimal wing area of the aircraft, as a function of wing loading (W/S) and weight to power ratio (W/P). The optimal design point occurs at the intersection of cruise speed, stall speed, and maneuvering loading as shown in Figure 5.

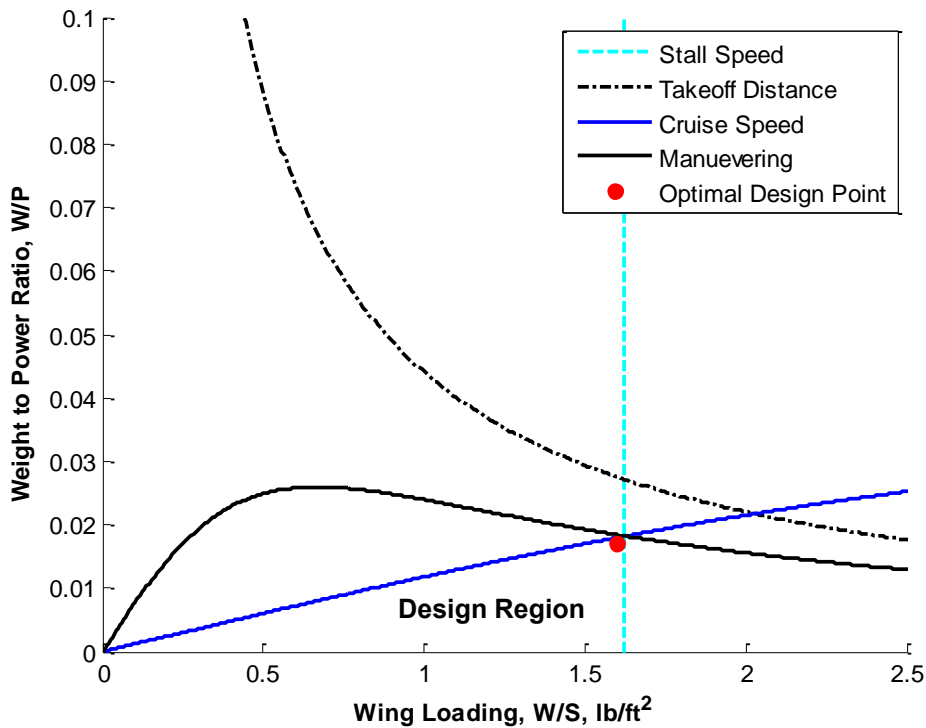


Figure 5: Performance Constraint Plot

This design point gave a wing loading, W/S of 1.60 lb/ft² and weight to power ratio, W/P of 0.0170. Using an estimated gross takeoff weight of 8.0 lb the necessary wing area was determined to be 5.2 ft². With a chosen aspect ratio, AR of 6.0 this area results in a span of 5.6 ft and a chord of 11.2 in. The power required was calculated from the weight to power ratio to be 470W. The performance constraint





shown in Figure 5 demonstrates an envelope of design points that meet all the performance requirements for stall, takeoff and cruise. An optimum point was chosen that would maximize the cruise speed while keeping weight to power ratio small. Lower weight to power ratios would result in more excess thrust and would further improve the time-to-climb mission.

4.2.4 Airfoil Selection

A selection of over 60 airfoils were chosen for analysis based on a number of airfoil characteristics, the most important being coefficient of lift and lift-to-drag ratio. The aerodynamic coefficients were found using thin airfoil theory, a theory that produces accurate results for incompressible and in viscid flow. The top ten airfoils analyzed are shown below in Figure 6 in a plot that compares their coefficient of lift to lift-to-drag ratio. A program called XFOIL (4), was used to determine the coefficients shown below.

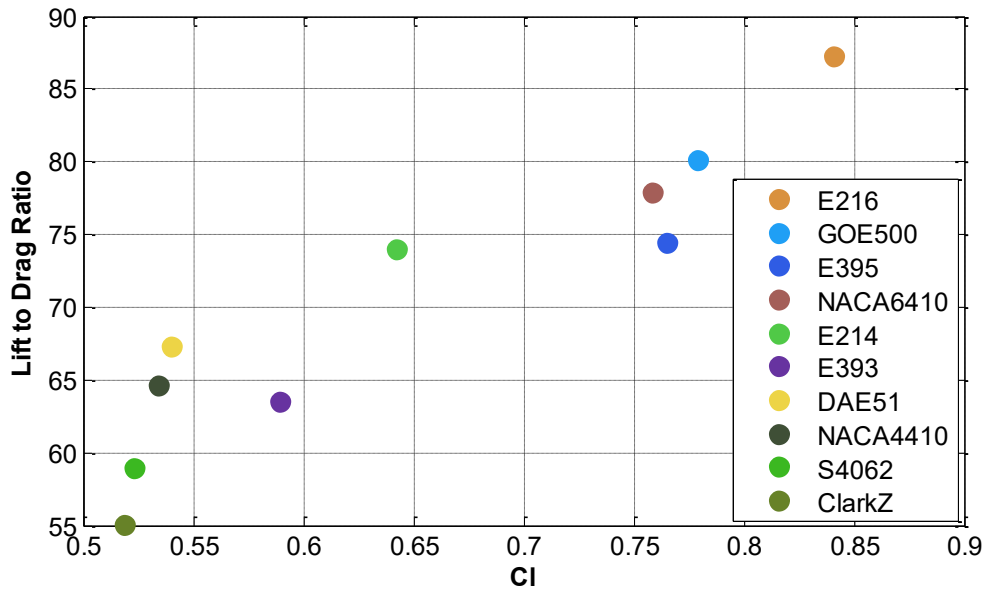


Figure 6: Lift-to-Drag Ratio versus Coefficient of Lift for Various Airfoils

The Eppler 216 airfoil was chosen due to its high coefficient of lift, about 0.84 at the cruising angle of attack. Along with the Eppler 216's high coefficient of lift, its lift-to-drag ratio at cruise was the highest of any airfoil at 87.32. The only downside to the chosen airfoil is its extremely high coefficient of moment when compared to the other airfoils analyzed shown below in Figure 7.



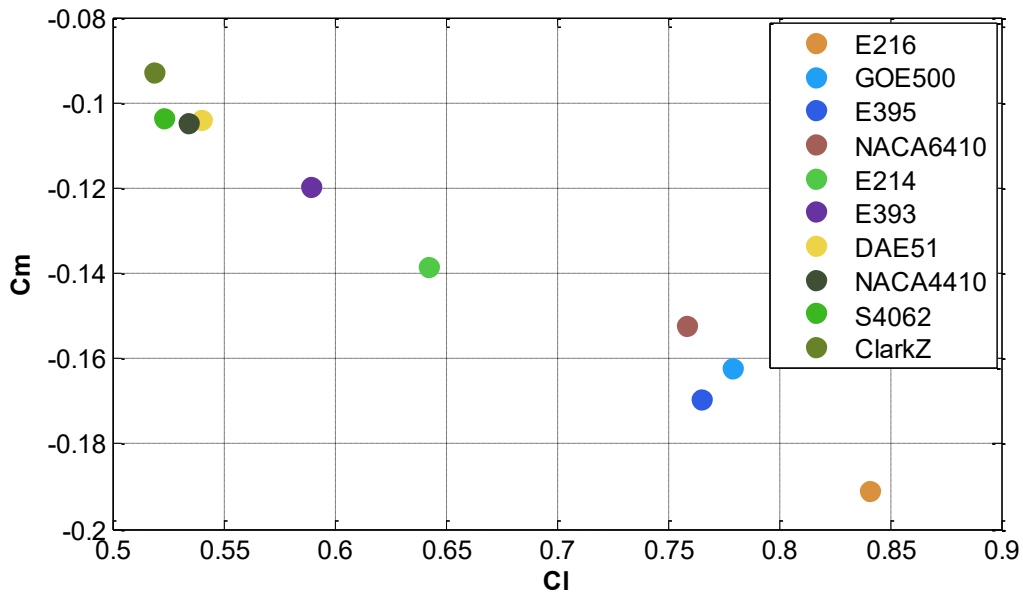


Figure 7: Coefficient of Moment versus Coefficient of Lift for Various Airfoils

The coefficient of moment for the Eppler 216 was -0.1975, -0.0255 higher than the Eppler 395. To counteract its higher coefficient of moment a larger tail is needed to keep the aircraft stable. It was ultimately decided that the high coefficient of lift and high lift-to-drag ratio outweighed the downside of a larger tail and increased weight and drag associated with it.

4.2.5 Empennage/Tail

Tail size was chosen using tail volume ratios in order to achieve the desired neutral point location for required stability and control authority. Since weight was determined to be the most critical parameter the tail was designed to optimize weight while still providing the appropriate stability characteristics. A program was written to iterate through various tail lengths. For each tail length the necessary tail area was calculated to maintain a constant tail volume. The structural weight was then calculated for each tail area and tail length combination. Results from this iteration can be seen in Figure 8.



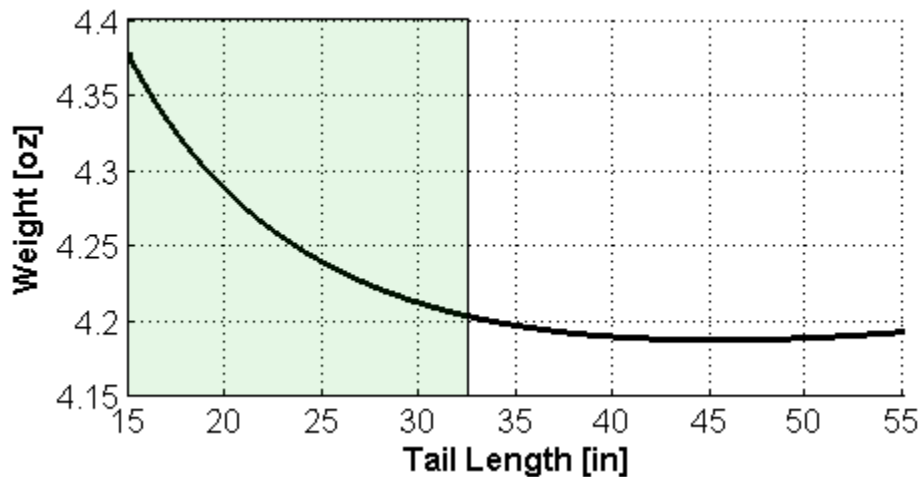


Figure 8: Tail Mass as a Function of Tail Length for a Constant Tail Volume

Lengthening the tail and increasing the tail area adds mass aft of the aircraft center of gravity, thus moving the total aircraft center of gravity aft. Therefore the center of gravity from the leading edge was also calculated for each tail length. Figure 9 shows how the center of gravity location changes with different tail length and tail area combinations.

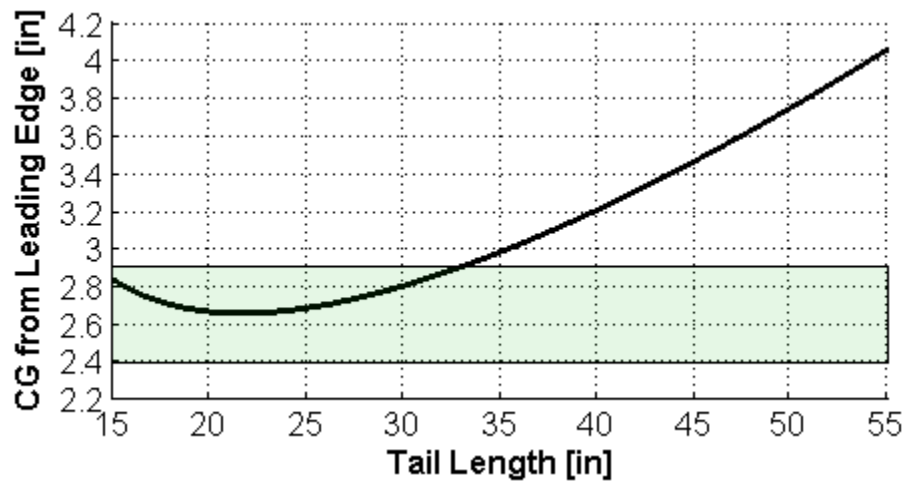


Figure 9: Center of Gravity Location for Each Tail Length

Given that weight is being optimized, inspection of Figure 8 reveals that a tail length of 45 inches would be optimum since it results in the lowest overall structural weight. However inspection of Figure 9 reveals that this tail length also results in a far aft CG. Therefore stability had to be considered. The static margin was calculated for various CG locations to determine the CG envelope that would result in the desired longitudinal stability. The shaded region on Figure 9 defines the forward most and aft most CG locations necessary for the desired stability to create tail length bounds. This region was then translated to Figure 8 based on the tail length at which the CG envelopes intersected the CG vs. tail length curve. The tail was then sized to minimize weight while remaining within the CG envelope. A tail length of 30 in was chosen to provide for a reasonable safety margin.





4.2.6 Battery Selection and Cell Quantity

The propulsion system had a variety of constraints; however, with the aid of several design tools, knowledge heritage, and numerical computations, the components of the system as well as the flight operations were selected to optimize the score. The propulsion system has several fundamental requirements: provide power enough to complete laps for ferry flight, provide adequate power for the passenger flight, and maximize the rate of climb of the aircraft for the time to climb mission, all while maintaining a low system weight. The first component necessary for the preliminary design of the propulsion system was the battery type, and quantity.

The battery chemistry is limited to nickel-metal hydride (NiMH) and nickel cadmium (NiCad) compositions. A NiMH chemistry provides a high-capacity density and a very repeatable charge and discharge cycle, allowing for consistent performance from well-conditioned cells; however, NiMH cells do experience a small voltage drop when under high amperage loads. As the empty weight of the aircraft is the most sensitive scoring attribute, the capacity density of the selected cells was of utmost importance; therefore, NiMH chemistry was selected. The size of the cell was then optimized using the values provided in Table 6.

Table 6: NiMH Cell Comparison Matrix

Cell (NiMH)	2/3A	4/5A	AA	AAA	Sub C
Capacity [mAh]	1600	2000	1700	1000	3300
Weight [oz]	0.81	1.16	1.00	0.46	1.93
Capacity [mAh/oz]	1975.31	1724.14	1700.00	2173.91	1709.84

The matrix provides the average weight and capacity density for five different cell sizes and capacities. As previously stated, the capacity density is the driving variable for cell selection; however, the 2/3A, 1600 mAh cell was selected. The AAA, 1700 mAh cell possess the ideal desired attributes, but lacks the ability to output high current for extended periods of time, as determined from experimental heritage.

Following the investigation of the cell size, the number of cells required to power the propulsion system was determined. In order to generate the most power from the system while keeping the pack weight under the 1.5 lbs and not blowing the 20 A slow-blow fuse mandated by the competition rules, the voltage was sought to be maximized to allow a lower current draw (per Ohm's Law, $P = I \cdot V$). Additionally, the required power values provided by aerodynamic analysis dictated the power output of the system. Assuming a 70% system efficiency, it was determined that a 14 cell battery configuration was well-suited for the aircraft.





4.2.7 Speed Controller

The purpose of the electronic speed controller (ESC) is to regulate current output and timing to an electric motor. Selection of the speed controller was derived from the estimated peak demand of the propulsion system. Since this system is limited by a 20 amp slow-blow fuse by the competition, the capabilities of the fuse must be known. By varying the current through the fuse and recording the time until it breaks down a relationship was established. This information can be found in Figure 10. As shown the fuse can actually sustain an amperage greater than 20 amps for an extended period of time. The power portion of the figure shows that for a flight time of approximately 425 seconds the power output of the motor is 470 W. Knowing that 25-30 amps could be drawn without blowing the fuse during a 1-2 minute climb, a speed control rating of 35 amps was chosen.

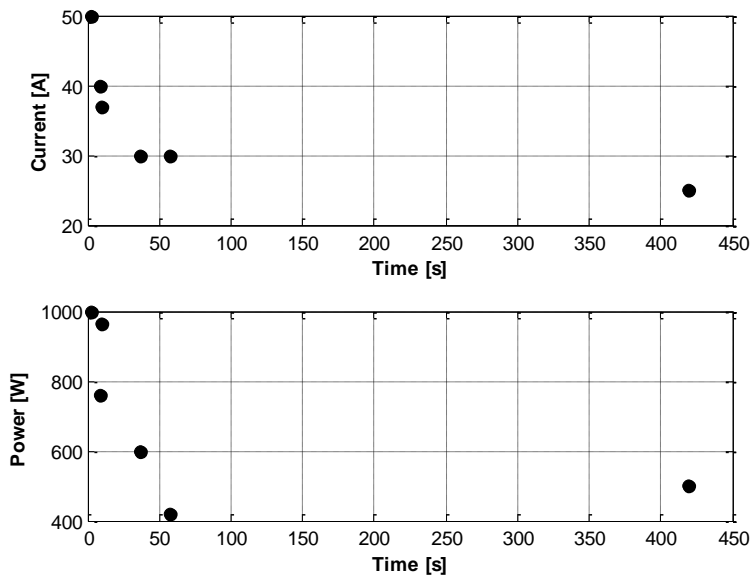


Figure 10: Power and Amperage Testing Data

Most Castle Creations ESCs have a built-in data logging system that can be accessed via a user friendly USB interface. The Castle ESCs offer throttle timing, range, and a motor break. Furthermore, previous use of Castle Creations ESCs in CU DBF has made the products and expertise more available. As weight is the most important parameter for this year’s mission, the ideal speed controller would be as light as possible. With the current limitations, only two Castle products were considered. The first, the Ice Lite, was chosen for flight test purposes as it possessed the data logging system mentioned above. For the final aircraft, however, the Phoenix 45 was chosen as it is slightly lighter.

4.2.8 Motor Selection

The competition requirements state that the motor is to be an electric, commercially available R/C motor. There are two main types of electric motors: brushed and brushless. Brushless motors are generally more reliable, overheat less, are more efficient than their brushed counterparts, and require no “breaking in” period. Gear reduction was also explored; however, a comparison of the thrust/system





weight ratio revealed that the additional weight of a gearbox offset the additional thrust in the overall score. For this reason, a brushless motor design was selected.

The mission requirements dictated the specific motor selection. Approximately 25 brushless motors were investigated, and input into an electric propulsion software, Electricalc (7). The motors that were investigated were from a wide range of Kv ratings and casing sizes. Using the 14 cell battery selected in the previous section, the theoretical maximum power output was determined for each motor using a propeller selected to optimize the thrust of each system (provided by the Electricalc (7) design software). This thrust was then compared to the approximated system weight of the propulsion sub-system. The results of this investigation are presented in Figure 11.

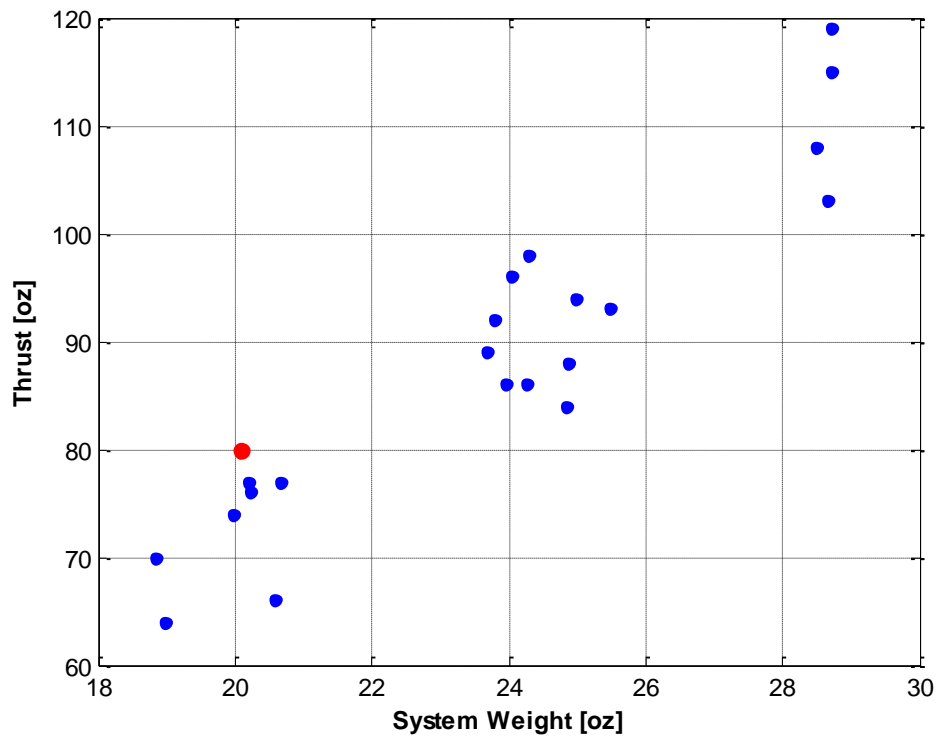


Figure 11: Propulsion System Weight vs. Theoretical Electricalc (7) Thrust for 25 Different Commercially Available Brushless Motors

The analysis interestingly seemed to divide the motors into three distinct groups: a low, mid, and high weight group, with low, mid, and high thrust, respectively. A motor configuration from each group was input to a mission analysis MATLAB (9) script to estimate a relative total score as a function of rate of climb and propulsion system weight. The results are provided in Figure 12 through Figure 15.



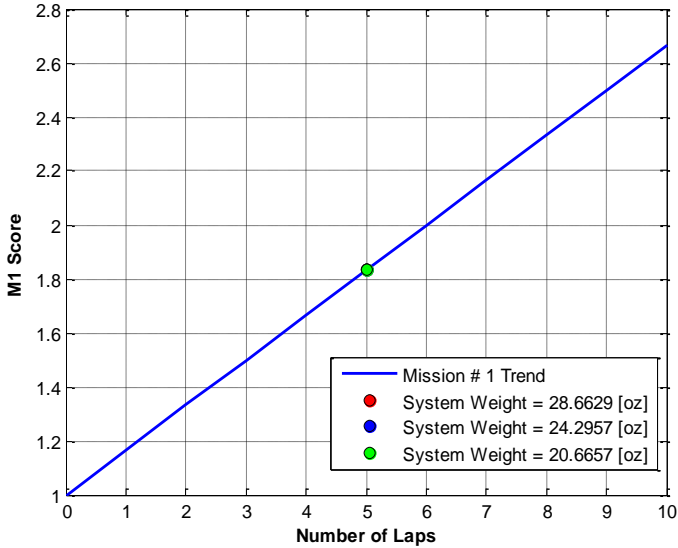


Figure 12: Mission 1 Score

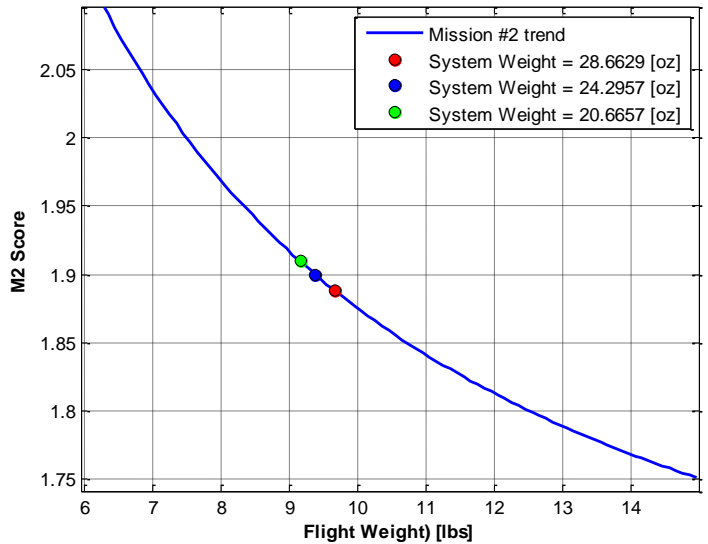


Figure 13: Mission 2 Score

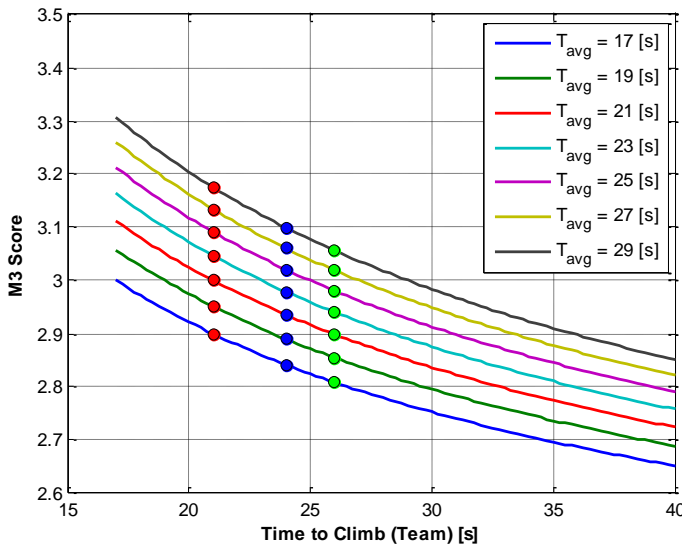


Figure 14: Mission 3 Score

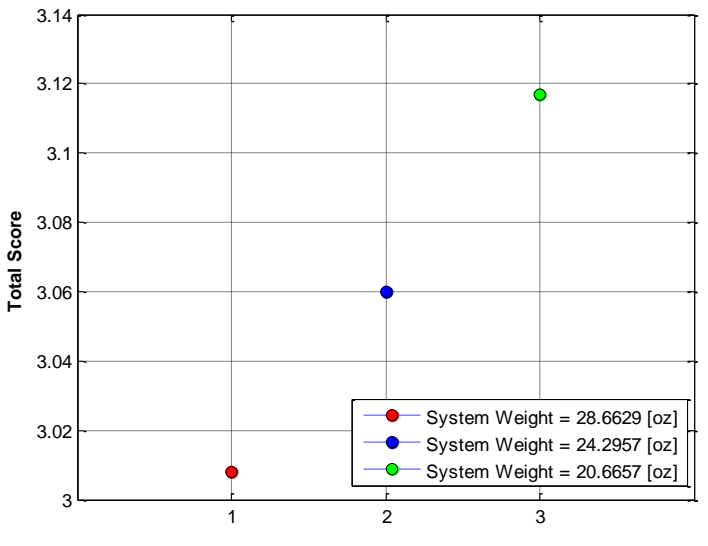


Figure 15: Total Mission Score

These results were computed by setting the number of laps completed to 5 because even with the increased propulsion performance from the heavier motors, the dynamics of the aircraft limited the completion of a full additional lap. This result was the first indication that a lighter system weight would be ideal. The score for mission two can be seen in Figure 13. The separation of the three motor groupings is quite small; however, the lighter motor configuration yields a slightly higher score. For the third mission, the heavier motor results in a higher score as it has the ability to achieve greater excess thrust. The plot provides an iterative depiction of the average time to climb of all of the competing teams, and the relative H₂Buffalo score for each case. The summations of the mission scores are provided in Figure 15. This score was generated using the lowest average time to climb of all of the teams. It should be noted





that for each mission three score iteration, the relative difference in score is independent of the competition average time to climb.

These results allowed for the selection of the light weight, high efficiency, HIMMAX HC3522-0700 brushless out-runner to be confidently selected as the optimal motor for the H₂Buffalo.

4.2.10 Propeller Diameter and Pitch

Following the preliminary design of the electrical components of the propulsion subsystem, the propeller diameter and pitch were optimized. The sizing was defined by the full-throttle current draw. For the payload missions, a high static thrust is desired, requiring a large diameter and smaller pitch. On the other hand, the no-payload ferry flight will score better with a faster top-end speed. The faster speed is obtained by choosing a propeller with a higher pitch value, allowing the propeller to “bite” through the air more as the aircraft is moving.

4.3 Mission Model

The competition consists of three unique missions. In all three missions, the aircraft must make a rolling ground takeoff within 100ft and begin to fly the course. The upwind leg ends 500 feet from the start line. Once the aircraft passes the marker at the end of the upwind leg, the aircraft may perform a 180° turn and begin the downwind leg. During the downwind leg of the lap, the aircraft is required to perform a 360° turn away from the runway before crossing the second marker 500 feet downwind of the start line. The aircraft then is allowed to turn and fly towards the start line. Once the aircraft crosses the start line in the air, the lap is complete.

4.3.1 Ferry Flight

The ferry flight puts the aircraft’s speed and agility to the test. With the goal of completing as many laps as possible within the four minute time limit, it was necessary to design the aircraft with a minimum drag and maximum corner velocity and straight away speed. With a corner velocity of 63.3 ft/s and a bank angle of 60°, the aircraft is calculated to have a turning radius of 72.3 ft at a load factor of 2 g’s. Assuming this turn radius, the turning portion of the flight path length is 908 ft long. The straight away distance of the course is 2000 ft and average cruise speed is estimated to be 86.5 ft/s. This makes the total time per lap equal to 35.1 seconds. Accounting for a slower take off velocity, the maximum number of laps is predicted to be 5 laps. This results in a score of 1.83 for the first mission.

This estimate will lose accuracy as the crosswind velocity increases on the day of the competition. As the crosswind component increases, the average flight course velocity decreases hyperbolically. Assuming a strong crosswind of 10 mph, the time per lap increases by approximately 3.1 seconds. This effect is surprisingly negligible. However, the effects of gusting wind and wind shear complicate the duties of the pilot and will increase the time per lap more than estimated above.





4.3.2 Passenger Transport

In the passenger transport mission, the only score contribution is dependent on aircraft weight. Optimizing this mission becomes a matter of structure to weight ratio. Having the minimum amount of structure not only improves this mission score, it also decreases RAC thus improving the overall score. Based on historical data a structure to payload ratio of about 0.8 is common for competitive aircraft of this scale optimized for low weight. Since the heaviest payload carried by this aircraft is 4.41 lb, the predicted score for the passenger transport mission is 2.56.

This calculation is made complicated by the fact that the current aircraft design includes a permanently waterproofed payload compartment rather than a removable one. The historic data of a structure to weight ratio of 0.8 may not be applicable to this style of aircraft.

4.3.3 Time to Climb

The third and final mission is the most challenging in terms of design. Completing the mission with a high score requires maintaining a sustained climb from the runway to 100m AGL. The minimum time to climb is dependent on the power output of the propulsion system and the maximum C_L attainable by the aircraft. The time to climb is estimated to be 26 seconds.

An additional consideration in the time to climb mission is the visibility of the time end indicating water plume upon reaching the target altitude. It is difficult to quantify the effects of atmospheric visibility and the flight line judge's reaction time to seeing the water plume.

4.4 Lift, Drag and Stability Characteristics

4.4.1 Control Surface Sizing

The aircraft's control surfaces were sized to produce the proper control authority for the loaded missions. The aircraft's ailerons spanned 50% of the wing's span and 25% of the chord. The elevator spans the entire horizontal stabilizer and 33% of the chord. The rudder spans the entire vertical stabilizer and 33% of the chord. Flight tests have proven these control surfaces provide ample control authority.

4.4.2 Lift and Drag

For drag analysis, XFOIL (4), XFLR5 (5), and AVL (6) were used to calculate viscous and lift-induced drag estimations. Parasite drag for the wing airfoil was calculated using XFOIL. AVL was used to calculate lift-induced drag for the entire aircraft. Fuselage viscous and pressure drag was calculated using XFLR5. A breakdown of the predicted drag coefficients for each aircraft component is shown in Table 7. The aircraft's drag polar is shown in Figure 16.





Table 7: Component Drag Values

Component	C _D	% of Total
Fuselage	0.00735	20.4%
Wings	0.02330	64.6%
Horizontal Stabilizer	0.00392	10.9%
Vertical Stabilizer	0.00151	4.2%
Total	0.03608	100%

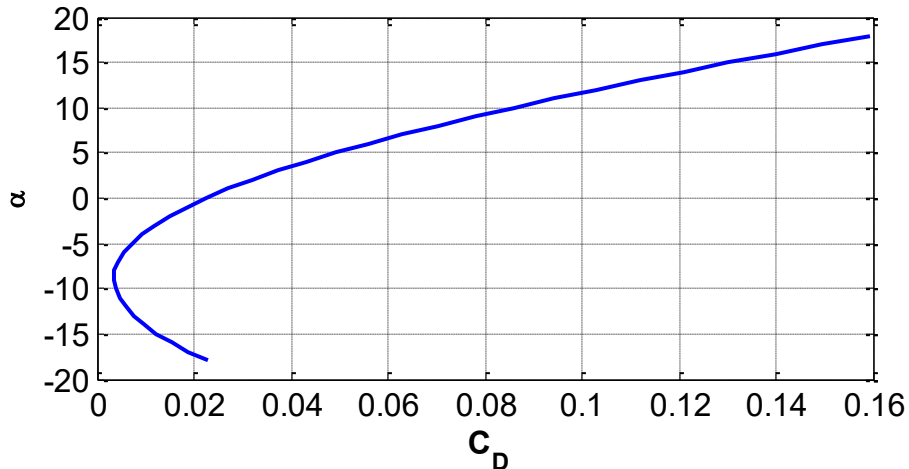


Figure 16: Aircraft Drag Polar

The drag polar above shows that at a 3.551 degree cruise angle of attack, the preliminary design has a 23.84:1 lift-to-drag ratio, which decreases to 16.36:1 before stall at 11.4 degrees, showing high rate of climb capability. The graph also shows that due to the high camber of the aircraft, the zero lift point occurs at -7.2 degrees angle of attack, giving a CD₀ of 0.0035.

In an attempt to reduce fuselage drag the fuselage was fitted with an aerodynamic trailing cone. The trailing cone was designed to fit within the low-pressure void immediately behind the fuselage. A simple SolidWorks (10) flow simulation, shown in Figure 17, was used to visualize the flow and determine the optimum location of the tail cone.

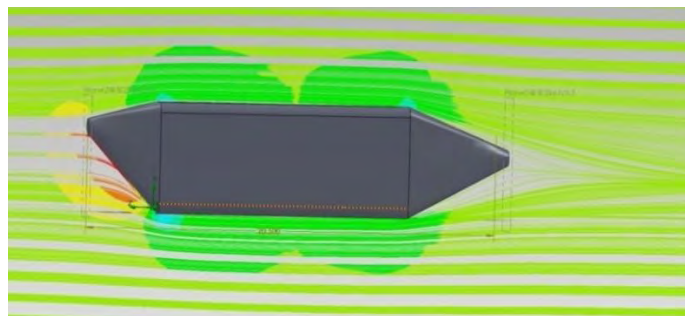


Figure 17: Fuselage Flow Simulation (10)





4.4.3 Stability

Longitudinal stability was vitally important for this aircraft. The aircraft must be stable enough to endure the sudden CG shift when water is ejected during the time to climb mission. However, an overly stable aircraft will sacrifice maneuverability resulting in a slower lap score and rate of climb. Aircraft stability was calculated primarily using AVL (6). Since the wing position was constrained due to structural requirements, iterations were performed in AVL to calculate the static margin with different CG locations. Figure 18 relates the X_{CG} location to static margin.

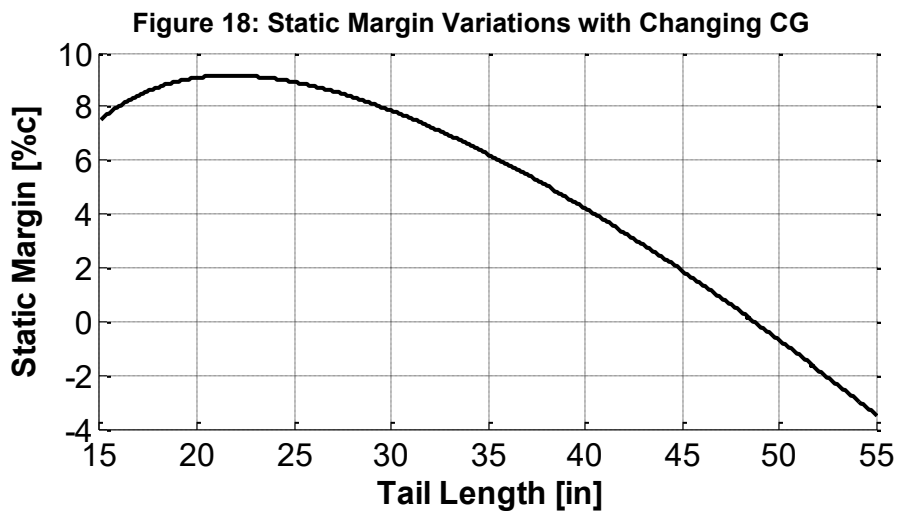
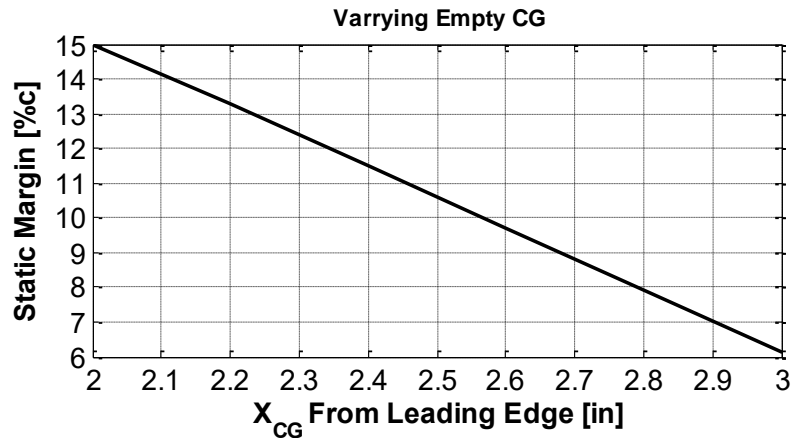


Figure 19: Static Margin Variations with Changing Tail Length

For the empty ferry mission the CG location is 2.7 in behind the leading edge, resulting in a static margin of 8.4%. For the time to climb mission at maximum takeoff weight the CG location moves to 1.62 in behind the leading edge, causing the static margin to increase to 18.5%. Although this static margin is pushing the limit of the ideal range of 5-15%, it is considered acceptable due to structural constraints.

AVL (6) was also used to calculate stability eigenvalues. Figure 20 shows the longitudinal stability modes of the aircraft.



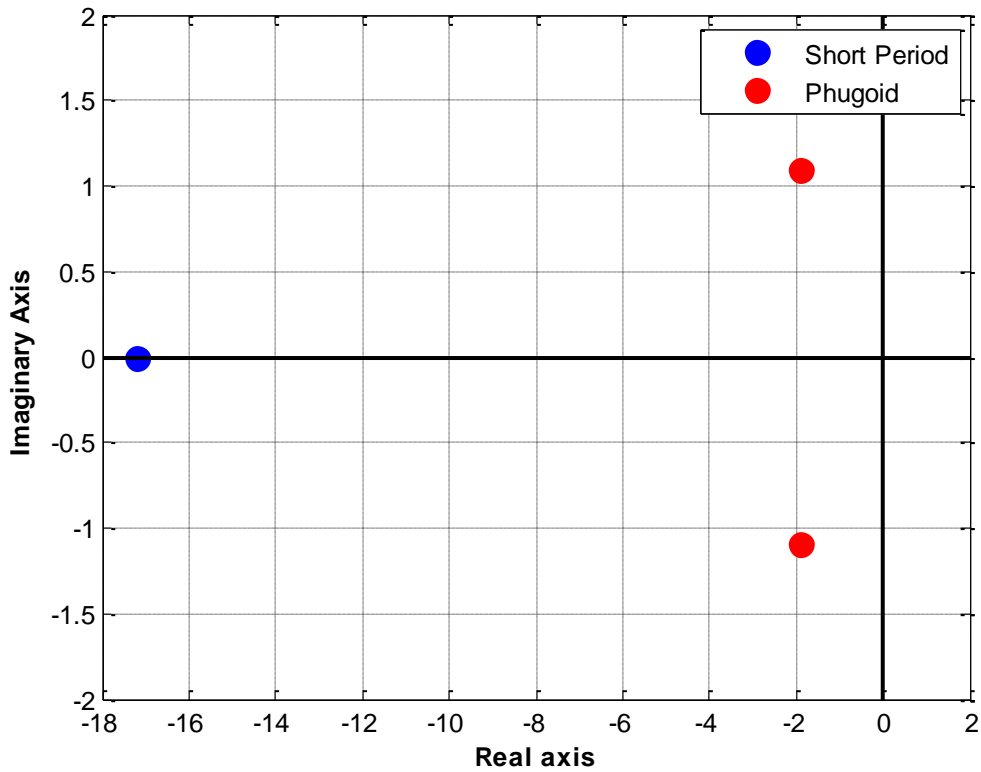


Figure 20: Longitudinal Stability Modes

Table 8: Longitudinal Stability Characteristics

Mode	Frequency [Hz]	Period [s]	Damping Ratio
Short Period	17.1874	0.0582	1.0
Phugoid	1.8950	0.5277	0.8653

The aircraft is stable in its longitudinal modes showing a high damping ratio for both the Phugoid and short period modes of the aircraft. The high damping, and lack of oscillations of the short period, in particular, is beneficial for the flight conditions due to a fast pitch up as experienced in the time to climb mission due to the efficient damping. Figure 21 shows the lateral stability modes of the aircraft.



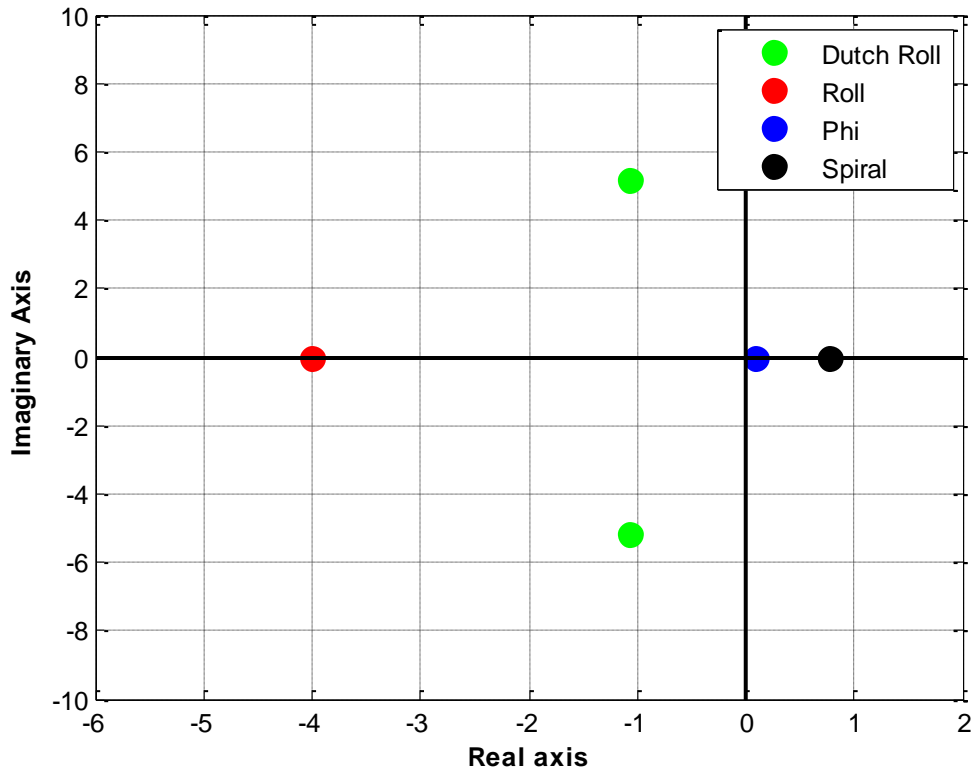


Figure 21: Longitudinal Stability Modes

Table 9: Lateral Stability Characteristics

Mode	Frequency [Hz]	Period [s]	Damping Ratio
Roll	4.0091	0.2494	1.0
Spiral	0.7738	1.2924	-1.0
Dutch Roll	1.0746	0.9305	0.2023
Phi	0.0970	10.3098	-1.0

The aircraft is stable in roll and Dutch roll, however, it has spiral instability and a phi Euler angle instability. The phi instability is a tendency of the aircraft to gain yaw and roll when the aircraft is perturbed in the y-direction with an initial phi angle. As Figure 21 shows, the magnitude at which the aircraft diverges in both cases is very low. Because of this both instabilities are acceptable, as they are easily correctable by the pilot.

4.5 Aircraft Mission Performance Estimation

4.5.1 Ferry Flight

The ferry mission does not require any payload; therefore, the aircraft will be significantly lighter than the other two missions. Because speed is the primary goal in the ferry mission, the propellers will be 14 x 10 inch to increase maximum speed. The aircraft is designed to cruise at 86.5 ft/s, make 180° turns in roughly 4 seconds, and make the 360° turn in 8 seconds. Based on early test flights and comparisons to





other University of Colorado DBF aircrafts, the aircraft should fly 5 laps within the allotted four minutes with approximately 600 mAh battery capacity remaining.

4.5.2 Passenger Transport

Speed is not a concern in the passenger transport mission therefore a 14 x 7 inch propeller will be used. This propeller should provide the aircraft with a higher static thrust. The aircraft is predicted to carry all 8 passengers for three complete laps with 1.2 minutes of flight time left over.

4.5.3 Time to Climb

As this mission requires the aircraft to climb at its heaviest weight, a 14 x 7 propeller will be used. It is expected that the aircraft will reach the 100m mark in 26 seconds as the aircraft was built for both lightness and climb rate. This climb time should place the team above the overall average.

5.0 Detailed Design

5.1 Dimensional Parameters

Following the extensive design and analysis process, the final aircraft design was selected. A preliminary design rendering is represented in Figure 22.



Figure 22: Complete Aircraft Design

The core dimensional parameters of the aircraft are presented in Table 10





Table 10: Dimensional Parameters

Fuselage	Value	Wing	Value	Vertical Stabilizer	Value	Horizontal Stabilizer	Value
Width (in)	4	Airfoil	Eppler 216	Airfoil	Flat Plate	Airfoil	Flat Plate
Height (in)	6.5	Span (in)	68	Span (in)	14	Span (in)	22
Length (in)	10	Chord (in)	11	Root Chord (in)	7.5	Root Chord (in)	7.5
Volume (in ³)	260	Area (in ²)	753	Area (in ²)	105	Area (in ²)	165
		Aspect Ratio	6	Aspect Ratio	1.9	Aspect Ratio	2.9
		Incidence Angle (deg)	0	LE Sweep Angle (deg)	20	LE Sweep Angle (deg)	20
		Ailerons	Value	Rudder	Value	Elevators	Value
		Area (in ²)	47	Area (in ²)	35	Area (in ²)	28
		% of Chord	25	% of Chord	33	% of Chord	33

5.2 Structural Characteristics: Component Selection, Integration, and Architecture

5.2.1 Wings Sections and Securement

The aerodynamic analysis indicated that the span of the aircraft needed to be 5.48 ft. An attachment involving a single wing spar and a moment pin was integrated in order to minimize the moment and weight experienced by the connection of the wing. The wings are connected to the fuselage via a carbon fiber joiner with an additional smaller carbon fiber alignment pin aft of the main joiner. This joiner extends across the width of the fuselage and is inserted into the carbon spar in the wing itself as shown in Figure 23. The wings are secured using a rubber band pin system, where a small pin is attached through each of the wings and rubber bands are hooked around the wing pins. The servos are nested and secured within the bottom of the wing for aileron control.

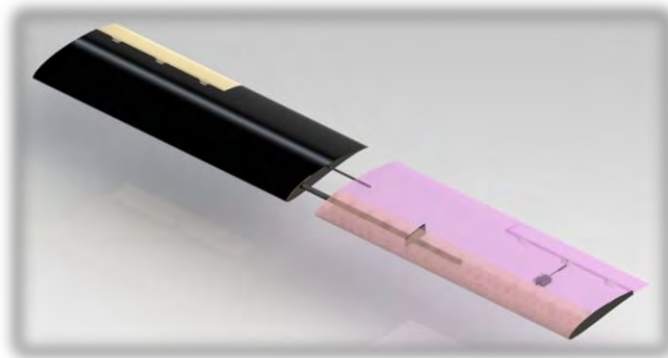


Figure 23: Wing Attachment





5.2.2 Water Tank, Fuselage and Airframe

The fuselage design needed to accommodate for the two liter water payload and the aluminum block passengers. After obtaining the necessary volumetric dimensions for the fuselage to carry both the water and the passengers, different materials for the fuselage structure were explored. A foam fuselage with a waterproofed inner lining was investigated. The foam provided feasible structural support, however, proved to be difficult to waterproof completely. The use of a plastic vacuum-formed shell with structural bulk heads was also investigated. This option had the appealing aspect of being entirely waterproof. The plastic, however, proved to be very frail and weak, even with the bulkheads providing structure. The vacuum-formed plastic was also difficult to work with when trying to incorporate the passenger restraints. The vacuum-formed fuselage had better weight savings, however, the issues with the structural support resulted in the foam fuselage being explored for the final design. Ultimately it was concluded that the foam fuselage would be the best option for the water and passenger mission and is shown in Figure 24.



Figure 24: Foam Fuselage

5.2.3 Nose Cone

The vacuum-forming technique, however, was useful for nose and tail cone configuration. Although the structural capabilities of the plastic were found to be minimal, the nose cone would only need to support its weight and any aerodynamic loads. Plastic was the favorable material due to the weight optimization, the formability around the fuselage, and the ease of manufacturing. The formability of the plastic also made for easier modifications with the design of the nose and tail cones. The nose cone and tail cones attach with tape that successfully secures the cones to the fuselage with no drag influence. The nesting of the nose cone is shown in Figure 25.



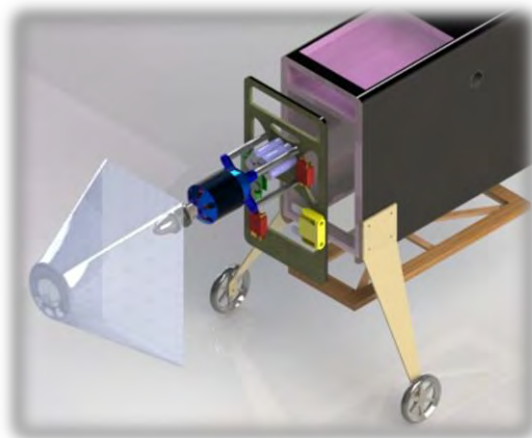


Figure 25: Expanded Nose Cone and Motor Assembly

5.2.4 Empennage Attachment

The vertical stabilizer of this aircraft was mounted using two carbon pins, which provided the structural support to endure the forces and moments it experienced. This idea was extrapolated to include both horizontal stabilizers by having two long carbon pins extruding from the base of the left stabilizer which, upon assembly, are inserted into the base of the right stabilizer as shown in Figure 26. This design allows for the tail to be easily assembled while maintaining a robust structure.

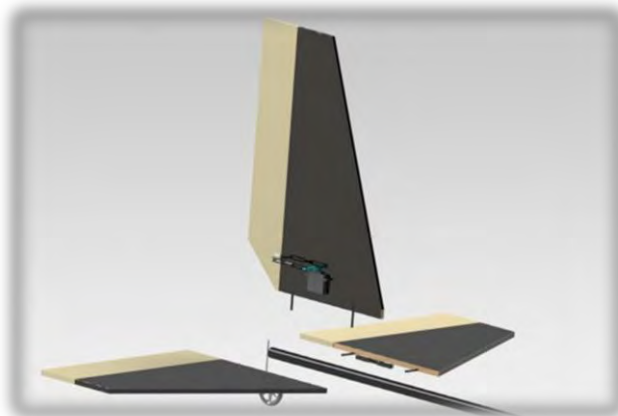


Figure 26: Empennage Attachment

5.2.5 Tail Boom Attachment

The tail boom securement involves a tail boom support bulkhead sandwiched between the fuselage and a 2" hollow foam fuselage extension. Due to the minimal allotted area, a cedar block was added for additional structural support for resistance against the torsion and moment forces on the tail. A final, half bulkhead is glued and secured to the foam extension, for additional moment resistance. The tail boom attachment is pictured in Figure 27.



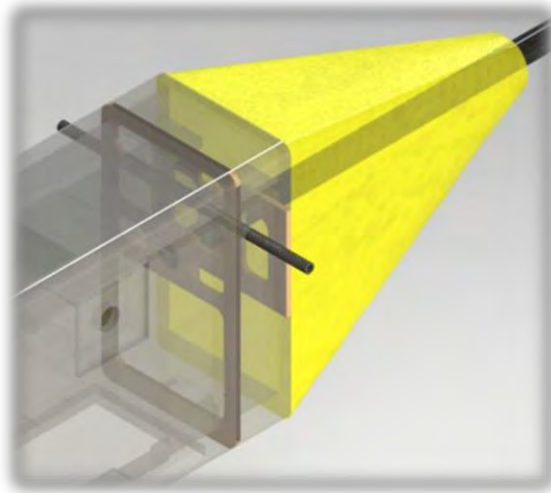


Figure 27: Tail Boom Securement

5.2.6 Water Release Mechanism

The current water release mechanism for mission 3 was designed to be on the bottom of the fuselage due to the ease of dropping the water. The design involves a hatch mechanism, containing an open frame and a coupling door. The frame is created from layered plywood such that the door can nest adequately in the frame in order to create a leak-proof seal. The door is a truss structure from plywood and a layer of plastic for waterproofing. The door is made to nest perfectly with the frame. A servo is attached to the fuselage with the specific attachment to hold the door in place, and to rotate when activated by the CAM sensor to release the door. This mechanism however, is heavy and not entirely leak-proof, and other, lighter options are being explored. The design is shown in Figure 28.

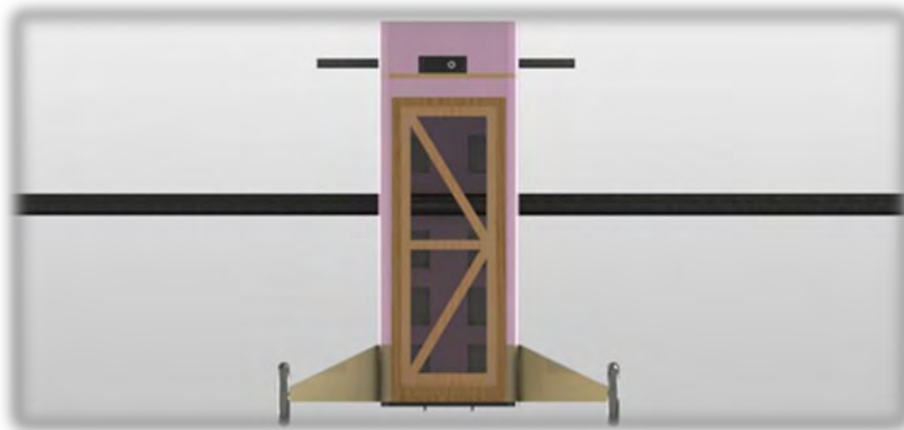


Figure 28: Access/ Water Release Hatch





5.2.7 Passenger Restraint

The aluminum passengers are held in place with a foam seat configuration. The passengers are slid into a foam cutout with eight 1”X 1” slots with proper spacing as required by the competition rules. The door of the water release mechanism then closes an additional foam cut-out , to restrain the other side of the passengers. This configuration fits within the requirements of Mission 2, and the fuselage dimensions, without affecting the water release mechanism. The foam provides a secure restraint and adequate weight optimization.

5.2.8 Electronics

The electronic components of the aircraft were chosen to minimize the RAC of the aircraft in an effort to further optimize scoring, and are provided in Table 11. A 5 cell receiver pack rated at approximately 6 V was selected to maximize the output torque of the servos, allowing for a lighter model servo to be used.

Table 11: Electrical Components

Component	Mission 1	Mission 2	Mission 3
Propeller	14x10	14x7	15x8
Component	All Missions		
Battery Pack	16 1600mAh 2/3A NIMH cells (19.2 V)		
Motor	Himax HC3522-0700		
Speed Controller	Phoenix ICE Lite 45		
Receiver	Spektrum AR6110 DSM2 Microlite 6-Chan.		
Receiver Battery	5 NiMh cells (6 V)		
Elevator Servos	HS 81 Metal Gear		
Rudder/Steering Servo	HS 65 Metal Gear		
Aileron Servos	HS 82 Metal Gear		

5.2.9 Propulsion

Following the preliminary design of the propulsion system, the selected components were further optimized for the desired time to climb performance. Above all else, the weight of the aircraft was aimed to be minimized; therefore, the detailed design was centered primarily on using the smallest battery pack possible.

Initially, a 14x7 propeller was selected for the time to climb mission. This propeller was conservatively chosen so as not to exceed the recommended operating ranges of the components. Additionally, this propeller allowed for a margin of safety on the current draw of the system so as not to exceed the peak current limit of the system safety, resulting in a blown fuse.

The preceding safety margins were then slightly modified to push the operating limit of the system by repeating the preliminary design using a 15x8 APC E propeller. Using this propeller, the static thrust was





increased by nearly 20% from 85 oz to 108 oz. The thrust and drag was then calculated as a function of velocity in order to compute the rate of climb for the aircraft in a loaded configuration. The obtained rate of climb was then plotted as a function of velocity to obtain an optimized velocity at which to climb (Figure 29).

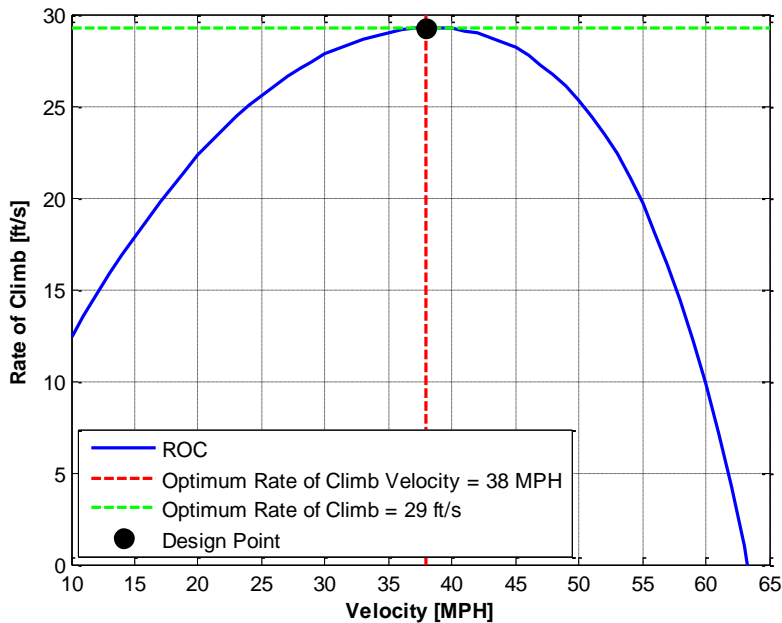


Figure 29: Optimized Rate Of Climb as a Function of Velocity

The ideal velocity to maximize the rate of climb of the aircraft was found to be 38 MPH, yielding a climb rate of 29 ft/s. It should be noted that this component configuration is exceeding the suggested operational envelopes of the propulsion system. This design decision was justified in an effort to maximize the University of Colorado’s total score.

5.3 Weight and Balance

Table 12 provides a weight breakdown of the aircraft as well as the CG location and moments of inertia for each main section of the assembly. The coordinate system is defined with the origin on the tip of the spinner, positive x towards the tail, positive y towards the tip of the right wing, and positive z down.





Table 12: Detailed Bill of Materials

Component	Weight (lbs)	Xcg (in)	Ycg (in)	Zcg (in)	lxx (sl-ft)	lyy (sl-ft)	lzz (sl-ft)
Total Aircraft (Ferry Flight)	3.78	12.42	0.06	-0.17	129.21	42.89	132.90
Total Aircraft (Passenger Flight)	8.17	10.98	-0.34	0.56	379.99	270.08	232.00
Total Aircraft (Time to Climb)	8.23	10.89	0.12	0.60	384.52	271.99	244.60
Payload							
Water	4.41	9.58	0.18	1.25	255.30	229.1	111.60
Passengers (x8)	3.90	8.84	0.21	1.18	250.90	227.2	99.12
Empennage							
Tail Monokote	0.20	39.10	-0.43	-1.87	10.10	10.20	10.14
Tail Servo, Clevice, and Servo Arm	0.08	14.78	-0.18	-1.64	1.26	1.19	1.28
Tail Wheel with Spar	0.01	41.15	-0.50	2.28	0.41	0.41	0.41
Horizontal Stabilizer (1)	0.04	39.37	4.85	0.36	1.83	1.68	2.10
Horizontal Stabilizer (2)	0.04	39.37	-5.21	0.32	1.84	1.68	2.10
Vertical Stabilizer	0.03	39.46	-0.16	-6.25	1.89	2.12	1.51
Landing Gear							
Wheel (1)	0.01	5.53	4.14	8.11	0.09	0.09	0.10
Wheel (2)	0.01	5.53	-4.49	8.11	0.09	0.10	0.10
Gear Support (1)	0.06	5.94	2.35	4.64	0.66	0.64	0.53
Gear Support (2)	0.06	5.94	-2.70	4.63	0.47	0.65	0.54
Wings							
Wing Left	0.25	12.54	-18.73	-0.74	29.40	7.20	31.00
Wing Left Spars and Ribs	0.09	10.76	-13.40	-0.69	8.83	1.62	8.92
Wing Left Servo and Control Surface	0.05	14.15	-27.33	-0.54	1.69	1.65	1.83
Wing Left Skin	0.05	9.71	-18.95	-0.57	5.26	1.02	5.31
Wing Right Spar	0.07	10.53	10.16	-0.67	2.87	1.08	2.87
Fuselage							
Door Servo	0.02	15.14	1.84	3.70	-----	-----	-----
Wing Right	0.28	12.71	19.79	-0.74	36.90	8.57	38.88
Main Wing Spar	0.24	10.53	-0.18	-0.67	24.90	2.52	24.99
Wing Spar 1	0.02	10.53	-0.18	-0.67	0.12	0.18	0.20
CAM Sensor	0.02	8.63	0.82	-1.57	0.13	0.13	0.13
Nosecone	0.03	12.91	-0.02	0.69	-----	-----	-----





5.4 Flight Performance

Between loaded and unloaded missions the performance parameters of the aircraft vary drastically. Table 13 below shows the expected flight performance parameters for the time to climb mission. This mission was chosen as it is the most demanding in terms of performance, and is expected to cause the greatest shift in performance values throughout the flight.

Table 13: Performance Parameters

Parameter	Value
Weight [lb]	8.4
Longitudinal Stability Empty	8.4%
Longitudinal Stability MTOW	15.3%
Horizontal Tail Volume Ratio	0.59
Vertical Tail Volume Ratio	0.3756
-10° Elevator Deflection Pitch	99.32 °/s
10° Aileron Deflection Roll	113.87 °/s
-10° Rudder Deflection Yaw	93.74 °/s
Drag [lb]	2.611
Power Required [W]	202.0
L/D	16.36
Rate of Climb [ft/s]	29

5.5 Mission Performance

The flight performance characteristics of the aircraft during each of the three missions are summarized below in Table 14.

Table 14: Predicted Mission Performance

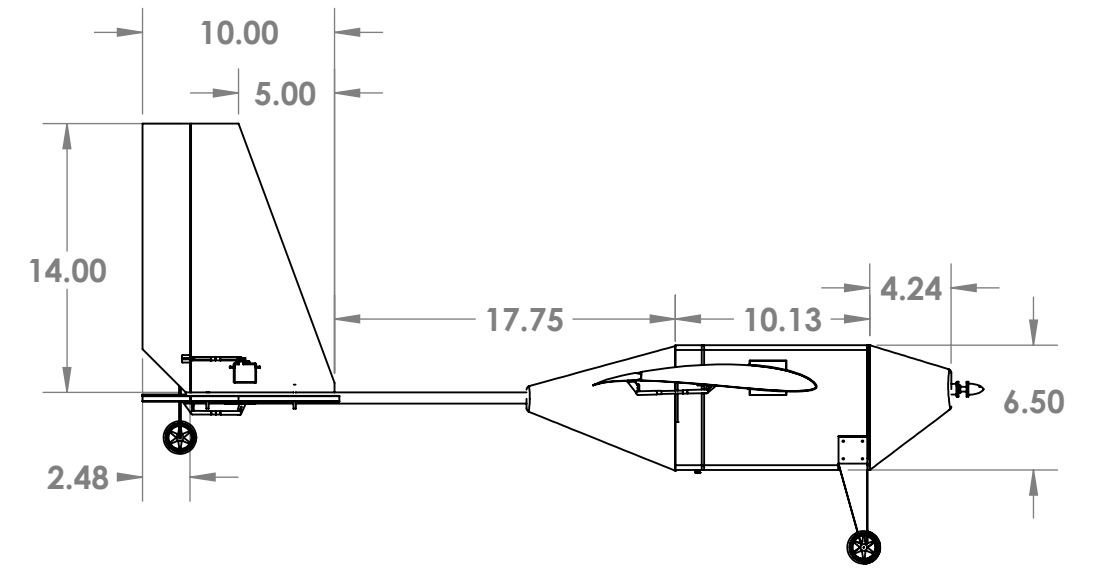
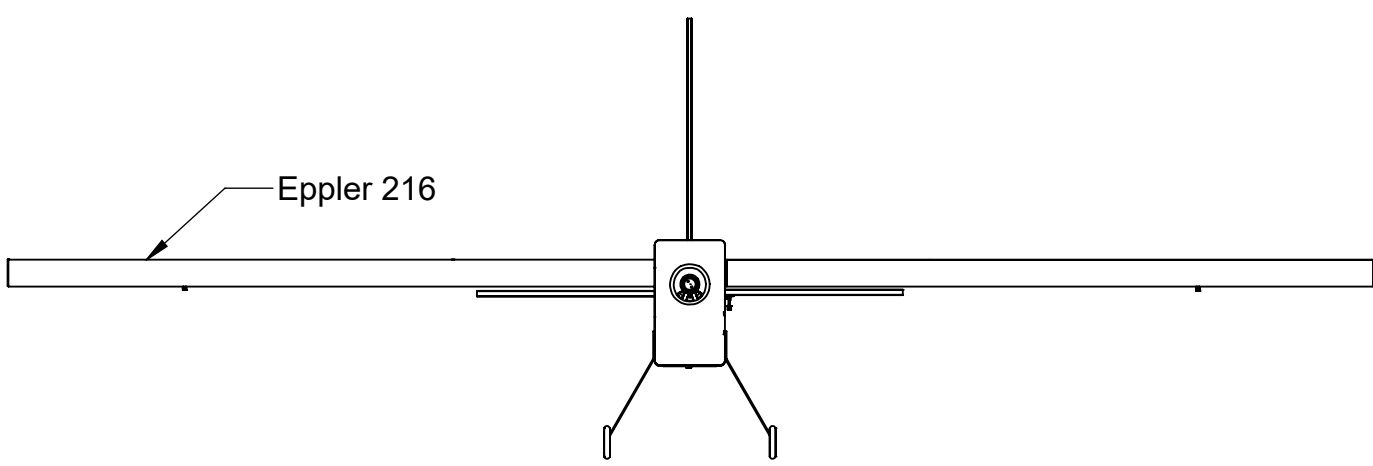
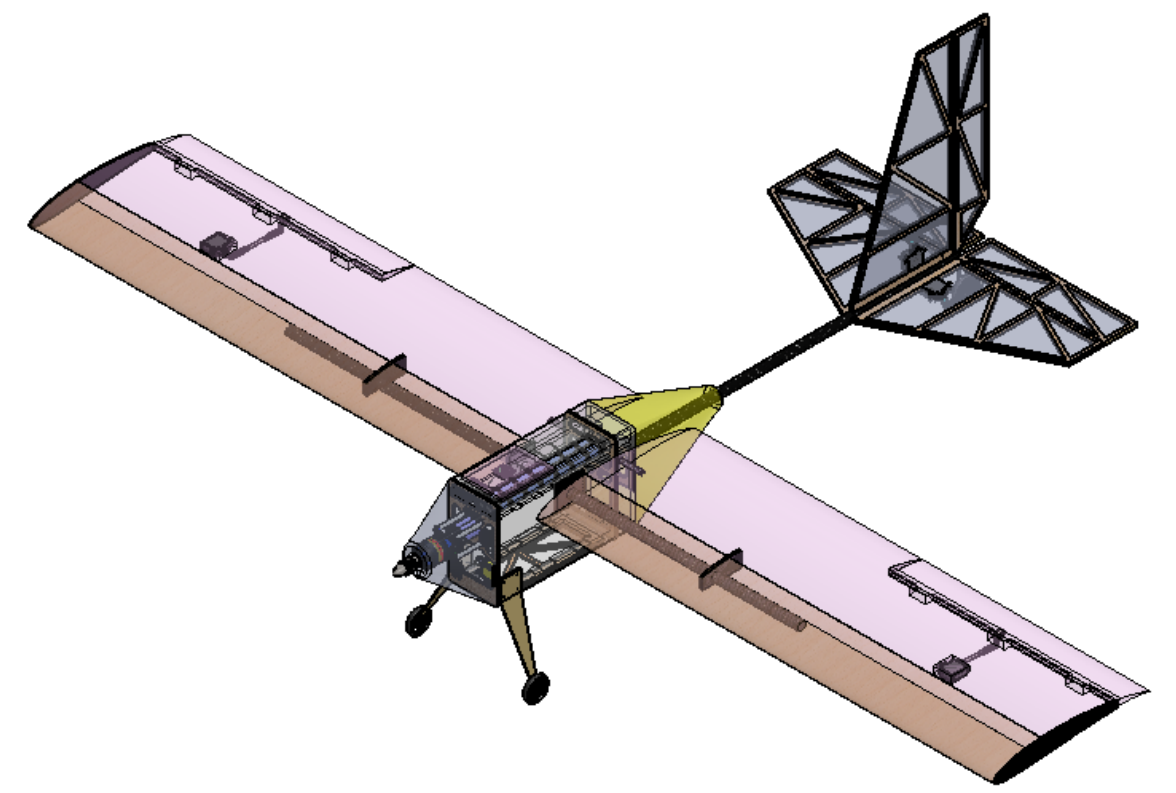
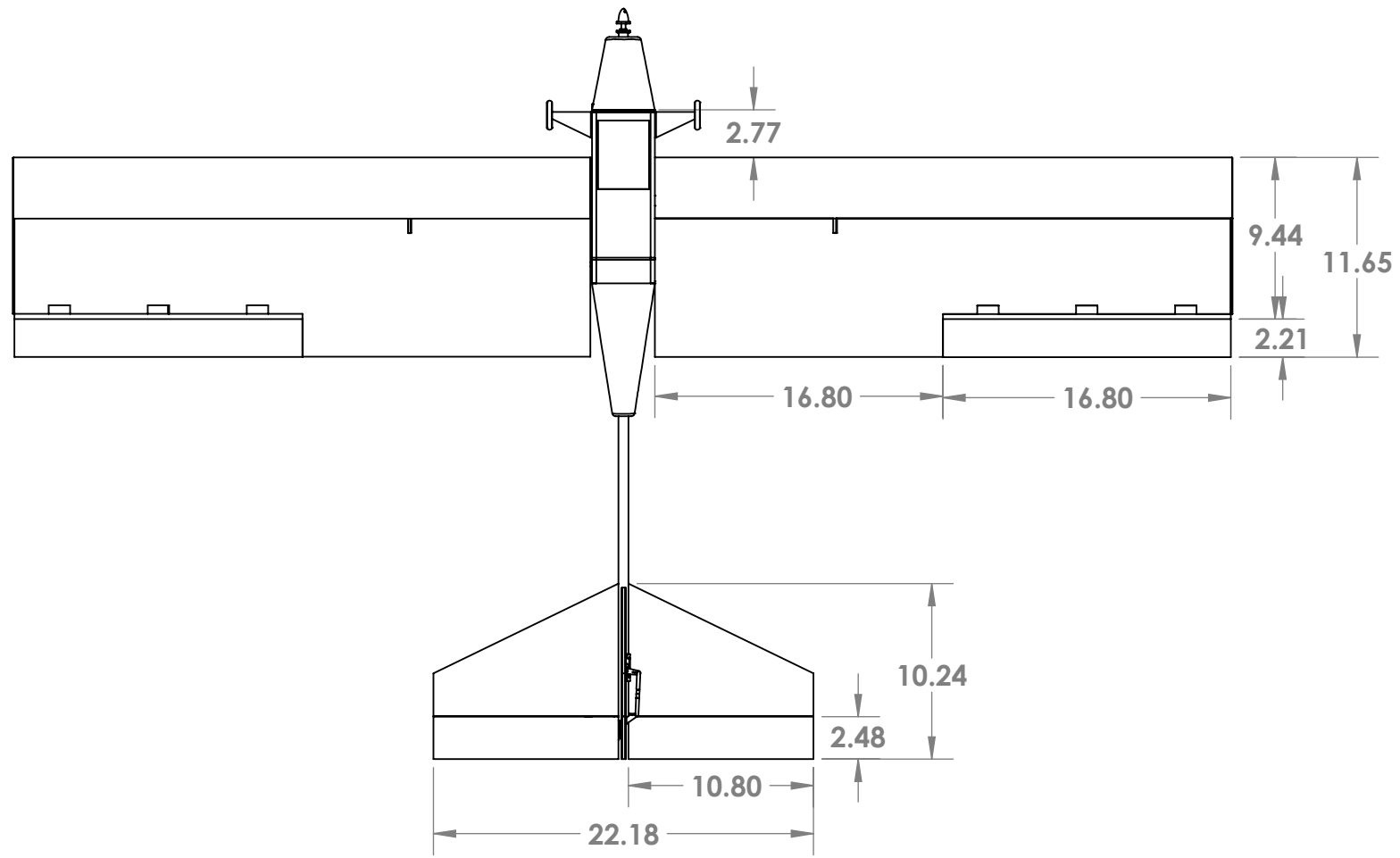
Mission Parameters	Mission 1	Mission 2	Mission 3
Flight Weight (lb)	3.44	7.34	7.84
Maximum Climb Rate (ft/s)	/		29
Turn Rate (deg/s)	50	50	50
Stall Speed (ft/s)	24.7	36.1	37.4
Cruise Speed (ft/s)	86.4	86.4	55.7 (Climb Velocity)
Predicted Mission Time (sec)	240	228	26 (Time to Climb)

Note that each value in the table above is estimated assuming the flight weight given.

5.6 Drawing Package

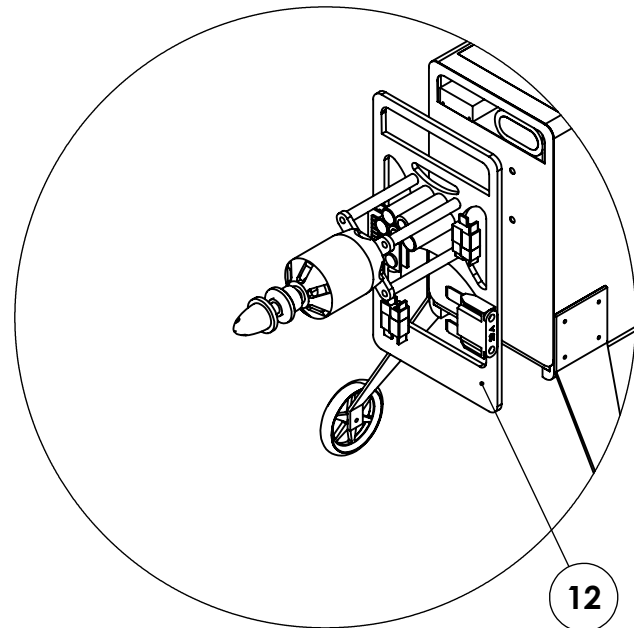
The drawing package includes a detailed three view drawing, structural arrangement, systems layout, and payload accommodation drawing for the aircraft.



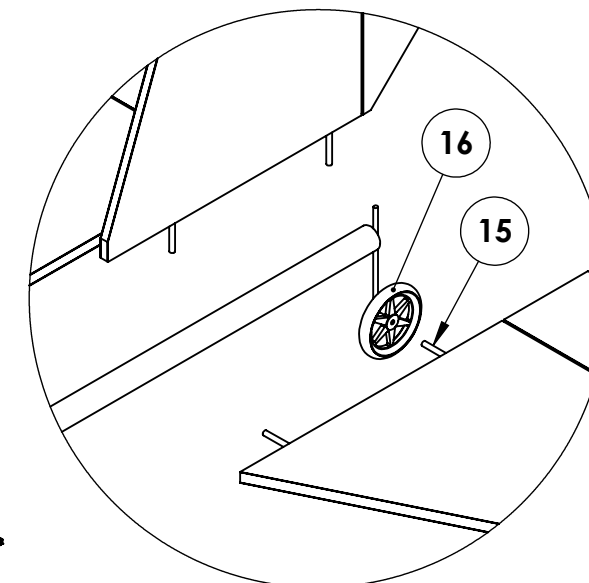
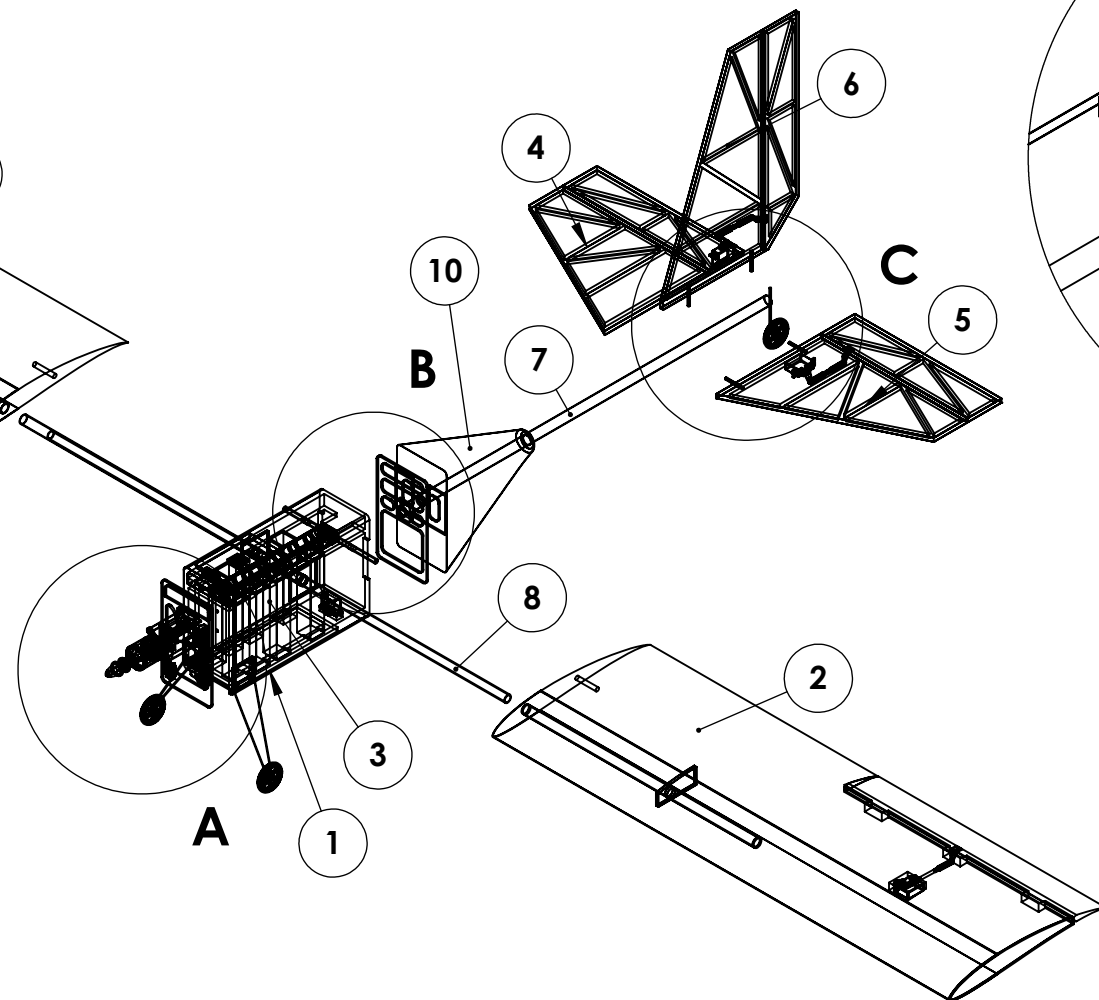
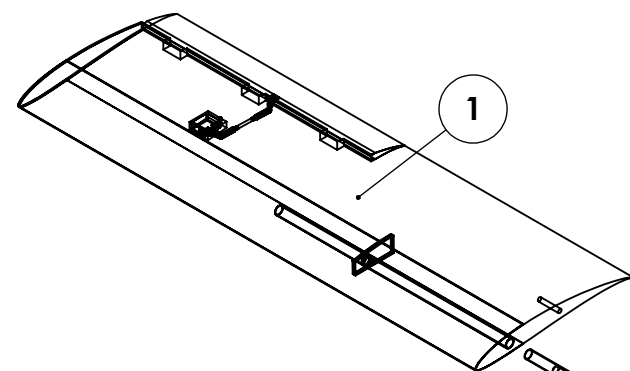


**SolidWorks Student Edition.
For Academic Use Only.**

University of Colorado - Boulder		
TITLE: 3-View Drawing		
AIAA Design Build Fly 2011-2012		
SCALE: 1:10	All Dimensions in Inches	SHEET 1 OF 4

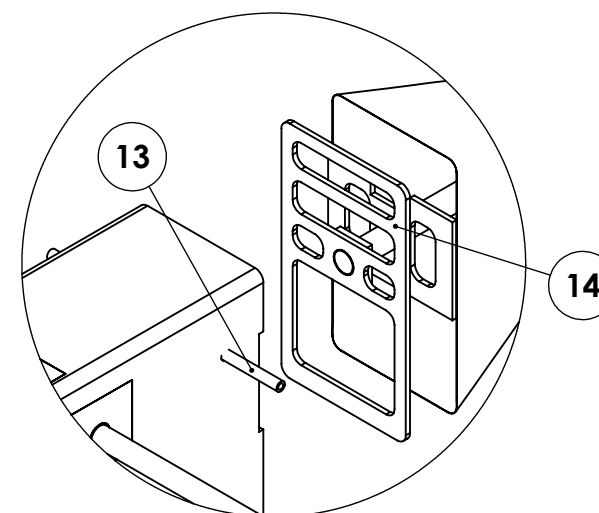


**DETAIL A
SCALE 1 : 4**



**DETAIL C
SCALE 1 : 4**

PART NO.	DESCRIPTION	MATERIAL	QTY.
1	Right Wing	Balsa/1# EPS	1
2	Left Wing	1# EPS	1
3	Fuselage	1# EPS	1
4	Right Horizontal	Balsa	1
5	Left Horizontal	Balsa	1
6	Vertical Stabilizer	Balsa	1
7	Tail Spar	Carbon Fiber	1
8	Wing Spar	Carbon Fiber	1
9	Water Drop Hatch	Plywood	1
10	Tailcone	Forming Plastic	1
11	Nosecone	Forming Plastic	1
12	Motor Bulkhead	Carbon Honeycomb	1
13	Wing Moment Pin	Carbon Fiber	1
14	Rear Bulkhead	Carbon Honeycomb	1
15	Tail Joiner	Carbon Fiber	4
16	Landing Gear Wheel	Plastic/Foam	3



**DETAIL B
SCALE 1 : 4**

**SolidWorks Student Edition.
For Academic Use Only.**

University of Colorado - Boulder

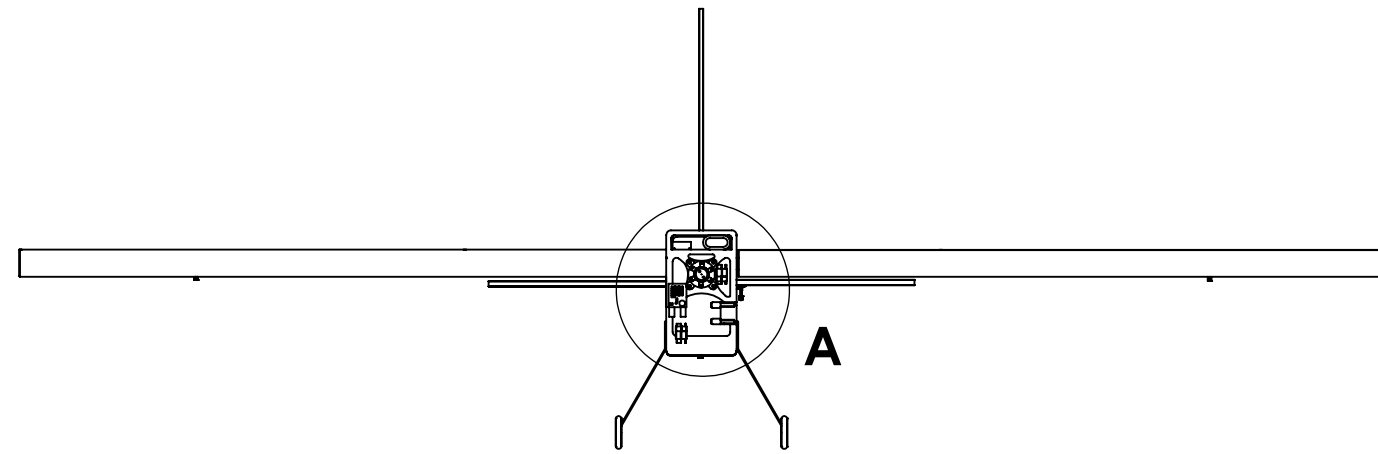
TITLE:
Structural Arrangement

AIAA Design Build Fly
2011 - 2012

SCALE: 1:10 All Dimensions in Inches SHEET 2 OF 4

8 7 6 5 4 3 2 1

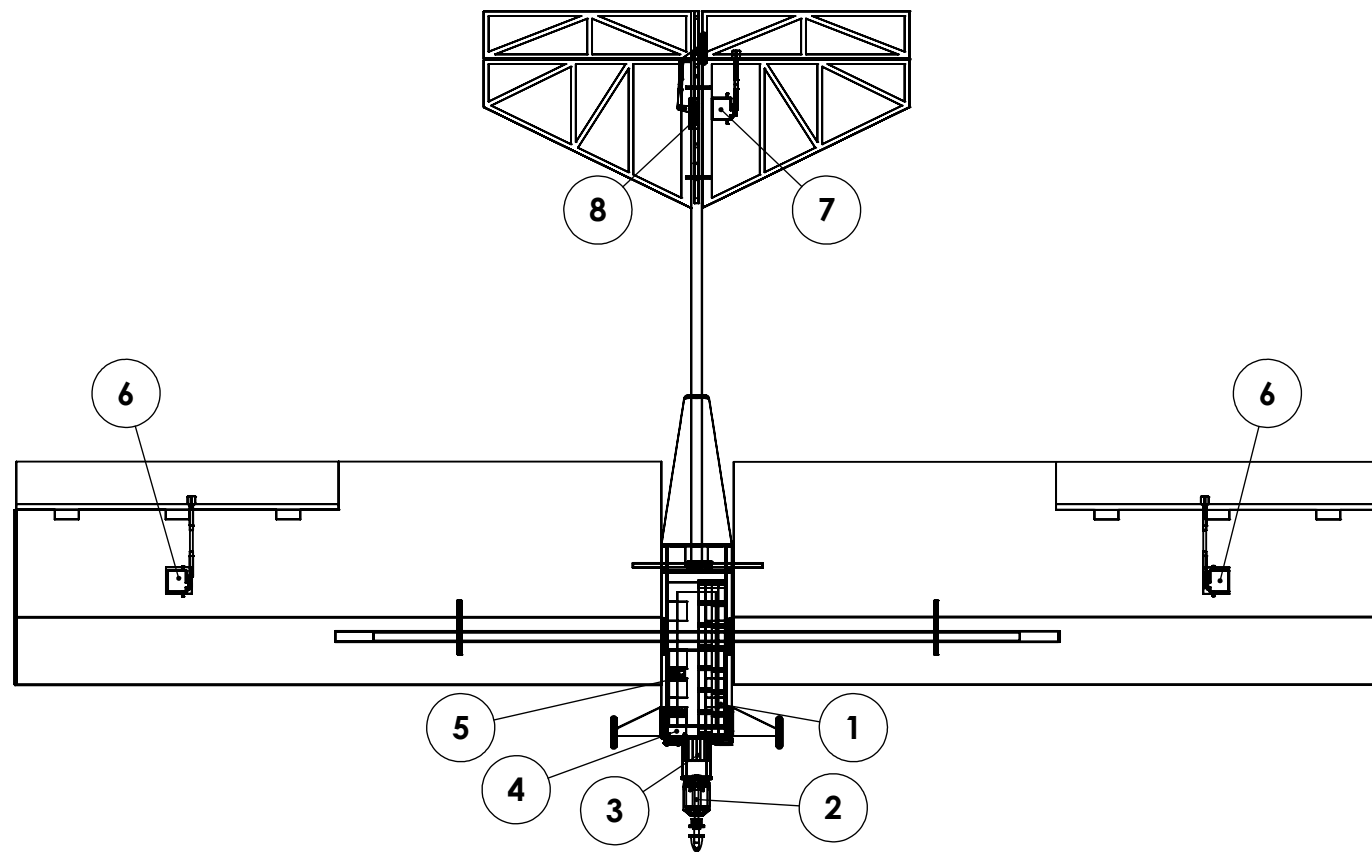
D



PART NO.	DESCRIPTION	QTY.
1	Main Battery - 14 Cell NiMH	1
2	Motor - Himax HC3522-0700	1
3	Flight Pack	1
4	Reciever - Spektrum	1
5	CAM Sensor	1
6	Aileron Servo - Hitec Hs-82	2
7	Elevator Servo - HitecHs-82	1
8	Rudder Servo - Hitec Hs-65	1
9	Speed Controller - Pheonix	1
10	20 Amp Slow Blow Fuse	1
11	Male/Female Deans Connector	2

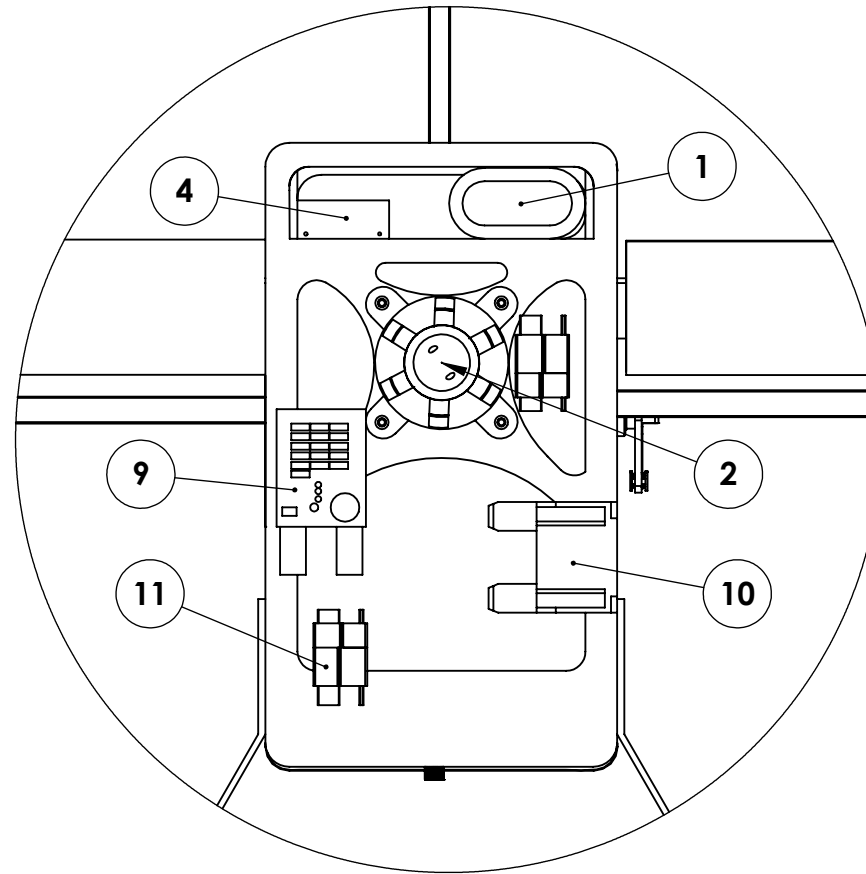
D

C



C

B



B

**DETAIL A
SCALE 1 : 2**

A

**SolidWorks Student Edition.
For Academic Use Only.**

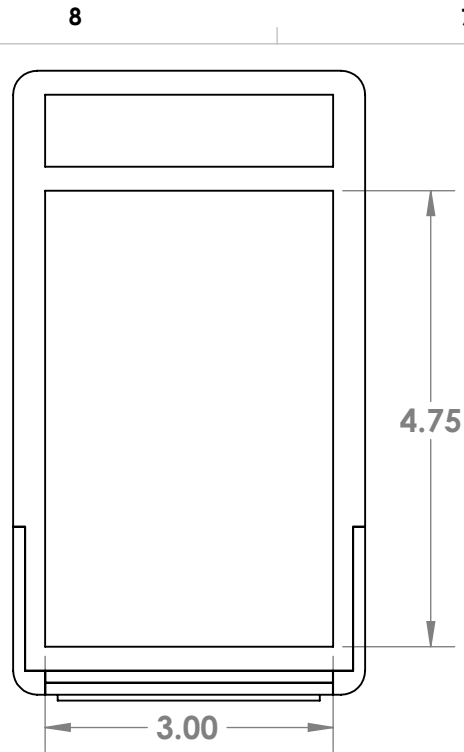
University of Colorado - Boulder

TITLE:
System Layout

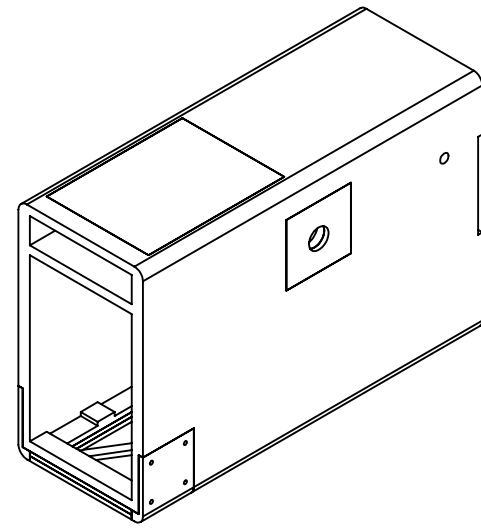
AIAA Design Build Fly
2011 - 2012

SCALE: 1:10 All Dimensions in Inches SHEET 3 OF 4

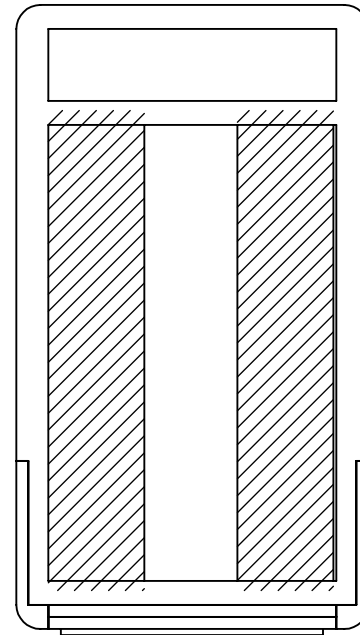
8 7 6 5 4 3 2 1



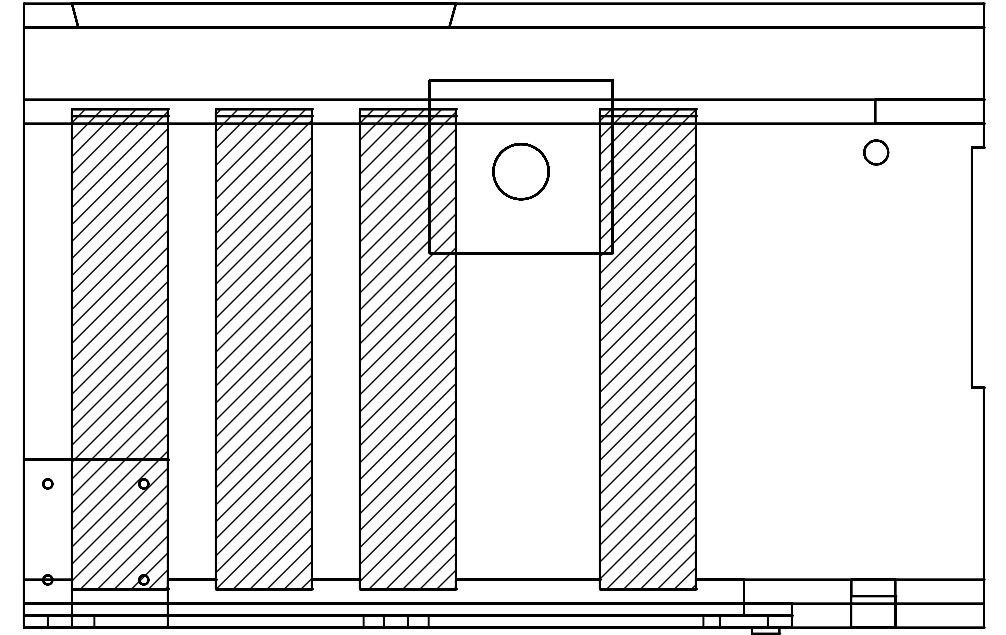
SCALE 1:2
EMPTY PAYLOAD COMPARTMENT



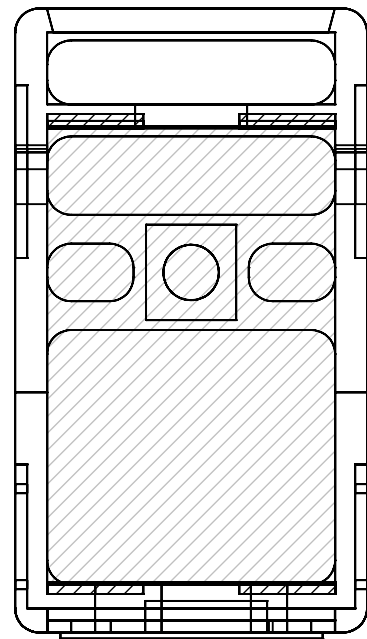
SCALE 1:4



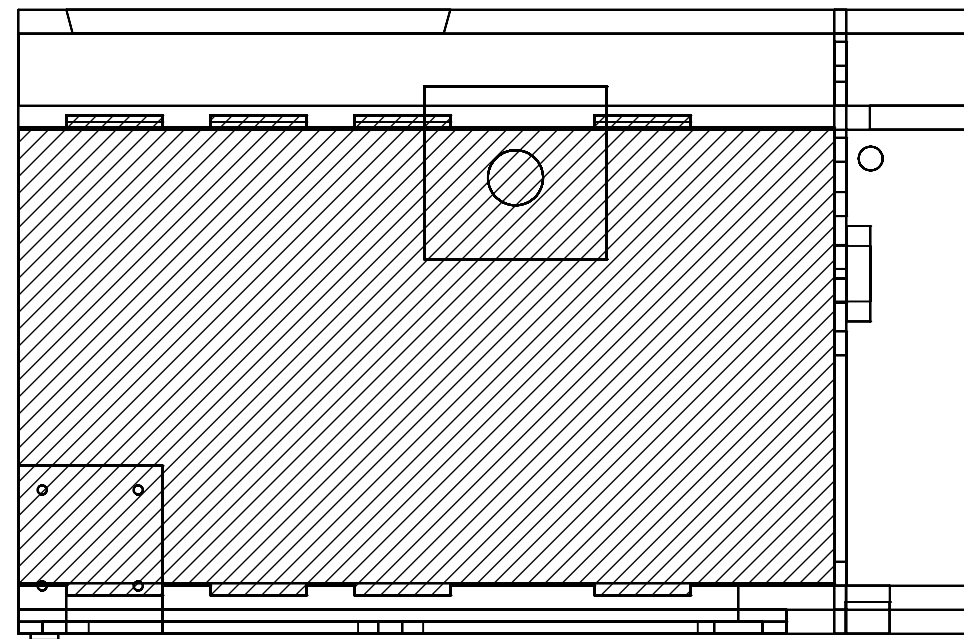
SCALE 1:2



SCALE 1:2



SCALE 1:2



SCALE 1:2

PAYLOAD COMPARTMENT WITH WATER

SolidWorks Student Edition.
For Academic Use Only.

University of Colorado - Boulder	
TITLE: Payload Accomodation	
AIAA Design Build Fly 2011 - 2012	
All Dimensions in Inches	SHEET 4 OF 4



6.0 Manufacturing Plan

6.1 Manufacturing Processes

Plans are in place to manufacture three aircraft. The first aircraft provided validation for the design analysis, and provided a durable test bed with which to explore the design's limitations and capabilities. It was decided that the first model would be capable of carrying the payload of water required in Mission 3. This test bed was manufactured with removable wings and tail to allow for the possibility of multiple, modular components. The second model, or manufacturing prototype, will incorporate all of the complex construction techniques and attachment mechanisms and will mimic the competition aircraft. The components of the manufacturing prototype will be nearly identical to that of the competition aircraft, allowing components to be interchanged in the event of the competition aircraft being damaged during transportation or testing. This aircraft will be developed prior to the competition aircraft, allowing the lessons learned from the aerodynamic and manufacturing prototypes to be applied to the competition aircraft. A detailed manufacturing schedule is provided in Figure 23.

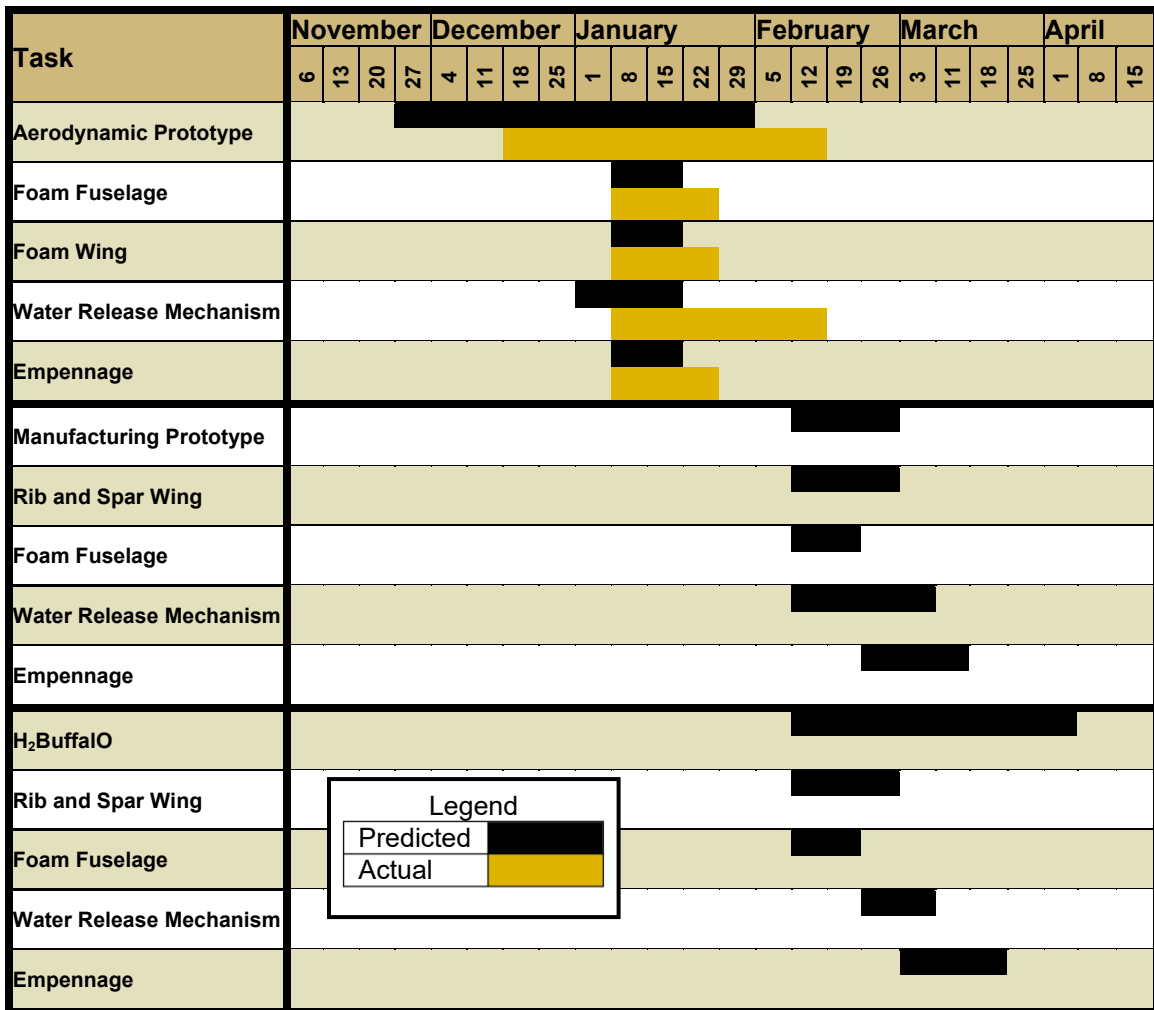


Figure 30: Manufacturing Schedule Gantt Chart





6.1.1 Wing Structure

The aerodynamic prototype was planned with Mission 3 in mind. The inclusion of the TEIS payload and water release system for the first flight encouraged a quickly manufactured wing. Since foam wing designs are easier to construct and durable designs, the initial selection of the wing structure of the H₂BuffalO was a foam and balsa composite. The wings were partially sheeted along the leading edges with 6" of balsa. In addition to producing the wings quickly, a removable wing design was favored for further flight tests. The removable wing design allowed for modifications to the wing design to be applied onto the fuselage immediately.

For the manufacturing prototype, a rib and spar wing design is planned to be integrated. The removability of the wings will still be integrated into the design; however, the carbon fiber spar will extend to the end of the wing. The ribs will be created using a laser cutter, for increased precision and accuracy. The balsa ribs will be attached along the carbon fiber spar and secured using glue. A layer of Monokote™ will provide a light yet robust skin for the wing.

6.1.2 Fuselage Structure

The fuselage must carry the internal payloads of the water and the aluminum passengers, be waterproof, absorb impact on landing, and withstand forces and moments produced by the tail. This resulted in the need for a strong yet light fuselage that could accommodate all three missions. The following design options were compared:

- **Foam:** The fuselage is cut out of the foam, and is easy to build but difficult to modify or repair. The weight is minimal but the foam is problematic when waterproofing.
- **Vacuum-Formed Plastic:** A foam mold is created to the necessary outer dimensions of the fuselage and plastic is vacuum formed around the mold. Four or five bulkheads are added to a longeron within the plastic to support the aircraft components and the passengers. A piece of plastic is placed and glued as the sixth and final wall of the fuselage. This design proved to be light weight and waterproof, but difficult to manufacture and modify. It was also found to be very delicate.
- **Foam/Plastic Composite:** The fuselage is also cut out of the foam, but has a plastic vacuum-formed inner lining for waterproofing. This design makes a particularly durable fuselage with unnecessary weight; however, it is easier to modify.

The foam fuselage was the chosen construction technique due to its optimal weight and structural capabilities. Although the foam is difficult to waterproof successfully, after many tests the foam was waterproofed with a wax-based surface coating. The foam also provided simpler securing methods for the aluminum passengers and stronger material for the wings and tail boom with which to attach. Additional bulkheads were added to the fuselage to provide rigidity. The bulkheads were constructed with





foam and plywood, and were sealed with a layer of plastic. The wing spar also runs through the fuselage, with support blocks that are waterproofed at the connection.

6.1.3 Tail Boom Structure

The tail-boom was chosen to be a 0.5" diameter, thin-walled carbon fiber rod. This was the simple and light-weight solution for the loads that the tail would experience. At the end of the fuselage, a section of the foam is sandwiched with two bulkhead supports for the tail boom. This contributes toward securing the tail boom and supporting the aerodynamic loads and moments that the tail experiences.

6.1.4 Empennage Structure

The tail and empennage structure was designed to optimize the center of gravity for the aircraft and to provide the pilot with enough control authority after takeoff. The tail structure is a standard truss for simplicity and strength. The vertical and horizontal stabilizers are connected with thin carbon fiber rods, threaded through and attached to the end of the carbon fiber tail boom. This method of attachment was proven to be a light solution and capable of enduring the moment and torsion of the tail. The control surfaces of the tail were controlled by servos mounted within the stabilizer surfaces. This design was implemented in order to minimize the total aircraft structure weight.

On an earlier prototype, the use of control rods was experimented with as an attempt to decrease weight near the aft of the aircraft. This approach, however, increased total aircraft weight which was unacceptable.

7.0 Testing Plan

7.1 Testing Objectives

In order to make successful predictions of the design of the aircraft, a series of tests were performed on the various components of the aircraft. From the individual subsystem tests, design decisions were made and integrated into the aircraft assembly.

7.1.1 Wing Testing

The initial design was a foam wing for ease of manufacturing. A preliminary test for deflection and strength was conducted with a foam section of airfoil. A half-wingspan test section was tested using a wiffletree weight distribution with the root fixed. The wing was tested until 14" deflection occurred and the wiffletree had failed. The wing yielded at 1.5" displacement with a 6-lb load added to it. The flexibility of the foam proved the need for a sheeted layer of balsa wood, which was integrated into the aerodynamic prototype. Further testing on deflection and torsion will be conducted on the rib and spar wing design.





Figure 31: Half-Wingspan Wiffletree Test

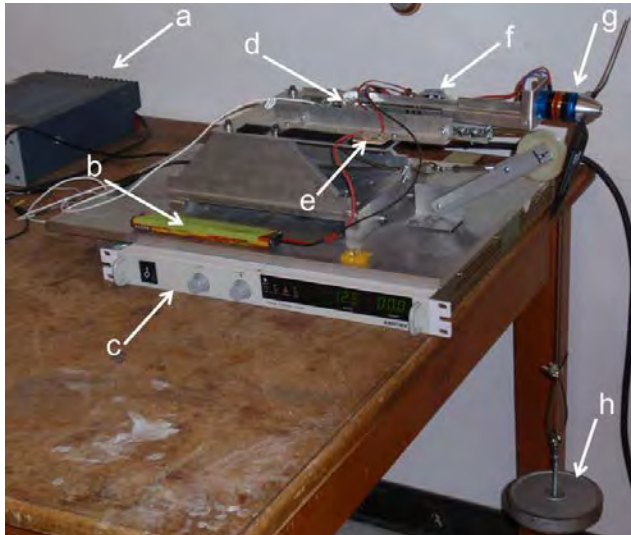
7.1.2 Fuselage Testing

A formal test of the structure of the fuselage was not conducted due to time constraints, but results were gathered from the aerodynamic flight tests. During the two primary aerodynamic flight tests, the fuselage proved to be a sturdy design, with the exception of several critical components. The second of the two flights conducted, resulted in a crash landing due to structural failure. On-board flight video revealed that the rear tail boom securement method failed and caused the aircraft to lose tail control and crash. The fuselage was later rebuilt in order to continue testing. Subsequent tests went without incident.

7.1.3 Static Propulsion Test

The static propulsion test stand consisted of several important components enabling a broad range of testing capabilities. The stand was equipped with roller-bearing sliding rails which allowed the propulsion assembly to apply a force to a load cell as shown below in Figure 32. The load cell's force capacity was 25 pounds and outputted an analog voltage signal to a 8-bit USB data acquisition card which fed into a LabView (8) script. In order to place the output signal in the middle of the output range, the load cell was pre-loaded with 5 lb of weight. This pre-load was also effective at eliminating the impulse force on the load cell from motor start. A 20 volt, 60 Amp power supply provided power to the propulsion system in place of batteries during some tests. The reason for this was the power supply proved to be a more reliable voltage and current source. The power system also included an integrated fuse block and an in-line speed controller. All of these parameters allowed propellers to be quickly switched out without altering other testing conditions. The only issues encountered with this test design was the low acquisition resolution and the noise from the load cell output.





a	Load Cell Power Supply
b	Battery Pack
c	20 V 60 A Max Power Supply
d	25 Pound Load Cell
e	Fuse Block
f	Electric Speed Controller
g	Motor/Propeller
h	Pre-load Weight

Figure 32: Static Thrust Test Stand

7.1.4 Aerodynamic Prototype Flight Testing

To verify the aerodynamic design, an aerodynamic prototype was constructed. The prototype was fabricated using high-density foam, vacuum-formed plastic, and balsa with carbon fiber reinforcements. A major goal of the first prototype was to fly with the Mission 3 payload of water. Although structurally the prototype did not match the final design, it resembled the same aerodynamic configuration and verified the operation of the propulsion, TEIS, and flight controls systems. The aircraft was outfitted with an accelerometer, and speed controller with data logging capabilities as well as a pitot-static system for airspeed data. Data taken from these instruments were used to identify performance in various flight regimes. A wing mounted camera was installed to observe the functionality and any unforeseen issues. An under-wing photo of the aerodynamic prototype in flight can be seen in Figure 33.



Figure 33: Aerodynamic Prototype Onboard Camera



The various flight test goals made for each trial are organized in Table 15.

Table 15: Aerodynamic Prototype Flight Test Plan

Task	Description
Maiden Flight	Small Battery (14 cell) Do not fly with probe installed Flight controls check out
Fly Empty Aircraft	Small Battery (14 cell) Pitot-Static Probe installed 6 + Laps
Water Payload	Big Battery (16 cell) Pitot-Static Probe installed Simulate Mission 3 Test Cam circuit Waterproof? Plume Size
Water Payload	Small Battery (14 cell) Pitot-Static Probe installed Simulate Mission 3 Test Cam circuit Waterproof? Plume Size

7.1.5 Water Release Testing

In order to ensure the Time End Indicating System design would work, several prototypes and tests were developed.

The first test conducted determined the necessary orifice area needed to expel the water at a rate that would be visible from the ground. The test rig consisted of a 2L container with a hole cut out of one side. For each trial, 2L of water was poured from the container and the time elapsed until the container was empty was recorded. After each trial, the hole was expanded. The results of these trials can be found below in Figure 34.



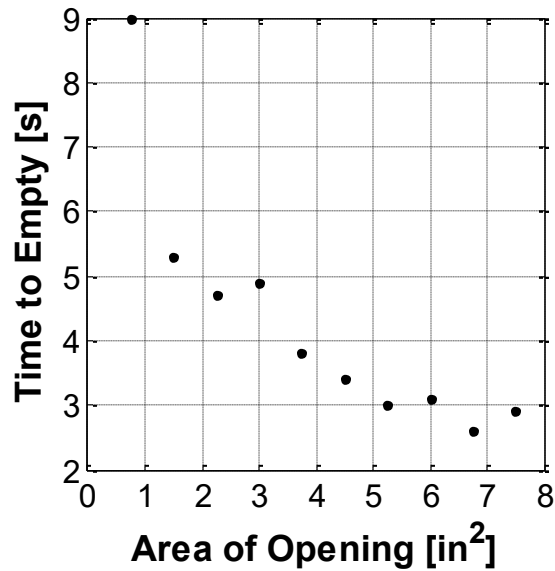


Figure 34: Results of Water Evacuation Trails

As shown in Figure 34, the trend in the data shows that the time it takes to empty the container decreases at a decreasing rate. Eventually, the time to empty remains nearly constant despite an increase in area. Because of this trend it was decided that the water release orifice would not need to be larger than 4.5 in² to evacuate the water quickly.

In addition to this test, several water release system prototypes were developed and tested. The biggest challenge during this process was constructing water-tight systems. One effective method was coating all boundaries in Vaseline. Though this technique stopped water from leaking through cracks, it made it more difficult to open and work with the hatch. For this reason it was important to add only the necessary amount of Vaseline. An image of one of the prototype hatches can be found below in Figure 35.

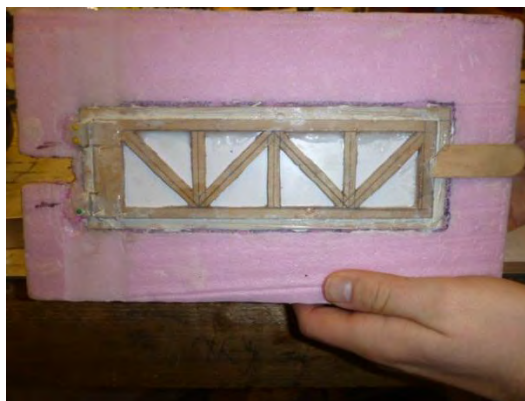


Figure 35: Water Release Hatch Prototype





The ideas that were explored most heavily were hatches, sliding doors, and hose release systems. A hose release system consists of a flexible rubber hose fixed to the bottom of the water tank. This hose is wrapped up and pinned in flight to avoid water leakage and is released at altitude to dump water. The main issue with this design is that it does not have a large enough opening to install the passengers.

7.1.6 Pitot Probe Testing

To ensure that the preliminary aerodynamic analysis was correct a pitot tube was constructed by using a PX 138 series pressure sensor connected to a Logomatic™ data logger. The pitot tube measured differential pressure between its static port and the pitot tube port. This pressure differential was output as a voltage differential that was recorded by the data logger. To calibrate the voltage differential to airspeed velocity the pitot tube was placed in an air flow with known velocity. The results of this calibration are shown in Figure 36.

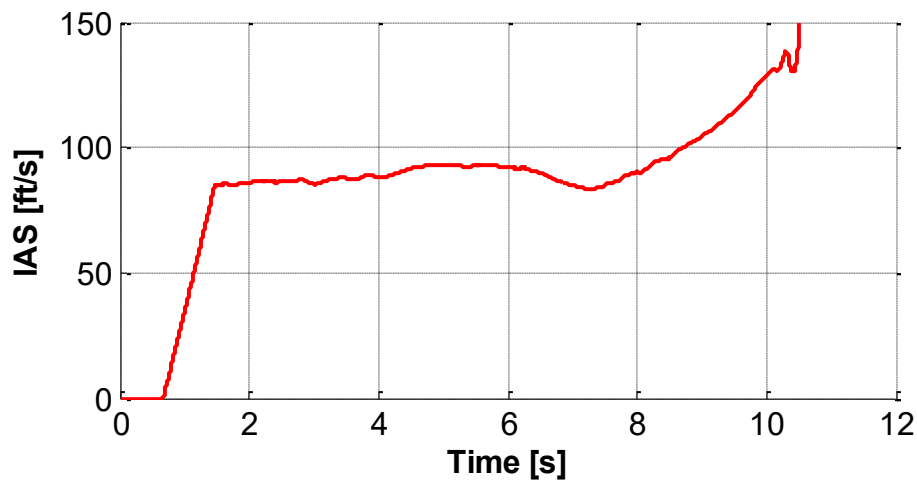


Figure 36: Calibration Data for Pitot Probe

The pitot probe first measured static pressure for the first second to set a baseline for the data. The airspeed was then accelerated up to 82 ft/s, which the pitot tube accurately measured. When the flow was increased up to 131 ft/s the accuracy of the pitot tube decreased and more noise was generated due to reaching the cutoff voltage for the data logger. The maximum predicted airspeed for the aircraft, though, was 85 m/s; thus the pitot tube is accurate enough for the flight conditions expected. The pitot tube will be used in future test flights to validate the aerodynamic analysis performed by AVL.





7.2 Testing Schedule

Figure 37, provides a testing schedule used to verify the functionality of the subsystems and monitor the performance and progress of the aircraft.

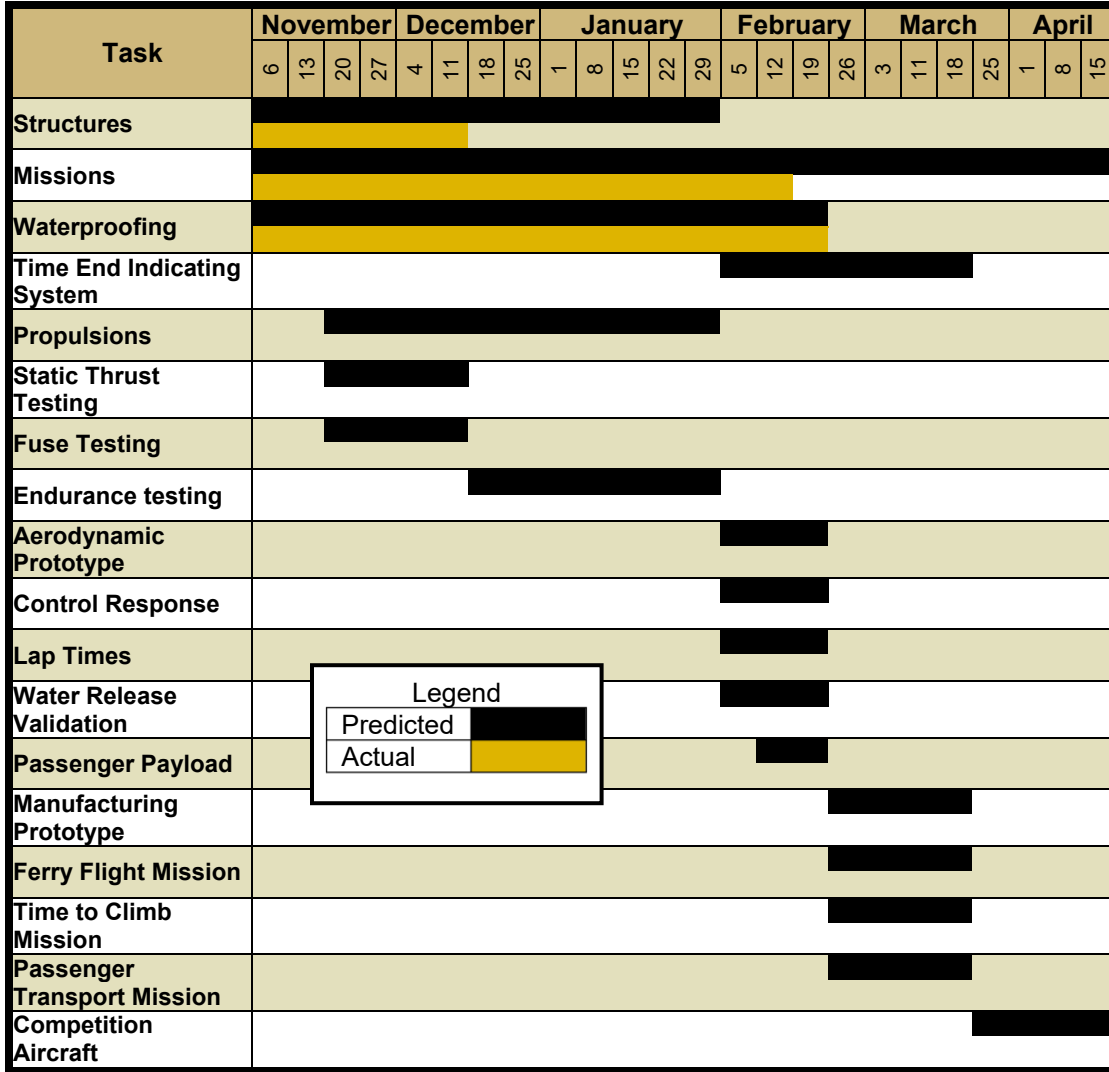


Figure 37: Testing Schedule Gantt Chart

7.3 Testing Checklists

Table 16 was used to ensure that all necessary equipment is taken to each test flight. Table 17 shows the pre and post flight checklist used for aerodynamic prototype testing.





Table 16: Equipment Checklist

Aircraft and Mission Equipment			
Aircraft		Transmitter	
Wings and Wing Spars		Fuses	
Tail Assembly		Speed Controller	
Nosecone		Receiver	
Propulsion Batteries		Receiver Batteries	
Propeller		CAM Altimeter	
Tools and Support Equipment			
Crescent Wrench		6 Minute Epoxy	
Allen Wrench Set		Utility Sticks	
Needle Nose Pliers		CA Medium	
Battery Charger		CA Activator	
Sand Bags		Dual Lock	
Scales		Ballast Weights	
Scissors		Foam Blocks for Repairs	
Screw Drivers		Servo Wire (extra)	
Xacto Handels		Wax for Waterproofing	
Xacto Blades		Screws	
Tape Measure		Balsa for Repairs	
Speed Square		Gaffers Tape	
Small Drill		Duct Tape	
Drill Bits		Masking Tape	
Sharpie Markers		Paper Towels	
Wire Cutters		Zip Ties	

Table 17: Pre/Post Operation Checklist

Before Departing for Field	
Gather and pack materials	
Battery packs charged	
Check weather report	
Preflight Checklist	
Verify speed controllers connected to motor	
Verify servo and throttle connections	
Remove fuse if installed	
Install propulsion battery pack	
Install and connect receiver battery pack	
Install payload	
Verify CG location	
Switch receiver on	
Transmitter on	
Flight controls check	
Range and failsafe check	
Activate data logger	
Connect propulsion battery pack	
Move aircraft to taxi/runway	
Install fuse	

Shut Down Checklist	
Uninstall Fuse	
Switch off receiver	
Check for damage/shifted payload	
Bring back to shelter	
Remove/replace battery	





8.0 Performance Results

8.1 Structures

8.1.1 Wing

The wiffletree deflection test revealed that the flexibility of foam wings was too flimsy for the flight forces and loads, and additional sheeting was necessary for increasing the rigidity of the wing. The deflection test also showed the great strength of the wing against shear forces. After the aerodynamic flight test crash, the balsa-sheeted wings endured an intense impact with no damage. The wings were reused for a new aerodynamic test and successfully endured the aerodynamic forces and moments generated during the flight. To increase the performance of the wings and the overall aircraft, the structure weight is planned to be reduced by using a rib and spar wing.

8.1.2 Tail Boom

The first aerodynamic flight test showed significant weakness in the tail and the tail boom structure. The video taken of the crash flight revealed that the ultimate cause of the crash was due to the failure of the tail boom securement. This was taken into account when rebuilding the aircraft for the second aerodynamic prototype. Additional reinforcements were added to help support the tail boom bulkhead, which resulted in a successful adjustment for the securement of the tail for the second test flight.

8.2 Aerodynamics

Aerodynamic performance results obtained from the test flights confirmed the aircraft's aerodynamic qualities performed as expected. The aircraft had the expected control authority from the control surface sizing. Pilot feedback confirmed the stability was appropriate for all missions. Even with a large static margin, the pilot was still able to perform the time to climb mission with full payload. Due to complications with the performance of the pitot-static system airspeed data was not accurately collected and therefore could not be compared to expected airspeed. However, ground speed measurements were similar to the expected airspeed. Future flights will be performed to collect accurate airspeed data. Figure 38, shows the aerodynamic prototype in flight.



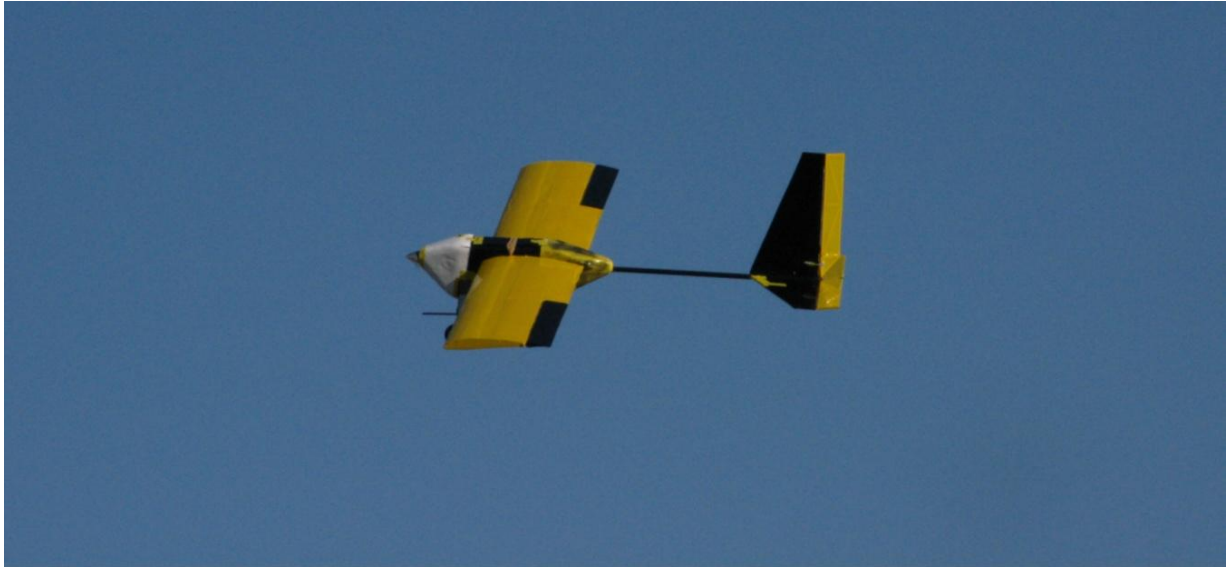


Figure 38: Aerodynamic Prototype in Flight

8.3 Propulsion

8.3.1 Batteries

The 1600 mAh NiMH packs have been tested several times to understand the constraints the battery systems pose to the propulsion of the aircraft. Using the propeller choices in the initial design, the batteries were able to pull approximately 40 amps of burst current for 30 second intervals. Although the endurance testing is not completed, the initial battery packs seem to be of adequate size and capacity. More testing will provide significant data as to how the batteries affect the propulsion system, including high current draw testing to determine the maximum output of the batteries as a function of time.

8.3.2 Propeller

The results of many static tests were able to quantify the performance of each propeller as a function of time using the ESC on-board speed controller and data acquisition module. These tests provide initial design data needed to choose a propeller. The initial designs show that a 14" diameter propeller will create adequate thrust from the available power. Following the preliminary design and testing, it was found that the system could be further optimized. For this reason, further testing will be conducted to maximize the thrust output of the system. A larger propeller will also improve the efficiency of the system. As of the drafting of this design document, a 15x8 propeller appears to be an ideal candidate for the optimization of the team's score.

8.3.3 Motor

The HC3522 – 0700 has proven to be an ideal motor for the H₂Buffalo. The current system is slightly exceeding the manufacture's recommended nominal limits; however, the motor's performance is still





within the rated burst values. By approaching the operating envelope of this motor, the propulsion output power to system weight ratio is better than that of a larger motor capable of higher power output.

8.4 System Performance

8.4.1 Unloaded Performance

In the flight tests performed using the unloaded configuration, the H₂Buffalo performed as expected. Taking off in 5 seconds after power-up, the aircraft demonstrated the ability to corner, perform the 360 degree turn, and fly for longer than 4 minutes, demonstrating the ability to complete the ferry flight mission. After initial complications were rectified, the aircraft also demonstrated the ability to successfully land gently and remain on the runway.

8.4.2 Loaded Performance

In its loaded configuration, the H₂Buffalo also performed as expected. In both of the loaded test flights, the aircraft was able to take off from the runway in 15 seconds and climb to an estimated 100m. Unfortunately, during these tests the TEIS was not fully operational and therefore a full water drop test was not possible. However, the aircraft was able to carry the maximum payload weight and climb. Further analysis will be performed in order to further increase the aircraft's performance during the loaded mission as well as completely test the TEIS.

9.0 References

- 1) "Aircraft Turn Information Calculator." *CSGNetwork.com Free Information*. 15 Aug. 2011. Web. 25 Feb. 2012. <<http://www.csgnetwork.com/aircraftturninfocalc.html>>.
- 2) "Castle Creations, Inc. 10 Jan 2011. <<http://www.castlecreations.com>>.
- 3) "DBF Rules." AIAA Student Design/Build/Fly Competition" 1 Nov. 2010 <http://www.aiaadb.org/2011_files/2011_rules.htm>.
- 4) Drela, Mark, and Harold Youngren. XFOIL. Computer software. 4 Aug. 2008. 1 November. 2010. <<http://web.mit.edu/drela/Public/web/xfoil/>>.
- 5) Drela, Mark, and Harold Youngren. XFLR5. Computer software. 23 May. 2008. 1 November. 2010. <<http://xflr5.sourceforge.net/xflr5.htm/>>.
- 6) Drela, Mark, and Harold Youngren. AVL. Computer software. 4 November 2003. 1 November. 2010. <<http://web.mit.edu/drela/Public/web/avl/>>.<
- 7) "ElectriCalc." MaxCim Motors. 10 Jan. 2009. <<http://www.maxcim.com/ecalc.html>>.
- 8) LabVIEW Ver. 9.0 (32-bit). National Instruments, Austin, TX, 2009
- 9) MATLAB. Vers. R2011. Natick, MA: MathWorks, 2011. Computer software.
- 10) *SolidWorks*. Vers. 2011. SolidWorks Corp., 2011. Computer software.

